The mechanism of action of LL-37 revisited:

exploring its activity and interaction with the Gram-positive model organism *Bacillus subtilis*

Madeleine Cate Humphrey

Thesis submitted in partial fulfilment of the requirements of the regulation

for the degree of Doctor of Philosophy

Biosciences Institute

Faculty of Medical Sciences

Newcastle University

September 2023

Abstract

LL-37 is a human antimicrobial peptide produced by neutrophils and epithelial cells, with broad activity against Gram-negative and Gram-positive bacteria. The ability of LL-37 to target bacterial membranes is largely agreed upon, however the mechanism by which it kills bacteria is still somewhat unclear.

Using a combination of fluorescence microscopy, growth, and viability assays on the Gram-positive model organism *Bacillus subtilis*, I show that permeabilisation by LL-37 is not sufficient to trigger bacteriolysis. Instead, LL-37 causes lysis in an indirect, autolysin-dependent manner. Surprisingly, a small subpopulation of cells can resume growth in the presence of LL-37. It emerged this phenomenon is caused by stochasticity in LL-37 binding, which enables these cells to grow and recover the culture. Intriguingly, cultures are then protected from subsequent exposure to LL-37. I found this was due to membrane debris from lysed cells sequestering LL-37, and not DNA from lysed cells as previously suggested by other research groups. Altogether, upon LL-37 treatment, the majority of cells die via membrane disruption which then induces autolysis; however, a small population of cells stochastically survive LL-37 and recover the culture, which is then protected from future LL-37 exposure by membrane debris from lysed sister cells.

Finally, I show that, unlike in other bacterial species, membrane headgroup composition, including the presence of lysyl-phosphatidylglycerol, has little impact on the susceptibility of *B. subtilis* towards first or repeated encounters with LL-37. Instead, only the loss of teichoic acids from the cell envelope increases susceptibility by a substantial degree, due in part to their D-alanylation. Contrary to previous postulations, membrane fluidity also has no impact on LL-37 activity, with both highly fluid and less fluid membranes being equally susceptible.

Taken together, these results shed surprising new light on the antibacterial mechanism of action of a major human immune system component.

Acknowledgements

I would first like to thank my supervisor Dr Henrik Strahl, whose guidance and support throughout my PhD candidature helped me to excel in my work and thoroughly enjoy my time in Newcastle. His knowledge and commitment to research were vital elements to me gaining a PhD. My research would not have been possible without funding from the Barbour Foundation, so I extend gracious thanks to Dame Margaret Barbour and her foundation. In completing this research, I was grateful to Dr Alan Koh for his help when working with L-forms. I also regularly used the microscopy and image analysis expertise of Dr James Grimshaw from the Newcastle University Image Analysis Unit. Additionally, I would like to thank the extremely useful websites that aid our everyday science, in my case these were Subtiwiki and Aureowiki (Fuchs *et al.*, 2018; Pedreira *et al.*, 2022). The original figures in this thesis were created using BioRender.com.

I am extremely grateful to the members of the Strahl lab for making my time in Newcastle so fun. Special thanks go to Jess, Laura and Maria for being the funniest, most supportive friends and lab mates that anyone could ask for. My thanks extend to all members of the CBCB, as they made our building such a friendly and cooperative place to work. I would finally like to give special thanks to my family who have always supported me in my educational endeavours.

Publications & Presentations

Publications

Humphrey, M., Abdelmesseh, Nekhala, I., Scheinpflug, K., Krylova, O., Schäfer, A.B., Buttress, J.A., Wenzel, M. & Strahl, H. (2023) Tracking Global and Local Changes in Membrane Fluidity Through Fluorescence Spectroscopy and Microscopy. In: Peter Sass (ed.). *Antibiotics: Methods and Protocols*. Methods in Molecular Biology. 2601:203-229. Springer US, New York.

Oral Presentations

"Autolysis triggered by LL-37 leads to accumulation of protective cell debris", Microbiology Society Annual Conference, Birmingham, 19th April 2023.

"Bacterial adaptation to the human antimicrobial peptide LL-37: more than just tuning lipid charge", NUBI Live!, Newcastle, 30th November 2022.

Poster Presentations

"Autolysis triggered by LL-37 leads to accumulation of protective cell debris", 4th Bacterial Cell Biology Conference, Cancun, 11th-14th February 2023.

Table of Contents

Table of Figures

Chapter 1

Chapter 3

Chapter 4

Chapter 5

Chapter 6

Appendix

Table of Tables

Chapter 2

Chapter 3

List of Abbreviations

ACP	acyl carrier protein
AMP	antimicrobial peptide
ANOVA	analysis of variance
BCFA	branched chain fatty acid
BKD	branched chain α-ketoacid dehydrogenase
CCCP	carbonyl cyanide *m*-chlorophenyl hydrazone
CDM	chemically defined medium
CDP	cytidine diphosphate
c.f.u.	colony forming units
CHDP	cationic host defence peptides
CL	cardiolipin
CLSI	Clinical & Laboratory Standards Institute
CoA	coenzyme A
cWFW	cyclo(RRRWFW)
DAG	diacylglycerol
DMF	dimethyl formamide
DMSO	dimethyl sulfoxide
EUCAST	European Committee in Antimicrobial Susceptibility Testing
FACS	fluorescence-activated cell sorting
FAS	fatty acid synthesis
GL	glycolipid
GlcNAc	*N*-acetylglucosamine
hBD1	human β-defensin-1
hBD3	human β-defensin-3

HI	heat inactivated
hNP-1	human neutrophil peptide 1
IB	isobutyric acid
ITPG	isopropyl β-D-1-thiogalactopyranoside
LB	lysogeny broth
L-PG	lysyl-phosphatidylglycerol
LPS	lipopolysaccharide
LTA	lipoteichoic acid
ManNAc	*N*-acetylmannosamine
MB	2-methylbutyric acid
MHB	Mueller Hinton broth
MIC	minimum inhibitory concentration
MurNAc	*N*-acetylmuramic acid
NA	nutrient agar
NB	nutrient broth
OD_{600}	optical density 600 nm
PA	phosphatidic acid
PBP	penicillin binding protein
PDH	pyruvate dehydrogenase
PDMS	polydimethylsiloxane
PE	phosphatidylethanolamine
PG	phosphatidylglycerol
PS	phosphatidylserine
ROI	region of interest
rpm	revolutions per minute
SFA	saturated fatty acid

SIFA	surface-induced fluorescence attenuation
SMM	Spizizen minimal medium
tPMP-1	thrombin-induced platelet microbial protein 1
TSB	tryptic soy broth
UFA	unsaturated fatty acid
UDP	undecaprenyl phosphate
WTA	wall teichoic acid
σ^D	sigma-D

Chapter 1 – Introduction

1.1 The bacterial cell envelope

Bacteria are broadly classified by the structure of their cell envelope into two groups: Gram-positive and Gram-negative. The bacterial cell envelope is the barrier between the interior of the cell and the extracellular environment. This barrier must be permeable to allow the transport of biological substances in and out of the cell, but also protect the cell from unfavourable conditions and compounds. Both Gram-positive and Gram-negative bacteria possess a cytoplasmic membrane, composed predominately of phospholipids interspersed with integral and peripheral proteins. Gram-positive cell envelopes additionally consist of a thick peptidoglycan cell wall layer surrounding the cytoplasmic membrane, with teichoic acids interwoven through the peptidoglycan (Fig. 1.1a) (Neuhaus & Baddiley, 2003). Gram-negative bacteria, in contrast, lack teichoic acids and instead encase their cytoplasmic membrane in a thin layer of peptidoglycan. This thin cell wall is in turn surrounded by an outer membrane, composed of phospholipids in its inner leaflet and lipopolysaccharides (LPS) in its extracellular-facing outer leaflet.

1.1.1 The peptidoglycan cell wall

The peptidoglycan cell wall is essential to protecting the cell, maintaining cell shape, and resisting turgor, which is caused by the differential solute concentrations within and outside of the cell. Likely due to the additional outer membrane providing protection against turgor in Gram-negative cells, their peptidoglycan is not required to be as thick as teichoic acid-containing peptidoglycan of Gram-positive bacteria (Rojas *et al.*, 2018). Peptidoglycan is composed of a mesh-like structure of glycan strands composed of alternating *N*-acetylglucosamine (GlcNAc) and *N*-acetylmuramic acid (MurNAc), which are cross-linked through short peptide bridges attached to the MurNAc residues (Fig. 1.1b) (Rogers *et al.*, 1980). The predominant structure of the peptide bridges is L-Ala-γ-D-Glu-(L-Lys or DAP)-D-Ala-D-Ala in nascent peptidoglycan, although species-specific variations are common (Vollmer *et al.*, 2008a). In general, most Gram-positive bacteria have L-Lysine in position 3 of their peptide bridges, and most Gram-negative bacteria have *meso*-diaminopimelic acid (DAP). The Gram-positive model organism *Bacillus subtilis*, however, forms a prominent exception to this rule as it carries a DAP at position 3 (Vollmer *et al.*, 2008a).

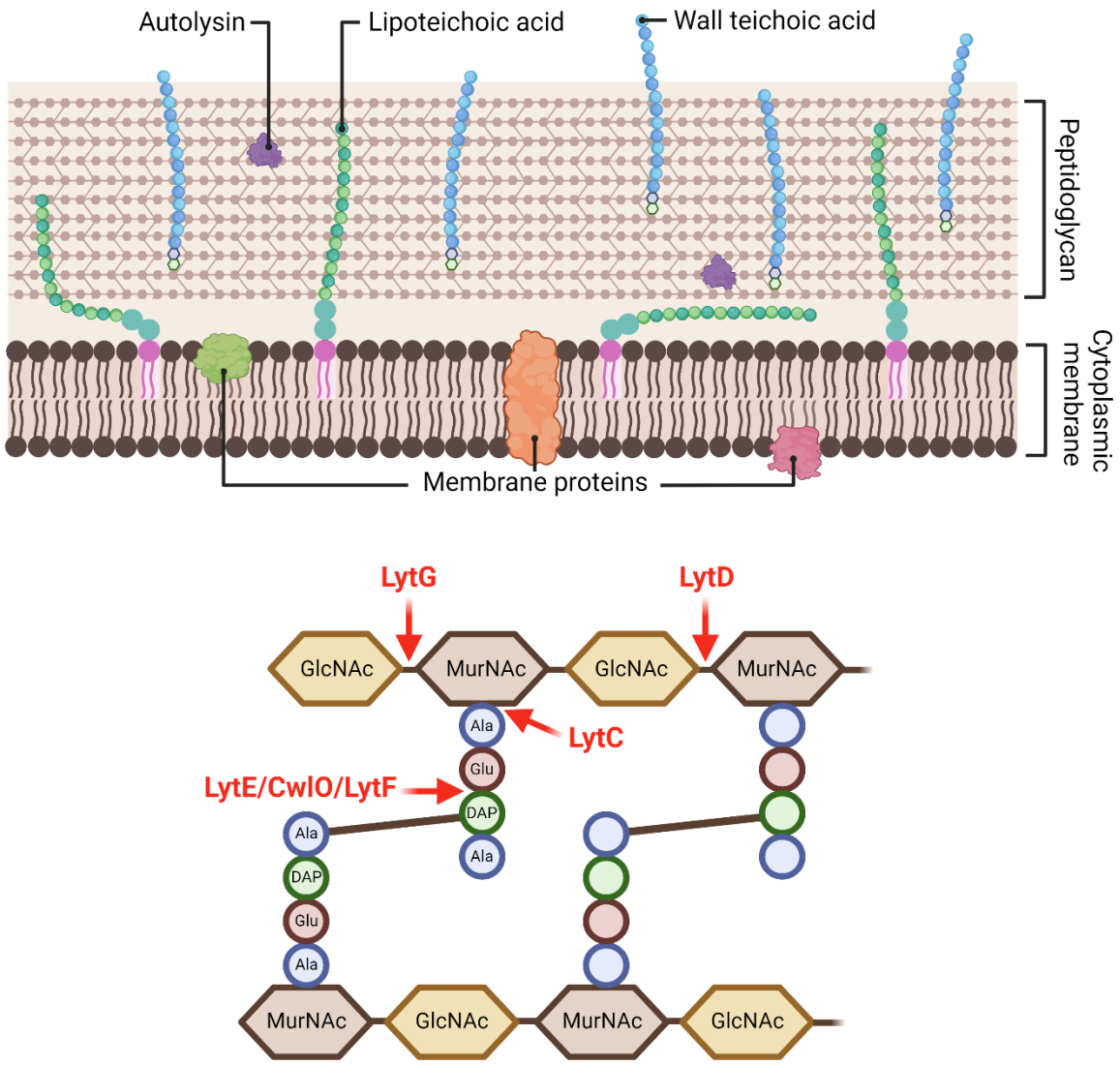

Figure 1.1. The cell envelope and peptidoglycan structure of *B. subtilis*, including its autolysin activity. a) The organisation of the Gram-positive cell envelope, with a thick peptidoglycan cell wall, through which teichoic acids are dispersed. **b**) The structure of *B. subtilis* peptidoglycan, with strands composed of repeating *N*-acetylglucosamine (GlcNAc) and *N*-acetylmuramic acid (MurNAc) residues, with crosslinks attached to MurNAc composed of L-alanine (Ala), D-Glutamine (Glu) and *meso*-diaminopimelic acid (DAP). Autolysins degrade the peptidoglycan at specific locations: LytG cleaves GlcNAc-MurNAc at the end of peptidoglycan strands; LytD cleaves GlcNAc-MurNAc within peptidoglycan strands; LytC cleaves MurNAc-L-alanine; LytE, CwlO and LytF cleave D-glutamine-*meso*-diaminopimelic acid.

Peptidoglycan synthesis starts in the cytoplasm, with the synthesis of UDP-*N*-acetylmuramyl-pentapeptide from UDP-GlcNAc by the enzymes MurABCDEF (Brown *et al.*, 1995; Benson *et al.*, 1995; Yan *et al.*, 2000; Gordon *et al.*, 2001; Deva *et al.*, 2006). This pentapeptide is then coupled to a membrane embedded undecaprenyl phosphate (UDP) by MraY, to yield lipid I (undecaprenyl-pyrophosphyl-MurNAc-

pentapeptide) (Heydanek *et al.*, 1969; Bouhss *et al.*, 2004). The glycosyltransferase MurG then adds GlcNAc to lipid I, to form lipid II (undecaprenyl-pyrophosphyl-MurNAc-pentapeptide-GlcNAc) (Ha *et al.*, 2000; Hu *et al.*, 2003). Lipid II is the mature cell wall precursor; however it needs to be flipped from the inner to the outer leaflet of the cytoplasmic membrane, this is mediated by MurJ and its homologues (Sham *et al.*, 2014). Lipid II in the outer leaflet can then be linked together by the glycosyltransferase activity of penicillin binding proteins (PBPs) and cross-linked into the existing peptidoglycan cell wall via the transpeptidase activity of PBPs, whilst UDP is recycled back to the cytoplasmic leaflet and reused (Goffin & Ghuysen, 1998, 2002).

Peptidoglycan expansion is mediated by dynamic and transient protein complexes – during elongation by the elongasome and during cell division by the divisome (Egan *et al.*, 2020). The elongasome mediates insertion of nascent peptidoglycan into the lateral part of the peptidoglycan mesh, this is organised by MreB, an actin homologue (Domínguez-Escobar *et al.*, 2011). Whereas the divisome mediates insertion of nascent peptidoglycan into the mesh during cell division, under the organisation of FtsZ, a tubulin homologue (Adams & Errington, 2009). These protein complexes, under the ultimate control of MreB and FtsW, recruit a number of additional proteins that enable interaction with PBPs to give directed synthesis of peptidoglycan. In *B. subtilis* MreB and its homologues are essential for the rod-shaped morphology of the cell (Schirner & Errington, 2009).

1.1.2 Autolysins

To enable turnover, cell elongation, division and separation, bonds within the existing peptidoglycan network must be broken to allow the insertion of nascent material. This is performed by autolysins, with their peptidoglycan hydrolase activity being essential to cell survival (Smith *et al.*, 2000). In *B. subtilis* there are potentially 42 autolysins, of which there are the essential LytE and CwlO, and, of other autolysins relevant to this project, there are also LytC, LytD, LytF and LytG (Fig. 1.1b) (Wilson & Garner, 2021).

LytC is 50 kDa *N*-acetylmuramoyl-L-alanine amidase, it is expressed from the *lytABC* operon during vegetative growth. Expression of the operon produces the small acidic membrane bound lipoprotein LytA and the LytC modifier LytB, as well as LytC (Lazarevic *et al.*, 1992). Insertional inactivation of *lytC* causes a 90% decrease in cell wall hydrolytic activity in stationary cells yet no changes in cell morphology, motility, competence or sporulation occur, showing the large but inessential role of LytC (Kuroda & Sekiguchi, 1991). Furthermore, LytC localisation has been observed to be

uniformally dispersed around the cell, indicating it is not solely responsible for cell separation (Yamamoto *et al.*, 2003)

LytD is a 90 kDa endo-β-*N*-acetylglucosaminidase that cleaves the bonds between GlcNAc and MurNAc. The expression of LytD is sigma D (σ^D)-dependent, σ^D is the motility sigma factor (Márquez *et al.*, 1990). Once LytD is synthesised its signal peptide is cleaved and it forms its dimeric active form. Deletion of *lytD* has no impact on the cell separation, motility, autolysis, cell wall turnover and growth of *B. subtilis*, making the physiological role of LytD unclear (Margot *et al.*, 1994).

In *B. subtilis* only 2 autolysins are synthetically lethal, these are LytE and CwlO, either one must be expressed for *B. subtilis* to be viable (Bisicchia *et al.*, 2007). LytE, 35 kDa, and CwlO, 50 kDa, are both D,L-endopeptidases active at the lateral cell wall (Margot *et al.*, 1998; Yamaguchi *et al.*, 2004). The two endopeptidases differ in their localisation within the cell envelope. LytE localises to the septa and poles as well as the cylindrical part of cells, whereas CwlO localises to the cylindrical part of cells only, indicating it is their activity at the cylindrical part of cells that makes these autolysins essential (Yamamoto *et al.*, 2003; Hashimoto *et al.*, 2012). LytE is secreted, with its distribution in the cylindrical part of the cell speculated to be governed by the MreB homologue MreBH (Carballido-López *et al.*, 2006). Whereas CwlO is tethered to the membrane by FtsEX, which regulates it activity (Domínguez-Cuevas *et al.*, 2013). Whilst the deletion of both *lytE* and *cwlO* is synthetically lethal, cells of each deletion exhibit distinct morphologies, suggesting that whilst the activity of one autolysin can rescue deletion of the other, they are not completely functionally redundant (Domínguez-Cuevas *et al.*, 2013).

LytF is a 50 kDa γ-D-glutamate-*meso*-diaminopimelate muropeptidase encoded on a monocistronic operon expressed by σ^D (Margot *et al.*, 1999). LytF localises to the cell septa and poles and its deletion results in filamentous growth, indicating its major role in cell separation (Ohnishi *et al.*, 1999; Yamamoto *et al.*, 2003).

LytG is a 32 kDa exo-*N*-acetylglucosaminidase implicated in cell division, lysis and motility, it acts processively from the end of glycan strands. Deletion of *lytG* significantly impacts the production of muropeptides by *B. subtilis*, whereas deletion of *lytD* does not have the same effect, indicating LytG provides the major glucosaminidase activity (Horsburgh *et al.*, 2003).

Staphylococcus aureus is also a member of the Firmicutes phylum along with *B. subtilis*, the close relation of these two species means many proteins and processes are homologous between the two. The similarity of the two makes *B. subtilis* a useful tool, as a Gram-positive model organism, to investigate findings that might also be relevant in the pathogenic species *S. aureus*. In *S. aureus* a major autolysin, Atl, is encoded; Atl has both *N*-acetylmuramyl-L-alanine amidase and endo-*N*-acetylglucosaminidase activity, the full array of autolysins encoded by *S. aureus* is less well characterised than *B. subtilis* (Oshida *et al.*, 1995; Monteiro *et al.*, 2015). A key difference between the two species is the lack of an elongasome machinery in *S. aureus*, instead a dispersive mode of cell wall synthesis takes place, this lack of an elongasome confers a coccoid shape to the bacterium (Pinho & Errington, 2003).

Autolysis is essential to the normal growth, division and separation of bacterial cells, however misregulation of autolysins can result in their over-activity, leading to bacteriolysis as the cell wall can no longer withstand turgor (Vollmer *et al.*, 2008b). There is a tight coupling between membrane energisation and the regulation of autolysins, which means their activity becomes dysregulated when membrane polarisation is lost and so cell lysis occurs (Jolliffe *et al.*, 1981). Indeed, a range of antibacterial compounds have been seen to induce autolysis, either through direct interaction with the membrane, or through the inhibition of cell wall synthesis which leads to a cascade of events indirectly causing their misregulation through depolarisation (Kitano & Tomasz, 1979; Lacriola *et al.*, 2013). Thus, the lysis induced by cell envelope interacting antimicrobials is a common feature resulting from their perturbance of energy and pH gradients across the cell, as this mis-regulates autolysins and results in their over-activity. Regulation of autolysins can also be mediated by the Gram-positive cell envelope component teichoic acids. In *B. subtilis* teichoic acids have also been found to regulate and directly interact with autolysins. The expression and localisation of LytF were found to be reduced in teichoic acid deficient mutants; whereas the opposite was true for LytE, in which deletion of teichoic acids caused increased LytE expression (Kiriyama *et al.*, 2014; Kasahara *et al.*, 2016; Guyet *et al.*, 2023). In *S.* aureus, both peptidoglycan synthesis and its degradation by the autolysin Atl have been shown to be regulated by teichoic acids (Schlag *et al.*, 2010; Atilano *et al.*, 2010). In *Streptococcus pyogenes*, teichoic acids sequester the major autolysin LytA, perturbation of teichoic acid synthesis results in the freeing of LytA which enables its cell wall degrading activity and results in lysis (Flores-Kim *et al.*,

2019). Altogether, autolysins are controlled through a range of regulatory processes, perturbation of any of which can result in misregulation of the cell wall-degrading enzymes and so deadly consequences for the cell.

1.1.3 Teichoic acids

A major component of the Gram-positive cell envelope is anionic teichoic acid polymers, accounting for up to 60% of the cell wall (Brown *et al.*, 2013). Teichoic acids are long polymers composed of repeating units of glycerol phosphate, their presence confers an anionic charge to the Gram-positive cell envelope (Neuhaus & Baddiley, 2003). There are two forms: lipoteichoic acid (LTA) and wall teichoic acid (WTA). LTA is attached to the cytoplasmic membrane via a glycolipid (GL) anchor whereas WTA is covalently linked to MurNAc residues in the peptidoglycan cell wall (Fig. 1.2). The teichoic acid-peptidoglycan matrix cell wall is responsible for a range of cellular functions, including cell elasticity and assisting in the trafficking of biological substances, as well as cell wall porosity and cation homeostasis (Fischer *et al.*, 1981; Wecke *et al.*, 1997).

LTAs are anchored to the membrane via GLs, these are synthesised by the addition of two glucose moieties to diacylgycerol (DAG) by the glycosyltransferase UgtP in the inner leaflet of the cytoplasmic membrane (Fig. 1.2) (Jorasch *et al.*, 1998). These diglucosyl DAG GLs are flipped from the inner to the outer leaflet of the cytoplasmic membrane by an unknown mechanism. After which, the major LTA synthase, LtaS adds glycerol phosphate groups to the GL to form LTA, this function can also be carried out by YfnI (induced upon stress), YqgS (induced upon sporulation) and YvgJ (a primase – only adds the first glycerol phosphate to the GL) (Gründling & Schneewind, 2007b; Jervis *et al.*, 2007; Schirner & Errington, 2009; Wörmann *et al.*, 2011).

WTA synthesis also starts in the inner leaflet of the cytoplasmic membrane, with the addition of GlcNAc to UDP by TagO, onto this *N*-acetylmannosamine (ManNAc) is added by TagA (Fig. 1.2) (Soldo *et al.*, 2002; Ginsberg *et al.*, 2006). To UDP-GlcNAc-ManNAc the first glycerol phosphate is added by the primase TagB, after which TagF adds a polymer of ~40 glycerol phosphate units to extend the WTA (Schertzer & Brown, 2003; Bhavsar *et al.*, 2005; Schertzer *et al.*, 2005). The ABC transporter TagGH flips the WTA to the outer leaflet of the cytoplasmic membrane (Lazarevic & Karamata, 1995). The WTA is then covalently attached to *N*-acetylmuramic acid in the peptidoglycan cell wall, by the LCP (LytR-CpsA-Psr) family of enzymes (Sewell & Brown, 2014; Gale *et al.*, 2017). WTA is attached in patches to newly synthesised

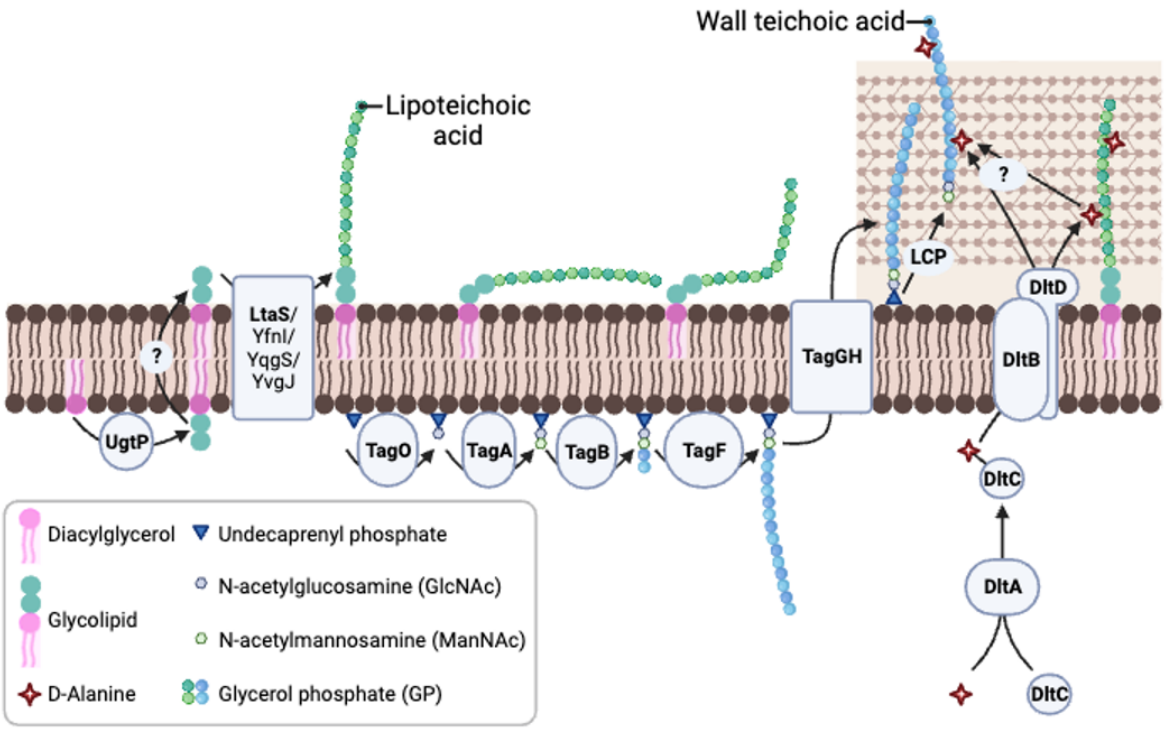

Figure 1.2. Teichoic acid synthesis in *B. subtilis*. Summary of the pathways in which lipoteichoic acid and wall teichoic are synthesised, and the mechanism by which they can both be modified with D-alanine residues. Detailed descriptions of these processes can be found in the written text.

peptidoglycan, the nascent peptidoglycan is then incorporated into the cell wall, dispersing the WTA across the peptidoglycan mesh (Koyano *et al.*, 2023).

Both WTA and LTA acid can be modified by the addition of D-alanine groups to their glycerol phosphate subunits. This process starts with the addition of D-alanine to the carrier protein DltC by DltA in the cytoplasm (Fig. 1.2) (Volkman *et al.*, 2001; Du *et al.*, 2008). It appears D-alanine is then transferred across the cytoplasmic membrane via DltB and added to LTA polymers by DltD; how D-alanylation of WTA occurs is unclear – the D-alanine is either transferred from LTA or directly from DltD (Debabov *et al.*, 2000; Pohl *et al.*, 2013; Reichmann *et al.*, 2013). In an LTA deficient mutant very little D-alanylation of WTA occurs, suggesting the dominant WTA D-alanylation process involves LTA (Haas *et al.*, 1984; Reichmann *et al.*, 2013). However, whether D-alanine is transferred from LTA directly or if other factors are involved remains unclear. D-alanylation of teichoic acids is impacted by growth conditions, with high pH, high temperature and high NaCl conditions reducing the amount of D-alanine on teichoic acids (Ellwood & Tempest, 1972; Novitsky *et al.*, 1974; Fischer *et al.*, 1981; Neuhaus & Baddiley, 2003). The arrangement of LTA within the cell envelope is unclear. A

consensus on whether LTA extends from the cytoplasmic membrane through the peptidoglycan cell wall, or if it lays flat on the cytoplasmic membrane beneath the cell wall has not been reached. The ability of DltBD to D-alanylate fully synthesised LTA polymers suggests a proximity of the length of LTA to the cytoplasmic membrane and as such a lying down arrangement (Kiriukhin & Neuhaus, 2001). Yet the transfer of D-alanine from LTA to WTA, implies proximity between LTA and WTA, and therefore favours the model of LTA extension into the cell wall (Haas *et al.*, 1984). Altogether, it may be that distribution of LTAs is flexible, with some proximal to the membrane and some extending into the cell wall. Additionally, it also remains unclear whether LTA, if extended through the cell wall, would be able to reach the cell surface, as LTA appears to be shorter than the span of the cell wall, meaning LTA may not be a surface exposed molecule (Labischinski *et al.*, 1991; Reichmann *et al.*, 2013).

In *B.* subtills, LTA is dispensable, as a quadruple mutant for the LTA synthases (LtaS, YfnI, YqgS, YvgJ) is viable and retains a normal morphology (Schirner & Errington, 2009). WTA is also dispensable, its removal is achieved through the deletion of TagO, however this results in a round cell shape, suggesting WTA is critical for the rod-shaped morphology of *B. subtilis* (D'Elia *et al.*, 2006a). Interestingly, WTA was previously thought to be essential as mutants for later genes in the WTA pathway were lethal, however this was found to be due to the accumulation of a toxic intermediate. Hence the first protein in the pathway (TagO) is deleted in the viable mutant, as this eliminates the accumulation of the toxic intermediate product (D'Elia *et al.*, 2006b). Despite being nonessential independently, deletion of both LTA and WTA in *B. subtilis* is lethal, showing some redundancies in their functions – however their individual deletions lead to strikingly different phenotypes, suggesting they also have distinct roles in cell physiology (Schirner & Errington, 2009). Deletion of UgtP, the glycosyltransferase that synthesises the LTA GL anchor, is thought to not abolish LTA synthesis, but LTAs in this mutant are thought to be anchored directly to DAG, without the diglucosyl group. However, this deletion results in slower growth, mild changes in cell morphology and increased susceptibility to cationic antimicrobials – suggesting cell envelope perturbations that are related to altered LTA content (Salzberg & Helmann, 2008). Similarly, deletion of D-alanine modifications, via a DltA deletion mutant, results in increased susceptibility to some cationic antimicrobials, as well as altered autolysin activity and increased susceptibility to cell wall targeting antibiotics (Wecke *et al.*, 1997). Altogether the impact of teichoic acid mutation has striking and wide-ranging

impacts on cell physiology, showing their multitude and variety of roles in maintaining and regulating *B. subtilis* envelope integrity.

In *S. aureus*, the synthesis of WTA yields a poly(ribotol phosphate) polymer, as opposed to the poly(glycerol phosphate) of *B. subtilis*. The synthesis of *S. aureus* WTA is a similar process to *B. subtilis*, with the TarOABFLGH proteins synthesising WTA. WTA of *S. aureus* is dispensable (D'Elia *et al.*, 2006b). The synthesis of LTA is also similar to *B. subtilis*, with the glycosyltransferase YpfP (UgtP homologue) synthesising the GL anchor (Kiriukhin *et al.*, 2001). The mechanism for the transfer of the GL anchor from the inner to the outer leaflet of the cytoplasmic membrane has been elucidated in *S. aureus*, in contrast to *B. subtilis*, with the lipid antiporter LtaA found to mediate this movement (Zhang *et al.*, 2020a). In *S. aureus* only one LTA synthase, LtaS, is encoded to extend the poly(glycerol phosphate) chain of LTA, and in contrast to *B. subtilis* LTA is essential (Gründling & Schneewind, 2007b; Percy & Gründling, 2014). Similar to *B. subtilis*, the teichoic acids of *S. aureus* have also been shown to influence autolysin activity (Fischer *et al.*, 1981).

1.1.4 The cytoplasmic membrane

The cytoplasmic membrane is composed of a bilayer of membrane phospholipids, with polar head groups facing outwards and hydrophobic fatty acids tails facing inwards towards each other. The bilayer is interspersed with integral and surface-attached membrane proteins (Fig. 1.1a). The cytoplasmic membrane is key to bacterial cell viability, as it forms the main diffusion barrier between the extra- and intracellular-space and is the site of essential cell processes, such as energy production, lipid biosynthesis, cell wall synthesis, protein secretion, transport and cell division (Silhavy *et al.*, 2010; Adams & Errington, 2009). The membrane must regulate intracellular concentrations of essential ions, metabolites and enzyme cofactors, and maintain a biologically active state for the integral, surface-attached and peripheral proteins to function appropriately. A key parameter of a cell is its membrane potential, the electrical gradient across the cytoplasmic membrane. The membrane potential regulates a wide range of essential processes, including membrane transport, cell division and pH homeostasis (Flagg & Wilson, 1977; Zilberstein *et al.*, 1980; Strahl & Hamoen, 2010). The membrane potential of *B. subtilis* is estimated to be ~-110 mV from exterior to interior (Hosoi *et al.*, 1980; Zaritsky *et al.*, 1981; te Winkel *et al.*, 2016). Membrane targeting antimicrobials can function by either directly or indirectly dissipating the membrane potential, causing cells to become depolarised. This enables

the use of membrane polarisation to be used as a proxy for the health of bacterial cells upon antimicrobial treatment (te Winkel *et al.*, 2016).

1.1.5 Phospholipid composition

Lipid head group types differ between bacterial species but those commonly found include the phospholipids phosphatidylglycerol (PG), phosphatidylethanolamine (PE) and cardiolipin (CL); with PE being the predominant species in Gram-negative membranes while PG and CL are most common in Gram-positive membranes (Epand & Epand, 2009; Sohlenkamp & Geiger, 2016). In *B.* subtilis, the dominant phospholipid is PG (37.5%), followed by PE (30.5%), lysyl-phosphatidylglycerol (7.8%; L-PG) and CL (4.5%), and GLs (16.9%) are also present, these proportions can vary with growth conditions (Matsuoka *et al.*, 2011). The head group composition of the cytoplasmic membrane has wide-ranging effects on cellular processes, especially the presence of the anionic phospholipids PG and CL; processes found to be linked to phospholipid composition include DNA replication, cell division, protein folding and protein transport (Sekimizu & Kornberg, 1988; de Vrije *et al.*, 1988; Castuma *et al.*, 1993; Ichihashi *et al.*, 2003; van Dalen & de Kruijff, 2004; Vitrac *et al.*, 2013).

Membrane lipids are synthesised from the common precursor phosphatidic acid (PA) in *B. subtilis* (Fig. 1.3) (Salzberg & Helmann, 2008). GLs are synthesised from the dephosphorylation of PA to DAG, to which UgtP then adds glucose moieties (Jorasch *et al.*, 1998). Whereas the phospholipid head groups of *B. subtilis* originate from PA converted to cytidine diphosphate-diacylglycerol (CDP-DAG). The only essential head group, PG, is synthesised by PgsA, via condensation of CDP-DAG with glycerol-3-phosphate, followed by removal of the phosphate (Nishibori *et al.*, 2005; Salzberg & Helmann, 2008). From PG, CL and L-PG can be synthesised (Fig. 1.3). CL is formed by the condensation of two PG molecules by the CL synthases ClsA, YwjE and YwiE (Kawai *et al.*, 2004). L-PG is formed by the MprF-mediated transfer of an L-lysine residue from lysyl-$tRNA^{lys}$ to PG (Staubitz & Peschel, 2002). From CDP-DAG, phosphatidylserine (PS) is also synthesised, via the addition of a serine residue by PssA (Patterson & Lennarz, 1971). From PS, PE can then be synthesised by the decarboxylation activity of Psd (Patterson & Lennarz, 1971; Matsumoto *et al.*, 1998). Via deletion of the enzymes responsible for their synthesis, mutants lacking GL, CL, L-PG, PE and PS & PE (as PE is synthesised from PS, deletion of PS also prevents PE synthesis) can be obtained and grow well in *B. subtilis* (Salzberg & Helmann, 2008;

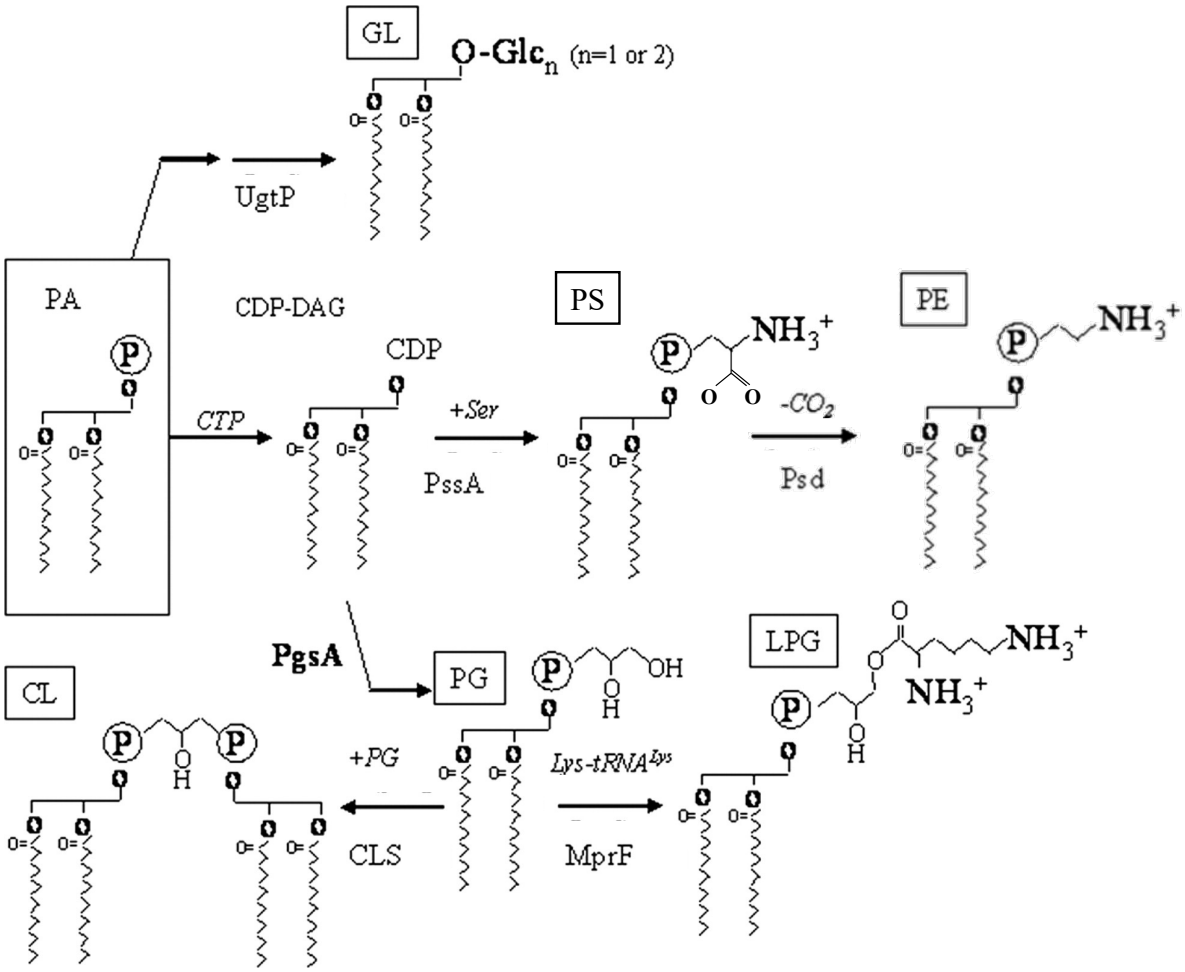

Figure 1.3. Synthesis of membrane lipids in *B. subtilis* from the common precursor phosphatidic acid. A detailed description of these processes can be found in the written text. GL = glycolipid; PA = phosphatidic acid; PS = phosphatidylserine; PE = phosphatidylethanolamine; CL = cardiolipin; PG = phosphatidylglycerol; LPG = lysyl-phosphatidylglycerol. Adapted from Salzberg & Helmann, 2008.

Humphrey *et al.*, 2023). Thus, there is a surprising level of malleability in *B. subtilis* lipid composition as only one head group species is essential to growth.

Head groups vary in their charge and size, in *B. subtilis* there are the anionic species PG, CL and PS, zwitterionic PE, neutral GLs and cationic L-PG (Salzberg & Helmann, 2008). Head groups also impact the overall shape of the phospholipid, the most notable of these being CL, due to its four fatty acid tails a cone shape occurs, giving the lipid preference for regions of membrane curvature (Fig. 1.4) (Renner & Weibel, 2011; Beltrán-Heredia *et al.*, 2019). Lipid head groups are attached to fatty acid chains of varying length that can also vary in their degree of saturation and branching, with each of these qualities affecting the shape of the overall phospholipid (Fig. 1.4).

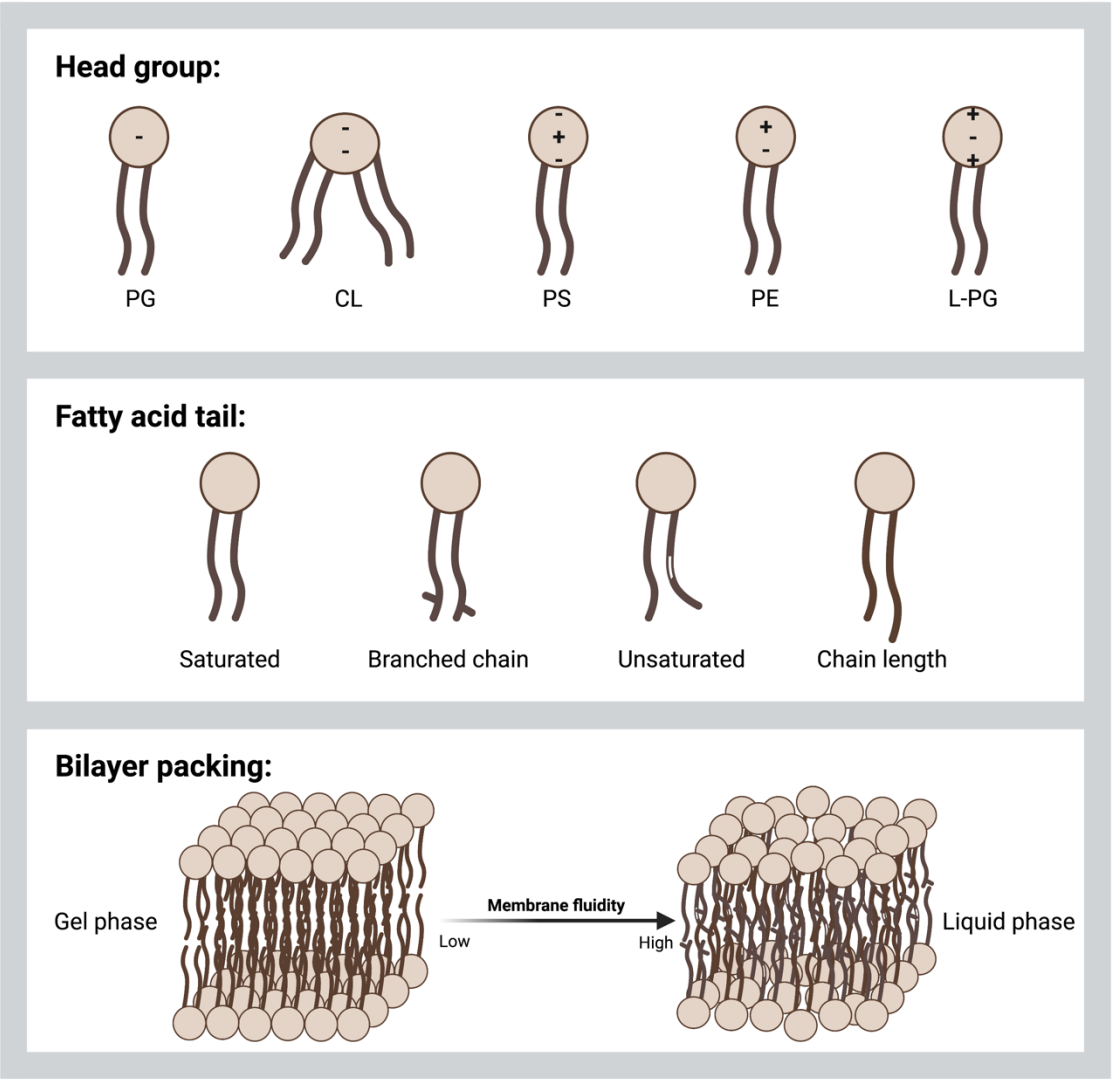

Figure 1.4. Lipid bilayer composition impacts the fluidity of a membrane. Membrane phospholipids can vary in their head group, fatty acid length and saturation/branching, with different head groups and fatty acid tails conferring different packing abilities. The packing of a lipid bilayer alters its fluidity, with densely packed, saturated, and long fatty acid chains giving a more viscous bilayer (gel phase), whereas loosely packed, unsaturated and short fatty acids give a more disordered and so more fluid bilayer (liquid phase).

The fatty acids of phospholipids are synthesised by the fatty acid synthesis (FAS) II pathway in bacteria, with the FAS I pathway being a mammalian process. In *B. subtilis* the pathway proceeds as follows (Fig. 1.5): firstly, the initiation complex AccABCD catalyses the conversion of acetyl-coenzyme A (CoA) to malonyl-CoA. FabD uses this to add a malonyl group to the acyl-carrier-protein (ACP) to form malonyl-ACP (White *et al.*, 2005). Malonyl-ACP is then condensed with acetyl-CoA to form the first intermediate of the elongation cycle by FabHA and FabHB. For the formation of branched chain fatty acids (BCFAs) FabHA and FabHB can use branched chain acyl-CoAs; in fact in *B. subtilis*, FabHA and FabHB preferentially utilise branched chain acyl-

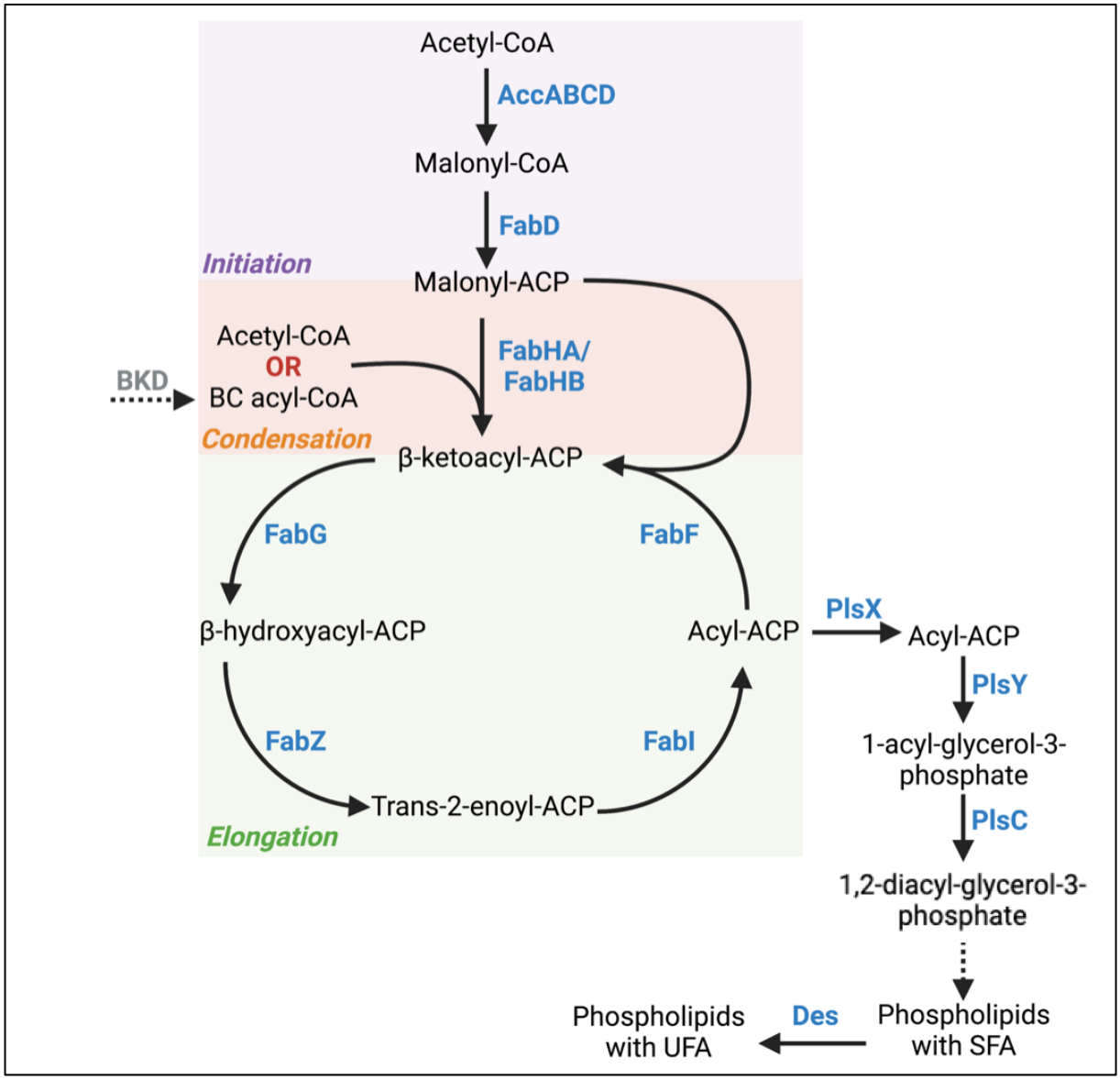

Figure 1.5. Fatty acid synthesis in *B. subtilis*. Simplified summary of the bacterial fatty acid synthesis (FAS II) pathway in which fatty acids are synthesised, involving initiation, condensation and elongation phases, and how this feeds into phospholipid synthesis – 1,2-diacyl-glycerol-3-phosphate is phosphatidic acid, the precursor used in phospholipid synthesis. The enzymes involved in catalysing each step are shown in blue text. Detailed descriptions of these processes can be found in the written text.

CoA as opposed to straight chain acetyl-CoA (Choi *et al.*, 2000). Branched chain acyl-CoAs arise from the metabolism of branched chain amino acids (valine, leucine and isoleucine) by the branched chain α-ketoacid dehydrogenase complex (BKD) (Willecke & Pardee, 1971). The FAS II pathway then enters the elongation phase, with the cyclical production of 3 intermediates by FabF, FabG, FabZ and FabI to produce acyl-ACP with a successively lengthened acyl chain through each cycle (White *et al.*, 2005; Diomande *et al.*, 2015). This acyl-ACP is either retained in the cycle and condensed

by FabF with malonyl-ACP to form the first intermediate again, or it is converted to acyl-phosphate by PlsX (Yoshimura *et al.*, 2007). The acyl group is then transferred to glycerol-3-phosphate by PlsY to form 1-acyl-glycerol-3-phosphate (Lu *et al.*, 2007). A second fatty acid chain is then added by PlsC, which uses acyl-ACP or acyl-CoA to form 1,2-diacyl-glycerol-3-phosphate, which is phosphatidic acid – the precursor for the synthesis of membrane lipids (Coleman, 1992). All *de novo* synthesis of fatty acids in *B. subtilis* produces saturated fatty acids (SFAs), however these can later be desaturated by the desaturase Des (Aguilar *et al.*, 1998). The Gram-negative model organism *Escherichia coli* also encodes the FAS II system but cannot utilise branched chain acyl-CoAs; alternatively, *E. coli* produces FabAB which alter FAS II elongation intermediates for the *de novo* synthesis of unsaturated fatty acids (UFAs) (White *et al.*, 2005).

The viscosity of the lipid bilayer, also known as membrane fluidity, is a key property in controlling membrane permeability and adaptation the extracellular environment. Membrane fluidity is a measure of the rotational and lateral diffusion of the membrane lipids and other membrane embedded species, such as proteins. It is determined by the packing of lipids within the membrane, which is affected mostly by lipid fatty acid tails, but also to a smaller degree by the size and charge of lipid head groups (Fig. 1.4) (Russell, 1984). Membrane fatty acids can vary in their length and saturation: longer, saturated chains give rise to lower fluidity in the membrane as the lipids are more densely packed together and so form more hydrogen bonds (Fig. 1.4). Thus, membrane fluidity can be maintained and adapted through altering the ratio of fluidity-promoting UFAs/ BCFAs and fluidity-reducing SFAs present in the lipid bilayer (Ernst *et al.*, 2016). In Gram-negative bacteria, membrane fluidity is predominately adapted through altering the ratio of UFA:SFA, whereas Gram-positive bacteria more commonly alter the fatty acid length or BCFA content, in addition to altering UFA:SFA (Yoon *et al.*, 2015). Fatty acid chain length increases bilayer stability, and so reduces fluidity, as the chain is able undergo increased interaction with other fatty acids chains (Rilfors *et al.*, 1984). Chain length is commonly between 14 and 24 carbons, and this remains fixed once the fatty acid has been synthesised, hence altering saturation is the more common strategy in altering membrane fluidity post synthesis (Mykytczuk *et al.*, 2007).

Lipid bilayers can transition between three distinct bilayer forming lipid phases: gel phase, liquid ordered phase and liquid disordered phase (Jouhet, 2013). The gel (solid)

phase consists of densely packed lipids with SFA chains, this compact composition results in very little lateral or rotational diffusion and so decreased membrane protein activity (Fig. 1.4) (Elson *et al.*, 2010). The liquid ordered phase is also characterised by well-packed SFA chains, however fast lateral diffusion is able to occur (Hjort Ipsen *et al.*, 1987). This liquid ordered phase is dependent on additional molecules that promote this formation, such as cholesterol and hopanoids, which do not exist in the bacterial species studied in this thesis (Mouritsen & Zuckermann, 2004; Sáenz *et al.*, 2015). The liquid disordered phase contains lipids that are loosely packed and likely to be shorter and/or unsaturated, enabling high diffusion rates – this phase is the regular state of biological membranes (Fig. 1.4) (Schmid, 2017). The organisation of bacterial membranes was thought to be a homogeneous distribution of phospholipids, interspersed with peripheral, integral and transmembrane proteins, as described in the classical fluid-mosaic model (Singer & Nicolson, 1972). However, it has now been shown that different lipids phases can co-exist, with liquid ordered and liquid disordered phases within the same bilayer, resulting in membrane domains with distinct composition and characteristics (Baumgart *et al.*, 2007; Heberle & Feigenson, 2011).

1.1.6 Homeoviscous adaptation

All poikilothermic organisms, including bacteria, adapt their membrane fluidity in response to a range of environmental changes, including temperature, pH, osmotic pressure and antimicrobial substances (Yoon *et al.*, 2015). The cytoplasmic membrane of bacterial cells compensates for environmental changes through homeoviscous adaptation, in which the membrane composition is altered in a manner that strives to maintain constant membrane fluidity. In doing so, homeoviscous adaptation also prevents extracellular changes from causing the membrane to transition away from its biologically active liquid state to a gel state, in which it is less: permeable, flexible, and protective (Sperotto *et al.*, 1989). This was first observed in the Gram-negative bacteria *E. coli*, which was found to synthesize and incorporate an increased proportion of UFA chains into its membrane lipids when growth temperature was decreased (Marr & Ingraham, 1962). *E. coli* synthesizes UFAs through the activity of three Fab enzymes, the most important being FabA – a protein that introduces a double bond into an intermediate in the fatty acid synthesis pathway (Mansilla *et al.*, 2004). Membrane fluidity is regulated through the temperature-dependent activity of the Fab proteins,

with low temperatures increasing their activity, causing more UFAs to be synthesised, enabling homeoviscous adaption to maintain the bilayer liquid phase.

In the Gram-positive bacterium *B. subtilis* normal synthesis of fatty acids and phospholipids is controlled by the FapR regulatory system (Schujman *et al.*, 2003). Additionally, *B. subtilis* encodes a rapid adaptation mechanism in response to changes in membrane fluidity, via the membrane-bound phospholipid desaturate Des (Aguilar *et al.*, 1998). Des introduces double bonds into the pre-existing fatty acid chains of membrane lipids, thereby increasing the fluidity of the lipid bilayer. Transcription of *des* is activated by an increase in the lipid order of the bilayer, caused by a decrease in temperature or limited synthesis of BCFAs and is switched off again once optimal fluidity has been restored (Mansilla & de Mendoza, 2005). This sensing of increased order is achieved by the transmembrane protein DesK, which upon increased membrane thickness phosphorylates the response regulator DesR, which induces the transcription of *des* (Cybulski *et al.*, 2010, 2015; Inda *et al.*, 2016). In addition to this rapid-response mechanism, *B. subtilis* also undertakes *de novo* synthesis of BCFA synthesis through the branched chain α-ketoacid dehydrogenase (BKD) complex (Willecke & Pardee, 1971). The BCFAs synthesised can be *iso*- or *anteiso*-BCFAs, which is another mechanism through which *B. subtilis* can alter its membrane fluidity, as *anteiso*-BCFAs are more fluidity promoting than *iso*-BCFAs due to their methyl branch being further from the end of the fatty acid (Zhang & Rock, 2008). The majority of *B. subtilis* fatty acids are BCFAs, as BCFAs account for over 90% of membrane fatty acids – ~40% iso-BCFAs and ~50% *anteiso*-BCFAs (Beranová *et al.*, 2008; Gohrbandt *et al.*, 2022). Thus, *B. subtilis* has multiple levels of homeoviscous control, through the rapid response activity of Des, the long-term homeostasis mediated through synthesis of *iso*- or *anteiso*-BCFAs, and also through the length of fatty acids incorporated into its membrane phospholipids.

Investigation into the consequences of insufficient homeoviscous adaptation had been hampered by the difficulty of modifying lipid composition, and so membrane fluidity, *in vivo*. Whilst previous work has associated sufficient membrane fluidity with promoting membrane protein folding, catalytic activity and diffusion, and excessive fluidity with increased protein permeability *in vitro*, comprehensive *in vivo* studies are required to improve our understanding (Andersen & Koeppe, 2007; Lee, 2004; Valentine, 2007). Recently, approaches to generate *B. subtilis* and *E. coli* with tuneable fatty acid composition and so membrane fluidity were described by Gohrbandt *et al*. (2022). In

both species an essential protein(s) in their UFA synthesis pathway was targeted, FabA in *E. coli* and the BKD complex and Des in *B. subtilis*, the strains were grown under specific conditions to control the composition of the membrane. Through this method, it was found that too low membrane fluidity in both *E. coli* and *B. subtilis* resulted in growth arrest and lipid phase separation between liquid-disordered and gel phase membrane, which in turn induced the segregation of normally disperse membrane proteins. A key finding of this research also negated the homeoviscous adaptation model, as bacterial cells were found not to maintain constant membrane fluidity, instead over-correction of fluidity to different growth temperatures was observed (Gohrbandt *et al.*, 2022). This work not only enables validation of *in vitro* work that came before it, but also lays the groundwork for investigation of the role of membrane composition and fluidity in these bacteria and other species.

1.2 Cell envelope-targeting antimicrobials

The bacterial envelope is an attractive target for antibiotics for multiple reasons: i) it is essential to cell viability, and as such any damage sustained to the cell envelope is likely to be bactericidal; ii) the bacterial cell envelope is composed and arranged differently from mammalian membranes, enabling selectivity and reduced off-target damage to host cells; iii) the cell envelope is difficult to mutate without disrupting cell function and viability, reducing the likelihood of resistance developing; iv) the cell envelope is directly accessible for extracellular compounds (Hamoen & Wenzel, 2017). A range of different cell envelope-targeting antimicrobials exist, with a variety of targets and activity specific to either Gram-positive, Gram-negative or both classes of bacteria (Fig. 1.6). The structural differences between Gram-negative and Gram-positive bacteria afford Gram-negative bacteria better protection from cell envelope-targeting antimicrobials, due to the protective presence of the outer membrane, making Gram-negative more resistant to antimicrobials in general (Breijyeh *et al.*, 2020).

1.2.1 Cell wall-targeting antibiotics

Peptidoglycan is unique to bacteria, making it an excellent antimicrobial target, there are multiple classes of cell wall-targeting antibiotics:

β-Lactam antibiotics have been used for over 80 years, initially against Gram-positive cocci, and then extended to Gram-negative and aerobic bacteria through the invention of broad-spectrum β-Lactams (Bush, 2016). The antibacterial activity of β-Lactams is mediated through their interaction with PBPs, essential enzymes in the last steps of

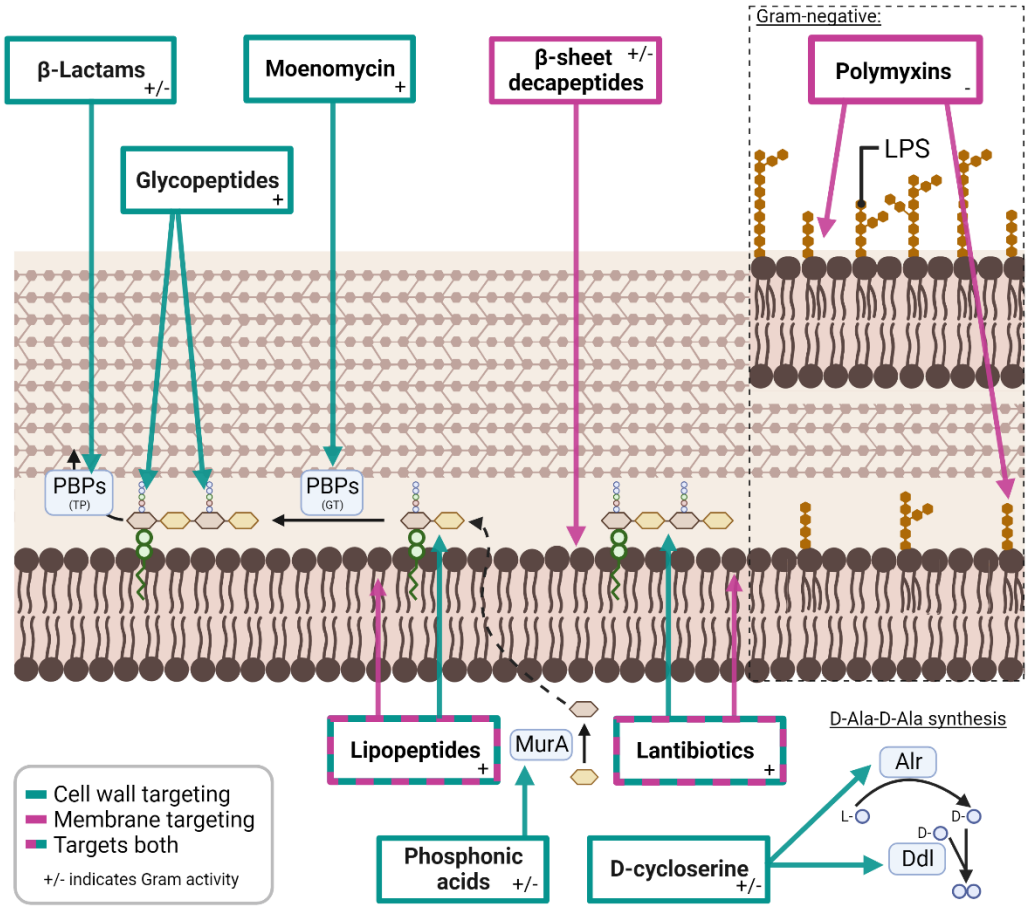

Figure 1.6. Summary of the targets of the main classes of cell envelope-targeting antimicrobials. Both Gram-negative and Gram-positive bacteria can be targeted by β-lactams, β-sheet decapeptides, phosphonic acids and D-cycloserine. Glycopeptides, moenomycin, lipopeptides and lantibiotics can only target Gram-positive bacteria as the outer membrane of Gram-negatives acts as a barrier to their entry to the cell. Polymyxins are specific to Gram-negative bacteria as they target lipopolysaccharide (LPS) which is only present in the outer membrane. These antibiotics have the following targets: β-lactams – penicillin binding proteins (PBPs); glycopeptides – D-alanine-D-alanine residues on cell wall precursors; moenomycin – glycosyltransferase PBPs; β-sheet decapeptides – cell membrane; polymyxins – LPS; lipopeptides – cell wall precursors and cell membrane; lantibiotics – cell membrane and cell wall precursors; phosphonic acids – MurA, the enzyme that catalyses the first committed step in peptidoglycan synthesis; D-cycloserine – the D-alanine-D-alanine synthesis enzymes alanine racemase (Alr) and D-alanine-D-alanine ligase (Ddl).

cell wall biosynthesis. PBPs have transpeptidase and transglycosylase/carboxypeptidase activity, catalysing the essential cross-linking of glycan strands to make the mesh-like structure of peptidoglycan (Goffin & Ghuysen, 1998, 2002). β-Lactams bind the transpeptidase catalytic cleft of PBPs and become covalently attached to the active site serine residue, acylating the PBP, thus reducing the rate of peptidoglycan cross-linking in the cell and eventually leading to lysis of the

cell (Macheboeuf *et al.*, 2006). The effectiveness of β-Lactams is limited by the multiple resistance mechanisms evolved by bacteria to evade their activity, these include inactivating β-Lactams through the production of β-Lactamases, modifying the target site of the PBPs and using efflux pumps to remove β-Lactams from within the cell envelope (Bush, 2016).

Moenomycin is the only known antibiotic to target the glycosyltransferase activity of PBPs (Goldman & Gange, 2000). It mimics the nascent peptidoglycan chain that glycosyltransferases extend, enabling it to inhibit glycosyltransferases and thus prevent cell wall synthesis (Yuan *et al.*, 2008). Resistance to moenomycin has been observed through mutation of the glycosyltransferase domains of PBPs, this mutation causes the synthesis of shorter peptidoglycan which causes major cell division defects – evidencing a link between cell wall structure and cell division (Rebets *et al.*, 2014).

Glycopeptides also inhibit cell wall synthesis, they do so by forming a complex with the D-Ala-D-Ala residues found on the cell wall precursor lipid II and at the C-terminus of nascent peptidoglycan peptide chains, thereby preventing the formation of mature peptidoglycan through PBP activity (Arthur & Courvalin, 1993). The first glycopeptide introduced was Vancomycin. It was assumed there would be limited resistance ability against glycopeptides due to the conserved nature of their target, however resistance mechanisms have been observed in which the terminal D-Alanine is replaced by D-lactate or D-serine (Arthur & Courvalin, 1993).

There are two classes of antibiotics that target the cytoplasmic stage of cell wall synthesis, firstly phosphonic acids, like Fosfomycin. Fosfomycin inhibits the cell wall enzyme MurA, which catalyses the first committed step of peptidoglycan synthesis through its enolpyruvate transferase activity (Kahan *et al.*, 1974). Resistance to phosphonic acids can be acquired through a multitude of strategies: mutation of *murA* to a protein with reduced affinity for the antibiotics, increased production of MurA so that higher concentrations of antibiotic are required to be inhibitory, and increased efflux pump activity (Nair & van der Donk, 2011).

D-cycloserine also targets cytoplasmic cell wall synthesis, via its inhibition of D-Ala-D-Ala ligase and alanine racemase preventing the formation of D-Ala-D-Ala. D-cycloserine is a cyclic analogue of D-alanine, this causes it to irreversibly block alanine racemase activity and also exhibit reversible binding as a phosphorylated form to the two active sites of D-Ala-D-Ala ligase (Neuhaus & Lynch, 1964; Lambert & Neuhaus,

1972; Batson *et al.*, 2017). Due to it having two targets, resistance to D-cycloserine is rare, however natural resistance in some *Mycobacterium* species has been observed through high expression of D-Ala-D-Ala ligase and alanine racemase, or through mutation of *cycA*, the gene that encodes the D-cycloserine transporter (Cáceres *et al.*, 1997; Chen *et al.*, 2012)

1.2.2 Membrane-targeting antibiotics

Many membrane-targeting antibiotics disrupt the function of the membrane diffusion barrier, resulting in depolarisation and even leakage of cell contents, mostly achieved through altering membrane properties, but also through forming ion channels or pores. Membrane-targeting antibiotics function by altering the properties of the membrane, such as by affecting the curvature, clustering and packing of the membrane and its constituent phospholipids. Bacterial envelopes have anionic phospholipids on the cell surface, exposing a negative charge to the extracellular environment, whereas eukaryotic membranes sequester anionic lipids within the inner leaflet of their membrane, this enables specific targeting of bacterial cells via the use of cationic antimicrobials (Epand *et al.*, 2016).

The lipopeptide daptomycin is rapidly bactericidal against Gram-positive cocci and has long been shown to inhibit cell wall synthesis in addition to causing membrane depolarisation (Alborn *et al.*, 1991). The native daptomycin molecule is negatively charged, but its membrane-targeting activity is dependent upon the presence of calcium ions, which convey an overall cationic charge to the active antibiotic (Ho *et al.*, 2008). Its specific mechanism of action is hotly debated but it was shown to target fluid lipid domains, impacting overall membrane fluidity, leading to membrane depolarisation and the detachment of the essential cell wall synthesis protein MurG and the phospholipid synthase PlsX (Müller *et al.*, 2016). Subsequently, daptomycin was found to form tripartite complexes with the membrane phospholipid PG and undecaprenyl coupled cell wall precursors, with this interaction providing an explanation for the previously observed detachment of essential cell wall synthesis proteins (Grein *et al.*, 2020). The authors suggested this work could explain the inhibition of cell wall synthesis, as essential proteins have been delocalised, and the previously observed depolarisation was suggested to be due to the hydrophobic mismatches between fluid and more ordered lipid domains. However, more recent work from the Strahl lab has shown that depolarisation by daptomycin does not require the presence of undecaprenyl coupled cell wall precursors, indicating that

depolarisation is a distinct mechanism of action of daptomycin (Buttress, 2022). Resistance to daptomycin is rare, but has been found to be associated with increased membrane fluidity, reduced membrane permeability, and increased net positive surface charge (Jones *et al.*, 2008; Bush, 2012). Further work has associated daptomycin resistance with redistribution of membrane phospholipids, moving CL-rich domains away from the cell septum and increasing the L-PG content of the outer leaflet of the cytoplasmic membrane (Mishra *et al.*, 2009; Tran *et al.*, 2013).

β-sheet decapeptides were amongst the first antibiotics to be used clinically, the most notable being tyrothricin and gramicidin, which are used for topical wound treatment. Tyrothricin and Gramicidin are both mixtures of polypeptide antibiotics, with some of their constituent antibiotics being cyclic β-sheet decapeptides. Tyrocidines and Gramicidin S both function through inserting into the membrane at the interface between phospholipid head groups and fatty acid chains (Prenner *et al.*, 1999; Loll *et al.*, 2014). Tyrocidines act by forming ion-conducting pores, inducing lipid phase separation and reducing membrane fluidity, causing membrane proteins to delocalise. Gramicidin S has 50% sequence identity to tyrocidines but has been found to cause mild lipid phase separation and delocalisation of only peripheral membrane proteins (Wenzel *et al.*, 2018). However, Gramicidin A, B & C, despite having a linear instead of cyclic structure, have similar activity to tyrocidines, as these forms of Gramicidin also form ion-conducting channels to disrupt ion-gradients (Kessler *et al.*, 2004).

Lantibiotics are peptides that contain intramolecular ring structures, they have activity against cell membrane components and are especially active against Gram-positive bacteria (McAuliffe *et al.*, 2001). The most well characterised lantibiotic is nisin, which has a dual mechanism of action. Nisin induces membrane pore formation and interacts with lipid II to induce inhibition of cell wall biosynthesis, this activity has also been shown to dysregulate autolysins, leading to autolysis (Bierbaum & Sahl, 1985; Breukink *et al.*, 1999; Hasper *et al.*, 2006; Reiners *et al.*, 2020). Resistance to nisin can be achieved through modifying the cell envelope with cationic charges, such as L-PG, as this repels the positively charged nisin (Peschel *et al.*, 2001).

The unique presence of LPS in the outer membrane enables the specific targeting of Gram-negative bacteria. Polymyxins, such as colistin, are cationic peptide antibiotics that bind to lipid A, the anchor for LPS, they are rapidly bactericidal but the specific mechanism by which they permeabilise cells has only recently been elucidated (Biswas *et al.*, 2012). Whilst already known to interact with LPS in the outer membrane,

colistin was also found to interact with newly synthesised LPS within the cytoplasmic membrane (LPS awaiting transport to the outer membrane), and it was this interaction and disruption of the cytoplasmic membrane that led to cell permeabilisation and death (Sabnis *et al.*, 2021). Resistance to polymyxins can be mediated through the modification of lipid A with positively charged moieties, such as aminoarabinose and phosphoethanolamine so as to reduce its affinity for the cationic polymyxins (Poirel *et al.*, 2017).

1.2.3 Antimicrobial peptides

Antimicrobial peptides (AMPs) are a component of innate immunity throughout the animal and plant kingdoms, with not only antibacterial activity but also antiviral, antifungal, anticancer and immunomodulatory activity. The shared structure of AMPs is an amphipathic design, in which hydrophobic and cationic residues are organised into discrete sectors. This structure enables disruptive interaction with the bacterial cell envelope, due to the presence of anionic phospholipids, LPS in Gram-negative bacteria and teichoic acids in Gram-positive bacteria (Zasloff, 2002). AMPs will interact with and disrupt the cytoplasmic membrane of both Gram-positive and Gram-negative bacteria, in addition to perturbing the outer membrane of Gram-negative species (Jenssen *et al.*, 2006). Whilst AMPs share a general amphipathic structure, there is much variation in their specific mode of actions and, as of 2015, there were over 2000 natural AMPs identified, this has been further contributed to with the development of synthetic AMPs (Wang, 2015).

There are three basic mechanistic models proposed for the inner membrane insertion of AMPs, these are the carpet, toroidal pore and barrel-stave models (Fig. 1.7) (Jenssen *et al.*, 2006). The carpet model suggests the amphipathic nature of the AMP causes it to self-associate with the surface of the membrane and, once a threshold concentration of the AMP is reached, it inserts between the phospholipids causing the membrane to break into pieces causing cell lysis (Oren & Shai, 1998). The toroidal pore model proposes the peptide coats the membrane, with membrane disruption that results in transient peptide channels that are stabilised by the hydrophilic regions of the peptide interacting with the lipid head groups, as such the membrane surface bends to form a pore lined by membrane head groups in addition to the peptide (Ludtke *et al.*, 1996). In contrast, the barrel-stave model describes direct insertion of the peptide between phospholipids to form a barrel-like peptide pore, with the exterior of the ring being the hydrophobic regions of the peptide interacting with the fatty acid chains of

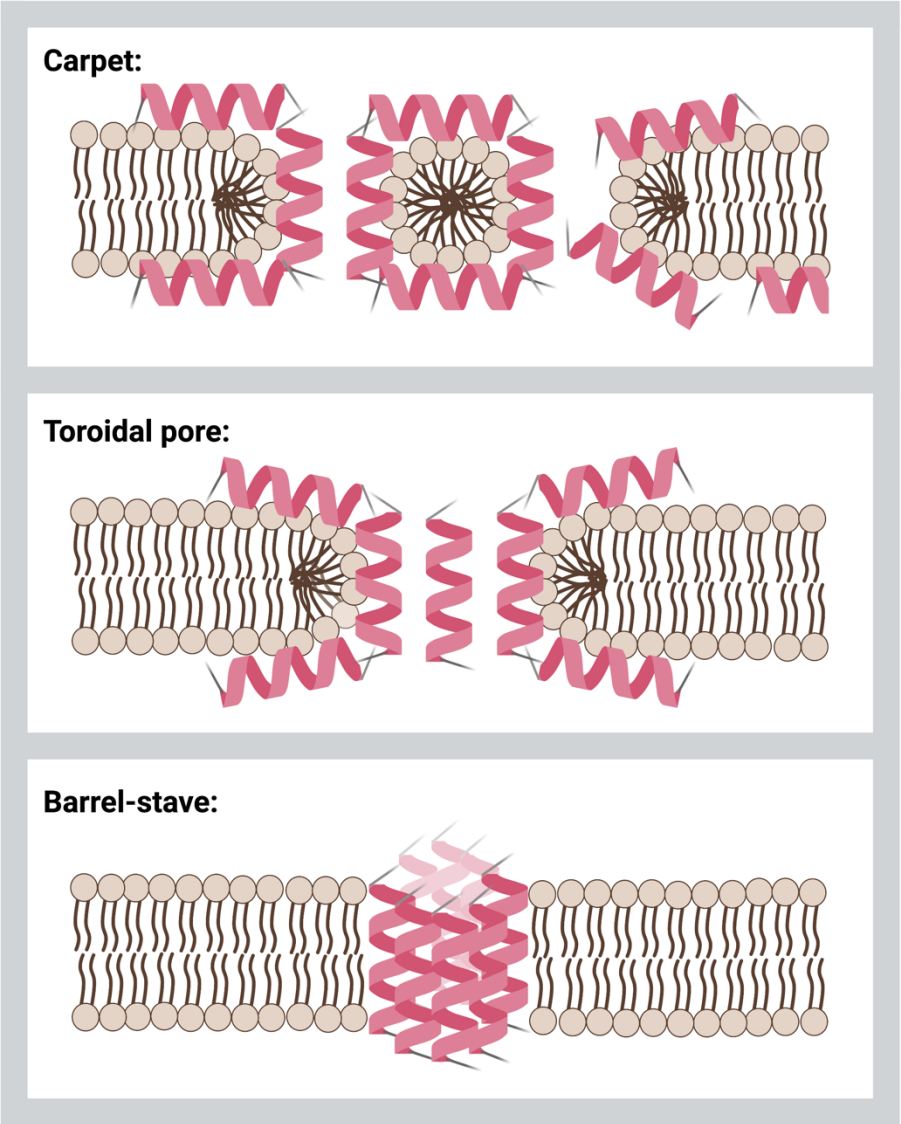

Figure 1.7. There are three proposed models for the activity of antimicrobial peptides. Following folding of the peptide into its amphipathic structure, the antimicrobial peptide (AMP) interacts with the bacterial membrane. The carpet model proposes the AMP coats the membrane to such an extent that parts of the membrane break away, causing permeabilisation of the cell. The toroidal pore model involves the AMP interacting with phospholipid head groups, this coating distorts the membrane, causing it to bend in on itself, resulting in transient pores lined by both AMP and head groups. The barrel-stave model involves the AMP inserting itself between membrane phospholipids to form a pore composed of oligomerised peptide.

the membrane phospholipids (He *et al.*, 1996). A significant point of contention arises from the pore-forming activity of AMPs, as it remains hotly debated whether pore formation is solely sufficient to cause bacteriolysis, or if instead pore formation triggers autolysis. In this thesis lysis is used to describe cells that have their membrane disrupted to such an extent that intracellular contents are released from the cell – this is measured through a decrease in optical density or the visibility of phase light cells.

There are two major classes of human AMPs, defensins and cathelicidins, with multiple defensins but only one cathelicidin encoded. Both classes are produced as propeptides, which are cleaved to release active peptides. Defensins are a class of AMP encoded in a wide range of plant and animal species, they are small cationic peptides with a 6-cysteine signature (Ganz, 2004). The structure of defensins is an α-helix linked to a two-stranded β-sheet domain, with defensin types having either a linear structure (α- and β-defensins) or a cyclic structure (θ-defensins). The human defensins human neutrophil peptide 1 (hNP-1), human β-defensin-1 (hBD-1) and human β-defensin-3 (hBD-3) have been seen to be active against a range of Gram-positive and Gram-negative bacteria (Pachón-Ibáñez *et al.*, 2017). These AMPs have been characterised to have a range of antibacterial activity, with destabilisation of the bacterial membrane through the mechanistic models described above, and via interacting with other envelope constituents such as the peptidoglycan precursor lipid II (Leeuw *et al.*, 2010).

Cathelicidins are primarily cationic α-helical amphipathic peptides, this structure enables their interaction with bacterial membranes. Cathelicidins are produced as prepropeptides, with a structure composed of N-signal peptide – cathelin-like domain – mature peptide-C; following secretion, the cathelin-like domain is cleaved by serine proteases to release to the mature peptide (Gudmundsson *et al.*, 1996; van Dijk *et al.*, 2009). The only cathelicidin produced by humans is LL-37, it has antimicrobial activity against both Gram-positive and Gram-negative bacteria (Sochacki *et al.*, 2011; Barns & Weisshaar, 2013). Cathelicidins interact with and perturb bacterial membranes, whilst also having immunomodulatory roles within the human body (van Harten *et al.*, 2018; Mookherjee *et al.*, 2020).

Synthetic AMPs have added a new dimension to AMPs, potentially broadening the definition from natural immunity peptides to include similar molecules synthesised in the laboratory. The synthetic AMP MP196 was developed through characterisation of the minimum antibacterial motif of AMPs, giving the minimal pharmacophore structure of RWRWRW-NH_2 (Strøm *et al.*, 2003). MP196 is active against Gram-positive, and to a lesser extent Gram-negative, bacteria and has been seen to mediate its antibacterial activity through integrating into the cytoplasmic membrane, inducing the delocalisation of essential peripheral proteins (Albada *et al.*, 2012; Wenzel *et al.*, 2014). A synthetic antimicrobial peptide was recently developed, in the form of a small cyclic hexapeptide called cWFW (cyclo(RRRWFW)), that was found to be potent against both Gram-

positive and Gram-negative bacteria (Scheinpflug *et al.*, 2015). cWFW was first described as having an affinity for CL-rich PE matrices, and thus inducing partitioning of the membrane into lipid domains. However, subsequent work showed that domains induced by cWFW were instead driven by lipid phase separation as opposed to clusters of specific lipid species, with these differing fluidity domains impacting on the organisation of membrane proteins, halting cell wall synthesis, and eventually triggering autolysis (Scheinpflug *et al.*, 2017). The advent of synthetic AMPs provides therapeutic and scientific benefits: they can be developed to avoid off-target effects, and their simplified structures can enable informed comparisons when investigating AMP mechanisms of action.

1.3 The antimicrobial peptide LL-37

One of the best studied AMPs is the cathelicidin LL-37, a 37-residue AMP that is active against both Gram-positive and Gram-negative bacteria. The structure of LL-37 is an α-helix with charged residues segregated to one side of the helix and hydrophobic residues opposite; this organisation confers the amphipathic nature of the AMP,

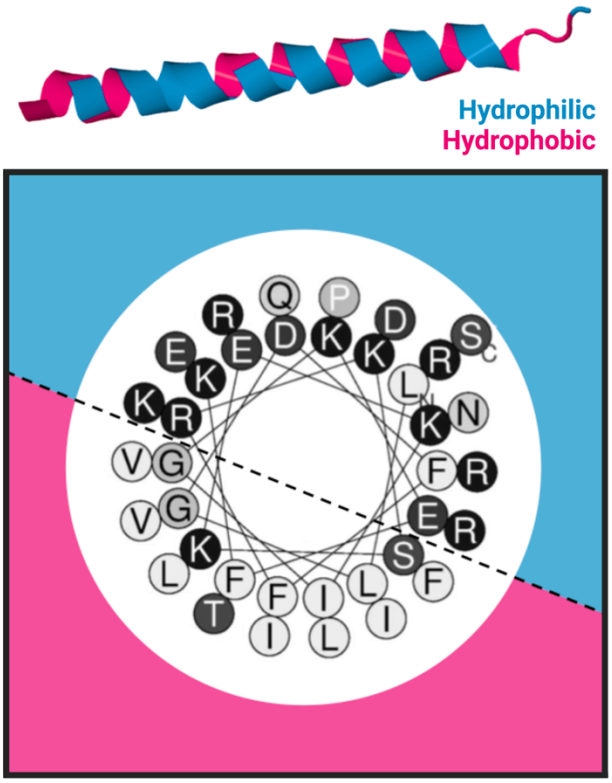

Figure 1.8. LL-37 has an amphipathic structure. The structure of LL-37 is a linear α-helix in which the majority of hydrophilic residues are on one face of the helix, with a majority of hydrophobic residues on the opposite face. Created using heliquest.ipmc.cnrs.fr and RCSB.org (Berman *et al.*, 2000; Gautier *et al.*, 2008).

enabling it to interact with negatively charged bacterial envelopes (Fig. 1.8) (Dürr *et al.*, 2006). LL-37 is derived from the prepropeptide hCAP18, *hCAP18* is composed of 4 exons, the first 3 encode the signal peptide and cathelin domain, with the 4th domain encoding the mature LL-37 peptide (Gudmundsson *et al.*, 1996; Murakami *et al.*, 2004).

LL-37 is active against both Gram-positive and Gram-negative bacterial species, in 2012 more than 40 bacterial species were known to be killed by LL-37 (Vandamme *et al.*, 2012). Notably it is active against the pathogenic genera *Pseudomonas, Escherichia, Staphylococcus, Acinetobacter* and *Enterococcus* (Neshani *et al.*, 2019). In addition to its direct antibacterial activity, LL-37 also has immunomodulatory activity that can further make the human body an inhospitable environment for bacterial infections.

1.3.1 The mechanism of action LL-37

LL-37 is thought to first interact with LPS or teichoic acids in Gram-negative and Gram-positive bacteria, respectively, and then interact with membrane phospholipids to disrupt the cell (Neville *et al.*, 2006). The specific mechanism of action of LL-37 has not yet been fully characterised, however work in *E. coli* and *B. subtilis* has described its effect on cells. Against *E. coli* LL-37 was found to inhibit cell growth once it had translocated across the outer membrane, permeabilisation of the cytoplasmic membrane occurred subsequent to growth arrest, suggesting LL-37 was somehow disrupting the cell wall and this was the cause of growth inhibition (Sochacki *et al.*, 2011). In *B. subtilis* lower concentrations of LL-37 caused the growth rate to decrease without inducing cell permeabilisation, whereas high concentrations caused abrupt cell shrinkage and permeabilisation from which the cells could not recover (Barns & Weisshaar, 2013).

There is much debate about the exact mechanism of action of LL-37. Some findings point towards the carpet model, with LL-37 being observed to interact with negatively charged membranes as monomeric units (Oren *et al.*, 1999; Porcelli *et al.*, 2008). Yet in other research, toroidal pore and barrel-stave models have been supported, by observations of pores formed by peptides lying parallel or perpendicular to the membrane plane, respectively (Henzler Wildman *et al.*, 2003; Lee *et al.*, 2011). Interestingly, when research on LL-37 is collated, its antibacterial activity does not strictly follow any of the three basic mechanistic models proposed for the activity of AMPs (Fig. 1.7). Firstly, the structure of LL-37 has been shown to depend on pH, ion

strength and peptide concentration, suggesting its mechanism of action will vary with these factors (Johansson *et al.*, 1998). Secondly, structural work has shown i) LL-37 doesn't insert into the membrane but remains parallel to the membrane; ii) LL-37 does not cause the membrane to break into small pieces but induces pore formation; iii) LL-37 forms supramolecular fibre-like structures (Henzler Wildman *et al.*, 2003; Barns & Weisshaar, 2013; Lee *et al.*, 2011; Zeth & Sancho-Vaello, 2017). In addition, it was recently shown *in vitro* that the mode of action of LL-37 is dependent upon fatty acid chain composition, with LL-37 changing between pore-forming activity against UFAs and lipid-clustering activity against SFAs (Shahmiri *et al.*, 2016). There is evidently much more to be characterised of the mechanism of action of LL-37 and the cellular factors that can affect it. There is also much to be seen in whether LL-37 functions through specific interactions with membrane moieties – whether specific phospholipid species or membrane domains are inherent to its activity, and as such whether membrane composition could affect bacterial susceptibility to LL-37.

In addition to its activity at the cell envelope, LL-37 may also have intracellular activity. LL-37 is cell-penetrating peptide that is capable of traversing both bacterial and eukaryotic cell membranes; the passage of LL-37 across membranes may even be promoted by its cationic charge and the membrane potential of the cell (Zhang *et al.*, 2010). Sub-inhibitory concentrations of LL-37 against *P. aeruginosa* and *E. coli* enabled LL-37, once in the cytoplasm, to bind DNA, with this binding inducing mutagenesis (Limoli *et al.*, 2014). LL-37 has also been observed to target the cytoplasmic protein AcpP (also known as AcpA in *B. subtilis*), with this interaction impacting the fatty acid synthesis of AcpP and so altering the fatty acid composition of the bacteria (Chung *et al.*, 2015). Additionally, active transport of LL-37 from the periplasm to the cytoplasm of *Haemophilus influenzae* by the Sap ABC transporter has also been reported (Shelton *et al.*, 2011). These observations suggest LL-37 may have multiple mechanisms to interfere with bacterial cells, with major disruptive activity at the cell envelope but also activity within the cytoplasm of cells, made possible by low concentrations of LL-37 that are not sufficient to cause the bactericidal membrane activity.

1.3.2 LL-37 in immunity

LL-37 is produced by a range of cell types, including neutrophils, macrophages, natural killer cells and mucous epithelial cells of the skin, airways, ocular surface and intestines (Larrick *et al.*, 1995; Kahlenberg & Kaplan, 2013). In epithelial cells, expression of LL-

37 is most commonly constitutive, as it forms part of the first line of defence against infection in sites that are directly in contact with the environment (Vandamme *et al.*, 2012). In neutrophils, natural killer cells and mast cells, LL-37 expression is also constitutive. However, the propeptide is stored in granules awaiting immune activation, which then causes the cells to degranulate and the propeptide to be released and cleaved (Sørensen *et al.*, 1997, 2001; Di Nardo *et al.*, 2003; Büchau *et al.*, 2009). LL-37 acts as a link between the innate and adaptative immune system, as it recruits immune cells to the site of infection and activates specific immune receptors for an adaptive response; the lytic activity of LL-37 causes the release of peptidoglycan, LTA and LPS which induce tumour necrosis factor alpha and interleukins 6 and 10 in T cells and monocytes (Wang *et al.*, 2000; Verjans *et al.*, 2016).

LL-37 also exhibits immunomodulatory activity, both activating and suppressing immune responses to bacterial infection. LL-37 functions as a chemoattractant for immune cells, it has been observed to attract neutrophils, T cells and eosinophils (Yang *et al.*, 2000; Tjabringa *et al.*, 2006; Hemshekhar *et al.*, 2018). As neutrophils both produce LL-37 and respond to its presence, this leads to very high concentrations of LL-37 at the site of infection, giving a potent immune response and higher likelihood of clearing the bacterial infection (Vandamme *et al.*, 2012). The presence of LL-37 enhances the antimicrobial activity of human neutrophils exposed to bacterial products; whilst the AMP also controls inflammatory mediators – its presence reduces the release of proinflammatory cytokines and induces the internalisation of chemokine receptors (Zhang *et al.*, 2009; Alalwani *et al.*, 2010). LL-37 also modulates the adaptive immune response, enhancing dendritic cell and B cell activation (Lande *et al.*, 2007; Kim *et al.*, 2017). The response of macrophages in response to bacterial products (such as LPS and LTA) is regulated by LL-37, this limits the damage that a strong immune response could cause, such as sepsis, whilst also recruiting immune cells to clear the infection (Scott *et al.*, 2002; Balhuizen *et al.*, 2022). The success of immunomodulatory activity by LL-37 is evidenced by its promotion of clearance of a *Pseudomonas aeruginosa* infection *in vivo,* without direct bactericidal activity – instead by modulating the inflammatory responses of host cells (Beaumont *et al.*, 2014). Altogether, this means when describing the mechanism of action of LL-37 against bacterial infections, its direct antibacterial activity should not be the sole focus, as the part that it plays in enhancing other immune system factors is also vital to its activity within the human body.

1.3.3 Factors that impact LL-37 activity in vivo

The natural context of LL-37 activity is within the human body, in which conditions vary strongly from those in laboratory experiments. The complex conditions within the body have been seen to inactivate LL-37, through LL-37 being bound by glycosaminoglycans, DNA and F-actin bundles, and proteolytically degraded by host immune cell factors (Bucki *et al.*, 2007; Bergsson *et al.*, 2009). Whilst other AMPs have been shown to be impaired under physiological salt concentrations, LL-37 has instead evolved to be resilient in this regard (Goldman *et al.*, 1997; Huang *et al.*, 2006; Kandasamy & Larson, 2006). Instead, LL-37 is sensitive to acidic conditions – increasingly acidic pH has been shown to increasingly impair LL-37-mediated killing of *S. aureus*, as well as impairing its ability to synergise with other antimicrobial factors (Abou Alaiwa *et al.*, 2014; Simonin *et al.*, 2019). This is likely linked to the effect of pH on the structure of LL-37, with acidic pH causing increased disorder and a decrease in the number of α-helical oligomers forming (Johansson *et al.*, 1998; Berkebile & McCray, 2014). Acidic conditions are especially common in the cystic fibrosis lung, this is a location in which LL-37 is found in very high concentrations, yet it fails to clear the chronic infections cystic fibrosis patients endure – likely due to the low pH interfering with its activity (Chen *et al.*, 2004; Pezzulo *et al.*, 2012; Elborn, 2016). Altogether, although LL-37 has been seen to be potent against a wide range of bacterial species, it must be considered that this activity may not be replicated in physiological conditions. This means that a holistic view of the activity of LL-37 should be taken, including not only its antimicrobial activity, but also the other immune functions described above. Due to the range of immunomodulatory roles that AMPs have outside of their antimicrobial activity, it has been suggested that a better name for this class would be cationic host defence peptides (CHDP). It is thought that the term CHDP better encompasses the variety of functions that AMPs, such as LL-37, can have and takes account of the possibility that host conditions may limit the antimicrobial functions of these peptides (Mookherjee *et al.*, 2020). Here in this thesis, I will be focussing on the direct antimicrobial properties of LL-37.

1.3.4 Bacterial resistance strategies against LL-37

As AMPs target the cell envelope, and have highly common and conserved targets, it was thought that resistance against them would be rare or even impossible. However, multiple studies have observed that passage of bacteria with LL-37 leads to the acquisition of resistance, and this can give cross-resistance to other AMPs and

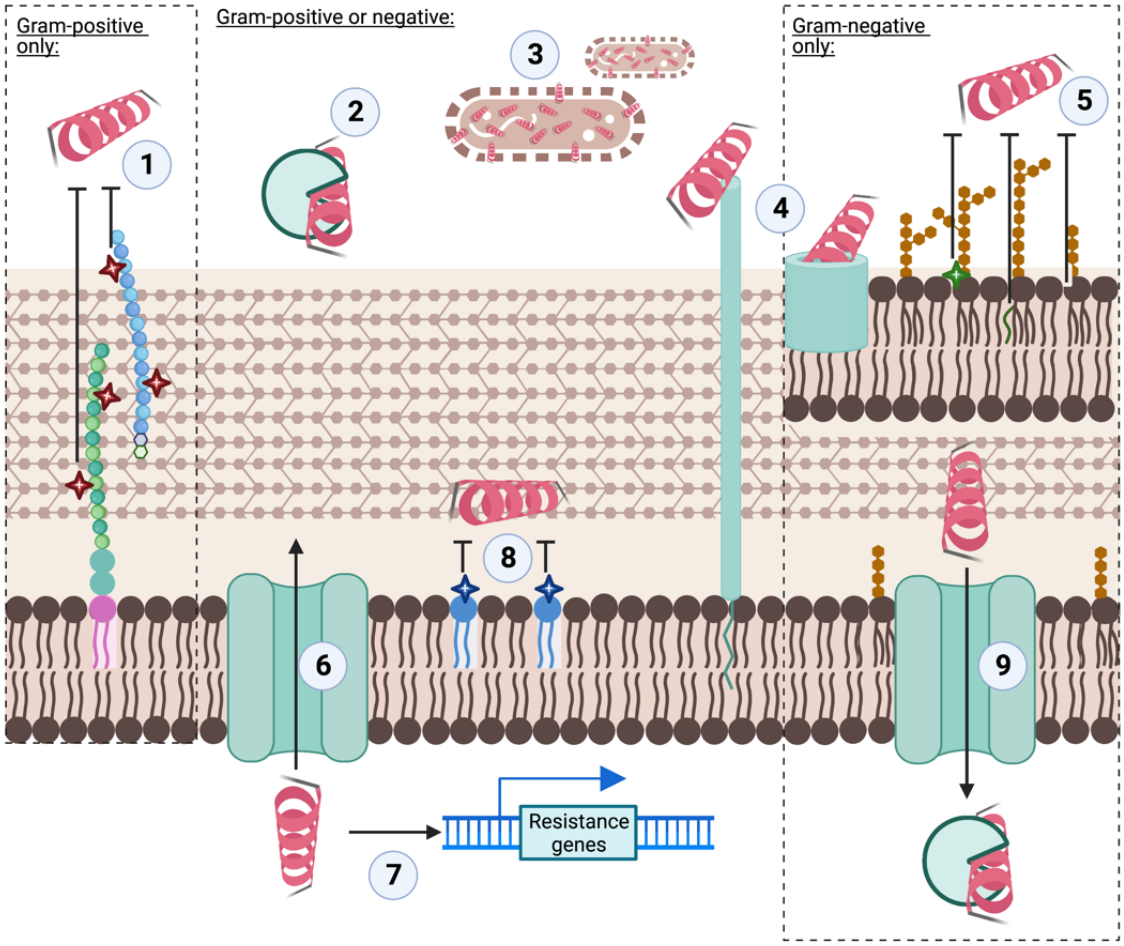

Figure 1.9. Resistance strategies against LL-37. **1**: Teichoic acids in the Gram-positive cell envelope can be modified with cationic D-alanine residues that repel cationic LL-37. **2**: Secreted proteases can degrade LL-37. **3**: Dead cells can bind and sequester LL-37, preventing it from binding surviving cells. **4**: Proteins in the cell envelope can sequester LL-37, preventing it from interacting with more vulnerable areas of the cell. **5**: The LPS of Gram-negative bacteria can be modified with aminoarabinose/acylation/dephosphorylation which repel or prevent interaction with LL-37. **6**: Efflux pumps can export LL-37 from the cell. **7**: LL-37 can trigger the expression of genes that contribute to resistance to LL-37. **8**: Positively charged phospholipids, generated by modification with L-lysine, can repel LL-37 from interacting with the cytoplasmic membrane. **9**: Some Gram-negative bacteria encode systems that uptake LL-37 into the cell so it can be degraded by intracellular proteases.

antibiotics (McQuade *et al.*, 2012; Lofton *et al.*, 2013; Kubicek-Sutherland *et al.*, 2017). Resistance to LL-37 can be mediated by a range of cellular strategies (Fig. 1.9) (Joo *et al.*, 2016; Mookherjee *et al.*, 2020):

The most evident resistance strategy against LL-37 is altering its target, bacteria achieve this by conferring a positive charge to their cell envelope and by doing so repel the cationic AMP. In Gram-positives, this is commonly achieved by the D-alanylation of teichoic acids, via the DltABCD proteins (Saar-Dover *et al.*, 2012). The membrane

itself can gain positive moieties via the activity of MprF adding L-lysine residues to PG phospholipids to form L-PG (Peschel *et al.*, 2001; Ernst *et al.*, 2009). Gram-negatives can reduce their susceptibility to LL-37 through LPS modifications (Ridyard & Overhage, 2021). The negative charge of LPS can be lessened by the removal of anionic charged phosphate groups from the LPS structure (Cullen *et al.*, 2011; Bociek *et al.*, 2015). The addition of a palmitoyl chain to LPS has been observed to protect against LL-37 exposure, likely due to the palmitoyl chain conferring enhanced rigidity to the outer membrane and so better exclusion of LL-37 occurs (Martynowycz *et al.*, 2019). LPS can also be modified with positive charges, with the addition of an aminoarabinose residue – the same strategy employed against the polymyxin antibiotic colistin (Gooderham *et al.*, 2009; Poirel *et al.*, 2017).

Efflux pumps contribute to resistance to a wide range of antibacterial compounds, including LL-37. The resistance-nodulation-cell division family of efflux pumps have been shown to interact with LL-37 and so likely contribute to its extrusion from bacterial cells (Lyu *et al.*, 2022). Detoxification modules, composed of a two-component system and an ABC transporter, contribute to LL-37 resistance in *B. subtilis* (YxdJK-LM) and *S. aureus* (GraRS-VraFG & BraRSAB) (Li *et al.*, 2007; Staroń *et al.*, 2011; Yang *et al.*, 2019). The GraRS two-component system was also recently shown to contribute to *S. aureus* tolerance to Daptomycin via LL-37-induced increased peptidoglycan synthesis, yielding a thicker and so more protective cell wall, as well as regulating the expression of the *dlt* operon and the *mprF* gene (Falord *et al.*, 2011; Ledger *et al.*, 2022). An additional transporter mechanism involves the Sap (sensitive to AMPs) uptake ABC transporter; in which LL-37 is actively taken into the cell to enable its degradation before it can interact with the cytoplasmic membrane (Mount *et al.*, 2010; Shelton *et al.*, 2011).

Bacteria can also protect themselves from peptide antibiotics via protease digestion, proteases cleave and degrade proteins and can be intracellular or secreted extracellularly (Culp & Wright, 2017). This mechanism has been observed against LL-37 by a range of protease classes and in a range of genera, including *Pseudomonas*, *Staphylococcus* and *Bacillus* (Thwaite *et al.*, 2006; Sonesson *et al.*, 2017; Claunch *et al.*, 2018; Kany *et al.*, 2018). However, studies on LL-37 have shown that the peptide is resilient against proteolytic degradation, due to its preference for oligomerisation when in solution, suggesting this resistance mechanism may not be wholly effective (Oren *et al.*, 1999).

Protection against LL-37 can occur via sequestration of the AMP. The proteins Opr1 (*P. aeruginosa*), M1 (*Streptococcus*), OmpA (*A. baumanii*) and OmpT (*E. coli*) confer protection against LL-37. LL-37 binding these proteins is thought to prevent it from binding more susceptible regions of the cell and the interaction can enable subsequent degradation of LL-37 (Lin *et al.*, 2010; LaRock *et al.*, 2015; Lin *et al.*, 2015; Urashima *et al.*, 2017). Interestingly, whilst the release of outer membrane vesicles confers protection against other host defence peptides, this does not appear to be an effective strategy against LL-37 (Balhuizen *et al.*, 2021). Instead, sequestration by dead cells has been seen to occur, with dead *E. coli* cells being observed to absorb LL-37, protecting surviving cells – this strategy confers tolerance, not resistance, to LL-37 (Wu & Tan, 2019). Indeed, *E. coli* cells have been seen to rapidly adsorb LL-37 upon growth inhibition, giving a population in which LL-37-bound cells sacrifice themselves to protect surviving cells (Snoussi *et al.*, 2018).

Exposure to LL-37 can also up-regulate the above-described protective systems in bacteria. In *P. aeruginosa*, LL-37 was seen to induce LPS modifications and efflux pump expression, as well as quorum sensing and virulence systems (Strempel *et al.*, 2013). A similar response was seen in *S. pyogenes*, with exposure to LL-37 inducing an invasive phenotype, and the production of vesicle-like structures on the cell surface that protected against LL-37 (Uhlmann *et al.*, 2016). These examples highlight that upon exposure to LL-37, bacterial cells will not only activate pathogenic systems to target the host, but also try to protect themselves, making bacterial susceptibility to LL-37 a dynamic situation.

1.4 Research aims and objectives

In this research project I used the Gram-positive model organism *B. subtilis* to study LL-37. I used *B. subtilis* as it is an extremely valuable research tool, due to its genetically tractability and its malleability in lipid composition, with strains already existing to directly manipulate this. My first objective was to investigate factors that could impact susceptibility to LL-37. I studied the role of the cell envelope, by altering phospholipid composition, teichoic acids and membrane fluidity. The second aim was to elucidate more in-depth knowledge of the mechanism of action of LL-37, looking into the precise process in which cell permeabilisation, depolarisation and lysis occur. My final objective was to uncover the mechanisms behind bacterial survival in the presence of LL-37. This includes the survival of individual cells upon initial exposure

to LL-37, and the subsequent survival of whole cultures upon secondary exposure to LL-37. The findings I have made in *B. subtilis* can then be studied with an informed approach in pathogenic species, such as *S. aureus.* This will provide interesting comparisons between a bacterial species that has evolved to exist in the presence of LL-37 and a non-pathogenic species, revealing the important differences between these bacteria. By enhancing our understanding of LL-37, we can develop informed strategies to better potentiate its activity *in vivo*.

Chapter 2 - Materials and Methods

2.1 Bacterial Strains

The strains used in this thesis are detailed in Table 2.1.

Table 2.1. Bacterial strains used in this study.

Strain	Label in this study	Genotype	Reference
B. subtilis			
168CA	Wild-type	*trpC2*	(Barbe *et al.*, 2009)
AG600	ΔLTA	*trpC2 yfnI::erm yqgS::spc ltaS::cat*	(Guyet *et al.*, 2023)
AK094B	ΔWTA	*trpC2 tagO::MLS*	A. Koh, unpublished
AK0117B	ΔGL	*trpC2 ugtP::MLS*	A. Koh, unpublished
AK0118B	ΔL-PG	*trpC2 mprF::kan*	A. Koh, unpublished
AK0119B	ΔPE ΔPS	*trpC2 pssA::spc*	A. Koh, unpublished
AK0197B	L-form	*trpC2 ispA(D92E)::spc uppS::kan pLOSS (Pspac-uppS) (MLS)*	A. Koh, unpublished
ARK3	ΔCL	*trpC2 clsA::tet ywjE::spc yWiE::kan*	(Pogmore *et al.*, 2018)
BRB08	BRB08	*trpC2* Δ*nprB* Δ*aprE* Δ*epr* Δ*bpr* Δ*nprE* Δ*mpr* Δ*vpr* Δ*wprA*	(Pohl *et al.*, 2013)
ELD19	Δ*divIVA*	*trpC2 divIVA::tet*	H. Strahl, unpublished
HS550	Δ*bkd* Δ*des*	*trpC2 bkd::ery des::kan*	(Gohrbandt *et al.*, 2022)
KS6	Δ*cwlO*	*trpC2 cwlO::spc*	(Seistrup, 2018)
KS7	Δ*lytF*	*trpC2 lytF::spc*	(Seistrup, 2018)
KS8	Δ*lytE*	*trpC2 lytE::tet*	(Seistrup, 2018)

KS9	Δ*lytD*	*trpC2 lytD::tet*	(Seistrup, 2018)
KS10	Δ*lytABC*	*trpC2 lytABC::kan*	(Seistrup, 2018)
KS15	Δ*lytABCEF*	*trpC2 lytABC::kan lytE::tet lytF::spc*	(Seistrup, 2018)
KS19	Δ*lytABCDEF*	*trpC2 lytABC::kan lytD::tet lytE::cat lytF::spc*	(Scheinpflug *et al.*, 2015)
KS50	Δ*des*	*trpC2 des::kan*	(Gohrbandt *et al.*, 2022)
KS66	Δ*lytABCF CwlO*	*trpC2 lytABC::kan lytF::spc cwlO::erm*	(Seistrup, 2018)
KS119	ΔPE	*trpC2 psd::MLS*	(Pogmore *et al.*, 2018)
MDS07	Δ*spoIIE*	*trpC2 spoIIE::ery*	M. Dakes-Stavrakakis, unpublished
MH057	Δ*lytG*	*trpC2 lytG::kan*	This work, *lytG::kan* transformed into 168CA from BKK31120 (Koo *et al.*, 2017)
MH073	Δ*bkd* Δ*des Pspac-des*	*trpC2 bkd::ery des::kan pLIMBU1 (Pspac-des) (cat)*	This work, HS550 transformed with *pLIMBU.*
MH075	Δ*dltA*	*trpC2 dltA::kan*	This work, *dltA::kan* transformed into 168CA from BKK38500 (Koo *et al.*, 2017).
S. aureus			
SA113	Wild-type	SA113 wild-type	T. Palmer, lab collection
SA113 Δ*mprF*	*S. aureus* ΔL-PG	SA113 *mprF::ery*	(Peschel *et al.*, 2001)
SH1000	Wild-type	SH1000 wild-type	(Horsburgh *et al.*, 2002)
S *cls1*/*cls2*	*S. aureus* ΔCL	SH1000 *cls1::cat cls2::tet*	(Tsai *et al.*, 2011)
VKS102	Δ*lpdA*	SH1000 *lpdA::kan*	(Singh *et al.*, 2008)

2.2 Media & growth conditions

The media used in this thesis are detailed in Table 2.2. All *B. subtilis* experiments were conducted in lysogeny broth (LB), unless otherwise stated; all *S. aureus* experiments were conducted in Mueller Hinton broth (MHB), unless otherwise stated.

Table 2.2. Recipes for media used in this study.

Medium	Ingredient	Concentration
Nutrient Broth (NB; Oxoid)	'Lab-Lemco' powder	1 g L^{-1}
	Yeast extract	2 g L^{-1}
	Peptone	5 g L^{-1}
	NaCl	5 g L^{-1}
Lysogeny Broth (LB)	Tryptone (Oxoid)	10 g L^{-1}
	Yeast extract (Oxoid)	5 g L^{-1}
	NaCl (VWR)	10 g L^{-1}
Minimal Medium Basic Salts	$(NH_4)_2SO_4$ (VWR)	0.2% w/v
	K_2HPO_4 ((VWR)	1.4% w/v
	KH_2PO_4 (VWR)	0.6% w/v
	Na_3-citrate•$2H_2O$ (VWR)	0.1% w/v
	$MgSO_4.7H_2O$ (VWR)	0.09% w/v
	Ferric ammonium citrate (Sigma-Aldrich)	11 µg mL^{-1}
Spizizen Minimal Medium (SMM) fortified supplements:	Glucose (VWR)	0.96% w/v
	Tryptophan (FORMEDIUM)	20 µg mL^{-1}
	Casamino acids (BD Biosciences)	0.02% w/v
Supplements added to fortified SMM for *S. aureus* growth:	Biotin (Sigma-Aldrich)	0.1 µg mL^{-1}
	Thiamine (Sigma-Aldrich)	2 mg $µL^{-1}$
	Nicotinic acid (Sigma-Aldrich)	2 µg mL^{-1}
	Calcium pantothenate (Sigma-Aldrich)	2 µg mL^{-1}
S. aureus Chemically Defined Medium (CDM)	KCl (VWR)	3 mg mL^{-1}
	NaCl	9.5 mg mL^{-1}
	$MgSO_4.7H_2O$	1.3 mg mL^{-1}
	$(NH_4)_2SO_4$	4 mg mL^{-1}

	Tris (Melford)	12.1 mg mL^{-1}
Supplements:	Glucose	0.5% w/v
	Casamino acids	1% w/v
	Tryptophan	10 µg mL^{-1}
	Biotin	0.1 µg mL^{-1}
	Thiamine	2 µg mL^{-}
	Nicotinic acid	2 µg mL^{-1}
	Calcium pantothenate	2 µg mL^{-1}
	$CaCl_2.2H_2O$ (Alfa Aesar)	22 µg mL^{-1}
	KH_2PO_4	140 µg mL^{-1}
	$FeSO_4.7H_2O$ (BDH)	6 µg mL^{-1}
	$MnSO_4.4H_2O$ (Sigma-Aldrich)	10 µg mL^{-1}
	Citric acid (Fisher Bioreagents)	6 µg mL^{-1}
Mueller Hinton Broth (MHB)	Mueller Hinton Broth (Sigma-Aldrich)	21 g L^{-1}
	Mueller Hinton Agar (Oxoid)	38 g L^{-1}
Tryptic Soy Broth (TSB)	Tryptic Soy Broth (Sigma-Aldrich)	30 g L^{-1}
MSM Medium (for L-form medium)	$MgCl_2$	3.81 g L
	Sucrose	342.3 g L
	Maleic acid	4.64 g L

Bacteria were grown either on nutrient agar (NA; Nutrient Broth with 1.5% w/v Bacto Agar; BD Biosciences) at 37 ºC or in LB with shaking at 30 ºC overnight. To suppress *B. subtilis* spore production, overnight growth of *B. subtilis* was in LB supplemented with 0.2% w/v glucose. The overnight cultures were diluted 1:100 in fresh LB the following morning and grown to the desired optical density 600 nm (OD_{600}) with shaking at 37 ºC. Where required, overnight media were supplemented with antibiotic to maintain selection, the concentrations used are shown in Table 2.3.

For experiments involving the Δ*bkd* Δ*des* strain, fortified Spizizen minimal media (SMM) was used; the auxotroph strain was supplemented with either isobutyric acid or 2-methylbutyric acid (IB/MB, 100 µM, Sigma Aldrich; Spizizen, 1958). For transformation of *B. subtilis* SMM was also used, however lower concentrations of

glucose (0.48% w/v) and ferric ammonium citrate (1.1 μg mL^{-1}) were used. The SMM starvation medium used for these transformations was SMM supplemented with glucose (0.48% w/v) and $MgSO_4$ only (0.09% w/v). For the induction of genes from Pspac promoters, 1 mM isopropyl β-D-1-thiogalactopyranoside (IPTG) was added to the growth medium.

For BCFA-precursor feeding of *S. aureus*, two media were trialled: *S. aureus* nutrient supplemented-SMM (SMM^{++}) composed of fortified SMM with additional supplements (Table 2.2); and *S. aureus* chemically defined medium (CDM) (Machado *et al.*, 2019).

For L-form growth, cultures were grown in osmo-protective L-form medium (2 x MSM mixed 1:1 with 2 x NB) at 37 ºC without shaking.

For assays involving benzyl alcohol, the benzyl alcohol was prepared by mixing under argon degassed dimethyl sulfoxide (DMSO; VWR) with an equal volume of benzyl alcohol (Sigma-Aldrich), to give 5 M stocks ready for at least 1/100 dilution in cultures.

Table 2.3. Antibiotic concentrations used in this study. All Sigma-Aldrich.

Antibiotic		**Solvent**	**Final Concentration** (μg mL^{-1})	
			B. subtilis	***S. aureus***
Chloramphenicol		100% ethanol	5	1
Erythromycin		50% ethanol	1	2.5
Kanamycin		Water	2	-
MLS	Erythromycin	50% ethanol	0.5	-
	Lincomycin	Water	12.5	-
Tetracycline		50% ethanol	6	5
Spectinomycin		Water	50	-
Gramicidin ABC		DMSO	5 μM	5 μM
Nisin		Water	5 μM	5 μM
CCCP		DMSO	100 μM	-
LL-37		Water	variable	variable
MP196		DMSO	variable	-

2.3 Strain construction and analysis

2.3.1 Extraction of chromosomal DNA

Chromosomal DNA was extracted from *B. subtilis* using a Promega Wizard® Genomic DNA Purification Kit. 2 mL of cells grown overnight with selection was centrifuged at

17,000 x *g* for 1 minute, the pellet was resuspended in 100 µL 50 mM EDTA with 300 µg mL^{-1} Lysozyme (Sigma Aldrich) and 300 µg mL^{-1} RNase A (Sigma Aldrich) and incubated at 37 °C for 1 hour. 500 µL Nuclei Lysis Solution (Promega) was added to the sample and it was incubated at 80 °C for 5 minutes, once cooled to room temperature, 200 µL of Protein Precipitation Solution (Promega) was added to the sample and mixed by 20 seconds of vortexing before being incubated on ice for 10 minutes. The sample was centrifuged at 17,000 x *g* for 10 minutes. 600 µL of the supernatant was added to 600 µL of room temperature isopropanol, this was gently mixed by inversion. The chromosomal extract was then pelleted by centrifugation at 17,000 x *g* for 10 minutes. The pellet was washed with 70% ethanol before being centrifuged again at 17,000 x *g* for 5 minutes. The pellet was allowed to air dry to remove residual ethanol, before being resuspended in 100 µL of sterile Milli-Q® Ultrapure water via incubation at 65 °C for 15 minutes. Chromosomal DNA was then stored at -20 °C.

2.3.2 Transformation of B. subtilis

B. subtilis cells to receive DNA were thickly streaked on nutrient agar plates and grown overnight at 30 °C. 5 mL of SMM was inoculated with cells from the nutrient agar and incubated with shaking at 37 °C for 3 hours. Cultures were diluted by the addition of 5 mL SMM Starvation Medium and incubated for a further 2 hours at 37 °C with shaking to induce natural competence. 2 µL of chromosomal DNA was added to 400 µL of competent cells, with incubation at 37 °C for 1 hour. Cells were then plated on nutrient agar with selection and incubated at 37 °C overnight.

2.3.3 Whole genome sequencing

Chromosomal DNA extracted from *S. aureus* using a Promega Wizard® Genomic DNA Purification Kit and the same protocol as described for *B. subtilis*, except in place of lysozyme 50 µg mL^{-1} of lysostaphin (Sigma-Aldrich) was used and chromosomal DNA was resuspended in elution buffer (Machery-Nagel). Whole genome sequencing was performed by the MicrobesNG (http://www.microbesng.com) Standard Whole Genome Service, using Illumina next generation sequencing. Reads were trimmed by MicrobesNG using Trimmomatic (Bolger *et al.*, 2014). Trimmed reads were then mapped against a reference genome - either *B. subtilis* 168 (Barbe *et al.*, 2009) or *S. aureus* SH1000 (provided by Prof Simon Foster, Sheffield University); using CLC Genomics Workbench (Qiagen), a threshold of >50% occurrences was set for detection of insertions/deletions/structural variants.

2.4 Bacterial growth and viability

2.4.1 Minimum inhibitory concentration assay

The minimum inhibitory concentration (MIC) of LL-37 (Novopro) for different strains was determined through the preparation of a 2-fold serial dilution of LL-37 in 195 µL LB in a microtitre plate. Bacteria were grown to mid-log (OD_{600} 0.5) and diluted to OD_{600} 0.2, with 5 µL of each diluted culture added to the microtitre plate in triplicate, to achieve a final volume in each well of 200 µL and a starting OD_{600} of 0.005. The plate was incubated at 37 ºC with 700 revolutions per minute (rpm) shaking for 16 hours, and the MIC was read as the lowest concentration of LL-37 in which no bacterial growth could be observed visually.

2.4.2 Growth/lysis curve

Bacteria were grown to mid-log (OD_{600} 0.5), diluted to OD 0.05 and 200 µL of each strain was transferred to a microtitre plate in triplicate. The microtitre plate was placed in a plate reader (BMG Spectrostar/Fluostar) at 37 ºC with shaking and OD_{600} measurements were taken every 5 minutes. Once bacteria had grown to OD_{600} 0.3 (early log phase) the plate reader was paused, and 2 µL of compounds at varying concentrations were added to the wells in triplicate, the plate was replaced in the plate reader and OD_{600} continued to be measured.

With supernatant:

Culture supernatants were generated by centrifuging cultures grown to OD_{600} 1 for 1 minute at 17,000 x *g*. Supernatants were diluted 1:3 in fresh LB and heat-inactivated supernatant was achieved by incubation at 95 °C for 10 minutes. When 20 µg mL^{-1} LL-37 was added to supernatants it was present for 1 hour before exposure to cultures. Cultures to be grown in the presence of supernatant were grown to OD_{600} 0.5, then centrifuged at 6000 x *g* for 1 minute and resuspended in supernatant.

With cell lysate:

The addition of cell lysate was achieved through growing wild-type *B. subtilis* to stationary phase (OD_{600} ~1.5) and sonicating the culture until the OD_{600} was reduced to ~0.2, then filtering the lysate through a 0.45 µm filter. The filtered lysate was diluted 1:5 in fresh LB to give cell debris akin to that of a OD_{600} 0.3 culture. Cultures were diluted in this lysate-LB, and a lysate-LB only sample was also added to the plate to provide a blank media reading.

With ultracentrifugation fractions:

Bacterial fractions were obtained through growing wild-type and cell wall lacking L-form (Δ*uppS*) cells to stationary phase, adding 60 µg mL^{-1} lysozyme and sonicating until the cultures appeared clear. Followed by centrifugation at 7000 x *g* for 10 minutes to obtain a cell debris pellet. The supernatant was subjected to ultracentrifugation at 90,000 x *g* for 60 minutes at 4 °C, to give a cell membrane pellet and cytoplasmic contents in the supernatant. Pellets were resuspended in fresh LB and fractions were diluted to achieve media with fractions akin to that of an OD_{600} 0.3 culture.

With wash:

To remove cell debris, cultures were washed by removal from the 96-well plate to microcentrifuge tubes and centrifuged at 8000 x *g* for 1 minute and the cell pellet was resuspended in warm LB. The centrifugation and resuspension were repeated once more, and the cultures were returned to the 96-well plate. The plate reader programme was resumed, and growth was allowed to stabilise for a few cycles before subsequent treatment occurred.

2.4.3 Viability assay

The killing and lysis induced by antibiotics was assayed by measuring the colony forming units (c.f.u.) and OD_{600} of treated cultures over time. Bacteria were grown to OD_{600} 0.3, and 1 mL was taken into microcentrifuge tubes to be treated with antibiotic, cultures were incubated in a thermomixer at 37 °C with 850 rpm shaking. Growth/lysis was measured via OD_{600} of the cultures over time using a spectrophotometer. Alongside cell viability was estimated using a spot assay. 10 µL of culture was diluted in 90 µL LB in a 96-well plate, this was serial diluted to achieve 10^{-1}-10^{-8} dilutions. 5 µL of the culture dilutions was spotted onto a nutrient agar plate, plates were incubated at 37 °C for 24 hours before colony forming units (c.f.u.) were calculated as follows:

$$c.f.u.mL^{-1} = \frac{number\ of\ colonies\ \times dilution\ factor}{volume\ of\ culture\ plated\ (mL)}$$

2.5 Microscopy

2.5.1 General fluorescence microscopy

Wide-field fluorescence microscopy was performed using Metamorph software (Molecular Devices) or NIS-Elements (Nikon) on a Nikon Eclipse Ti. This microscope was equipped with Cool LED pE-4000 light source, Nikon Plan Apo 100×/1.40NAOil

Ph3 objective, Photometrics BSI sCMOS Prime camera and Chroma 49002 (EX470/40, DM49l5pxr, EM525/50) and Semrock Cy5-4040C (EX628/40, DM660lp, EM 692/40) filter sets.

Bacterial strains were grown to an OD_{600} of 0.3. Incubation with dyes and compounds (Table 2.4) was performed using 200 µL of cells in 2 mL microcentrifuge tubes with perforated lids and shaking at 850 rpm in a ThermoMixer (Eppendorf). Cells were immobilised on 1.2% (w/v) agarose dissolved in deionised water, and aliquoted onto Teflon-coated multi-spot slides (Thermo Shandon). This was compressed into a thin layer by pressing a microscope slide with sections of a Gene Frame (Thermo Fisher) attached over the aliquoted agarose. After the agarose had solidified, 0.5 µL of bacterial culture was applied to the agarose and allowed to air dry prior to application of a coverslip. Cells were imaged immediately after application of the coverslip in order to limit oxygen starvation.

When fluorescent LL-37 (5-FAM-LC-LL-37) was used, it was mixed at a 1:4 ratio with non-fluorescent LL-37 to ensure potency was comparable to non-fluorescent experiments. When compounds were used as controls for dye activity, such as gramicidin ABC and nisin, these were added to the culture 5 minutes before imaging.

Table 2.4. The fluorescent dyes and compounds used in this study. Final conc. indicates concentration in sample, stock samples were 100x this in the solvent indicated; treatments are distinguished between *B. subtilis* (*Bs*) and *S. aureus* (*Sa*).

Dye/ Compound	**Supplier**	**Final conc.** [solvent]	**Excitation (nm)**	**Emission (nm)**	**Addition time**
5-FAM-LC-LL-37	Anaspec	20 µg mL^{-1} [water]	470/40 or 500/20	525/50 or 535/30	From start
DAPI	Severn Biotech	100 ng mL^{-1} [DMSO]	377/50	447/60	15 m before imaging
$DiBAC_4(3)$	Invitrogen	2.5 µM [DMF]	466/40	525/50	From start
$DiSC_3(5)$	Anaspec	2 µM [DMSO]	628/40	692/40	*Sa*: from start; *Bs:* 5m before imaging *
Nile red	Sigma-Aldrich	50 µg mL^{-1} [DMSO]	560/40	630/75	From start
Propidium iodide	Thermo Fisher	10 µM [water]	562/40	641/75	From start

SYTOX Blue	Invitrogen	200 nM [water]	438/24	483/32	From start
SYTOX Green	Invitrogen	200 nM [water]	470/40	525/50	From start

* This is due to $DiSC_3(5)$ being growth inhibitory against *B. subtilis* but not *S. aureus*

2.5.2 Time-lapse microscopy

Wide-field time-lapse fluorescence microscopy was performed using Metamorph 7.7 software (Molecular Devices) or Nikon NIS-Elements (Nikon) on a Nikon Eclipse Ti. This microscope was equipped with a temperature control unit, Cool LED pE-300 white light source, Nikon Plan Apo 100×/1.40NAOil Ph3 objective, Photometrics Prime camera, and Chroma 49002 (EX470/40, DM495pxr, EM525/50) filter set.

Cultures were grown to an OD_{600} of 0.3, 100 µL was transferred to a 2 mL microcentrifuge tube with a perforated lid, shaking at 850 rpm in a ThermoMixer and incubated with the fluorescent dyes to be imaged (either SYTOX Green or a mixture of $DiBAC_4(3)$ and propidium iodide) in the presence or absence (untreated control) of LL-37 for 5 minutes. The culture was immobilised on 1.2% low melting point agarose (2-Hydroxyethyl agarose; Sigma-Aldrich), containing 10% LB (with normal LB salt concentration, 10 mg mL^{-1}; this maintains ionic conditions whilst reducing nutrients to minimise background fluorescence – this has no effect on cell growth over the incubation periods used in this thesis) or MHB and the fluorescent dyes. Slide preparation was achieved as described by Jong *et al.* (2011), in brief: the agarose mixture was added to the centre of a Gene Frame attached to a clean slide, and then compressed using an additional clean slide. After the agarose was allowed to solidify, extra material was removed to allow for better oxygenation, leaving only a thin strip approximately 5 mm in width. 2.5 µL of bacterial culture was added to the agarose, spread across the strip and allowed to air dry before application of the coverslip. Cells were imaged on a microscope that had been pre-heated to 37 °C.

To prevent interaction of fluorescent dyes with the glass coverslips used in time-lapse microscopy, the coverslips were coated in L-dopamine – this is essential for experiments using $DiBAC_4(3)$ (Zhang *et al.*, 2013; Strahl *et al.*, 2015). Glass coverslips were coated in 2 mg mL^{-1} L-dopamine (Sigma-Aldrich) dissolved in 2 mM Tris at pH 8.3 for 30 minutes. The coverslips were aspirated and washed in deionised water, then dried at 37 °C.

2.5.3 Image analysis & quantification

Image analysis and fluorescence quantification were performed using Fiji (Schindelin *et al.*, 2012).

Quantification of single cell fluorescence was performed in a semi-automated process using the Cropping Multiple Images and Phase Contrast Cell Average Fluorescence plugins (Newcastle University Image Analysis Unit, 2023) – https://github.com/NCL-ImageAnalysis/General_Fiji_Macros/blob/main/Cropping_Multiple_Images.py and https://github.com/NCL-ImageAnalysis/General_Fiji_Macros/blob/main/Phase_Contrast_Cell_Average_Fluorescence.py; as follows: the 2048x2048 pixel images were cropped to the central 1800x1800 pixels; the average background fluorescence intensity was subtracted; phase contrast images were thresholded to select individual cells as regions of interest (ROI), cells that neighboured each other were manually separated by a thin line to aid automatic cell detection; the mean fluorescence across each ROI was obtained, to give single cell fluorescence values across the cell population.

Quantification of fluorescence along a line was conducted as follows: a segmented line was drawn along the cell line of the phase contrast image; this was overlaid on the fluorescence channels. A density plot profile was plotted from this line selection of each fluorescent channel. The data was normalised against the maximum fluorescence value of each channel to give percentage fluorescence.

To correct for microscope drift, time-lapse merged images were aligned using the MultiStackRegistration plugin – https://github.com/miura/MultiStackRegistration (Thévenaz *et al.*, 1998).

2.6 Statistical analysis

Experiments were conducted in triplicate with at least two biological repeats. All statistical analyses were conducted in Graphpad Prism 9.5.0 for Windows, GraphPad software, San Diego, California USA, www.graphpad.com. The following analyses were used: an unpaired, two-tailed t-test; an ordinary one-way analysis of variance (ANOVA) with – Dunnett's multiple comparisons test, when comparing conditions to wild-type, or Tukey's multiple comparisons test, when comparing between all conditions.

Growth/lysis assays were analysed by comparison of the time taken for cultures to recover growth to the OD_{600} at which antibiotic was added to the culture, each graph represents one biological repeat, with statistical analysis of that repeat only; analysis of the second biological repeat of each experiment can be found in the appendix of this report.

Chapter 3 – Membrane composition and fluidity in susceptibility to LL-37

3.1 Introduction

The role of membrane composition in susceptibility to cationic AMPs has been studied in a range of bacterial species (Ernst & Peschel, 2011). It is well established that the presence of cationic L-PG in the cytoplasmic envelope of *S. aureus* protects it from cationic AMPs – in a mutant lacking L-PG, susceptibility to LL-37 is significantly increased (Ernst *et al.*, 2009). However, to the best of my knowledge, this research has not yet been extended to the Gram-positive model organism *B. subtilis*. *B. subtilis* is a useful tool in studying the factors that make bacteria susceptible to antibacterial substances, as it is genetically tractable and very well studied, including its lipid and overall envelope composition. This means it is easy to make and understand the outcome of genetic mutations – much of the understanding and manipulation achieved with *B. subtilis* has not yet been matched in other bacterial species.

B. subtilis strains lacking the non-essential membrane lipid head groups have provided an invaluable tool in investigating the role of membrane head groups in cellular processes (Salzberg & Helmann, 2008). The *B. subtilis* deletion library established by Koo *et al.* (2017) enables analysis of the role of any non-essential gene of the bacterium, by comparing wild-type and gene knockout phenotypes. From this library, and strains constructed by the Strahl group, we also have strains lacking LTA, WTA and D-alanylation. By using these lipid head group and teichoic acid mutant strains, the role of *B. Subtilis* envelope composition can be investigated in relation to LL-37 susceptibility.

Additionally, the role of membrane fluidity in susceptibility to AMPs has long been hypothesised – it seems highly plausible that the packing of membrane phospholipids should impact the ability of membrane disrupting antimicrobials to interact with the membrane. Yet, this had not been possible to test due to a lack of means to alter membrane fluidity in a controllable manner in living cells. However, the recent development of *B. subtilis* strains in which the membrane fluidity can be directly altered in living cells provides a means to assay the impact of membrane fluidity on susceptibility to antimicrobials (Gohrbandt *et al.*, 2022). Membrane fluidity can also be altered via growth temperature. Whilst cells adapt to maintain constant membrane

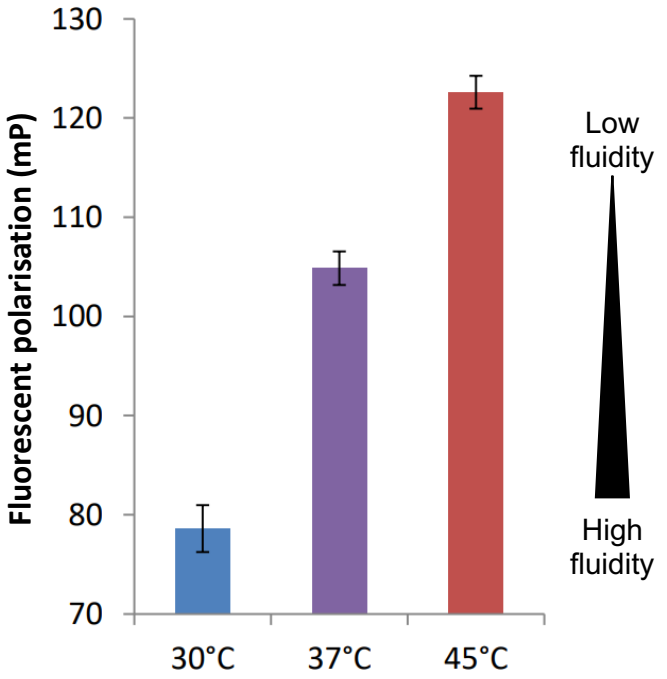

Figure 3.1. *B. subtilis* overcorrects membrane fluidity upon temperature change. Fluorescent polarisation of *B. subtilis* grown at 30, 37 and 45 °C as measured by DPH anisotropy by Dr Kenneth Seistrup, 2018. "Higher values signify more rigid membranes, while lower values signify more fluid membranes. Error bars represent standard deviation. n=3" (Seistrup, 2018, p. 74).

fluidity at different temperatures via homeoviscous adaptation, it was found by a previous PhD student that *B. subtilis* over-corrects when grown at varying temperatures (Fig. 3.1; Seistrup, 2018). Meaning when grown at 30 °C, which will cause the cytoplasmic membrane to become more rigid, the cells counter this and instead have a more fluid membrane than those grown at 37 °C. Likewise, when cells are grown at 45 °C, inducing more fluid membranes, the cells counter this and instead have more rigid membranes. A final method to alter membrane fluidity is by the addition of benzyl alcohol, which has a fluidising effect on the membrane (Coster & Laver, 1986; Friedlander *et al.*, 1987). The addition of benzyl alcohol counteracts the membrane solidifying effect of cold-shock in *B. subtilis*, leading to benzyl alcohol being established as a positive control for high membrane fluidity (Strahl *et al.*, 2014; Zielińska *et al.*, 2020). Altogether, there are now a range of direct and indirect methods by which membrane fluidity can be altered for the purposes of testing the role of membrane fluidity in cell envelope processes and interactions.

In this chapter, I aimed to use the range of *B. subtilis* cell envelope mutant strains and varying growth conditions to alter membrane fluidity established to provide a thorough investigation of the role of cell envelope composition in susceptibility to LL-37. I tested

the hypothesis that membrane fluidity would impact the ability of LL-37 to interact bacterial membranes. Where appropriate, and possible, comparisons have been made to the pathogenically relevant Gram-positive species *S. aureus*.

3.2 Results

3.2.1 Phospholipid head group composition has little effect on LL-37 susceptibility

I first used *B. subtilis* membrane phospholipid head group mutants, described by Salzberg & Helmann (2008), to assess the role of cytoplasmic membrane composition in susceptibility to LL-37. A MIC assay was undertaken, to identify strains in which the MIC deviated from that of wild-type *B. subtilis*. This assay showed that strains lacking CL, PE and PS & PE were as susceptible as wild-type, as their LL-37 MIC was the same as wild-type. Surprisingly there was also no change in MIC with the lack of L-PG, a cationic head group. Only the loss of GLs made *B. subtilis* more susceptible to LL-37, seen in the reduction of LL-37 MIC from 20 to 10 μg mL^{-1} (Table 3.1).

Table 3.1. Minimum inhibitory concentration (MIC) of LL-37 against *B. subtilis* (n=3).

***B. subtilis* strain**	**LL-37 MIC** (μg mL^{-1})
Wild-type	20
ΔL-PG	20
ΔCL	20
ΔGL	10
ΔPE	20
ΔPS & ΔPE	20

In addition to a MIC assay, susceptibility can also be assayed by growth/lysis assays, in which the growth of bacteria is followed over time upon addition of LL-37. When these head group deficient strains were assayed in this way, the clear increase in susceptibility of the GL deficient strain was immediately evident, as it took much longer than other strains to recover growth following LL-37 addition (indicated by an increase in OD_{600}; Fig. 3.2a). Analysis of the time taken for cultures to recover to the initial OD_{600} at which LL-37 was added, showed that whilst the recovery of most strains took just over 2 hours, when GLs were absent the time to recover was significantly increased to

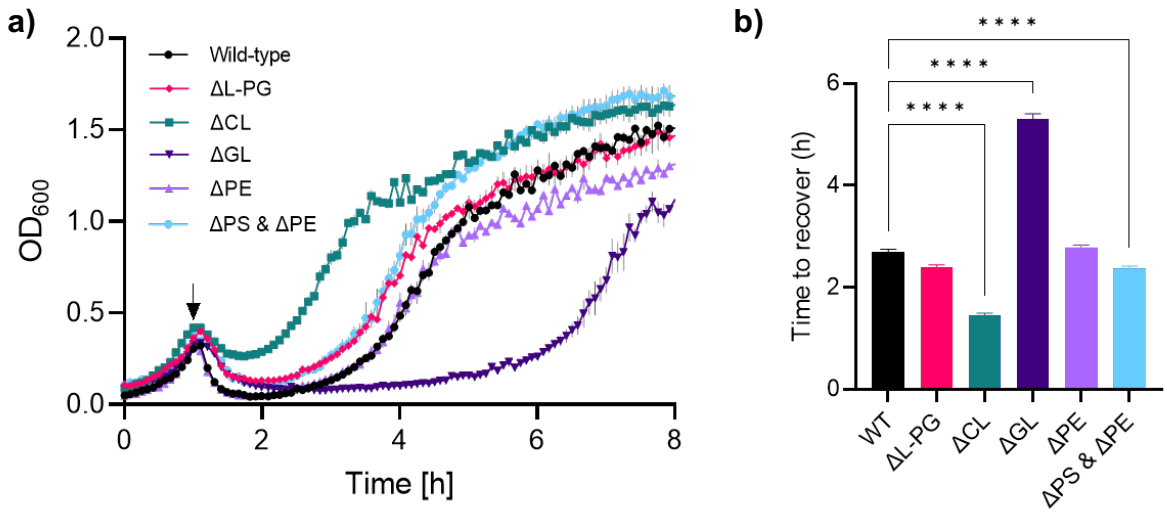

Figure 3.2. Glycolipid deficient *B. subtilis* is more susceptible to LL-37 than wild-type, whilst the loss of cardiolipin is protective. a) Growth/lysis of *B. subtilis* strains lacking lysyl-phosphatidylglycerol (L-PG), cardiolipin (CL), glycolipids (GL), phosphatidylethanolamine (PE), and phosphatidylserine (PS) & PE upon the addition of 20 µg mL^{-1} LL-37 (indicated by arrow). **b**) Analysis of the time taken for each strain to recover to the initial optical density at which LL-37 was added; analysed by unpaired ordinary ANOVA with Dunnet's multiple comparisons test comparing to wild-type (WT), **** represents $p < 0.0001$. Data represented as mean±SD (n=3).

5 hours (Fig. 3.2b). This assay also revealed that a lack of CL conferred a slight protective effect to *B. subtilis*, however this protection was not sufficient to increase the LL-37 MIC (Table 3.1) but did significantly improve recovery time (Fig. 3.2b). Through conducting both MIC and growth/lysis assays with these strains, it became clear that growth/lysis kinetics were more informative than MIC values. Therefore, growth/lysis assays are the preferred technique to assess LL-37 activity throughout this report.

3.2.2 Loss of teichoic acids sensitises B. subtilis to LL-37

The increase in LL-37 susceptibility observed in the GL deficient strain (Fig. 3.2) indicated that GLs must contribute to a mechanism that protects *B. subtilis* from LL-37. GLs form the membrane domain of LTAs, anchoring the teichoic acid to the outer leaflet of the cytoplasmic membrane (Toon *et al.*, 1972). In a ΔGL mutant LTA synthesis is impacted, it may be that this change in LTAs is responsible for the increased susceptibility of the ΔGL strain to LL-37 (Salzberg & Helmann, 2008). Therefore, I investigated the susceptibility of teichoic acid deficient strains to LL-37.

Both forms of teichoic acid present in *B. subtilis*, LTA and WTA, were investigated. One complication in this experiment was the phenotype of the ΔWTA strain, as in addition to lacking WTA, this strain also loses its rod-shaped morphology and instead

transitions into slow-growing round cells (Soldo *et al.*, 2002). This round cell morphology lowers the OD_{600} of a given cell density, meaning the cell density suggested by the OD_{600} of ΔWTA is not equivalent to that of wild-type and ΔLTA; however, the effects of differing concentrations of LL-37 could still be compared between the cultures despite the differences in OD_{600} range.

The effect of a range of LL-37 concentrations was first assessed by lysis assay against wild-type *B. subtilis* cells; in this assay I used a range of LL-37 concentrations as this enables the effect of a low concentrations of LL-37 to also be assessed – this is only possible experimentally when fewer strains are assayed. The highest concentration of LL-37, 20 μg mL^{-1} caused rapid lysis, reducing the culture OD_{600} before the cells were then able to recover and grow to stationary phase (Fig. 3.2a). Both 10 & 5 μg mL^{-1} LL-37 caused a lesser degree of lysis, whereas the lowest concentration of 2.5 μg mL^{-1} caused very little effect relative to the untreated culture. In comparison to wild-type *B. subtilis*, 20 μg mL^{-1} had a much more striking effect against both the ΔWTA and ΔLTA strains, with lysis that reduced the culture OD_{600} but also remained at this low level for a longer duration, showing the cells were less able to recover from treatment with 20 μg mL^{-1} LL-37 (Fig. 3.3a,b&c). A similar dramatic lysis was seen with 10 μg mL^{-1} LL-37 against both strains, however whilst ΔWTA did not recover from this, ΔLTA was able to recover growth after an extended period of low OD_{600}. Lower concentrations of LL-37 also had an increased effect against the teichoic acid-deficient strains, as seen through the ability of wild-type cells treated with all concentrations to recover growth to that of untreated cells by ~5 hours growth, whereas no ΔWTA and ΔLTA cells treated with LL-37 recovered growth to untreated levels by the end of the 8-hour period. The striking lytic effect and inability to recover of either LTA or WTA deficient cells (Fig. 3.3b&c), meant it was not possible to assess the time to recover from 20 μg mL^{-1} of these strains.

3.2.3 D-alanylation of teichoic acids is protective against LL-37

To examine how teichoic acids may be protecting *B. subtilis* from LL-37, the role of D-alanylation was assessed. Both LTAs and WTAs can be modified with cationic D-alanine residues, conferring positive charges to the normally anionic polymers – it is thought this decoration with positive residues can repel cationic AMPs (Wecke *et al.*, 1997; Saar-Dover *et al.*, 2012). In the absence of D-alanylation (Δ*dltA*), *B. subtilis* was much more susceptible to LL-37 than wild-type (Fig. 3.4a). Initial lysis of Δ*dltA* was dramatic when treated with both 20 and 10 μg mL^{-1} LL-37, these cultures also took far

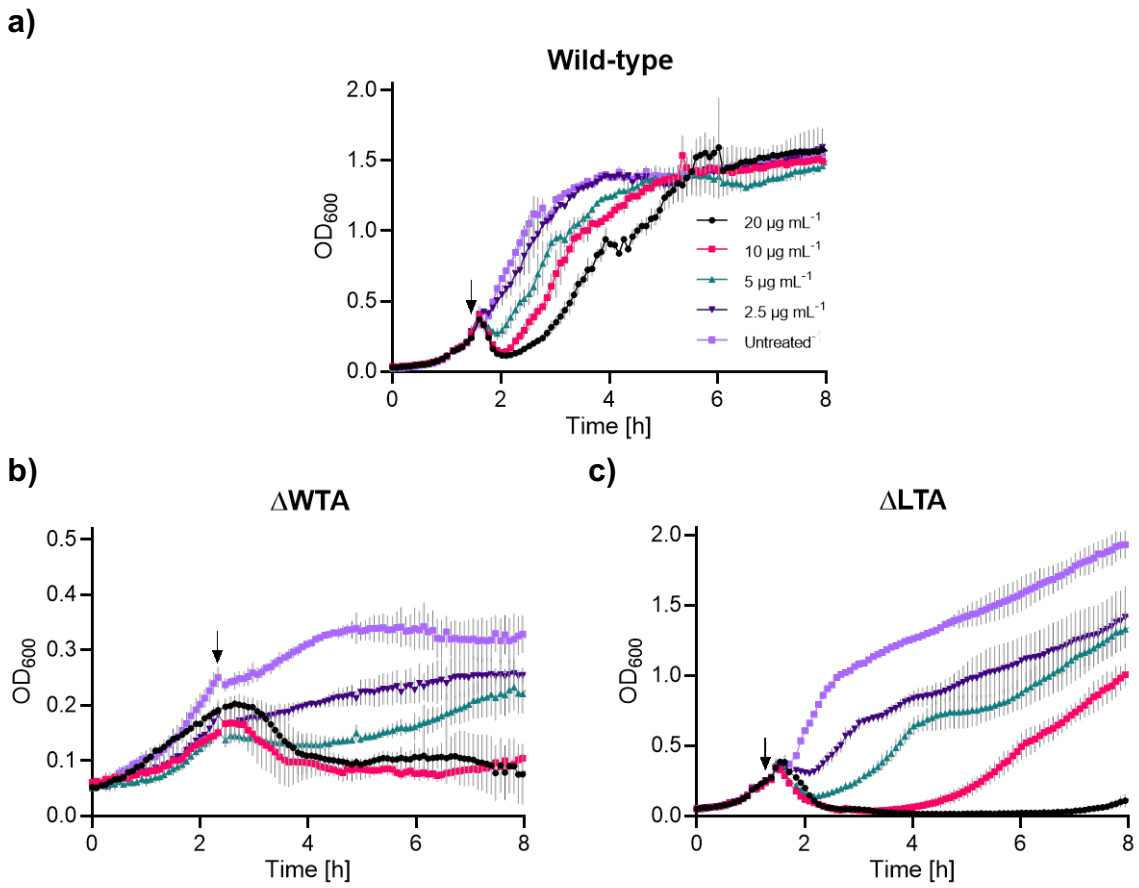

Figure 3.3. Wall teichoic acid and lipoteichoic acid deficient strains have increased susceptibility to LL-37. Growth/lysis of (**a**) wild-type, (**b**) wall teichoic acid (WTA) deficient, and (**c**) lipoteichoic acid (LTA) deficient *B. subtilis* upon the addition of LL-37 (indicated by arrow). Data represented as mean±SD (n=3).

longer to recover their growth (Fig. 3.4b). Lower concentrations of LL-37 were also more effective against Δ*dltA*, as wild-type treated with 2.5 µg mL^{-1} LL-37 had no discernible growth lag compared to untreated, whereas this concentration caused a slight growth delay from which Δ*dltA* cells had still not recovered by 8 hours. When comparing the time to recover to the initial OD_{600} at which LL-37 was added to the 20 µg mL^{-1} cultures, Δ*dltA* took significantly longer to recover, evidencing its increased susceptibility to LL-37 whilst not fully accounting for the extended lysis of teichoic acid lacking strains (Fig. 3.4c).

3.2.4 Membrane fluidity altered through Δbkd Δdes auxotrophy does not impact susceptibility to LL-37

I next looked at the role of fatty acid composition and membrane fluidity in susceptibility to LL-37. I employed the recently developed method of Gohrbandt *et al.* (2022) in combination with LL-37 treatment. This method uses *B. subtilis* Δ*bkd* Δ*des*, these deletions mean it cannot synthesise its own BCFA precursors or UFAs and so is an

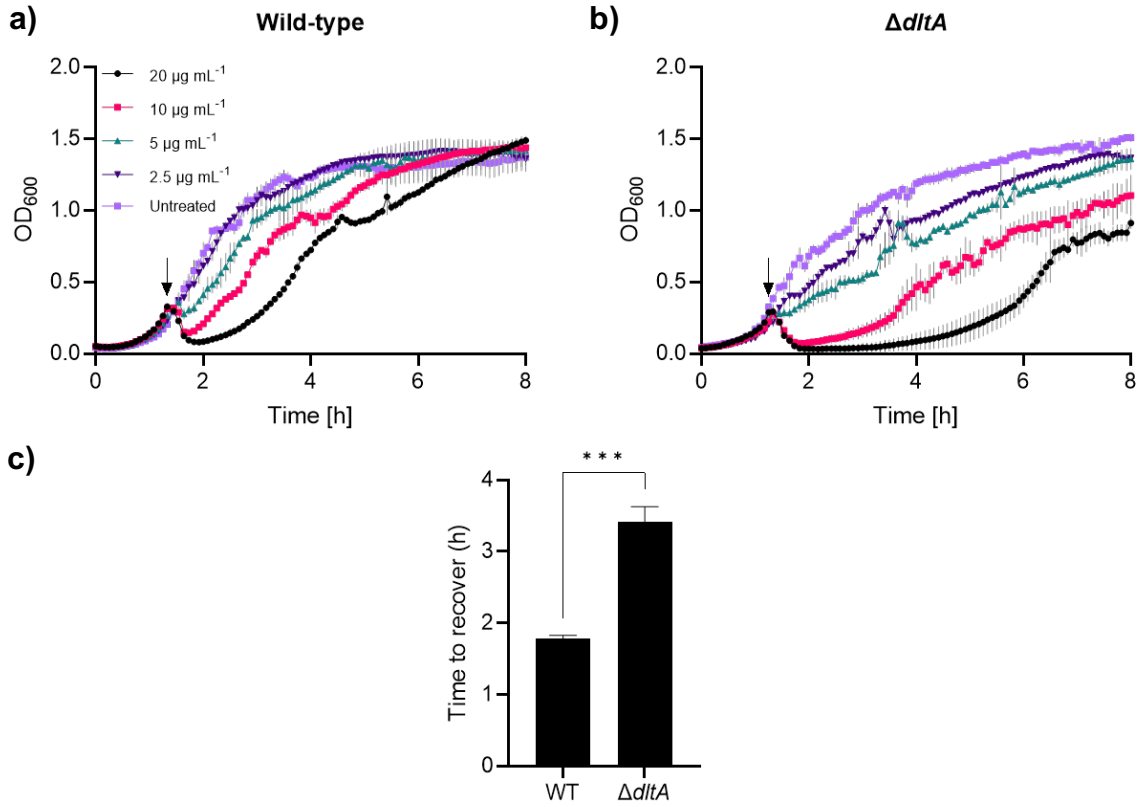

Figure 3.4. D-alanylation deficient *B. subtilis* is more susceptible to LL-37. Growth/lysis of (**a**) wild-type and (**b**) D-alanylation (Δ*dltA*) deficient *B. subtilis* upon the addition of LL-37 (indicated by arrow). **c**) Analysis of the time taken for each strain treated with 20 µg mL^{-1} LL-37 to recover to the initial optical density at which LL-37 was added; analysed by unpaired two-tailed t-test, *** represents $p < 0.001$. Data represented as mean±SD (n=3).

auxotroph for BCFA precursors. Through the feeding of specific BCFA precursors the BCFA content of Δ*bkd* Δ*des* can be specified, resulting in a means to control membrane fluidity *in vivo* in *B. subtilis*. The precursors used to alter membrane fluidity are isobutyric acid (IB) and 2-methylbutyric acid (MB), IB provides the primer for the synthesis of *iso*-BCFAs and MB provides the primer for the synthesis of *anteiso*-BCFAs, with *anteiso*-BCFAs being highly fluidity-promoting and *iso*-BCFAs being low fluidity promoting. In the absence of precursor this strain cannot grow as the *bkd* deletion prevents BCFA synthesis through the FAS II pathway and the deletion of *des* prevents the synthesis of UFAs to compensate for this (Gohrbandt *et al.*, 2022; Humphrey *et al.*, 2023). To enable specific feeding the strain is grown in SMM, a minimal medium (Spizizen, 1958).

I first tested the phenotype of the Δ*bkd* Δ*des* strain by growing it with IB and MB at different temperatures – 22, 30 and 37 °C. At 22 °C, growth of precursor free and IB-fed Δ*bkd* Δ*des* was not supported, indicated by the lack of growth/ colonies in the Δ*bkd*

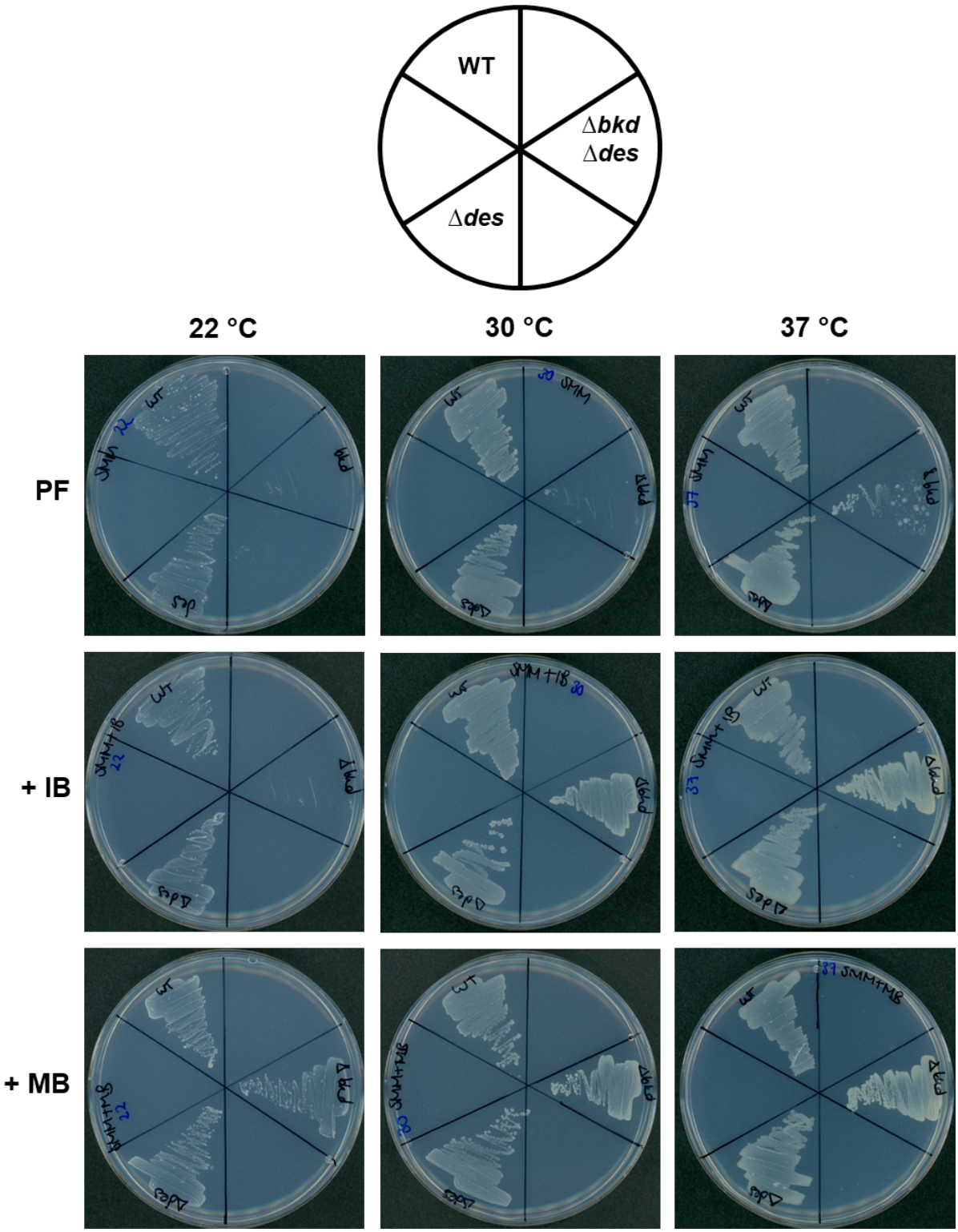

Figure 3.5. Growth of Δ*bkd* Δ*des* with IB and MB at different temperatures shows fluidity promotion of MB. Wild-type (WT), Δ*des* and Δ*bkd* Δ*des* *B. subtilis* grown on SMM plates either precursor free (PF) or containing isobutyric acid (IB) or 2-methylbutyric acid (MB). Plates were incubated at 22 (4 days), 30 and 37 (2 days) °C before being imaged.

Δ*des* section of the plates (Fig. 3.5). Whereas, the most fluid phenotype, MB-fed Δ*bkd* Δ*des*, was viable at this temperature, as shown by the opaque growth on the plate. At

30 °C both IB- and MB-fed Δ*bkd* Δ*des* were able to grow, but the precursor free Δ*bkd* Δ*des* was not viable. At 37 °C, Δ*bkd* Δ*des* grew in all 3 conditions, precursor free, IB-fed and MB-fed; however, the growth of precursor free Δ*bkd* Δ*des* was limited compared to the other conditions, seen in the small colonies of precursor free, compared to the dense lawn streak of IB- and MB-fed (Fig. 3.5). Having observed the expected phenotype of Δ*bkd* Δ*des* – with growth at low temperatures dependent on *anteiso*-BCFA synthesis, I continued to assay the susceptibility of the strain to LL-37 when grown with the different BCFA precursors, as this results in highly variable levels of membrane fluidity.

The auxotrophy of Δ*bkd* Δ*des* for BCFA precursors was seen in the inability of precursor free Δ*bkd* Δ*des* to grow in liquid medium, whereas IB- and MB-fed Δ*bkd* Δ*des* grew well (Fig. 3.6a). Treatment of wild-type *B. subtilis* grown in SMM with LL-37

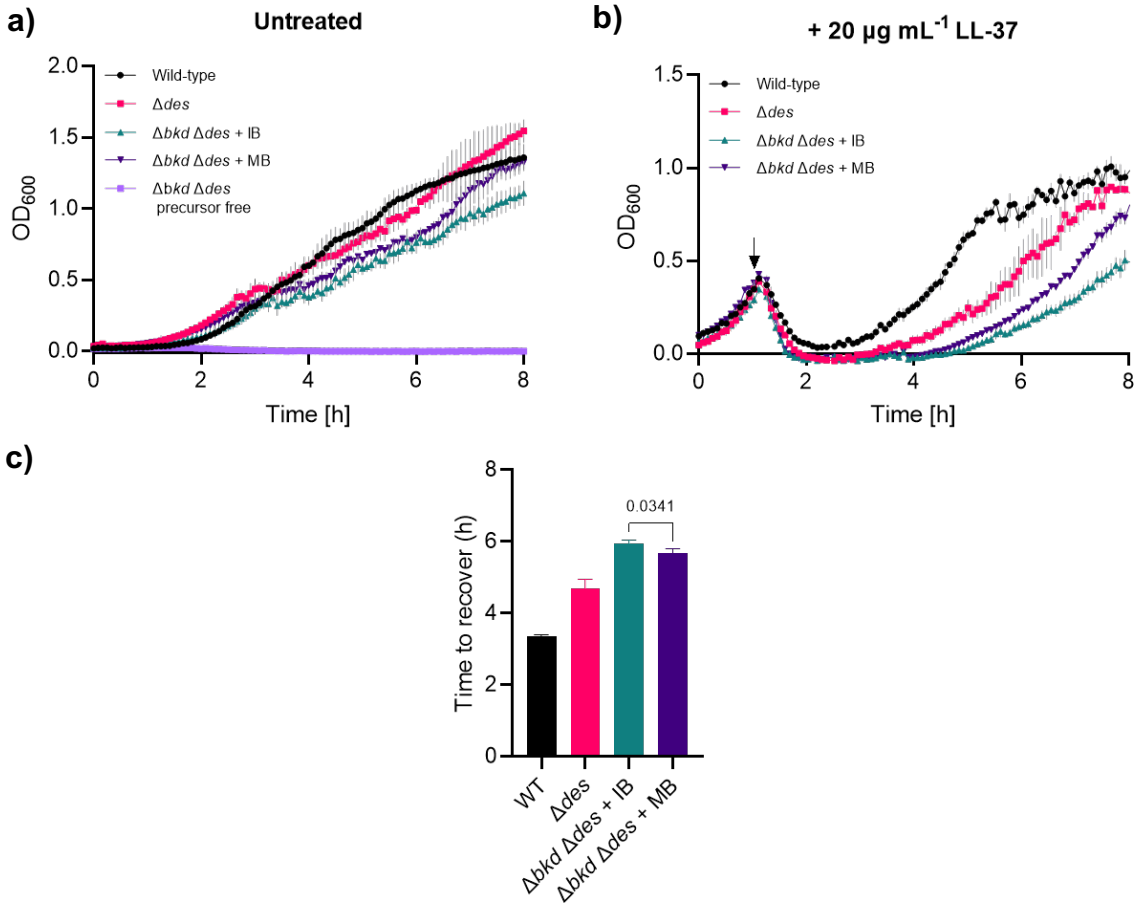

Figure 3.6. Fluidity altered by BCFA feeding has little impact on susceptibility to LL-37. Growth/lysis of *B. subtilis* wild-type, Δ*des* and Δ*bkd* Δ*des* with isobutyric acid (IB), 2-methylbutyric acid (MB) or no precursor either (**a**) untreated, or (**b**) upon the addition of 20 µg mL^{-1} LL-37 (indicated by arrow) at 37 °C. **c**) Analysis of the time taken for each strain treated with 20 µg mL^{-1} LL-37 to recover to the initial optical density at which LL-37 was added; Δ*bkd* Δ*des* + IB/MB analysed by unpaired two-tailed t-test, p value is indicated. Data represented as mean±SD (n=3).

resulted in the same lysis and recovery seen previously (Fig. 3.6b), except the recovery took slightly longer due to the minimal medium supporting slower growth – this slow growth was also seen in the untreated cultures (Fig. 3.6a). The strains lacking Des and BKD all recovered slower than wild-type and suffered a higher degree of lysis when treated with LL-37. The strain lacking both BKD and Des was more susceptible than that lacking Des alone, however there was only a small difference in recovery time of Δ*bkd* Δ*des* fed IB or MB. Whilst the difference between their recovery time was found to be significant (Fig. 3.6c), the values themselves were very similar – 5.96 h and 5.67 h for IB and MB, respectively. These findings suggested that fluidity does not impact susceptibility to LL-37, so I sought to confirm this key result by pursuing additional methods in which fluidity can be altered.

Feeding Δ*bkd* Δ*des* with MB gives the most fluid membrane composition of this strain (Gohrbandt *et al.*, 2022). Through the artificial expression of *des*, to synthesise UFAs, this could make the MB-fed strain have even higher membrane fluidity, and thus would provide a means to assay whether very fluid membranes impact LL-37 activity; therefore, I looked to test this. As previously seen, wild-type *B. subtilis* recovered better from LL-37 than the Δ*bkd* Δ*des* mutant (Fig. 3.6b, 3.7a). Between the Δ*bkd* Δ*des* + MB un/induced cultures treated with LL-37 there were very few differences (Fig. 3.7b&c). The highly fluid induced culture suffered significant lysis and delayed recovery when treated with 20 μg mL^{-1} LL-37 but as did the culture in which *des* was not induced – when the time to recover from 20 μg mL^{-1} LL-37 between the two was compared the values were very similar and not found to be significantly different (Fig. 3.7d). Similarities remained at lower concentrations of LL-37, with 10 and 5 μg mL^{-1} also inducing lysis in both uninduced and induced cultures, but to a lesser extent so that cells recovered from more quickly. Between all three cultures, 2.5 μg mL^{-1} LL-37 had very little effect, with the growth being only very slightly below that of untreated (Fig. 3.7a,b&c). In summary, altering membrane fluidity of Δ*bkd* Δ*des* through precursor feeding or induction of *des* did not hugely impact *B. subtilis* susceptibility to LL-37. To enable a firm conclusion to be drawn surrounding the potential role of membrane fluidity in LL-37 activity, I decided to pursue further membrane fluidity altering techniques, in combination with LL-37 susceptibility testing.

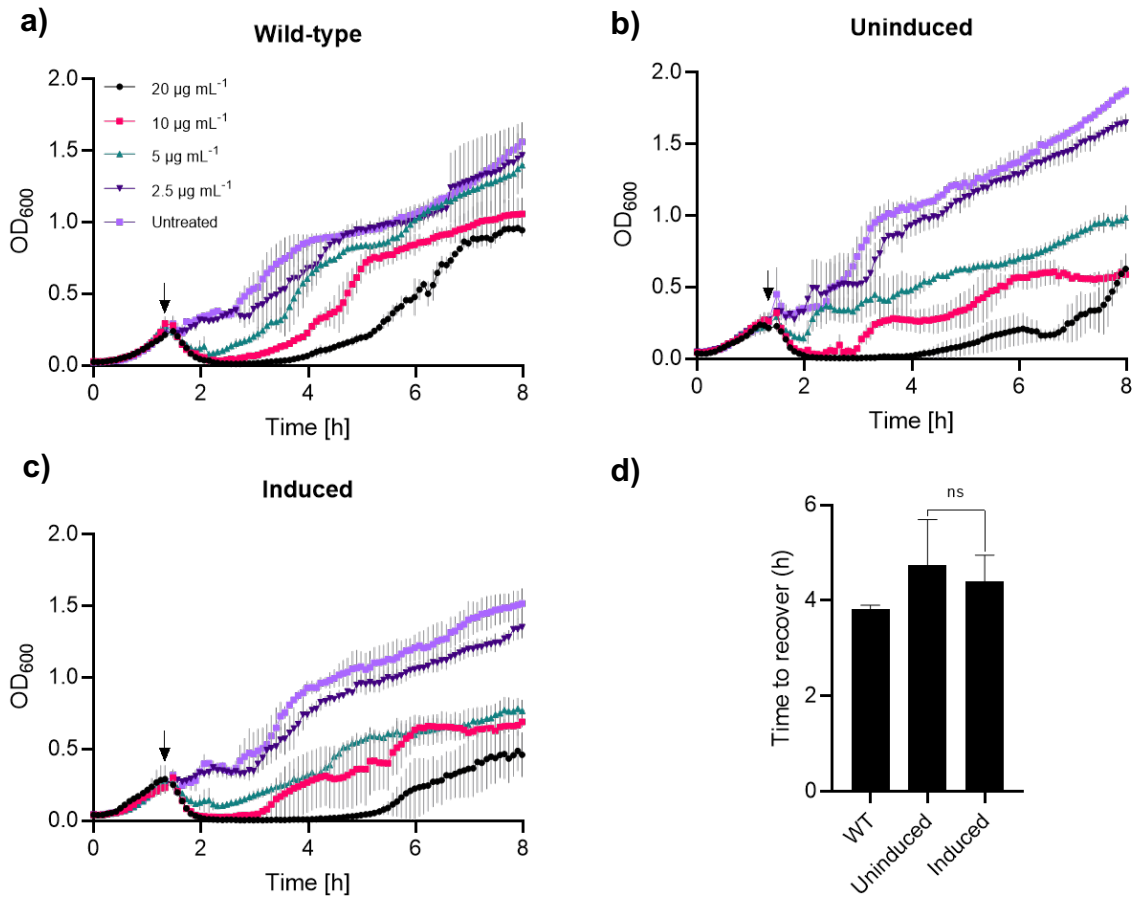

Figure 3.7. High membrane fluidity does not change susceptibility to LL-37. Growth/lysis of *B. subtilis* (**a**) wild-type, Δ*bkd* Δ*des* Pspac-*des* with 2-methylbutyric acid (MB) and *des* expression (**b**) uninduced and (**c**) induced by 1 mM IPTG, upon the addition of 20 µg mL^{-1} LL-37 (indicated by arrow) at 37 °C. **d**) Analysis of the time taken for each strain treated with 20 µg mL^{-1} LL-37 to recover to the initial optical density at which LL-37 was added; Δ*bkd* Δ*des* + MB with *des* expression un/induced analysed by unpaired two-tailed t-test, p value is not significant (ns). Data represented as mean±SD (n=3).

3.2.5 Membrane fluidity altered by temperature does not impact susceptibility to LL-37

I next used growth temperature as a proxy for membrane fluidity, as described by Seistrup (2018). I combined LL-37 susceptibility assays with growth at 30, 37 and 45 °C. As a control for generic AMP activity, this assay was also conducted with MP196. MP196 is a synthetic hexapeptide composed of six alternating residues of tryptophan and arginine residues; the structure of MP196 represents the minimal pharmacophore of positively charged and hydrophobic amino acids of cationic AMPs (Strøm *et al.*, 2003; Chantson *et al.*, 2006; Wenzel *et al.*, 2014). At all three temperatures both 20 and 10 µg mL^{-1} LL-37 induced lysis, whereas 5 µg mL^{-1} induced a slight growth inhibition (Fig. 3.8a). When treated with 2.5 µg mL^{-1} LL-37, cultures grown at the three temperatures all appeared unaffected, as their growth was very similar to that of the

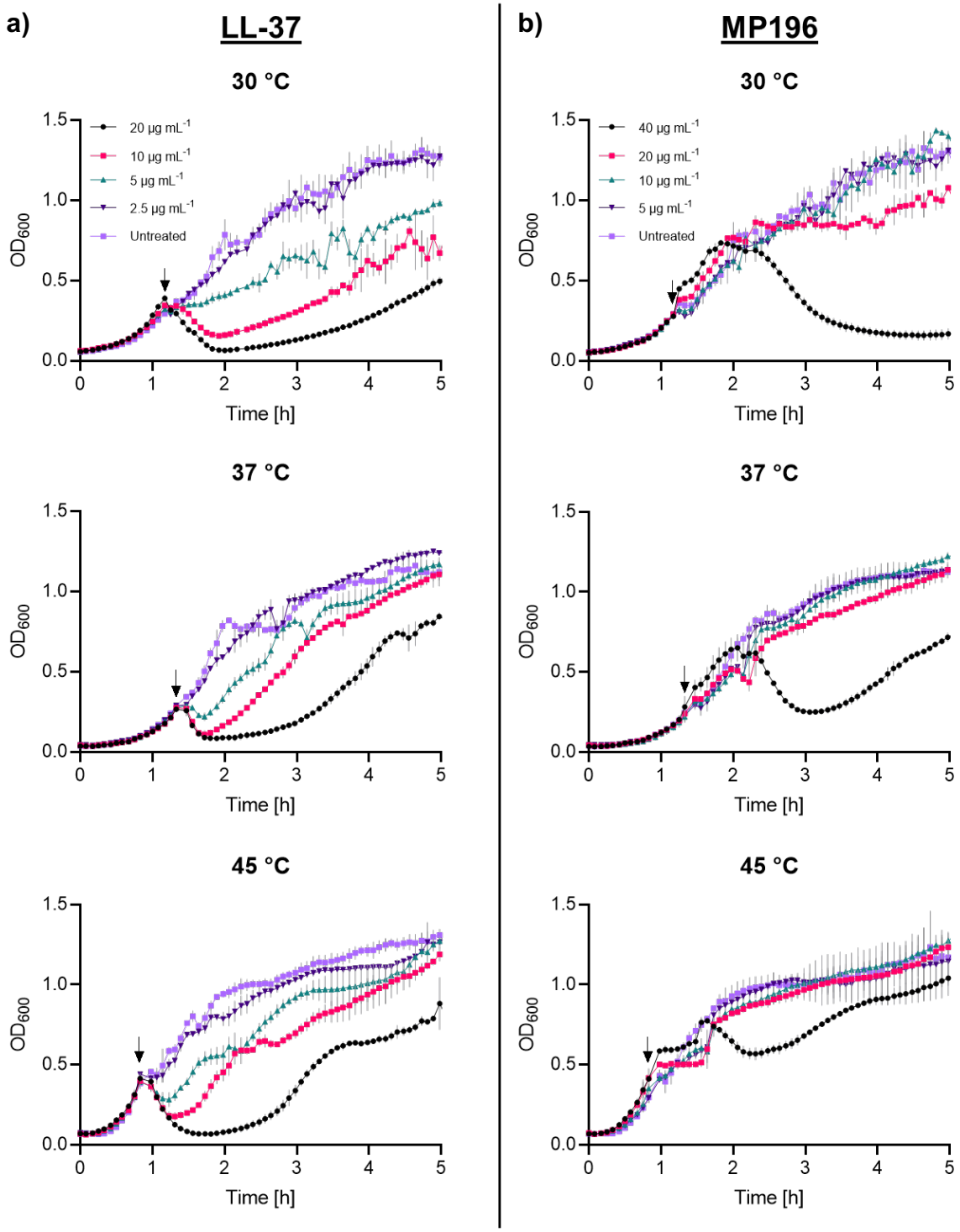

Figure 3.8. Fluidity altered by temperature has little impact on susceptibility to LL-37. Growth/lysis of *B. subtilis* wild-type grown at 30, 37 and 45 °C upon the addition of (**a**) LL-37 or (**b**) MP196 (indicated by arrow). Data represented as mean±SD (n=3).

untreated culture in each condition. Between the growth temperatures the notable difference was the time it took for cultures to recover their growth, the 30 °C culture recovered slower than the 37 °C whereas the 45 °C recovered more quickly. However, it wasn't pertinent to compare the time to recover of the different cultures as the varying

temperatures impact the growth rate of the cultures, which made the time to recover comparison an uninformative metric in this case (Ratkowsky *et al.*, 1982).

In contrast, the activity of MP196 varied with temperature. At 30 °C, the culture treated with the highest concentration of MP196 (40 μg mL^{-1}) exhibited continued growth for ~1 hour post-addition, followed by lysis from which the cells had not recovered by 5 hours (Fig. 3.8b). Additionally, 20 μg mL^{-1} MP196 also impacted the growth of *B. subtilis* at 30 °C – following continued growth for ~1 hour post treatment, this culture then exhibited slower growth relative to the lower concentrations and untreated cultures. At 37 °C, the same ~1 hour of continued growth occurred post-addition of 40 μg mL^{-1} MP196, followed by lysis, however the culture only lysed for ~1 hour before growth started to recover as the OD_{600} increased (Fig. 3.8b). At 37 °C there was also little difference between the growth of cultures treated with lower concentrations of MP196. At 45 °C, when membranes are most solid, 40 μg mL^{-1} MP196 instead caused ~1 hour of growth inhibition, before a small degree of lysis occurred, from which the culture rapidly recovered, with growth nearly akin to that of the untreated *B. subtilis* by 5 hours. Membrane fluidity, as controlled by temperature, did not impact the activity of LL-37 against *B. subtilis*, whereas it had a significant impact on the activity of the minimal pharmacophore MP196. MP196 against highly fluid membranes (30 °C) caused continued growth followed by dramatic lysis, and low fluidity (45 °C) led to immediate growth inhibition followed by a very low level of culture lysis from which growth could recover quickly.

3.2.6 Membrane fluidity altered by benzyl alcohol does not impact susceptibility to LL-37

Altering membrane fluidity through temperature can be confounded by the impact that temperature has on the growth rate of bacteria. Therefore, I decided to also employ benzyl alcohol as chemical means to assay the impact of membrane fluidity on LL-37 activity. Benzyl alcohol has been established as a membrane fluidiser, however there is limited information available on the concentrations to use and the effect these have on cells (Konopásek *et al.*, 2000; Strahl *et al.*, 2014). I decided to first investigate the impact of different concentrations of benzyl alcohol on the growth of *B. subtilis* via a MIC assay. This revealed the MIC of benzyl alcohol to be 50 mM, however the growth observed at this temperature was very limited – the wells appeared cloudy as opposed to the opaque cultures seen at lower concentrations (Fig. 3.9a). Due to the limited growth of cultures incubated with 50 mM benzyl alcohol, I decided to look at the

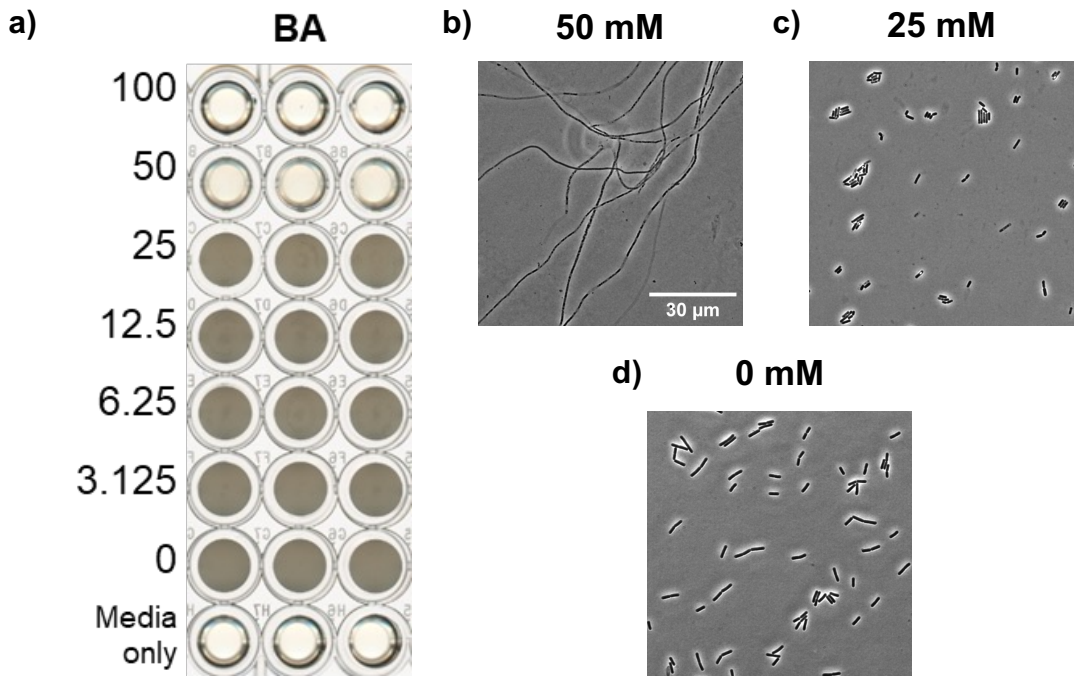

Figure 3.9. High concentrations of benzyl alcohol cause cells to become elongated and phase light, even higher concentrations inhibit growth. **a**) Minimum inhibitory concentration (MIC) assay of wild-type *B. subtilis* with 100, 50, 25, 12.5, 6.25, 3.125 and 0 mM benzyl alcohol (BA). Phase contrast microscopy of wild-type *B. subtilis* taken from the MIC assay wells grown with (**b**) 50 mM, (**c**) 25 mM and (**d**) 0 mM benzyl alcohol (BA); scale bar is 30 µm.

morphology of the cells. Cells from the MIC assay that had been incubated with 50 mM benzyl alcohol were very elongated and appeared phase light, indicating the cells had lysed (Fig, 3.9b). Whereas cells incubated with half that concentration, 25 mM benzyl alcohol, appeared much healthier, with a normal short, rod-shaped *B. subtilis* morphology similar to untreated (0 mM) cells (Fig. 3.9c&d).

Incubation with 50 mM benzyl alcohol resulted in elongated and phase light cells, suggesting these cells were able to initially grow, although in a chainy morphology, before eventually becoming phase light, indicating cell lysis (Fig. 3.9b). As, to the best of my knowledge, there is limited research on the effects of benzyl alcohol on growing cells, I wanted to better characterise the activity of benzyl alcohol before using it as a membrane fluidiser. To achieve this, I undertook microscopy with wild-type *B. subtilis* incubated with 50 mM benzyl alcohol and imaged the culture over time. The DNA-intercalating dye SYTOX Green was used as an indicator of cell permeabilisation, as it can only enter permeabilised cells and upon entering fluoresces when bound to DNA (Roth *et al.*, 1997). I used nisin as a positive control for permeabilisation, the rapid permeabilisation caused by nisin can be seen in the high SYTOX green signal it caused after 5 minutes of incubation with *B. subtilis* (Fig. 3.10). When *B. subtilis* was incubated

with benzyl alcohol, its morphology was akin to that of untreated cells for the first 30 minutes. By 1 hour of incubation, cells were slightly longer than untreated cells, this lengthening progressed over time with some cells at 4 hours of incubation appearing over ~5 times as long as untreated cells (Fig. 3.10). Alongside increased cell length, the *B. subtilis* treated with benzyl alcohol also became slightly leaky to SYTOX Green over time - by 4 hours of incubation with benzyl alcohol, faint SYTOX Green signals occurred within the cells (Fig. 3.10). The phase light cells seen in Fig. 3.8c are the end result of this elongated and increasingly leaky growth with 50 mM benzyl alcohol, showing cells incubated with this concentration whilst initially viable are increasingly unwell and eventually die.

Having established 50 mM as the maximum concentration of benzyl alcohol to use, I then combined benzyl alcohol, to increase membrane fluidity, with LL-37 susceptibility testing. This experiment was conducted at 30 °C, as this is the most fluidity-promoting temperature (Fig. 3.1). Wild-type *B. subtilis* was grown with a range of benzyl alcohol concentrations (6.25 – 50 mM), before antimicrobials were added once OD_{600} reached 0.3 – 20 μg mL^{-1} of either LL-37 or MP196. I again tested MP196 susceptibility alongside, as its fluidity-dependent activity (seen in Fig. 3.8b) could function as a positive control in this experiment. When *B. subtilis* was grown with benzyl alcohol alone, 6.25 and 12.5 mM benzyl alcohol had no impact on growth, with the OD_{600} following that of the 0 mM culture (Fig. 3.11a). 25 mM benzyl alcohol caused a slight slowing of growth, but the culture was still able to achieve stationary phase; whereas *B. subtilis* grown with 50 mM benzyl alcohol, whilst initially able to grow slowly, soon started to lyse (indicated by a decrease in OD_{600}; Fig. 3.11a). This aligns with what was seen in Fig. 3.9b and Fig. 3.10, where cells have initially grown to achieve a chainy phenotype, but then lysed to give phase light cells.

When 20 μg mL^{-1} LL-37 was added to the cultures grown with benzyl alcohol, the previously seen LL-37-induced rapid lysis and recovery dynamics (Fig. 3.2a) occurred with 0, 6.25 and 12.5 mM benzyl alcohol (Fig. 3.11b). When 25 mM benzyl alcohol was present recovery was delayed, but the culture was able to recover its growth, as indicated by the eventual increase in OD_{600}. When 50 mM benzyl alcohol and the addition of 20 μg mL^{-1} LL-37 were combined, the culture could not recover following lysis. Whereas with 20 μg mL^{-1} MP196, all cultures grown with benzyl alcohol were more sensitive to MP196. The cultures grown with 6.25 and 12.5 mM benzyl alcohol exhibited longer growth inhibition and slower recovery of growth relative

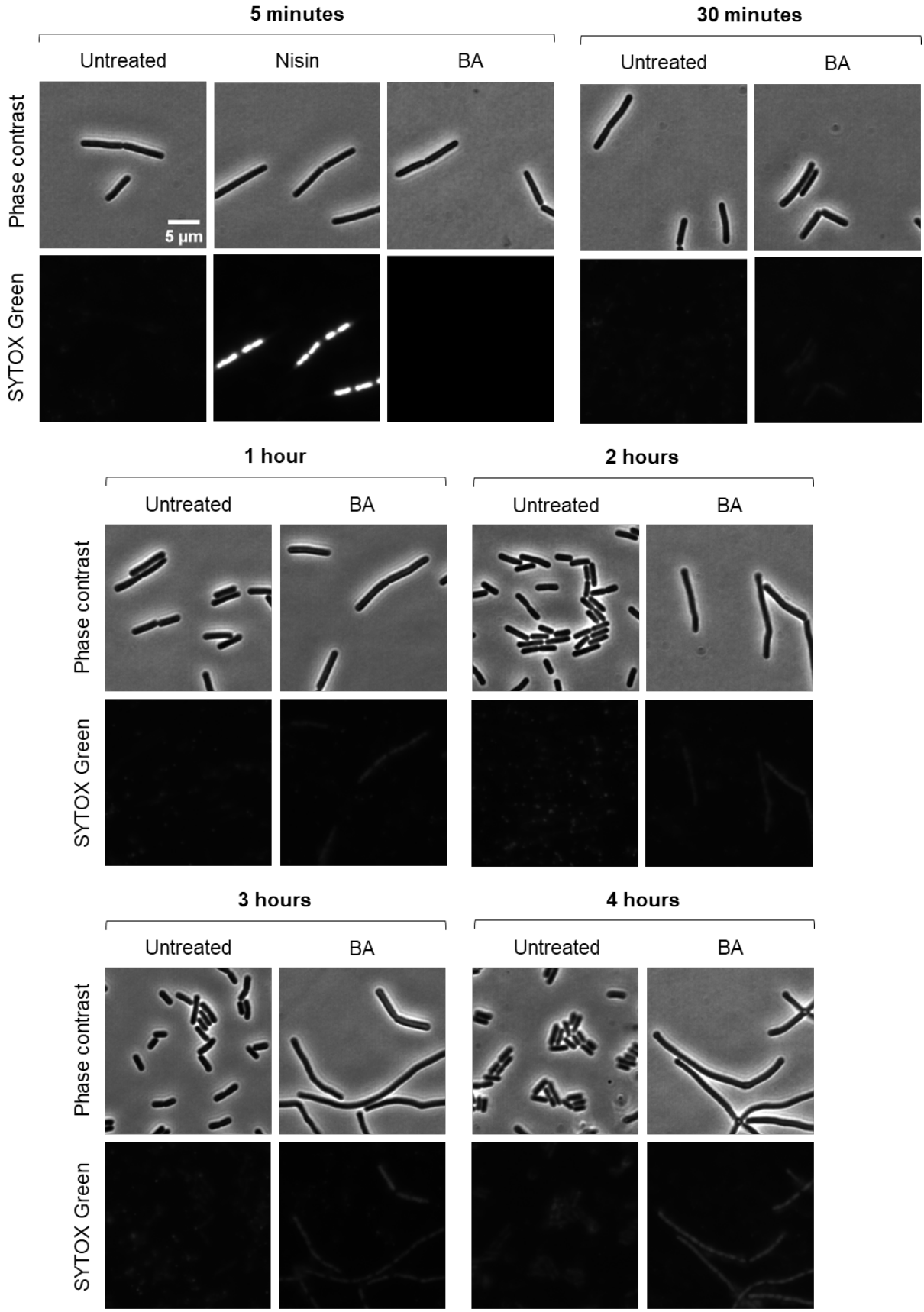

Figure 3.10. Incubation with benzyl alcohol causes *B. subtilis* cells to become elongated and leaky over time. Time-course phase contrast and fluorescent microscopy of wild-type *B. subtilis* untreated or incubated with 50 mM benzyl alcohol (BA), stained with 200 nM SYTOX Green. Nisin (5 µM) used as a positive control for membrane permeabilisation; scale bar is 5 µm (figure best viewed digitally).

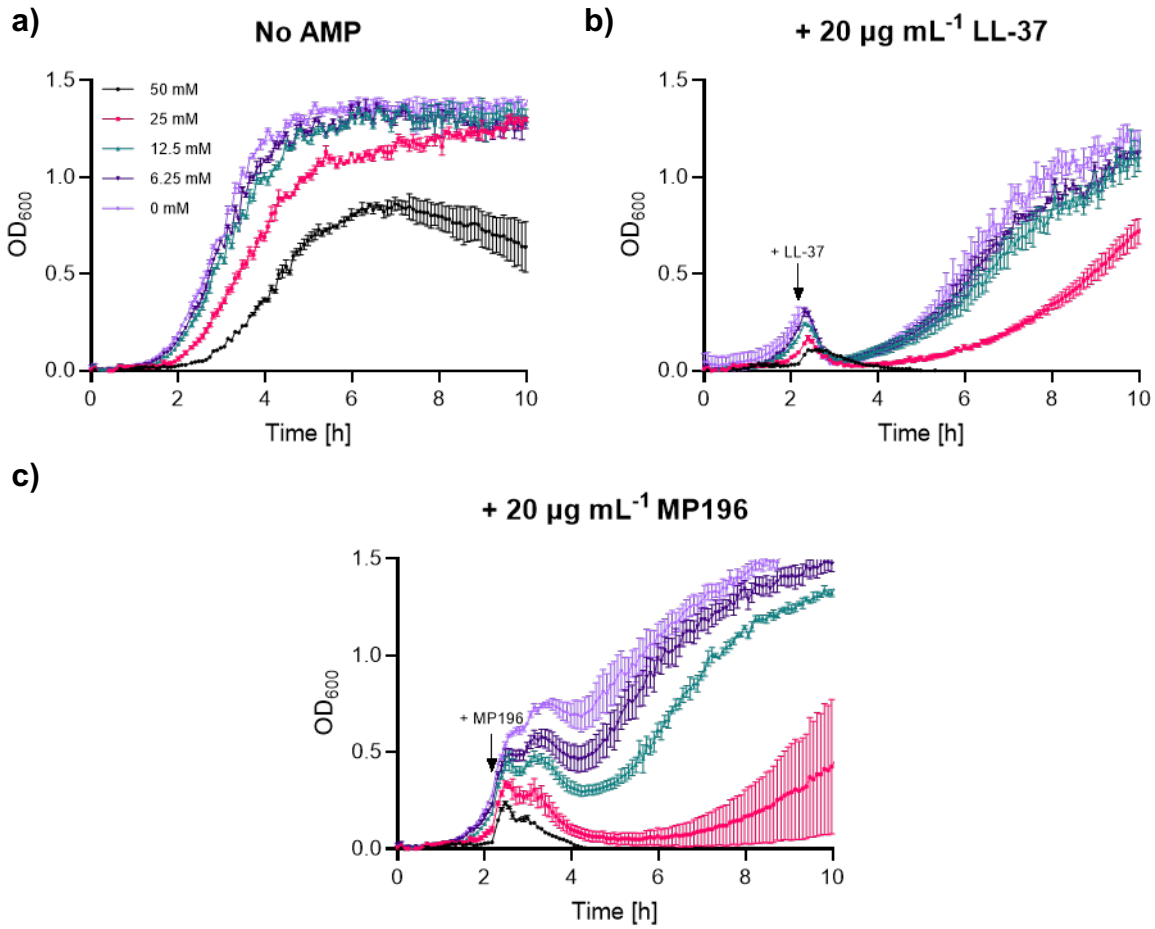

Figure 3.11. High fluidity induced by benzyl alcohol has little impact on susceptibility to LL-37 but enhances MP196 activity. Growth/lysis of *B. subtilis* wild-type grown with 50, 25, 12.5, 6.25 and 0 mM benzyl alcohol at 30 °C, either (**a**) without the addition of an AMP, or upon the addition of (**b**) 20 µg mL^{-1} LL-37 or (**c**) 20 µg mL^{-1} MP196 (addition indicated by arrow). Data represented as mean±SD (n=3).

to the 0 mM benzyl alcohol culture (Fig. 3.11c). With 20 mM benzyl alcohol, lysis by MP196 was extended and recovery of culture growth was very delayed. The combination of 50 mM benzyl alcohol and 20 µg mL^{-1} MP196 was lethal, as was also the case with LL-37, with lysis occurring from which the culture could not recover (Fig. 3.11c). Altogether, high membrane fluidity, as induced by benzyl alcohol, significantly altered the activity of the synthetic pharmacophore MP196 but not the cathelicidin LL-37, confirming with the previous fluidity-altering techniques that LL-37 activity is not impacted by membrane fluidity.

3.2.7 Lysyl-phosphatidylglycerol protects S. aureus but not B. subtilis from LL-37

I next wanted to transfer the observations I had made in *B. subtilis* to the pathogenic Gram-positive species *S. aureus*. I started by comparing what was already known in *S. aureus* with the new findings I had made in *B. subtilis* regarding L-PG content and

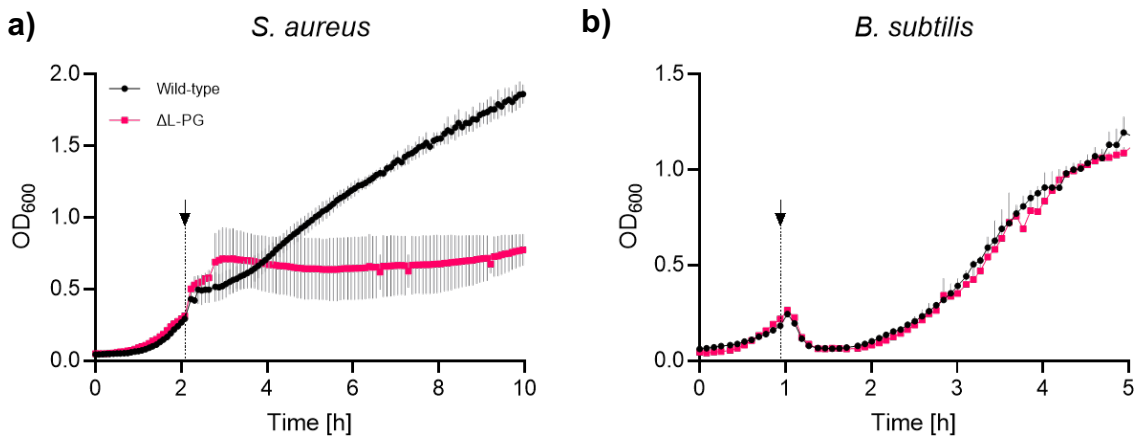

Figure 3.12. Lysyl-phosphatidylglycerol protects *S. aureus* but not *B. subtilis* from LL-37. Growth/lysis of wild-type and ΔL-PG (**a**) *S. aureus* in MHB treated with 100 μg mL^{-1} LL-37, and (**b**) *B. subtilis* in LB treated with 20 μg mL^{-1} LL-37; addition of LL-37 indicated by arrow. Data represented as mean±SD (n=3).

protection. To define the difference in protection conferred by L-PG to *B. subtilis* and *S. aureus*, growth/lysis assays of the two species, with wild-type and ΔL-PG strains, were undertaken. This confirmed that whilst L-PG is extremely protective in *S. aureus* – a strain lacking L-PG was unable to recover growth after 8 hours (Fig. 3.12a); the loss of L-PG causes no discernible difference from wild-type susceptibility in *B. subtilis* – ΔL-PG underwent the same degree of LL-37 induced lysis as wild-type (Fig. 3.12b).

Due to CL conferring a slight protective effect against LL-37 in *B. subtilis* (Fig. 3.2a), I investigated whether this may also be the case in *S. aureus*. To achieve this, a strain lacking the CL synthases Cls1 and Cls2 was used, ΔCL. However, it was not possible to observe any differences between wild-type and ΔCL *S. aureus*, as the LL-37 MIC of wild-type *S. aureus* was already above the maximum concentration used in the assay (Table 3.2). The limitations of observing wild-type *S. aureus* susceptibility to LL-37 in our laboratory meant that for the remainder of this project, *S. aureus* ΔL-PG was used to study the mechanism of action of LL-37 in *S. aureus*.

Table 3.2. Minimum inhibitory concentration of LL-37 against *S. aureus* (n=3).

***S. aureus* strain**	**LL-37 MIC** (μg mL^{-1})
Wild-type (SH1000)	>100
ΔCL (SH1000)	>100
Wild-type (SA113)	>100
ΔL-PG (SA113)	40

3.2.8 *S. aureus* treated with LL-37 dies, but does not lyse to the same extent as *B. subtilis*

I next wanted to establish the medium in which to grow *S. aureus* ΔL-PG and to define the effect of different concentrations of LL-37 against the strain. I compared the growth/lysis caused by a range of LL-37 concentrations against wild-type and ΔL-PG *S. aureus* in TSB and MHB. TSB is an established and preferred growth medium for *S. aureus* (Missiakas & Schneewind, 2013). Whereas MHB is the medium recommended for MIC testing by the European Committee on Antimicrobial Susceptibility Testing (EUCAST) and the Clinical & Laboratory Standards Institute (CLSI) (Kowalska-Krochmal & Dudek-Wicher, 2021). In both media against wild-type *S. aureus*, LL-37 had no discernible impact on the growth of the cultures, with the cultures treated with 100 μg mL^{-1} growing as well as untreated (Fig. 3.13). In TSB, LL-37 only had a little effect against ΔL-PG *S. aureus*, 100 μg mL^{-1} LL-37 caused temporary growth inhibition, from which the cells promptly resumed growing after ~2 hours, cultures treated with lower concentrations grew as well as untreated (Fig. 3.13). Whereas, in MHB ΔL-PG *S. aureus* was significantly more susceptible to LL-37, with

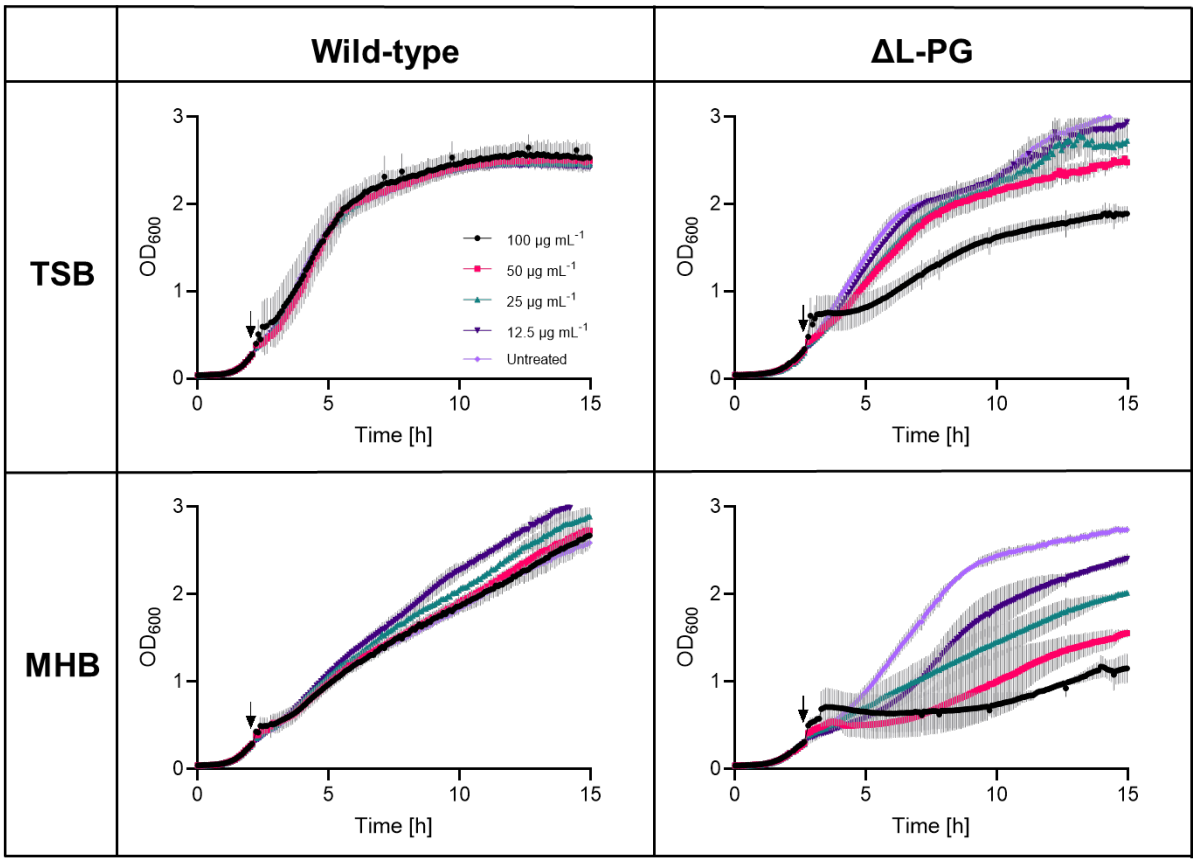

Figure 3.13. The antimicrobial effect of LL-37 is only seen against ΔL-PG *S. aureus* grown in MHB. Growth/lysis of wild-type (SH1000) and ΔL-PG *S. aureus* in TSB and MHB treated with 100, 50, 25, 12.5 and 0 μg mL^{-1} LL-37; addition of LL-37 indicated by arrow. Data represented as mean±SD (n=3).

reduced growth occurring in all cultures treated with LL-37 compared to wild-type. Both 12.5 and 25 μg mL^{-1} LL-37 caused *S. aureus* ΔL-PG to exhibit slower growth, from which the cultures had not reached the same OD_{600} as wild-type by the end of the experiment (~12 hours post LL-37 addition; Fig. 3.13). The higher 50 and 100 μg mL^{-1} LL-37 concentrations caused growth inhibition, lasting ~3 hours and ~10 hours, respectively. The clear effects of LL-37 observed against *S. aureus* ΔL-PG in MHB, led me to continue using MHB as the medium in which to grow *S. aureus* for the remainder of this project.

LL-37 significantly impacted the growth of *S. aureus* ΔL-PG, causing prolonged growth inhibition (Fig. 3.13). However, I noticed that whilst the effect was dramatic, it differed from the effect LL-37 had on *B. subtilis*. *B. subtilis* lysed when treated with LL-37, indicated by a decrease in OD_{600} (Fig. 3.2a), whereas the OD_{600} of *S. aureus* did not decrease (Fig. 3.12a), suggesting growth inhibition rather than lysis. To examine whether this was the case, I undertook a viability assay, in which the OD_{600} and c.f.u. of cultures are followed over time – with OD_{600} to indicate cell lysis, and c.f.u. to indicate cell death. When *S. aureus* ΔL-PG was treated with 25 μg mL^{-1} LL-37 (added at 0 hours) the culture was able to continue growing for the first 30 minutes, shown by the OD_{600} of the culture increasing to the same extent at untreated cells (Fig. 3.14a). The culture then exhibited the same growth inhibitory effect observed previously, as the OD_{600} neither significantly increased nor decreased for ~4 hours. However, the viability of the same culture indicated the *S. aureus* cells were indeed dying, as the c.f.u. mL^{-1} of the culture decreased rapidly upon exposure to LL-37, and only started to recover ~4 hours after LL-37 addition (Fig. 3.14b). Altogether, this assay showed that whilst *S.*

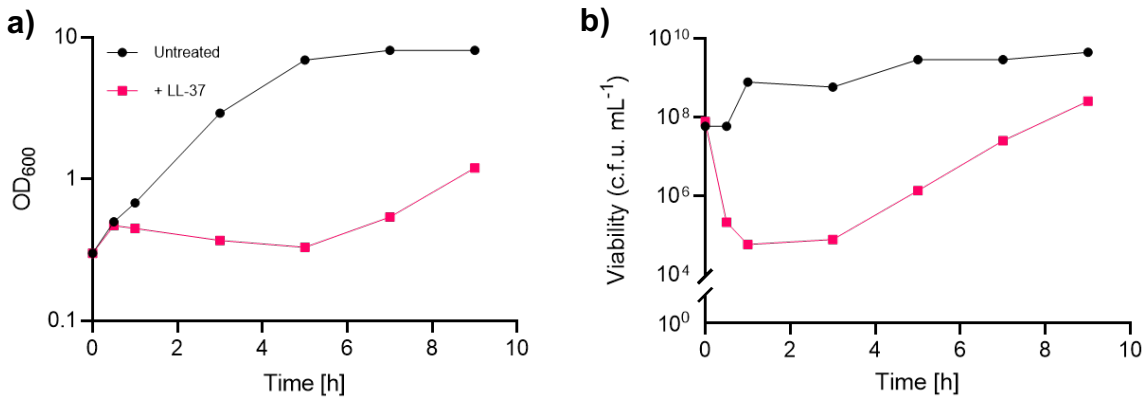

Figure 3.14. *S. aureus* cells die but do not lyse when treated with LL-37. **a**) Growth/lysis of *S. aureus* ΔL-PG treated with 25 μg mL^{-1} LL-37, and (**b**) viability measurements taken at the same time points, colony forming units (c.f.u.) were calculated via serial dilution and spot assay of the cultures.

aureus cells do not lyse when treated with LL-37, they do die, meaning LL-37 is bactericidal against *S. aureus* in a manner that is independent of cell lysis.

3.2.9 A S. aureus membrane fluidity control strain requires further research

To replicate the membrane fluidity experiments I conducted in *B. subtilis*, I wanted to establish a method comparable to *B. subtilis* Δ*bkd* Δ*des* in *S. aureus*. *S. aureus* has a similar BCFA synthesis pathway to *B. subtilis*, so a tuneable lipid composition strain should be achieved by a similar deletion in the *bkd* operon; additionally, *S. aureus* has not been found to encode a *des* desaturase so Δ*bkd* should be sufficient (Singh *et al.*, 2008). A strain with these requirements was constructed by Singh *et al.* (2008), this was achieved via the insertional activation of *lpdA* in the BKD operon, I have denoted this strain as Δ*lpdA*. I requested this strain to test whether it would have the same BCFA auxotrophy as *B. subtilis* Δ*bkd* Δ*des*, and thus could have its membrane fluidity altered by BCFA precursor feeding.

I first wanted to establish the best growth medium for this strain, as Δ*bkd* Δ*des* requires a minimal medium to ensure specific BCFA precursor feeding, I needed a similar medium for *S. aureus* Δ*lpdA* (Gohrbandt *et al.*, 2022). I compared growth in rich LB medium with two minimal media, SMM adapted for *S. aureus* and CDM (Spizizen, 1958; Machado *et al.*, 2019). Growth of wild-type in LB was dense with the typical yellow colour conferred by staphyloxanthin (Fig 3.15a; Pelz *et al.*, 2005). This yellow pigment also occurred in wild-type grown in CDM, whereas it was weak when grown in SMM. A similar robust growth occurred with Δ*lpdA* in LB, with CDM also supporting better growth than SMM (Fig. 3.15a). I decided to take CDM forward as the minimal medium in which to grow Δ*lpdA*, as it supported better growth than SMM and is an established minimal medium for growth of *S. aureus* (Machado *et al.*, 2019). To test the potential auxotrophy of *ΔlpdA* for BCFA precursors, I grew *ΔlpdA,* and wild-type *S. aureus* on CDM plates containing either no precursor or MB at 15, 22, 30 and 37 °C. I tested growth at 15 °C as *S. aureus* can grow better at lower temperatures than *B. subtilis*, meaning its membrane fluidity should be tested at a wider range of temperatures (Schmitt *et al.*, 1990). At 20, 30 and 37 °C, *ΔlpdA* growth was comparable to that of wild-type on precursor free plates, with thick streaks of growth on the plates (Fig. 3.15b). Only at 15 °C did *ΔlpdA* struggle to grow on precursor free CDM, whereas when MB was present the culture streak grew to a similar degree as wild-type. However, *ΔlpdA* was still able to somewhat grow at this temperature, compared with the complete lack of growth of *B. subtilis* Δ*bkd* Δ*des* at 20 °C, causing concern that

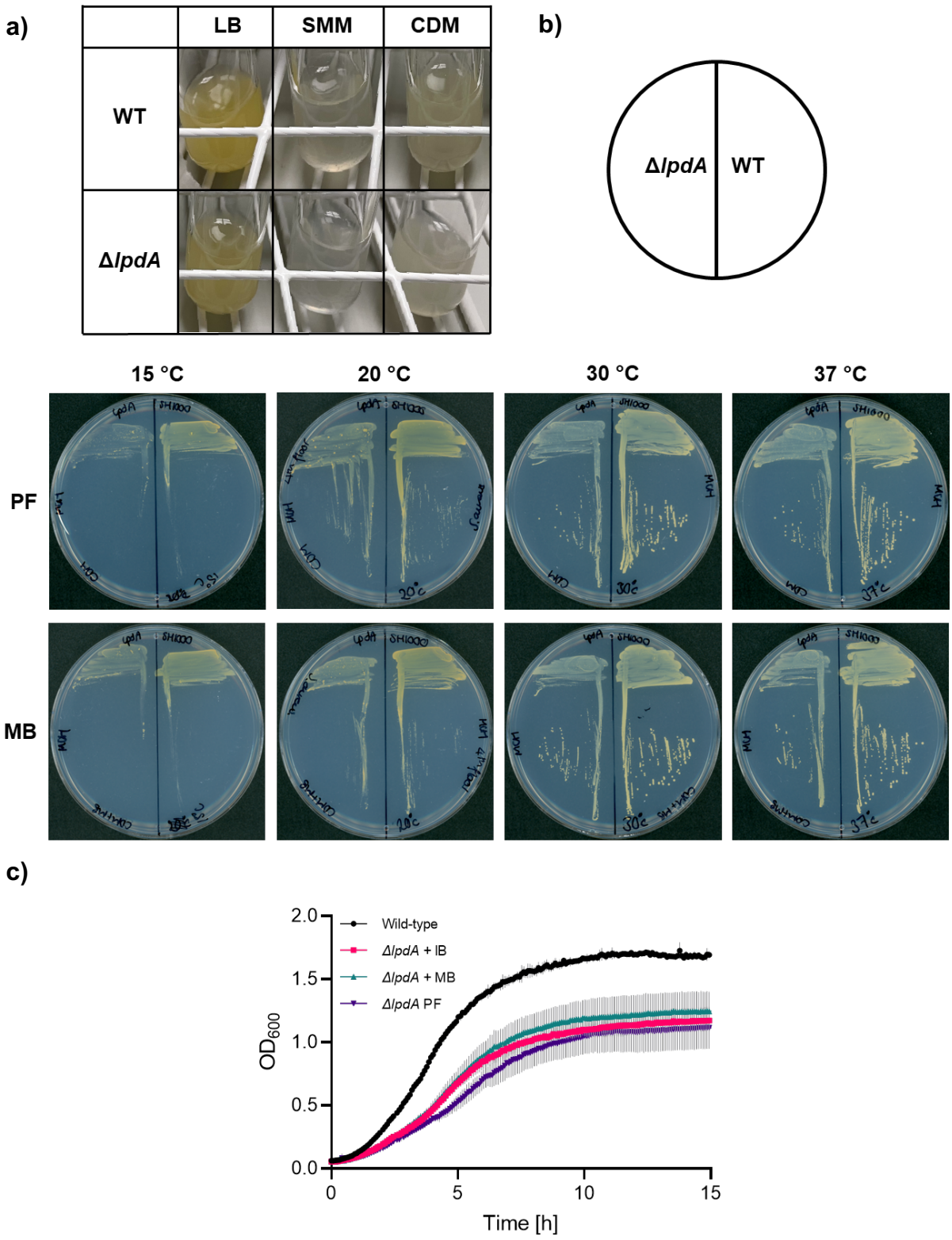

Figure 3.15. Growth of Δ*lpdA S. aureus* is not dependent on BCFA precursors. **a**) Overnight liquid growth of *S. aureus* SH1000 and *ΔlpdA* in LB, fortified SMM and CDM, *ΔlpdA* was supplemented with BCFA precursors. **b**) Solid growth of SH1000 and *ΔlpdA* on CDM plates either precursor free (PF) or containing 2-methylbutyric acid (MB), at 15, 20, 30 and 37 °C. **c**) Growth of SH1000 and *ΔlpdA* in CDM media, with the addition of isobutyric acid (IB), MB and PF; data represented as mean±SD (n=3).

ΔlpdA was not completely auxotrophic for BCFA precursors. Due to this, I conducted growth curves of *ΔlpdA* in CDM with and without precursors to visualise its growth. *ΔlpdA* was grown at 37 °C in CDM, with wild-type *S. aureus* used a positive control for healthy growth. This assay revealed no difference in growth between *ΔlpdA* supplemented with IB, MB or no BCFA precursor (Fig. 3.15c), indicating *ΔlpdA* is not an auxotroph for BCFA precursors, as it is able to grow in their absence.

The lack of BCFA auxotrophy in *ΔlpdA* caused me to use genomic sequencing to verify if there was indeed an insertion within *lpdA* to inactivate its activity in the BKD complex. The genomic DNA of wild-type and *ΔlpdA* was sequenced and the genomes were analysed for insertions, deletions, and structural variants. This analysis confirmed the presence of an insertion in the *lpdA* gene of the *ΔlpdA* strain, as no reads extended through the region in which the insertion was identified, whereas in wild-type, multiple reads traversed the insertion site (Fig. 3.16). Due to the surprising lack of BCFA auxotrophy in *ΔlpdA*, despite the confirmed insertion, I did not pursue using this strain

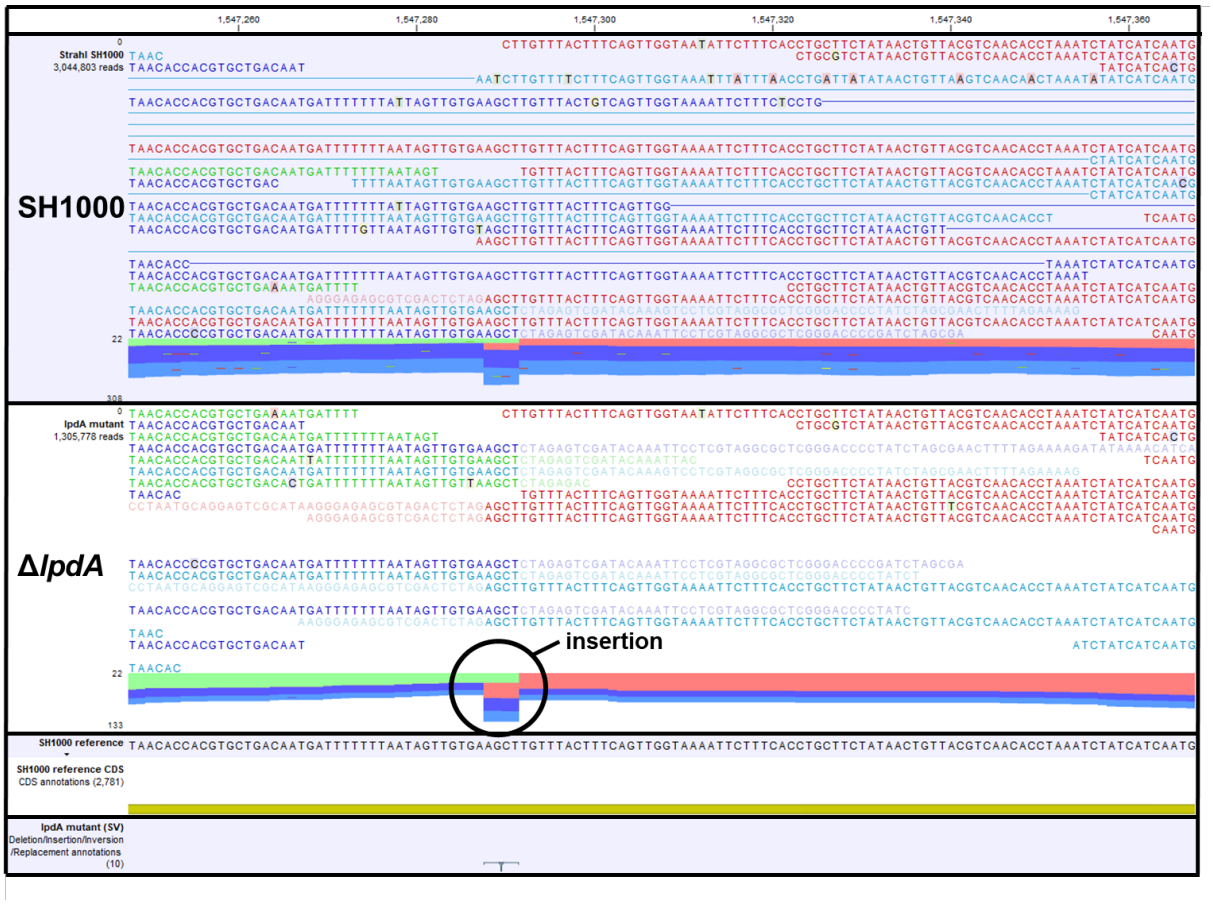

Figure 3.16. *S. aureus* Δ*lpdA* contains an insertion in *lpdA*. Sequence analysis of wild-type (SH1000) and Δ*lpdA* *S. aureus* using CLC Genomics Workbench (Qiagen), a threshold of >50% occurrences was set for detection of insertions/deletions/structural variants.

in combination with LL-37 susceptibility, as it would not give the same insights as *B. subtilis* Δ*bkd* Δ*des*. I instead focused on investigating the mechanism of action of LL-37 for the remainder of my project, as described in chapters 4 and 5. Altogether, more research is need for the development of fatty acid modification strains in *S. aureus*.

3.3 Discussion

The protective role of L-PG against cationic AMPs has been established in a range of Gram-positive and Gram-negative bacteria, including the pathogenic species *S. aureus* and *P. aeruginosa* (Ernst & Peschel, 2011; Golla *et al.*, 2020). L-PG confers a positive charge to the cytoplasmic membrane via the presence of a cationic lysine on PG (Staubitz & Peschel, 2002). In this chapter, I aimed to define whether L-PG also conferred a protective effect against the cathelicidin LL-37 in *B. subtilis* and looked into the role of other membrane lipid head groups in susceptibility to LL-37. By establishing the similarities between *B. subtilis* and pathogenic Gram-positive species, the suitability of using *B. subtilis* as a model organism for investigating LL-37 susceptibility against Gram-positives can be established. Investigating the role of other membrane lipid head groups also extends the current research, which mainly focuses on L-PG, to the wider composition of bacterial membranes and cationic AMP interactions.

MIC and lysis/growth assays revealed L-PG conferred no protection against LL-37, as strains lacking L-PG were equally susceptible to LL-37 in both the MIC of LL-37 and lysis/growth profiles (Table 3.1, Fig. 3.2). This contrasts with other Gram-positive bacteria, including the closely related species *B. anthracis* and also *S. aureus*, in which L-PG has been observed to protect against LL-37 (Fig. 3. 12a; Ernst & Peschel, 2011). In *B. anthracis*, L-PG deficient cells were found to be ~360-fold more susceptible to LL-37 than wild-type, contrasting with the lack of any increase in susceptibility I observed in *B. subtilis* (Samant *et al.*, 2009). The lack of any protection conferred by L-PG in *B. subtilis* against LL-37 is surprising and suggests differences in the interaction of LL-37 with different bacterial species. The lipid compositions of *B. subtilis* and *S. aureus* have been characterised as follows (Koch *et al.*, 1984; Matsuoka *et al.*, 2011):

Table 3.3 Membrane lipid composition of *B. subtilis* and *S. aureus*. As described by Koch *et al*. (1984) and Matsuoka *et al*. (2011). Included are phosphatidylglycerol (PG), phosphatidylethanolamine (PE), glycolipids (GL), lysyl-PG (L-PG) and cardiolipin (CL). PE is not produced by *S. aureus* (Hines *et al*., 2020).

Membrane Lipid	***B. subtilis*** (%)	***S. aureus*** (%)
PG	37.5	50.4
PE	30.5	-
GL	16.9	32.7
L-PG	7.8	9.9
CL	4.5	1.1

There is not a large difference in the amount of L-PG present in the cell envelopes of *B. subtilis* and *S. aureus* (Table 3.3). Suggesting the difference in protection conferred by L-PG in the two species is not due to the proportion of L-PG present in the membrane. Hence, it is not immediately clear why the L-PG protective mechanism, which is so efficient in *S. aureus* and *B. anthracis*, is not effective in *B. subtilis*.

In the growth/lysis assay with membrane lipid deficient strains, I also observed a slight improvement in recovery from LL-37 when CL was deleted (Fig. 3.2a); this protection was not sufficient to increase the MIC of LL-37 (20 μg mL^{-1}, same as wild-type), but did significantly reduce the time taken for cultures to recover (Fig. 3.2b). CL is anionic and has four fatty acid tails, this confers a conical shape to the phospholipid and so is thought to cause preferential localisation of CL at the cell poles and septal regions – this has been observed in *B. subtilis* and *E. coli* (Mileykovskaya & Dowhan, 2000; Kawai *et al.*, 2004; Muchová *et al.*, 2011). Previous visualisation of LL-37 attack on single *E. coli* cells revealed preferential attack on septating cells (Kristian *et al.*, 2007; Sochacki *et al.*, 2011). It may be that LL-37 has some preference for either regions of negative curvature, such as the cell poles and septa, or for CL itself – as CL is anionic and LL-37 is cationic this is possible. However, there are two more recent findings that negate this hypothesis. Firstly, similar visualisation of LL-37 attack on single *B. subtilis* cells did not observe the same preference for septal regions (Barns & Weisshaar, 2013). Secondly, the technique used to identify CL domains at the septa of *B. subtilis* by Kawai *et al*. (2004) has recently been shown to be flawed in its specificity for CL in *B. subtilis* and *E. coli*. This research found that the dye thought to preferentially strain

CL does not exhibit the same lipid species specificity in *B. subtilis*; and in *E. coli* it was shown that the domains bound are anionic phospholipid rather than solely CL (Oliver *et al.*, 2014; Pogmore *et al.*, 2018). Altogether, these factors make it difficult to draw a firm conclusion behind why the lack of CL is protective in *B. subtilis*. A surprising link between LL-37 and CL was also observed recently, as LL-37 exposure was found to increase the proportion of CL in *S. aureus* by 32% (Ledger *et al.*, 2022). This suggests in *S. aureus* upregulation of CL may confer protection, opposing the protective effect of CL loss I observed in *B. subtilis* (Fig. 3.2). These contrasting findings highlight the future need to directly investigate the role of CL in *S. aureus* susceptibility to LL-37, something I was unable to achieve due to concentration limits with the media and strains I was using (Table 3.2).

The increased susceptibility of the *B. subtilis* GL deficient mutant (Table 3.1, Fig. 3.2) immediately led me to look into the role of teichoic acids in susceptibility to LL-37, as GLs function as the lipid anchor for LTAs (Toon *et al.*, 1972). In GL mutants, LTAs are still synthesised but are anchored directly to the membrane, as opposed to through the GL DAG (Salzberg & Helmann, 2008). This change to anchoring could impact the localisation or number of LTAs in the membrane, changes to either of which would make the GL deficient strain more susceptible to LL-37 if LTAs protect against it. The increased susceptibility of WTA and LTA deficient strains confirmed that teichoic acids confer protection against LL-37 in *B. subtilis* (Fig. 3.3). The inability of either culture to recover to the initial OD_{600} at which LL-37 was added over the ~6 hours post addition, shows both WTA and LTA contribute to protection from LL-37 (Fig. 3.3b&c). To ensure the increased susceptibility of the WTA deficient strain is due to WTA-conferred protection, and not the general unwellness of the sick phenotype of these cells (Soldo *et al.*, 2002), it would be informative to repeat this experiment with an antimicrobial with a distinct mechanism of action that should be unaffected by teichoic acid composition such as valinomycin, a potassium ionophore (Huang *et al.*, 2021). However, we know so little mechanistically about how teichoic acids may protect against membrane targeting antibiotics that it is not straightforward to rule out that WTA deficiency would not impact the activity of valinomycin against the membrane. The difference in localisation of WTA and LTA also makes my observations interesting; WTAs are anchored to peptidoglycan and LTAs are anchored to the cytoplasmic membrane, it remains unclear whether LTAs lay against the cytoplasmic membrane or extend through the peptidoglycan cell wall (Brown *et al.*, 2013; Percy & Gründling, 2014). Both

WTA and LTA conferring protection indicates that whatever their localisation, both are protecting the cell from LL-37; however, due to the lethality of a double deletion, it is not possible to test the role of teichoic acids altogether (Schirner & Errington, 2009).

I observed that protection conferred by teichoic acids is supported by D-alanylation (Fig. 3.4), this mechanism has been seen to confer protection to LL-37 and other cationic antimicrobials in other Gram-positive species such as *Streptococcus* and *S. aureus* (Collins *et al.*, 2002; Saar-Dover *et al.*, 2012). As D-alanine residues are positively charged, their decoration on anionic teichoic acid polymers can reduce the net negative charge of the cell envelope, and in doing so reduce the affinity of cationic LL-37 for the cell (Wecke *et al.*, 1997). Investigating the role of teichoic acids in *S. aureus* is complicated by the essentiality of LTA in this species, indicated by the lethality of a *ltaS* deletion (Gründling & Schneewind, 2007b). However, *S. aureus* LTA content can be reduced by a *ypfP* deletion, the gene responsible for the synthesis of the GL anchor of LTA (Gründling & Schneewind, 2007a). It was found that Δ*ypfP* in the SA113 strain background causes an 87% reduction in LTA relative to wild-type (Fedtke *et al.*, 2007). WTA in *S. aureus* is not essential, and its synthesis can be abolished via deletion of *tagO* (Weidenmaier *et al.*, 2004). To ensure the protection by teichoic acids I observed in *B. subtilis* (Fig. 3.3&4), and other previous research has observed against similar AMPs, also occurs in *S. aureus*, susceptibility to LL-37 should be assayed with *S. aureus* Δ*ypfF*, Δ*tagO* and Δ*dltA*.

Defining the cell envelope composition that impacts susceptibility to membrane-targeting antimicrobials, such as LL-37, is important as it allows informed approaches in enhancing their antibacterial activity. For example, recent work by Slavetinsky *et al*. (2022) developed monoclonal antibodies that target *S. aureus* MprF, the L-PG synthase, preventing its transport activity and so reducing the L-PG content of the outer leaflet of the cytoplasmic membrane. This inhibition of MprF reduced *S. aureus* survival of 45 μg mL^{-1} LL-37 from 100% to less than 50% in the presence of antibody. This technique also restored susceptibility in a daptomycin-resistant clinical isolate of *S. aureus* (Slavetinsky *et al.*, 2022). It should be a priority, not just for fundamental understanding but also clinical outcomes, to continue elucidating the relationship between membrane and cell wall composition and membrane-targeting antimicrobial activity.

The lack of any change in susceptibility when membrane fluidity was altered was surprising and negates one of the main hypotheses of my project. I proposed that the

increased disorder and the related decreased lipid packing density of more fluid membranes would enhance interaction and penetration of LL-37 into the cytoplasmic membrane and so increase susceptibility. However, the summary of 4 distinct approaches indicates fluidity is not a factor in LL-37 susceptibility, whereas it appears to modulate the activity of the minimal pharmacophore MP196 (Fig 3.6,7,8&10). In previous research using model membranes, it was shown that the mechanism of action of LL-37 alters depending on the fatty acid structure of the membrane, with UFAs promoting pore formation and SFAs promoting lipid-clustering; interestingly, they observed that changing the temperature, and so fluidity, of UFA and SFA bilayers did not alter this FA-dependent activity, which is in agreement with my finding that LL-37 activity is not fluidity dependent (Shahmiri *et al.*, 2016).

Investigation of the role of *S. aureus* membrane fluidity in antimicrobial susceptibility is enigmatic, with different studies drawing opposing conclusions. Investigation into the resistance of *S. aureus* to thrombin-induced platelet microbial protein 1 (tPMP-1) found that increased fluidity was associated with protection from tPMP-1 (Bayer *et al.*, 2006). However, research using *S. aureus* cells, protoplasts and liposomes found that more rigid membranes protected against tPMP-1, in addition to another AMP hNP-1 (Xiong *et al.*, 2005). To follow my research in *B. subtilis* membrane fluidity with similar approaches in *S. aureus*, more dedicated work needs to go into establishing a complete *S. aureus* BCFA auxotroph, as opposed to the non-auxotroph Δ*lpdA* (Fig. 3.15). I was aware when using Δ*lpdA* that it may not have complete BCFA auxotrophy, as the research that constructed the strain found Δ*lpdA* had reduced, not abolished, BCFA synthesis – BCFA content was reduced from 63.5% in wild-type to 35.4% in Δ*lpdA* (Singh *et al.*, 2008). This indicates *S. aureus* encodes another means to synthesise BCFA. Subsequent work by the same group investigated whether pyruvate dehydrogenase (PDH), which has structural similarities to BKD, also contributed to *S. aureus* BCFA synthesis. However, a PDH deficient mutant (Δ*pdhA*) had increased BCFA content (~80%) and when Δ*lpdA* and Δ*pdhA* were combined the mutant had higher BCFA content than Δ*lpdA* alone (Singh *et al.*, 2018). This means that PDH evokes changes in BCFA synthesis, but not in the same manner at BKD. Before a *S. aureus* tuneable fluidity strain can be designed, full characterisation of *S. aureus* BCFA synthesis needs to occur, something which requires prolonged time and attention as it is an evidently complex process. To overcome these issues in the short-term, benzyl alcohol and temperature should be used as means to alter *S. aureus* membrane

fluidity; to achieve this, the concentrations and conditions used need to be established. Preliminary work using temperature and benzyl alcohol against *S. aureus* has been undertaken (Cebrián *et al.*, 2016); however, the strain and conditions used are not applicable to my work, meaning this would need repeating under the conditions used in this report.

My work with *S. aureus* showed the species to be much more resilient to LL-37 than *B. subtilis*. *S. aureus* required much higher concentrations to inhibit growth, and this inhibition could only be achieved in a strain lacking L-PG (Table 3.2). Lysis/growth profiles of *S. aureus* indicated cells were not lysing, as OD_{600} plateaued rather than decreased upon addition of LL-37 (Fig. 3.13), so I undertook a viability assay to show that whilst *S. aureus* treated with LL-37 are not liable to lyse, LL-37 is indeed bactericidal (Fig. 3.14). The inability of LL-37 to kill wild-type *S. aureus* in my assays does not necessarily mean that LL-37 is not effective against *S. aureus* in its native conditions within the human body. Multiple studies have found LL-37 to be more effective against clinical isolates of *S. aureus* than laboratory strains, and LL-37 has been found to be more efficacious than conventional antibiotics at clearing planktonic and biofilm *S. aureus* (Noore *et al.*, 2013; Kang *et al.*, 2019).

In this chapter, I showed that contrary to other Gram-positive species, *B. subtills* is not protected from LL-37 by L-PG; instead, only teichoic acids, and their D-alanylation, confer protection against LL-37 in cell envelope composition. In agreement with previous research, I showed that L-PG indeed protects *S. aureus* but was limited in further work with *S. aureus* by the essentiality of genes and the current strains available. I showed conclusively, by 4 different methods, that membrane fluidity does not alter susceptibility to LL-37 in *B. subtills*, whereas it does to the minimal pharmacophore MP196. This comparison also revealed differences between the effect of LL-37 and MP196, with LL-37 inducing rapid lysis, whereas MP196 induced a two-stage slow lysis – the mechanism behind LL-37 inducing such rapid lysis is something I explore in Chapter 4.

Chapter 4 – The mechanism of action of LL-37

4.1 Introduction

The current consensus on the mechanism of action of LL-37 is it interacts with the bacterial cell envelope and permeabilises cells via pore formation to cause cell death. However, there are gaps in this knowledge, such as the type of pore formed by LL-37, and whether this pore-forming activity is the only bactericidal activity of LL-37 (Sochacki *et al.*, 2011; Zeth & Sancho-Vaello, 2017). Additionally, LL-37 has been found to mediate distinct depolarising and permeabilising activity at different concentrations against *B. subtilis* (Barns & Weisshaar, 2013). Where and how LL-37 binds bacterial cells is also an important research question. Research of LL-37 interacting with LPS observed cooperative binding – as LL-37 bound LPS, more LL-37 was recruited to bind the LPS as well (Turner *et al.*, 1998). Furthermore, Snoussi *et al.* (2018) recently showed *E. coli* cells that are bound by LL-37 recruit more LL-37, which again is indicative of cooperative binding. Due to its cationic nature, it is widely hypothesised that LL-37 would be attracted to anionic components of a bacterial cell, including not just the cell envelope but also interior components such as DNA and maybe even the negative transmembrane potential of the cell. Altogether, this leaves many unknowns in the step-by-step mechanism of action of LL-37, including the binding of LL-37, how depolarisation is linked to pore formation and other "off-target" effects; elucidating these would enable informed approaches to potentiating LL-37, by using other antimicrobials that could enhance the antibacterial activity of the AMP.

Previous comparison of LL-37 against the ion-pore-forming decapeptide gramicidin and the cell envelope-targeting lipopeptide daptomycin showed LL-37 to induce lysis much more rapidly than these other antimicrobials - with lysis by LL-37 initiating immediately, whereas a delay of ~1 hour occurred before gramicidin and daptomycin treated cultures started to lyse (Kessler *et al.*, 2004; Müller *et al.*, 2016; Seistrup, 2018). Due to these previous findings, in this chapter I aimed to establish how LL-37 is able to cause bacteriolysis so quickly, and whether autolysins could be involved in this process. Autolysins are of interest in this context as previous work by the Strahl group has shown what was previously thought to be pore formation by daptomycin was in fact the triggering of autolysis by the lipopeptide, with this autolysis inducing permeabilisation (Buttress, 2022).

To elucidate the precise step-by-step mechanism of LL-37's antibacterial activity, I wanted to expand on the observations that high and low concentrations have different depolarising and permeabilising effects against *B. subtilis* (Barns & Weisshaar, 2013). To achieve this, I used fluorescent dyes to indicate the permeability and membrane polarisation of cells treated with LL-37, in combination with fluorescently labelled LL-37 and different *B. subtilis* mutant strains. I also aimed to unpick the relationship between cooperative binding of LL-37 and the effect of different LL-37 concentrations against *B. subtilis*, and also explored the targeting of LL-37 to different anionic components. Finally, I looked into the role of autolysis in the mechanism of action of LL-37. Throughout this chapter I have again used *B. subtilis* to investigate the mechanism of action of LL-37, due to the extended knowledge and mutants available in this species.

4.2 Results

4.2.1 LL-37 exhibits cooperative binding against B. subtilis

I first examined how concentration impacts the binding of LL-37 to the Gram-positive model organism *B. subtilis* at the single cell level. To do this, I used fluorescently labelled LL-37 at a range of concentrations and correlated the effects of these concentrations to growth and lysis. This showed low concentrations of LL-37 to exhibit concentration-dependent and gradual binding of cells, with the fluorescence intensity of cells treated with 2.5 and 5 μg mL^{-1} fluorescent LL-37 comparable to that of the background fluorescence seen in untreated cells (Fig. 4.1a). At 10 μg mL^{-1} an increase in LL-37 binding occurred, giving a heterogeneous increase of fluorescence intensity across the cell population, with some cells being highly bound while others remained similar to the less bound cells treated with lower concentrations of LL-37. At 20 μg mL^{-1} the whole population of cells were very highly bound by LL-37, the highly bound state of 10 and 20 μg mL^{-1} treated cells is confirmed by their high fluorescence intensity (Fig. 4.1a). When these binding states are compared to the growth/lysis kinetics of *B. subtilis* treated with LL-37, the states coincide with different effects of LL-37. Growing cells treated with 2.5 and 5 μg mL^{-1} LL-37 do not suffer lysis, instead only, transient or no growth inhibition occurs (Fig. 4.1b). In contrast, cultures treated with 10 and 20 μg mL^{-1} suffer pronounced lysis, which takes longer to recover from when 20 μg mL^{-1} is added. The presence of high and low bound cells at 10 μg mL^{-1} may explain why this culture was able to recover faster, as the less bound cells would not lyse and so growth would be recovered more rapidly. Altogether, at low concentrations LL-37 exhibited low

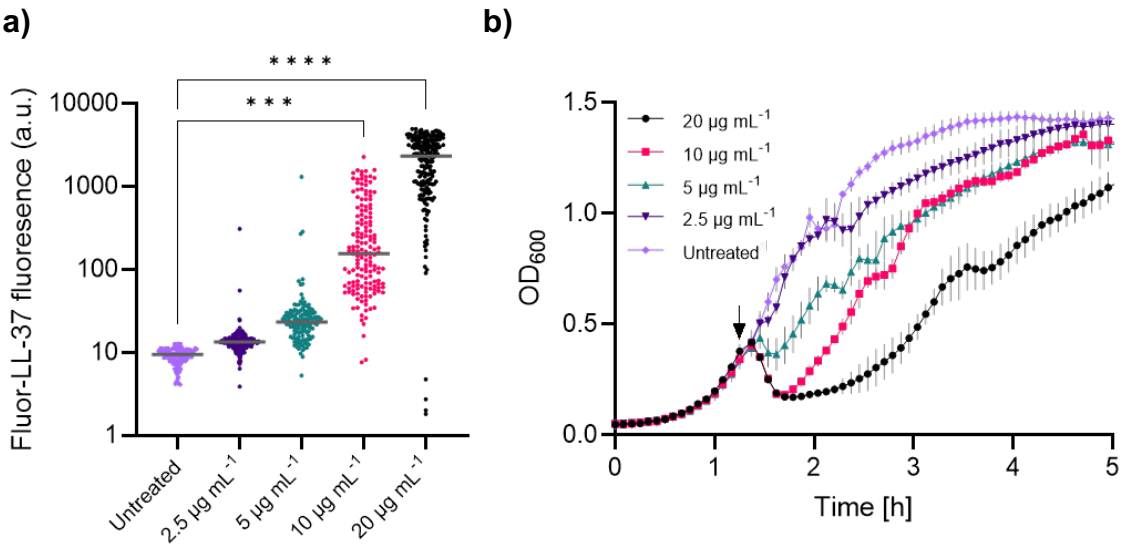

Figure 4.1. High binding of LL-37 induces cell lysis, whilst low binding induces growth inhibition. a) Single cell fluorescent microscopy quantification of 5-Fam-LC-LL-37 (Fluor-LL-37) binding to wild-type *B. subtilis* after 5 minutes incubation; grey bar indicates median fluorescence intensity; analysed by unpaired ordinary ANOVA with Dunnet's multiple comparisons test comparing to untreated, *** represents $p < 0.001$, **** represents $p < 0.0001$; $n \geq 150$. **b**) Growth/lysis of wild-type *B. subtilis* upon the addition of LL-37 (indicated by arrow). Data represented as mean±SD (n=3).

binding of cells and this caused growth inhibition at most. LL-37 at high concentrations was able to highly bind cells and this induced cell lysis. The sudden change from negligible to high binding between 5 and 10 µg mL^{-1} LL-37 (Fig. 4.1a) is implicit of cooperative binding, as high LL-37 binding does not occur incrementally with concentration but rather suddenly occurs once a threshold concentration has been reached. Under these experimental conditions this threshold lies somewhere between 5 and 10 µg mL^{-1} LL-37.

To further explore the relationship between LL-37 binding and membrane permeabilisation, I combined these different concentrations of fluorescently labelled LL-37 with the permeability indicator SYTOX Blue. In this thesis, permeability dyes (such as SYTOX Blue) and the phase contrast of imaged cells are used as indicators of permeability, whereas OD_{600} is used to indicate cell lysis. Untreated cells had no LL-37 bound and no SYTOX Blue fluorescence, indicating they were unpermeabilised (Fig. 4.2). At 2.5 and 5 µg mL^{-1} LL-37 the majority of cells remained unbound by LL-37 and impermeable. By 10 µg mL^{-1} LL-37 two sub-populations of cells occurred, with a small number of cells remaining impermeable, and the majority of cells being permeabilised – seen in their high SYTOX Blue fluorescence intensity. Many of these

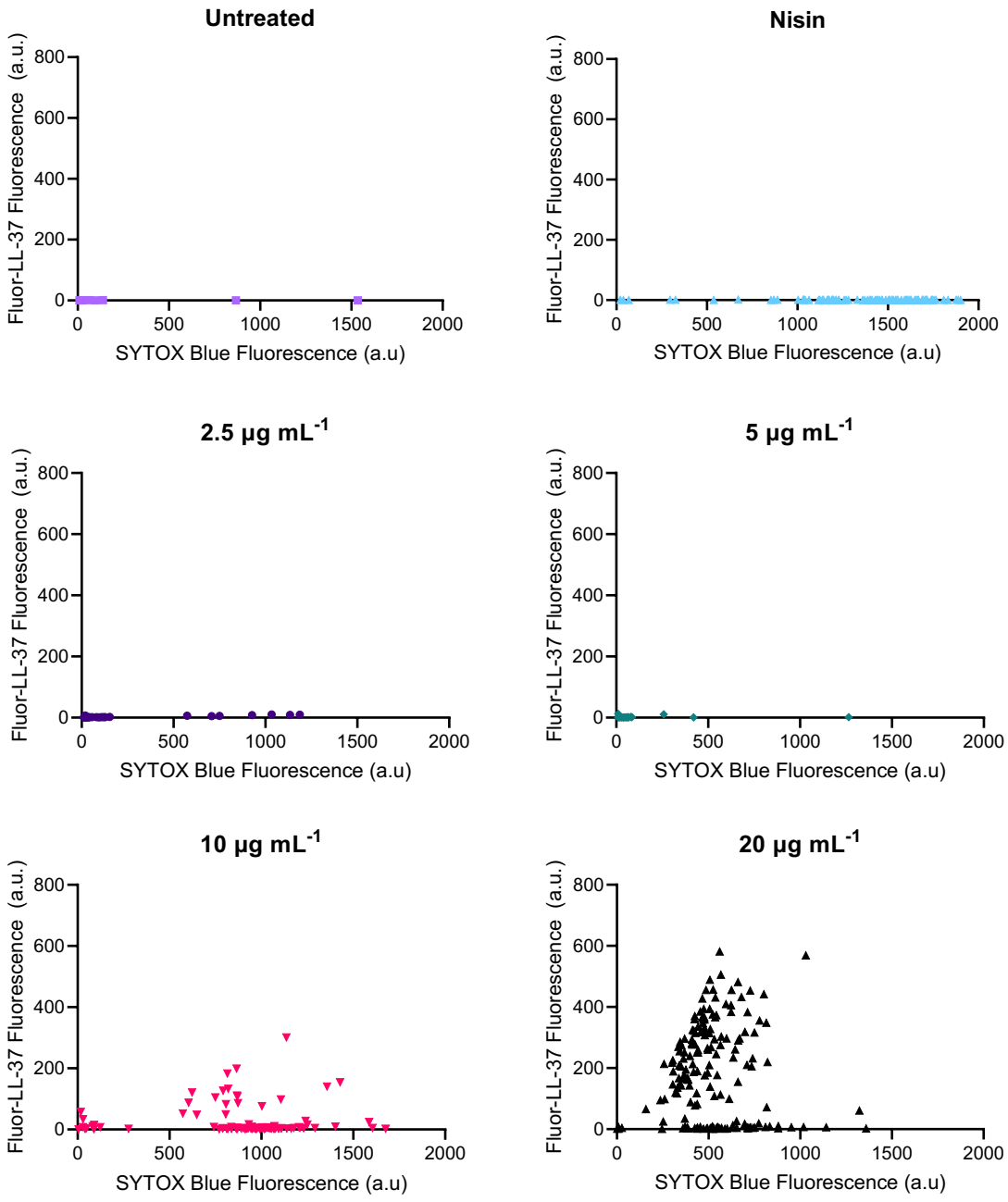

Figure 4.2. High concentrations of LL-37 cause more LL-37 to bind cells than is required for permeabilisation. Single cell fluorescent microscopy quantification of SYTOX Blue fluorescence (200 nM) and 5-Fam-LC-LL-37 (Fluor-LL-37) at 0, 2.5, 5, 10, and 20 µg mL^{-1} in wild-type *B. subtilis* after 5 minutes incubation; n ≥ 107.

permeabilised cells however did not have high fluorescent LL-37 binding, with Fluor-LL-37 values appearing at the same minimal value of untreated cells (Fig. 4.2). When 20 µg mL^{-1} LL-37 was added, this sub-population of lowly bound but permeabilised cells again occurred; however, a second sub-population was highly-bound by LL-37 and also permeabilised – seen in the high SYTOX Blue intensity (Fig. 4.2). It should be noted that the Fluor-LL-37 values from this assay and the previous quantification of

Fluor-LL-37 alone (Fig. 4.1a) are not directly comparable, as different microscopes and settings were used. However, when the observations of these experiments (Fig. 4.1&2) are combined, LL-37 at low concentrations hardly bound *B. subtilis* cells and did not permeabilise them, whereas higher concentrations caused permeabilisation and a sub-population of these permeabilised cells exhibited extremely high binding of LL-37.

4.2.2 Low concentrations of LL-37 depolarise cells, high concentrations then permeabilise cells

Having observed this dose-dependent, surprisingly complex permeabilisation by LL-37, I next wanted to establish how this related to the depolarising activity of LL-37. To do so I used a dilution series of LL-37 in fluorescence microscopy with the permeability indicator SYTOX Green and the cationic membrane polarisation dye $DiSC_3(5)$ combined (Kepplinger *et al.*, 2018). As positive controls for depolarisation and permeabilisation, gramicidin ABC and nisin were used. When *B. subtilis* was treated with gramicidin ABC, $DiSC_3(5)$ fluorescence was lost, indicating depolarisation. With nisin, $DiSC_3(5)$ fluorescence was lost and SYTOX Green fluorescence was high, indicating that in addition to being depolarised the cells were also permeabilised, in this case through pore formation (Fig. 4.3a). Analysis of these microscopy images revealed three different states of cell present when *B. subtilis* was treated with LL-37; these were: polarised; depolarised; and permeabilised cells (permeabilised cells are also depolarised). Polarised cells, indicated by high $DiSC_3(5)$ fluorescence, only occurred in cultures in the absence or presence of low concentrations of LL-37, such cells were observed at 0, 2.5 and 5 μg mL^{-1} (green arrows, Fig. 4.3a). Depolarised only cells, indicated by low $DiSC_3(5)$ and low SYTOX Green fluorescence, were only present in cultures treated with low concentrations, indicating this depolarisation was caused by low binding of LL-37 (orange arrows, Fig. 4.3a). At high concentrations (10 & 20 μg mL^{-1}) of LL-37, all cells were both depolarised and permeabilised – shown by their high SYTOX Green and lack of $DiSC_3(5)$ signal (blue arrows, Fig. 4.3a). To establish the proportion of these cell states in each culture, I quantified this microscopy, with the portion of the graph into which each cell type should fall shown as guidance in Fig. 4.3b. Untreated cells had high $DiSC_3(5)$ fluorescence intensity, indicating these cells were polarised (Fig. 4.3b). When low concentrations of LL-37 were present (2.5 and 5 μg mL^{-1}), many cells remained polarised; some cells were depolarised, and a minority were also permeabilised – indicated by low $DiSC_3(5)$ and high SYTOX Green fluorescence, respectively. When LL-37 concentration was increased to above the threshold for high binding (10 & 20 μg mL^{-1}, threshold seen in Fig. 4.1a), all cells in the

a)

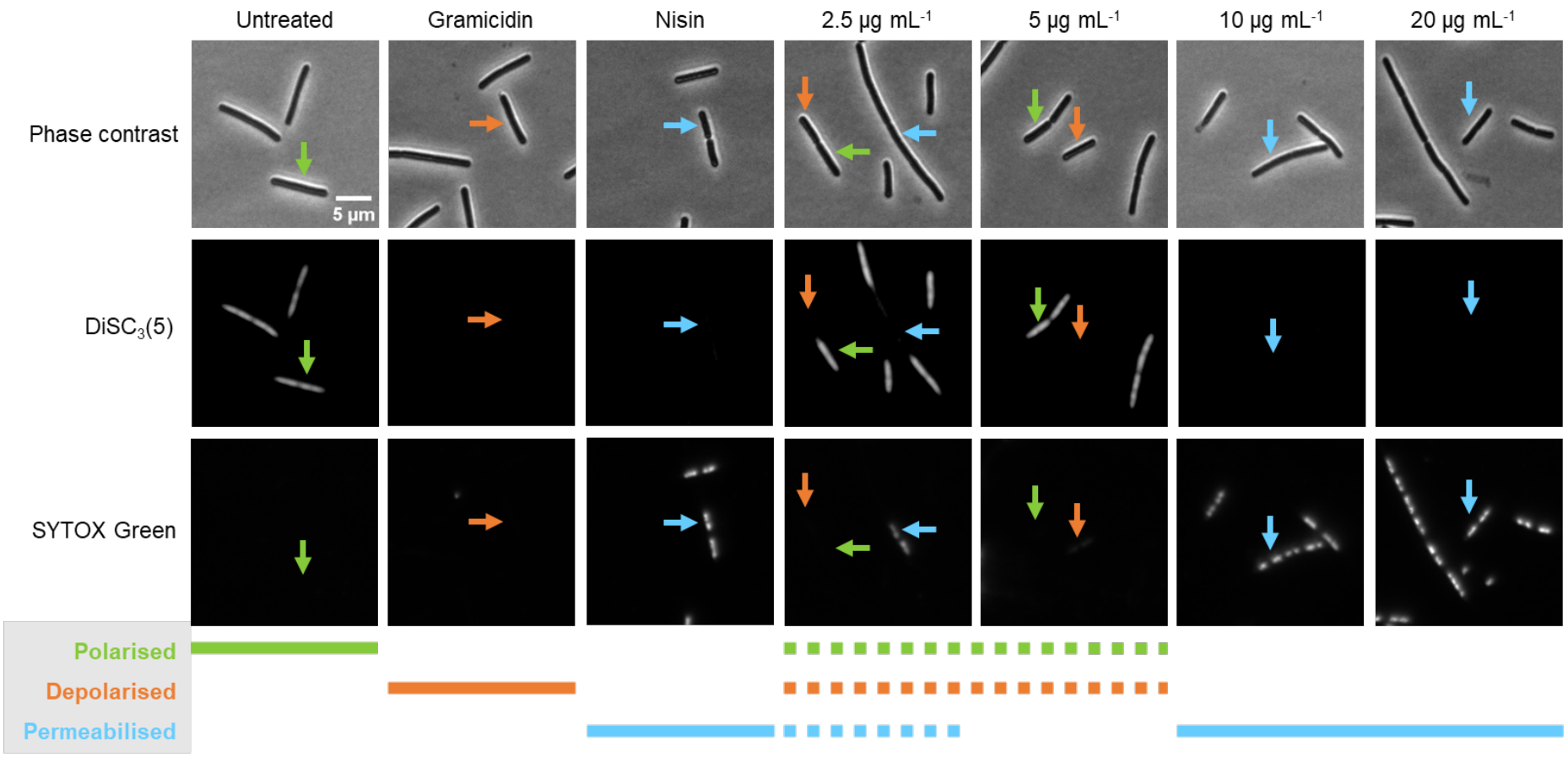

figure continued on next page...

b)

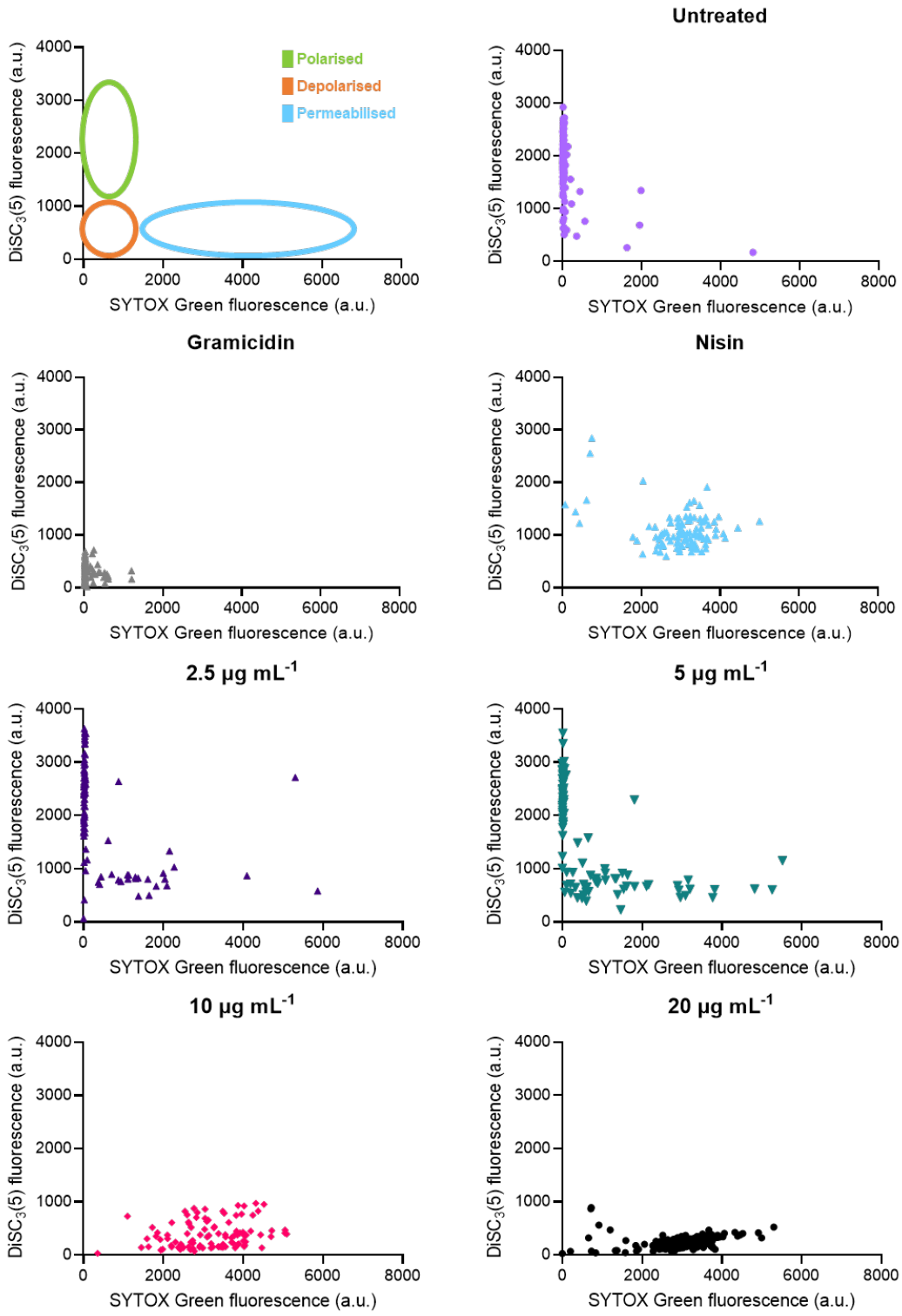

Figure 4.3. Low concentrations of LL-37 depolarise *B. subtilis*, whilst high concentrations also permeabilise cells. a) Fluorescent microscopy images of $DiSC_3(5)$ (2 µM) and SYTOX Green fluorescence (200 nM) at 0, 2.5, 5, 10, and 20 µg mL^{-1} LL-37 in wild-type *B. subtilis* after 10 minutes incubation, and with gramicidin ABC (5 µM) and nisin (5 µM) after 5 minutes. Examples of different cell states are indicated: polarised (green), depolarised (orange), depolarised and permeabilised (blue) – full line beneath indicates all cells, dotted line indicates some cells; scale bar is 5 µm. **b**) Single cell quantification of this microscopy; n ≥ 97.

cultures were depolarised and had high SYTOX Green signals, indicating they were also permeabilised (Fig. 4.3b). In summary, this assay showed LL-37 at low concentrations caused a heterogenous population of polarised and depolarised cells, whereas high concentrations caused complete permeabilisation and depolarisation of the vast majority of *B. subtilis* cells in the culture.

4.2.3 LL-37 does not exhibit a preference for transmembrane potential or DNA

As LL-37 is a cationic antimicrobial peptide, it could be attracted to negatively charged regions of a bacterial cell. In addition to the cell envelope factors I examined earlier, such as teichoic acids and CL, DNA is also negatively charged, and the interior of the cell is negatively charged relative to the exterior (known as transmembrane potential) (Flagg & Wilson, 1977; Maffeo *et al.*, 2014). Therefore, I looked to establish whether transmembrane potential and DNA localisation could impact the binding of LL-37 to *B. subtilis* cells. I first compared the ability of LL-37 to bind polarised and depolarised cells. Cells were depolarised by the addition of carbonyl cyanide *m*-chlorophenyl hydrazone (CCCP), a well-established depolarising agent (Strahl & Hamoen, 2010), then I imaged the cells upon the addition of fluorescently labelled LL-37. This microscopy showed similar binding by LL-37 to cells with and without CCCP, indicating LL-37 was able to bind both states of *B. subtilis* (Fig. 4.4a). When this microscopy was

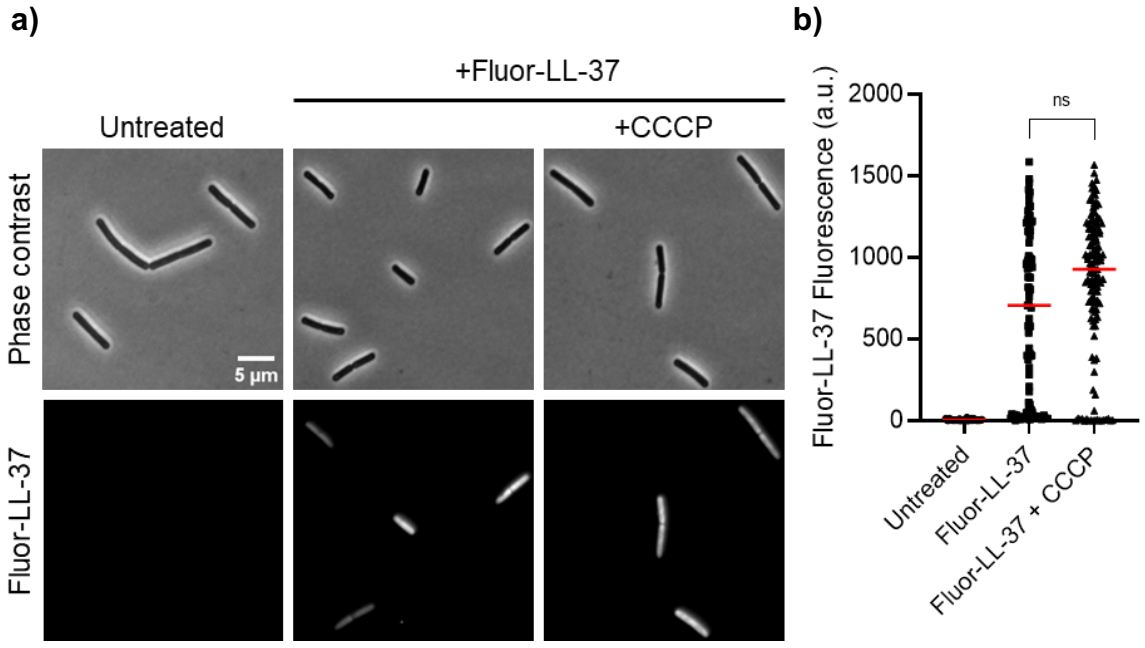

Figure 4.4. LL-37 does not exhibit preference for polarised cells. a) Fluorescent microscopy images of wild-type *B. subtilis* treated with 5-Fam-LC-LL-37 (Fluor-LL-37; 20 µg mL^{-1}) and CCCP (100 µM) for 5 minutes, scale bar is 5 µm. **b**) Single cell quantification of this microscopy; red bar indicates median fluorescence intensity; analysed by unpaired two-tailed t-test, p value is not significant (ns); n ≥ 119.

quantified no difference in the ability of LL-37 to bind polarised and depolarised cells occurred, with both being equally bound by the fluorescently-labelled AMP (Fig. 4.4b), showing LL-37 to bind cells independent of membrane polarisation. This also rules out the possibility that the cooperative binding that LL-37 exhibits is due to the depolarisation induced by the AMP, as the depolarised cells were not significantly more highly bound than the initially polarised cells.

I next investigated whether internalised LL-37 exhibited a preference for DNA, as suggested earlier (Wu & Tan, 2019); to do so I used fluorescently labelled LL-37 in combination with the DNA stain DAPI. I did this in Δ*divIVA* cells as the deletion of *divIVA* results in a chainy cell phenotype in which minicells devoid of DNA arise due to issues with cell division in this mutant (Edwards & Errington, 1997; Strahl *et al.*, 2015).

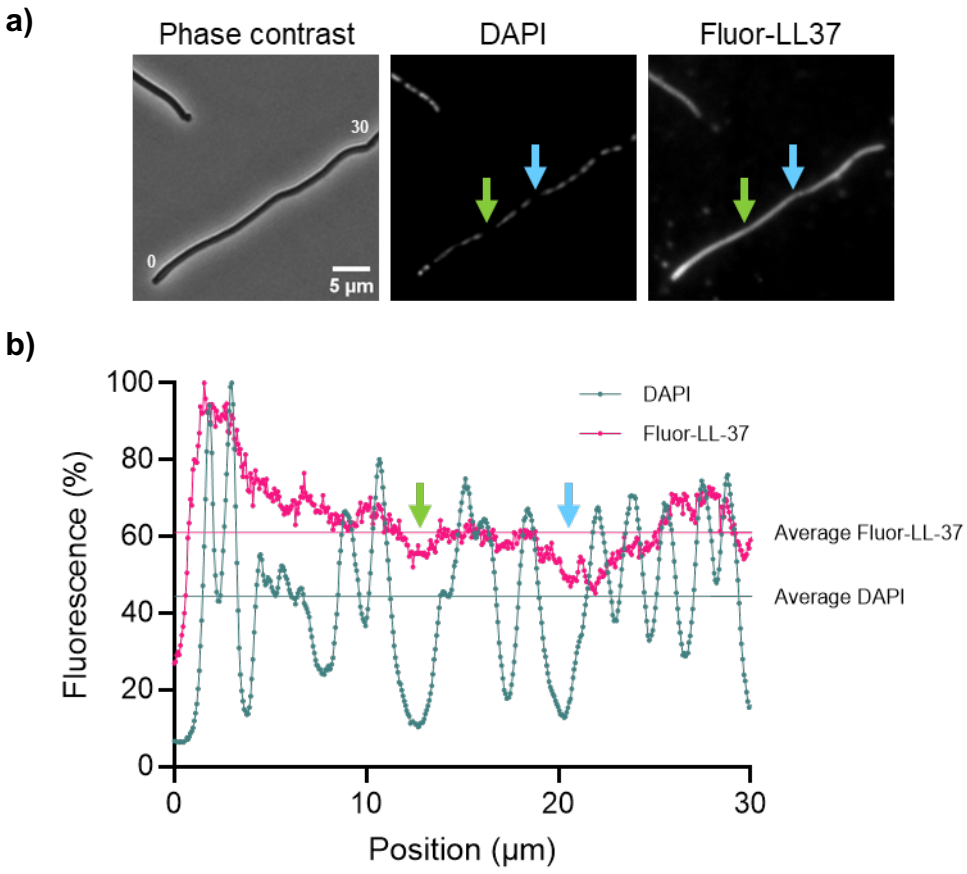

Figure 4.5. LL-37 does not exhibit preference for DNA-containing regions of cells. a) Fluorescent microscopy images of *B. subtilis* incubated with DAPI (100 ng mL^{-1}) and 5-Fam-LC-LL-37 (Fluor-LL-37; 20 µg mL^{-1}) for 5 minutes, arrows indicate regions devoid of DNA that contain LL-37; scale bar is 5 µm, region used for fluorescent quantification contained between 0 and 30. **b**) Fluorescence intensity profile of the above microscopy, the fluorescence was normalised against the maximum fluorescence value in each profile to give a percentage from raw DAPI fluorescence (a.u.) and Fluor-LL-37 fluorescence (a.u.), the mean fluorescence of each dye is shown.

The minicell regions of these chainy cells were used to assay whether LL-37 could bind DNA-containing and DNA-devoid regions of *B. subtilis* cells. This microscopy revealed a diffuse binding pattern of LL-37, with regions of Δ*divIVA* cells that were devoid of DNA still being bound by LL-37 (indicated by arrows, Fig. 4.5a). I generated a fluorescence intensity profile across the cell indicated in this microscopy, and this showed some regions of the cell that contained LL-37 were devoid of DNA, with LL-37 binding always remaining close to the average value (Fig. 4.5b). It does appear that LL-37 did bind slightly better at regions containing more DNA, as indicated by the high LL-37 fluorescence at the start and end of the profile where DAPI fluorescence was also high (Fig. 4.5b), however as LL-37 was also able to bind areas lacking DNA this relationship doesn't appear strong or necessary for binding. Together, these experiments show that LL-37 does not exhibit a preference to DNA or depolarised cells, with it instead having a diffuse binding throughout the cell.

4.2.4 LL-37 induces rapid lysis

Next, I moved on to looking at the processes in a cell that occur subsequent to LL-37 binding. Previous research has shown LL-37 is able to rapidly trigger cell lysis in *B. subtilis* (Seistrup, 2018), I first repeated this experiment myself to ensure this was indeed the case. I compared lysis induced by LL-37 to the well characterised lytic agent CCCP. CCCP is a proton ionophore that depolarises the cell, leading to a cascade of events that eventually trigger cell lysis due to misregulation of autolysis (Jolliffe *et al.*, 1981; Ghoul *et al.*, 1989). In comparison to the gradual lysis that CCCP induced, LL-37 instead induced rapid lysis, with OD_{600} decreasing within 10 minutes post-addition, compared to ~1 hour for CCCP (Fig. 4.6a).

Having affirmed the rapid lysis that LL-37 causes in *B. subtilis*, I wanted to establish how this related to the depolarising and permeabilising activity of LL-37. I used time-course microscopy to follow the membrane polarisation and permeabilisation, using $DiSC_3(5)$ and SYTOX Green, of a culture treated with a high concentration of LL-37 over time. Untreated cells had high $DiSC_3(5)$ fluorescence and no SYTOX Green fluorescence, showing they were polarised and unpermeabilised; after just 10 minutes of LL-37 treatment however, cells were depolarised and highly permeabilised, as indicated by the loss of $DiSC_3(5)$ fluorescence and high SYTOX Green fluorescence (Fig. 4.6b). Cells remained depolarised and permeabilised for the following 90 minutes, and phase light cells were visible in the phase contrast images – showing cell lysis to have occurred. Only 120 minutes post-addition were polarised cells starting to become

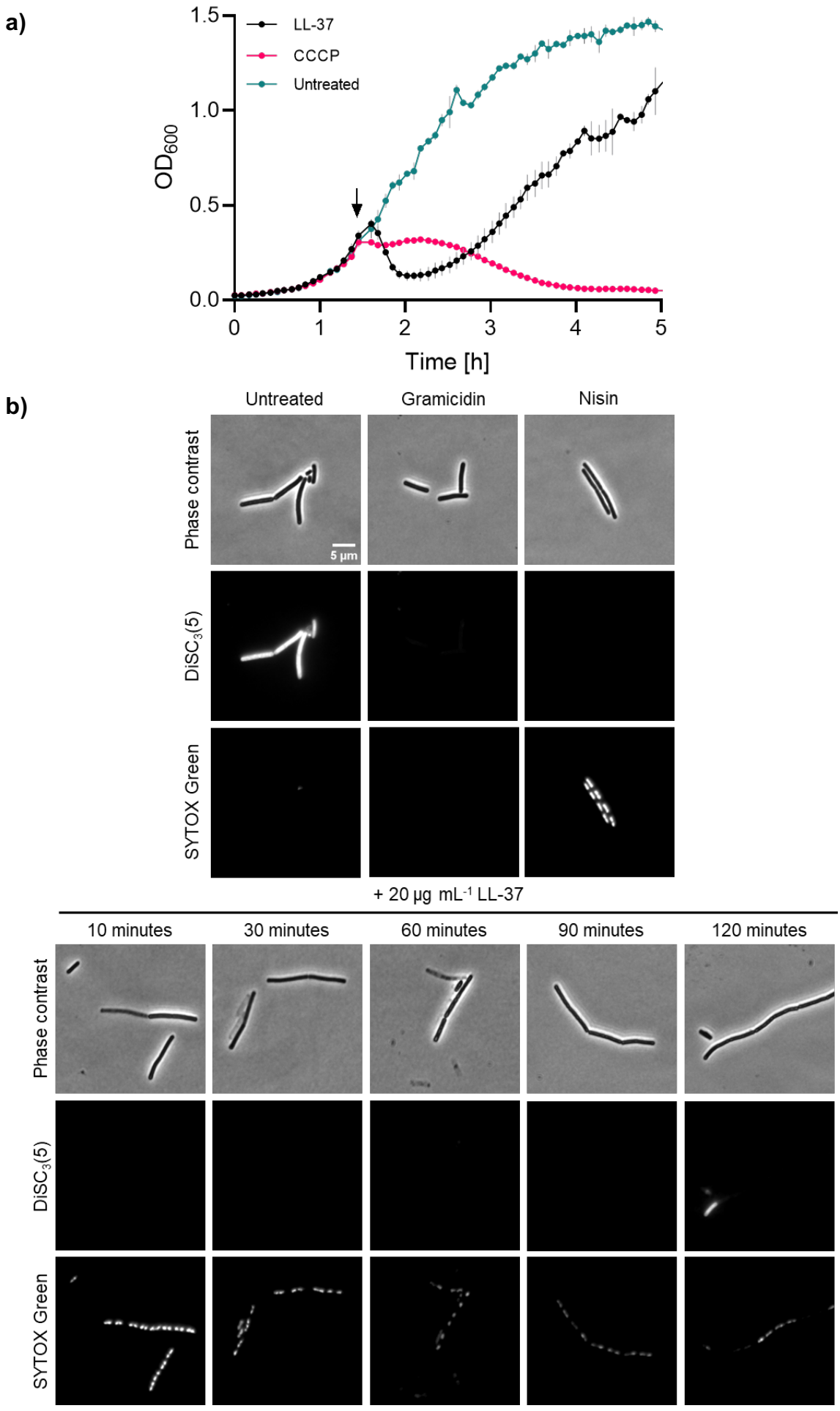
a)
LL-37
CCCP
Untreated
OD600
Time [h]
b)
Untreated
Gramicidin
Nisin
Phase contrast
DiSC3(5)
SYTOX Green
5 µm
+ 20 µg mL-1 LL-37
10 minutes
30 minutes
60 minutes
90 minutes
120 minutes

Figure 4.6. LL-37 induces rapid lysis. a) Growth/lysis of wild-type *B. subtilis* upon the addition (indicated by arrow) of LL-37 (20 µg mL^{-1}) and CCCP (100 µM). Data represented as mean±SD (n=3). **b**) Time-course fluorescent microscopy images of wild-type *B. subtilis* with $DiSC_3(5)$ (2 µM) and SYTOX Green fluorescence (200 nM) untreated, treated with gramicidin ABC (5 µM) and nisin (5 µM) after 5 minutes and with 20 µg mL^{-1} LL-37 over time; scale bar is 5 µm.

visible in the culture again, with a heterogenous population of polarised, depolarised and permeabilised cells occurring (Fig. 4.6b).

4.2.5 LL-37 permeabilises and kills cells independent of autolysis, but the lysis induced by LL-37 is autolytic

The rapid lysis induced by LL-37 suggested one of two things, either LL-37 was somehow rapidly triggering autolysis; or the pore-forming activity of LL-37 was directly responsible for causing cell lysis. To investigate whether LL-37 triggers the autolytic pathway to induce lysis in *B. subtilis*, I conducted experiments in a mutant lacking the autolysins LytABCDEF (LytCDEF are autolysins whilst LytA and LytB are auxiliary to LytC). I first looked at the permeabilisation and polarisation of Δ*lytABCDEF* via SYTOX Green and $DiSC_3(5)$ microscopy. Due to the lack of the LytABCDEF autolysins, there are cell division defects in this mutant that cause a chainy phenotype (Ohnishi *et al.*, 1999); however, the mutant is well energised when untreated, as seen in the high $DiSC_3(5)$ fluorescence the cells had (Fig. 4.7a). Within 10 minutes of the addition of 20 µg mL^{-1} LL-37 cells were already highly permeabilised and depolarised, indicated by the high SYTOX Green and low $DiSC_3(5)$ fluorescence, respectively. Throughout the 120 minute assay, the Δ*lytABCDEF* cells remained depolarised and exhibited retention of SYTOX Green – where wild-type cells lost SYTOX Green fluorescence over time (Fig. 4.6b), these Δ*lytABCDEF* cells instead retained high SYTOX Green fluorescence and no phase light cells were observed (Fig. 4.7a). This experiment proved permeabilisation by LL-37 to be independent of autolysis, as these autolysin deficient cells were still rapidly permeabilised by the AMP.

The retention of SYTOX Green and lack of phase light cells observed throughout this microscopy suggested that whilst cells are permeabilised independently of autolysis, bacteriolysis by LL-37 may require the autolytic process. To test this, I followed the growth/lysis of Δ*lytABCDEF* treated with LL-37. However, due to the chainy phenotype of Δ*lytABCDEF*, following growth/lysis in a plate reader is not possible as the cell shape interferes with OD_{600} readings (Ohnishi *et al.*, 1999). Instead, the OD_{600} had to be

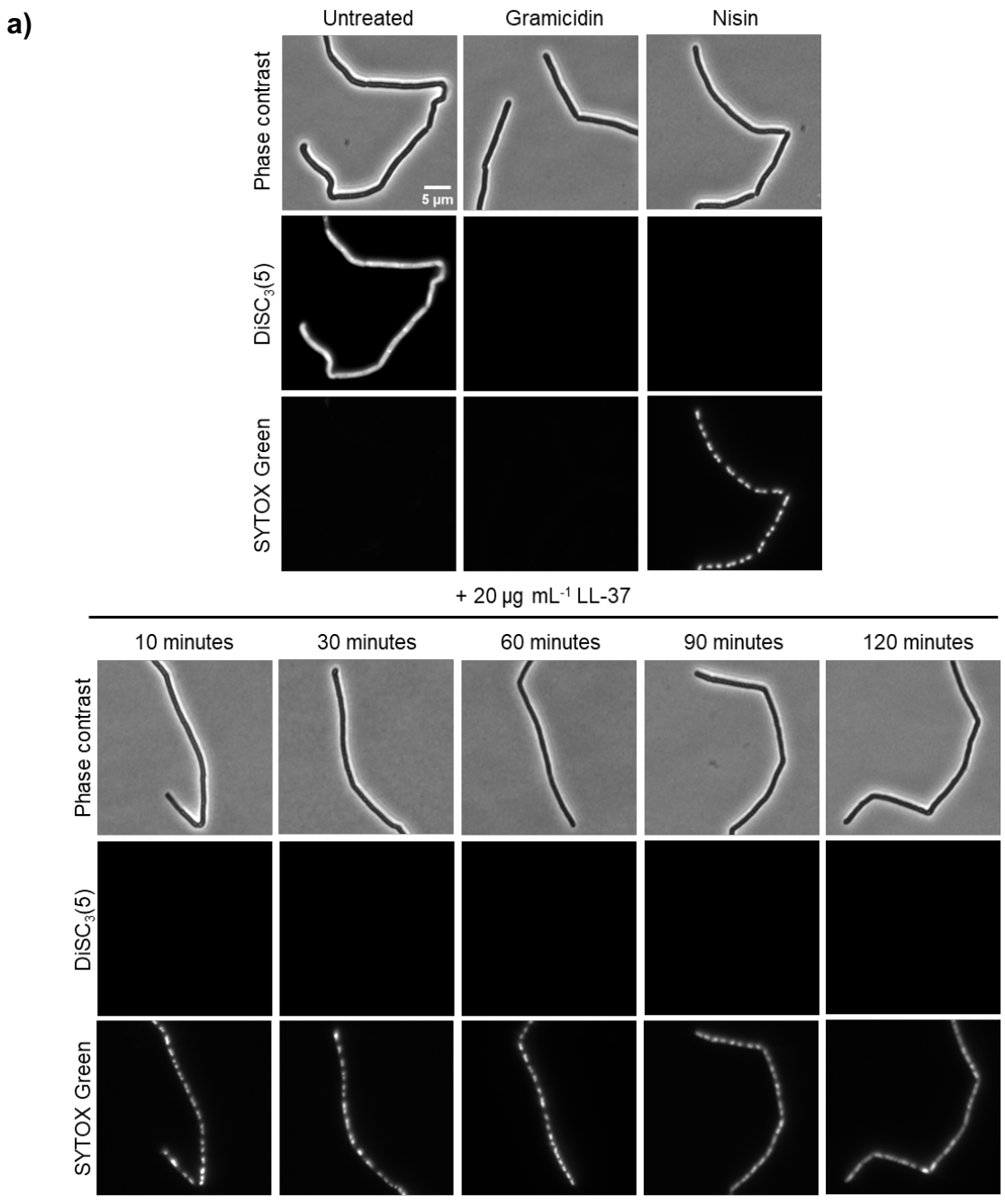

figure continued on next page...

d)

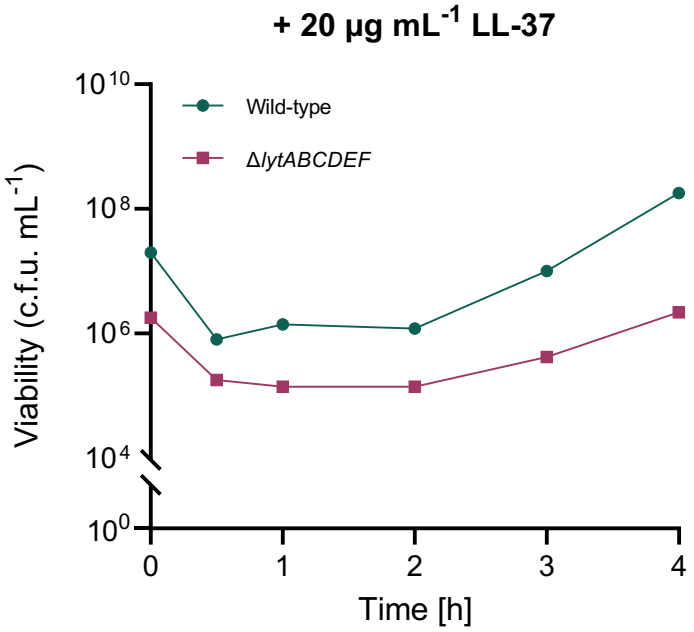

Figure 4.7. Permeabilisation by LL-37 is independent of autolysis, but autolysins are required for bacteriolysis. a) Time-course fluorescent microscopy of Δ*lytABCDEF B. subtilis* with $DiSC_3(5)$ (2 µM) and SYTOX Green fluorescence (200 nM) untreated, treated with gramicidin ABC (5 µM) and nisin (5 µM) after 5 minutes and with 20 µg mL^{-1} LL-37 over time; scale bar is 5 µm. Growth/lysis of (**b**) wild-type and (**c**) Δ*lytABCDEF B. subtilis* treated with LL-37 at 0 hours, and (**d**) viability of the cultures treated with 20 µg mL^{-1} LL-37, colony forming units (c.f.u.) were calculated via serial dilution and spot assay of the cultures.

followed manually, I did this in both wild-type and Δ*lytABCDEF B. subtilis*. As seen previously, wild-type cells started to lyse almost immediately upon treatment with 20 µg mL^{-1} LL-37, within 10 minutes; 10 µg mL^{-1} also caused lysis, whereas 5 µg mL^{-1} gave growth inhibition followed by recovery (Fig. 4.7a). When Δ*lytABCDEF* was treated with 20 µg mL^{-1} the culture OD_{600} did not immediately decline, instead it plateaued for the duration of the assay. Lower concentrations of LL-37 against Δ*lytABCDEF* also did not induce lysis, instead a profile akin to growth inhibition occurred, from which the cultures then recovered growth (Fig. 4.7b). This lack of lysis in Δ*lytABCDEF* could be taken to mean these cells were not dying in the presence of LL-37. To test if this was the case a viability assay was conducted alongside of the cultures treated with 20 µg mL^{-1}, to enable distinction between cell death and cell lysis. This revealed that the viability of both wild-type and Δ*lytABCDEF* reduced to similar extents, meaning both were killed by LL-37, and both cultures had started to recover viability by the end of the experiment (Fig. 4.7c). The lower c.f.u. mL^{-1} of *ΔlytABCDEF* is due to its chainy phenotype (Fig. 4.7a), this likely also results in the underestimation of the loss of

viability. Altogether, this experiment showed that the rapid bactericidal activity of LL-37 is independent of autolysis, as cells were rapidly permeabilised and lost viability in the absence of autolysins; however, LL-37 does trigger autolysis in *B. subtilis,* and it is this autolysis that is responsible for the rapid bacteriolysis observed when cultures are treated with LL-37.

4.2.6 LL-37 induces autolysis through LytD and LytE

Having established this link between LL-37-induced lysis and autolysins, I wanted to identify the specific autolysins that LL-37 induces. To do this, I used *B. subtilis* strains lacking LytABC/LytD/LytE/LytF individually, and also tested CwlO, the autolysin that is synthetically lethal in combination with LytE; and LytG, the major glucosaminidase (Horsburgh *et al.*, 2003; Bisicchia *et al.*, 2007). I compared the lysis of these strains to the lysis experienced by wild-type *B. subtilis* upon the addition of 20 μg mL^{-1} LL-37. The lysis of strains lacking LytABC, LytE, LytF LytG and CwlO did not appear much different from that of wild-type, with all sharing a rapid reduction in OD_{600} over 30 minutes followed by recovery within ~2 hours (Fig. 4.8a,b,d,e,f,g). The LytD deficient strain did not suffer rapid lysis, instead a gradual decline in OD_{600} occurred over a 2 hour period, followed by a slow growth recovery (Fig. 4.8c). To enable comparison, I measured the time to recover to the initial OD_{600} at which LL-37 was added for each strain, this confirmed the delay in recovery for LytD relative to wild-type (Fig 4.8h). It should be noted that this comparison in this case is slightly complicated by the somewhat slower growth of the Δ*lytD* strain, but nonetheless the rate of lysis in this strain is still reduced relative to the other autolysin deletion mutants. This shows that LytD is involved in the autolysis that LL-37 induces in *B. subtilis*, as in a LytD deficient strain the OD_{600} did not decrease as much or as rapidly as strains expressing LytD.

To assess the extent to which LytD was responsible for the autolysis triggered by LL-37, I compared the lysis of strains lacking the other autolysins to that lacking just LytD. As LytE and CwlO are synthetically essential, I used two strains to compare against: Δ*lytABCEF* and *ΔlytABCFcwlO* (Bisicchia *et al.*, 2007). When untreated, all of these strains were able to grow as well as wild-type *B. subtilis* (Fig. 4.9a). Upon the addition of a lower concentration of 10 μg mL^{-1} LL-37, the Δ*lytD* strain did not lyse, instead ~1 hour growth inhibition occurred before the culture was able to continue growing (Fig. 4.9b). This lack of lysis and instead short period of growth inhibition also occurred in the strain lacking LytABCDEF, whereas the Δ*lytABCFcwlO* strain had a growth/lysis

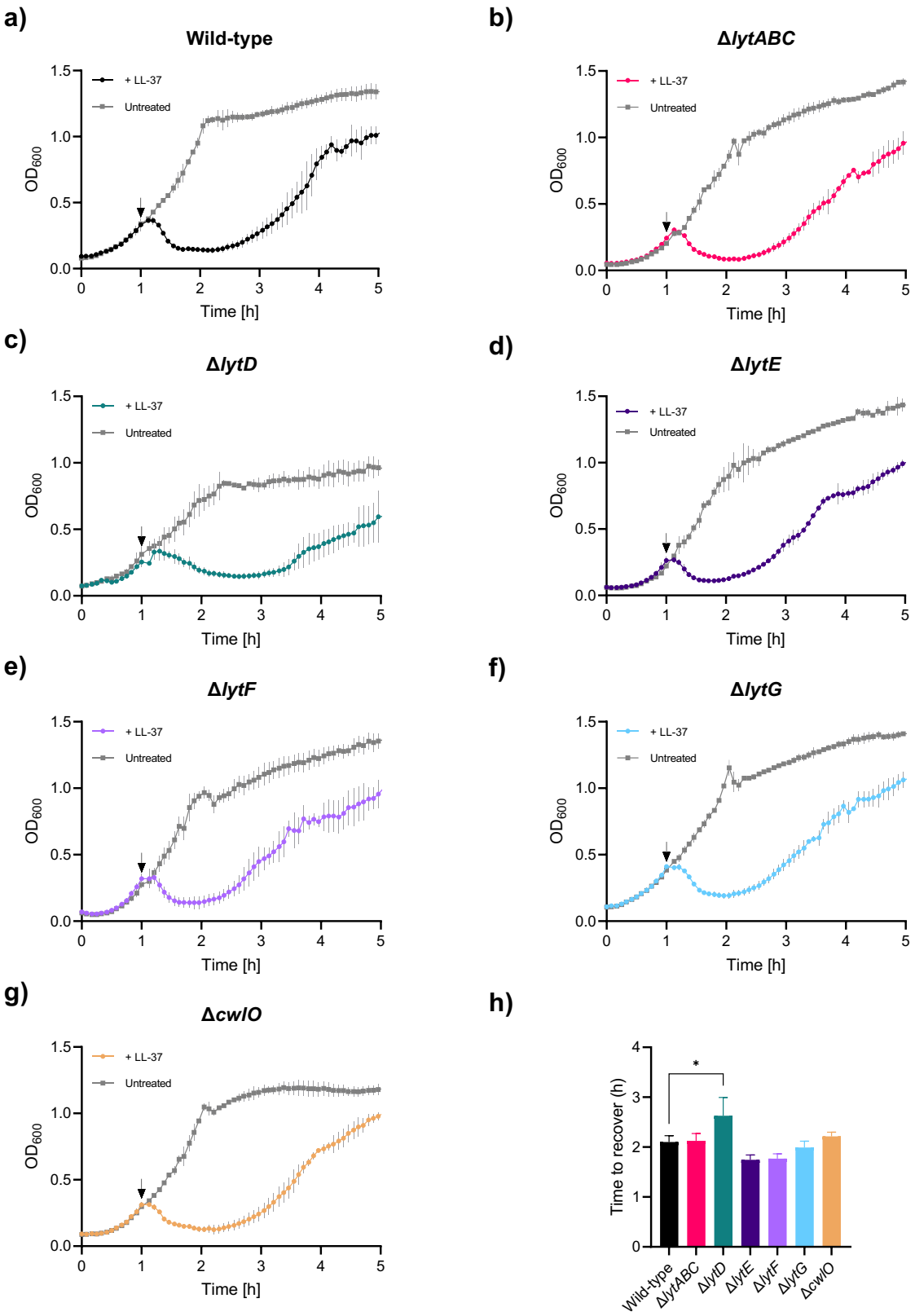

Figure 4.8. LytD is involved in the autolysis triggered by LL-37. Growth/lysis of *B. subtilis* strains (**a**) wild-type, (**b**) Δ*lytABC*, (**c**) Δ*lytD*, (**d**) Δ*lytE*, (**e**) Δ*lytF*, (**f**) Δ*lytG*, (**g**) Δ*cwlO* untreated and upon the addition of 20 µg mL^{-1} LL-37 (indicated by arrow). **h**) Analysis of the time taken for each strain to recover to the initial optical density at which LL-37 was added; analysed by unpaired ordinary ANOVA with Dunnet's multiple comparisons test comparing to wild-type, * represents $p < 0.05$. Data represented as mean±SD (n=3).

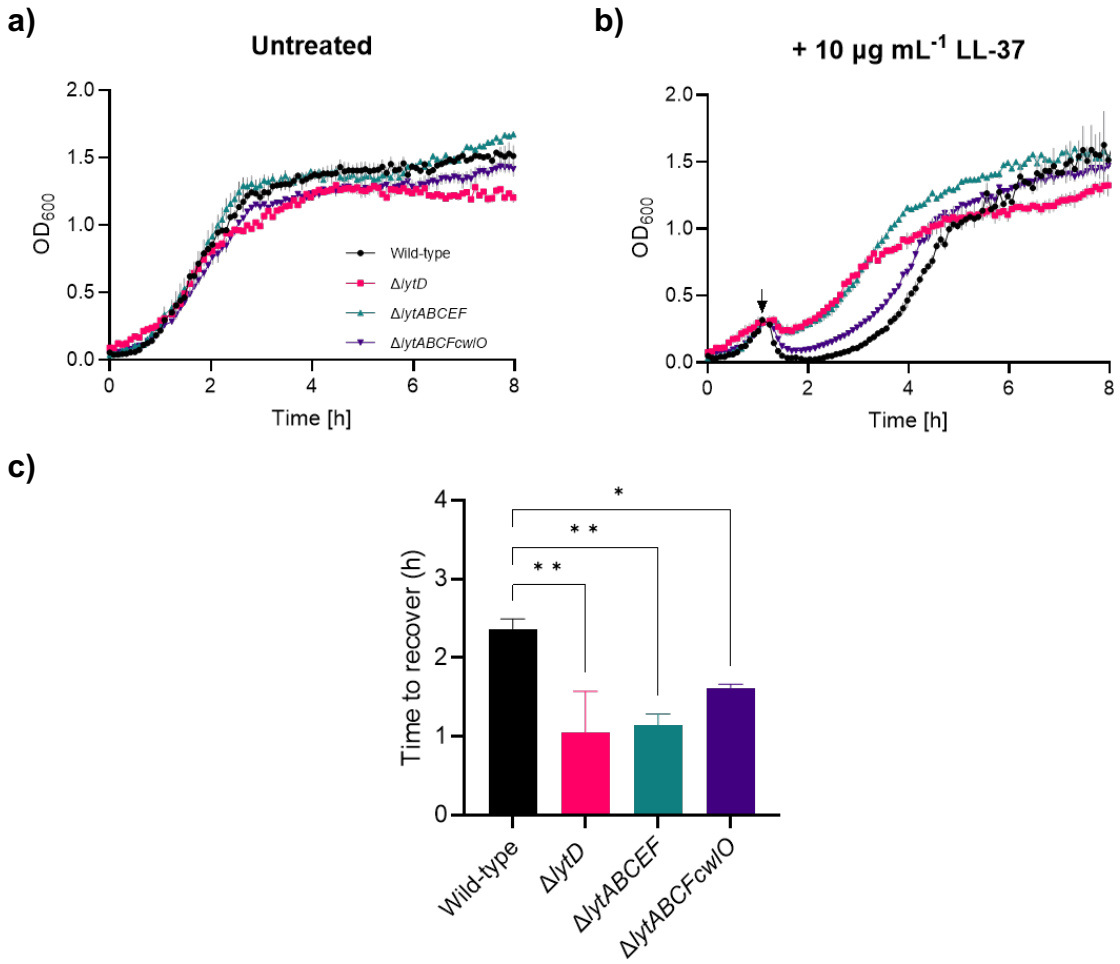

Figure 4.9. LytD and LytE are involved in the autolysis triggered by LL-37. Growth/lysis of wild-type, Δ*lytD*, Δ*lytABCEF*, Δ*lytABCFcwlO B. subtilis* strains (**a**) untreated and (**b**) upon the addition of 10 µg mL^{-1} LL-37 (indicated by arrow). **c**) Analysis of the time taken for each strain to recover to the initial optical density at which LL-37 was added; analysed by unpaired ordinary ANOVA with Dunnet's multiple comparisons test comparing to wild-type; * represents $p < 0.05$, ** represents $p < 0.01$. Data represented as mean±SD (n=3).

profile more similar to wild-type *B. subtilis* (Fig. 4.9b). When the time to recover of these strains was quantified, the ability of the LytD and LytABCEF deficient strains to recover was significantly improved compared to wild-type (Fig. 4.9c). These comparisons indicate that in addition to LytD, LytE is also somehow involved in the autolysis induced by LL-37; as in the absence of LytE, lysis induced by LL-37 is abrogated, whereas when LytE is expressed, lysis occurs to a more similar extent as wild-type.

As the deletion of *lytD* had such a striking impact on the lytic activity of LL-37, I decided to test whether this was due to its σ^D-dependent expression. σ^D is the motility RNA polymerase (RNAP) sigma factor, meaning it promotes the attachment of RNAP to the initiation sites of specific genes, including *lytD* (Margot *et al.*, 1994; Márquez-Magaña

& Chamberlin, 1994). To examine the role of σ^D in the activity of LL-37 against *B. subtilis*, I used a strain deficient for the σ^D gene *sigD* and followed its lysis and recovery when treated with LL-37. This growth/lysis assay revealed Δ*sigD* to be more susceptible to LL-37 than wild-type *B. subtilis*. At all concentrations of LL-37 Δ*sigD* took longer to recover growth following lysis than wild-type, and 2.5 μg mL^{-1} which against wild-type had no discernible effect relative to untreated caused reduced growth against the Δ*sigD* strain (Fig. 4.10a&b). Comparison of the time taken to recover from 20 μg mL^{-1} LL-37 of wild-type and Δ*sigD* affirmed this visual comparison, with Δ*sigD* taking significantly longer to recover than wild-type *B. subtilis* (Fig. 4.10c). Here, again, slow growth rate complicates comparison as Δ*sigD* has a slower growth rate than wild-type; however, the evident effect of low concentrations against Δ*sigD*, that have no impact against wild-type, provides clear evidence of increased susceptibility of a strain lacking σ^D. Altogether, following permeabilisation of *B. subtilis*, which itself is sufficient

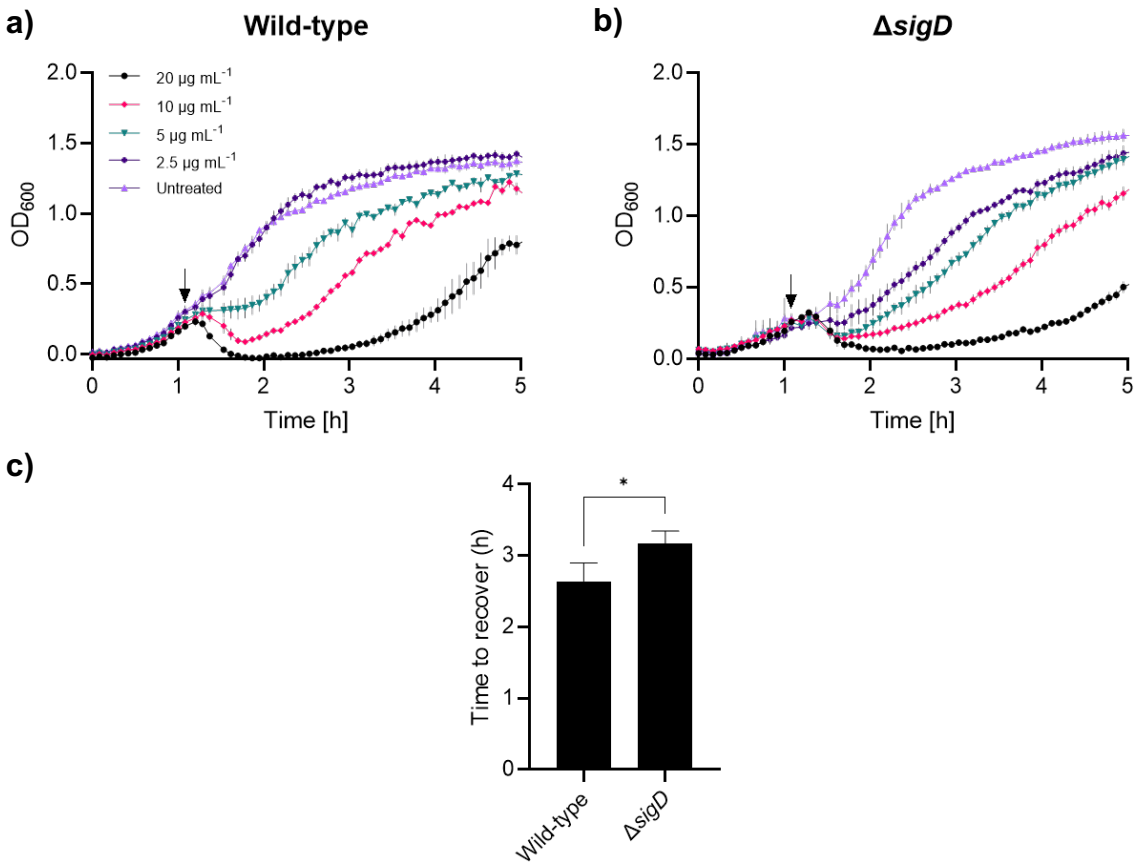

Figure 4.10. σ^D deficient *B. subtilis* is more susceptible to LL-37. Growth/lysis of (**a**) wild-type and (**b**) σ^D deficient (Δ*sigD*) *B. subtilis* upon the addition of LL-37 (indicated by arrow). **c**) Analysis of the time taken for each strain treated with 20 μg mL^{-1} LL-37 to recover to the initial optical density at which LL-37 was added; analysed by unpaired two-tailed t-test, * represents $p < 0.05$. Data represented as mean±SD (n=3).

to kill cells, LL-37 triggers autolysis through LytD and LytE, likely with σ^D involvement, to cause bacteriolysis of the cell.

4.3 Discussion

Elucidating the mechanism of action of LL-37 would enable informed approaches to potentiate its activity and so aid immune clearance of bacterial infections. This knowledge would also aid understanding of similar AMPs and perhaps the development of synthetic AMPs with enhanced activity for therapeutic purposes. I first investigated the binding of LL-37 to *B. subtilis* cells, this revealed a cooperative binding dynamic, in which binding was either low or high, with no/low binding until the threshold concentration was reached at which point cells were very highly bound by LL-37 (Fig. 4.1). This supports the previous findings of Turner *et al*. (1998) and Snoussi *et al.* (2018) in which they observed similar cooperative binding by LL-37 to LPS and *E. coli* cells, respectively. Cooperative binding is also supported by the small presence of permeabilised cells at 2.5 and 5 μg mL^{-1} (Fig. 4.3), as this indicates LL-37 is recruited to these few cells bound by LL-37 at sufficient concentrations to permeabilise the cells, rather than it exhibiting low binding to all cells within the culture.

The LL-37 binding assay revealed the shift to high binding of LL-37 to *B. subtilis* to occur between 5 and 10 μg mL^{-1} (Fig. 4.1a). When the permeability of cells treated with a LL-37 concentration range was assayed alongside LL-37 binding, this revealed very limited permeabilisation by 2.5 and 5 μg mL^{-1} (Fig. 4.2). Together this indicates that low level of binding of LL-37 is not sufficient to permeabilise cells, suggesting the cooperative binding property of high concentrations of LL-37 is required for its permeabilising activity. The correlation of high cooperative binding of LL-37 and permeabilisation of *B. subtilis* cells could occur by two different mechanisms. Firstly, LL-37 might cooperatively bind *B. subtilis* cells to such an extent that the cell envelope loses integrity and so is permeabilised. Or secondly, initial binding of LL-37 might disrupt the cell envelope, permeabilising the cell, which once permeabilised then facilitates the cooperative binding of more LL-37, giving highly bound, permeabilised cells. The data presented in this thesis cannot distinguish between these two possibilities. High concentrations of LL-37 revealed first a shift to high permeabilisation and then at the highest concentration a sub-population of very highly-bound cells (Fig. 4.2). This supports that high concentrations are required for the pore-forming activity of LL-37 to permeabilise cells, and also suggests that permeabilised cells recruit more

LL-37 to become very highly-bound. This high-binding by already permeabilised cells is suggestive of sequestering activity, in which these dead cells take on more LL-37, potentiating the survival of other cells in the population that may not be bound by LL-37. Dead cell sequestration of LL-37 has previously been observed in *E. coli* (Snoussi *et al.*, 2018; Wu & Tan, 2019); my findings suggest the ability of permeabilised cells to continue binding LL-37 is shared across bacterial species. These observations are important, as they indicate a shortcoming in the antibacterial activity of LL-37, as once a proportion of a bacterial population have been killed by LL-37, the ability of the AMP to kill the remaining cells is reduced by the protective effect these dead cells have by sequestering LL-37 – this is something I investigate further in Chapter 5.

A rather complex relationship between LL-37 concentration, its binding, and the effect LL-37 has against *B. subtilis* cells was revealed in my experiments. Low concentrations, with low binding, induced only depolarisation, whereas high concentrations, with high binding, induced both depolarisation and permeabilisation of cells (Fig. 4.3), again indicating high binding is necessary for the permeabilising activity of LL-37. Similar observations have also been made in *B. subtilis* by Barns & Weisshaar (2013), with low concentrations inducing growth inhibition and high concentrations causing cell shrinkage, which was associated with a loss of turgor. Together with my results, this suggests their observed growth inhibition at low concentrations is caused by depolarisation, and that high concentrations cause cell shrinkage by permeabilisation via the pore-forming activity of cooperatively-bound LL-37. As only high concentrations of LL-37 cause permeabilised cells, an important question going forward is how LL-37 can induce depolarisation when at low non-permeabilising concentrations. The impermeable state of cells treated with 2.5 and 5 μg mL^{-1} LL-37 is evident in their lack of SYTOX Blue and Green fluorescence (Fig. 4.2&3). Thus, future work should include elucidating the activity of LL-37 at low concentrations. One potential mechanism for depolarisation could be a precursor to the carpet model of AMP activity, which involves AMP coating the cytoplasmic membrane to such an extent that parts of the membrane start to break away, permeabilising the cell (Oren & Shai, 1998). Recent work in model membranes suggested LL-37 does indeed follow the carpet model of membrane disruption, with LL-37 changing the conformation of phospholipid fatty acid tails and altering the tilt angle of phospholipids to bring about membrane dissolution (Majewska *et al.*, 2021). It may be that at low concentrations LL-37 interacts with the membrane sufficiently to

disrupt its normal organisation, leading to membrane depolarisation, but not at sufficient amounts to lead to membrane breakaway and permeabilisation. Investigating this low level activity of LL-37 could be important in enabling synergy with its activity *in vivo*, as the depolarising effect of LL-37 could potentiate the activity of other antimicrobials, giving an enhanced antibacterial response. Barns & Weisshaar (2013) observed that the cells treated with low concentrations of LL-37 that experience growth rate inhibition can recover if the LL-37 is washed away, if these cells are akin to the depolarised only cells I observed in Fig. 4.3 this suggests *B. subtilis* may be able to recover from membrane depolarisation induced by LL-37 – this is a question I investigate further in Chapter 5.

The presence of DNA and membrane polarisation were found to not impact the ability of LL-37 to interact with *B. subtilis* cells (Fig. 4.4&5). This negates a previous hypothesis in which it was proposed DNA would attract LL-37 into the cytoplasm due to its negative charge (Wu & Tan, 2019). I also investigated transmembrane polarisation as it is responsible for the internalisation of cell penetrating peptides, short cationic or amphipathic peptides that are used to deliver molecules across the cell membrane; their translocation across the membrane is driven by membrane polarisation pushing the peptide to the interior of the cell (Hoffmann *et al.*, 2018; Trofimenko *et al.*, 2021). However, in contrast to membrane polarisation being necessary for the internalisation of cell-penetrating peptides, this was not the case for LL-37 (Fig. 4.4). These experiments did however reveal a surprising observation, as after just 5 minutes incubation, LL-37 was bound diffusely across the cell, with no clear preference for the cytoplasmic membrane (Fig. 4.4&5). This contrasts with the established dogma of the mechanism of action of LL-37, which centres around the interaction of LL-37 with the cell envelope (de Miguel Catalina *et al.*, 2019). These observations do not mean LL-37 does not interact with the cytoplasmic membrane; however, it does indicate at least that LL-37 is rapidly translocated across the membrane. To characterise this process fully, an insightful assay would be combining fluorescence microscopy with microfluidic devices, to enable visualisation of the transient membrane association step of LL-37 binding. However, this approach is currently challenging due to the hydrophobic nature of polydimethylsiloxane (PDMS) used in microfluidic devices, meaning LL-37 would bind to the experimental equipment and so have limited interaction with the bacterial cells. This experimental impasse would need to be overcome before such visualisation can take place.

The rapid cell permeabilisation LL-37 induces in *B. subtilis* is unlike that seen with many other membrane active compounds, including CCCP, daptomycin and gramicidin, which permeabilise the membrane through the autolytic process (Fig. 4.6a; Seistrup, 2018). This rapid permeabilisation LL-37 induces is evidenced by SYTOX Blue staining after only 5 minutes of incubation with *B. subtilis* (Fig. 4.3). This immediate permeabilisation by LL-37 is similar to that caused by the AMP nisin, which functions by interacting with lipid II to induce pore formation and inhibition of cell wall biosynthesis (Breukink *et al.*, 1999; Hasper *et al.*, 2006; Reiners *et al.*, 2020). As LL-37 remains active against model membranes, whereas nisin loses its potency, this supports that LL-37 interacts with membrane phospholipids directly (Breukink *et al.*, 1999; Majewska *et al.*, 2021). This rapid permeabilisation also occurred in *B. subtilis* deficient for the autolysins LytABCDEF, indicating permeabilisation by LL-37 is distinct from the autolytic pathway (Fig. 4.7a). Yet, whilst permeabilisation was independent of autolysis, the bacteriolysis of *B. subtilis* required autolysins, as seen in the lack of OD_{600} decrease in the Δ*lytABCDEF* culture (Fig. 4.7c). This differs from the activity of the lipopeptide antibiotic daptomycin, for which autolysins are required for its permeabilising activity, with this permeabilisation not occurring immediately and instead starting to occur after ~20 minutes treatment (Buttress, 2022). Therefore, in contrast to each other: daptomycin induces autolysis to cause permeabilisation, whereas LL-37 induces permeabilisation to trigger autolysis. However, the depolarised and highly permeabilised state of the Δ*lytABCDEF* cells and their loss of viability indicates this autolysis is a subsequent or independent activity to that that kills the cell (Fig. 4.7c&d). The mechanism through which LL-37 triggers autolysis is unclear, it may be that LL-37 somehow directly triggers autolysis, potentially through teichoic acids – as I have shown teichoic acids to be involved in LL-37 interaction and teichoic acids have been shown to regulate autolysins (Guyet *et al.*, 2023), or it may be that the LL-37-induced permeabilisation of cells triggers autolysis through an unknown rapid mechanism. The ability of LL-37 to induce permeabilisation and lysis so rapidly by direct interaction with the cytoplasmic membrane is impressive, and further unpicking how it is able to do so so quickly is an important research question for future antibiotic understanding and design.

Assessment of the lysis of individual autolysin mutants treated with LL-37 revealed LytD to be specifically important in LL-37-induced autolysis, as Δ*lytD* exhibited reduced lysis (Fig. 4.8). LytD is a major autolysin with N-acetylglucosaminidase activity, it is

expressed within the σ^D regulon (Margot *et al.*, 1994). In addition to LytD, it also appeared that the endopeptidase LytE contributes to LL-37-induced autolysis (Margot *et al.*, 1998). This is because when *lytD* was expressed in the absence of *lytABCEF*, lysis was reduced to the same extent as a single *lytD* deletion; whereas when *lytE* was expressed but its synthetically essential opposite *cwlO* was deleted with *lytABCF*, lysis more akin to wild-type occurred, showing LytE to be responsible for the reduced lysis of Δ*lytABCEF* (Fig. 4.9). However, when *lytE* was deleted on its own, no change in lysis and time to recover occurred (Fig. 4.8), indicating the contribution of LytE to LL-37-induced lysis is less than that of LytD and also more complex. Previous characterisation of LytE found that its cell wall-degrading activity at specific regions of the cell enabled more targeted degradation by the amidase LytC (Margot *et al.*, 1998); it may be that the same is true for LytD, with LytE activity enabling rapid autolytic activity by LytD to cause the rapid permeabilisation and cell lysis I observe in *B. subtilis* treated with LL-37. When σ^D was deleted, *B. subtilis* was significantly more susceptible to LL-37, as it took longer to recover growth and was more impacted by low concentrations of LL-37 than wild-type (Fig. 4.10). This supports that genes within the σ^D regulon are involved in the cellular outcomes of LL-37 treatment, as these outcomes changed in the absence of σ^D. Interestingly, in addition to LytD, the autolysins LytC and LytF are also in the σ^D regulon; LytD and LytF are under exclusive control of σ^D, whereas ~70% of LytC expression is controlled by σ^D (Lazarevic *et al.*, 1992; Margot *et al.*, 1994, 1999). However, no change in lysis or time to recover occurred in strains deficient for LytC and LytF (Fig. 4.8), meaning the entire σ^D regulon does not appear to be involved in the response to LL-37. It may be that LL-37 somehow directly triggers misregulation of LytD, but σ^D is required for there to be an existing pool of LytD to be misregulated. LL-37 has previously been observed to trigger a stress response in *B. subtilis*, through the extracytoplasmic function sigma factors σ^W and σ^M, both of which have established roles in adaptation to membrane-active compounds (Pietiäinen *et al.*, 2005). σ^W and σ^M are triggered by membrane-activate agents and impaired peptidoglycan synthesis, respectively (Helmann, 2016). This leads me to speculate that in addition to its membrane active activity, which is well documented and further evidenced in Chapter 5 of this thesis, LL-37 may also interact with the peptidoglycan cell wall or components of its biosynthetic pathway. It has previously been established that AMPs interfere with cell wall synthesis machinery (Pag *et al.*, 2008); thus, it may be that regions of the cell wall with active synthesis are weak points that are easier for AMPs, such as LL-37, to penetrate. This speculation of LL-37 interaction with

components of the cell wall is supported by the direct triggering of LytD activity that LL-37 appears to have, and its previously documented activation of the σ^M regulon, which occurs under peptidoglycan synthesis impairment. To explore this, interactions of LL-37 with different cell wall components should be investigated, similar to what has already been conducted with the lipid II-interacting peptides nisin and daptomycin (Breukink *et al.*, 1999; Grein *et al.*, 2020). This could first be achieved by pre-incubating *B. subtilis* with antibiotics that bind cell wall precursors, such as oxacillin, teixobactin and oritavancin to see if this impacts the activity of LL-37 (Grein *et al.*, 2020). By unpicking how LL-37 triggers autolysis so rapidly, and whether this is due to direct interaction with the cell wall components relevant for regulation of autolysis or autolysins directly, we can use informed approaches to enhance its activity and have a better understanding of which antibiotics could help or hinder its lytic activity. Another approach to research the potential interaction of LL-37 with the cell wall would be to test the susceptibility of *B. subtilis* L-forms to LL-37. L-forms lack a cell wall and *E. coli* has been observed to readily transition to L-forms to evade cell wall targeting antibiotics (Kawai *et al.*, 2014; Mickiewicz *et al.*, 2019). So, if cell wall interaction is part of the mechanism of action of LL-37, L-forms should have reduced susceptibility to the AMP – a new PhD project is commencing in the Strahl group this year to research this hypothesis. Additionally, L-forms can also be used to distinguish between the permeabilising and autolytic activity of LL-37, as the autolytic process will be absent in these cell wall-deficient cells.

In this chapter, I showed that LL-37 exhibits cooperative binding against the Gram-positive bacterium *B. subtilis*, and this is independent of DNA or transmembrane polarisation. This cooperative binding dynamic means low exposure to LL-37 causes depolarisation only, the mechanism of which is unknown but could be due to low level membrane disruption that is not sufficient to cause larger scale membrane permeabilisation. High concentrations of LL-37 exceed the threshold required for cooperative binding, thereby triggering permeabilisation of *B. subtilis*. This permeabilisation is independent of autolysis, however autolysis is required for the subsequent bacteriolysis that LL-37 causes. LL-37 induces autolysis predominately through the N-acetylglucosaminidase LytD and also to a lesser extent through the endopeptidase LytE. These insights into the mechanism of action of LL-37 lay the groundwork for further investigation of the AMP.

Chapter 5 – Recovery and protection from LL-37

5.1 Introduction

LL-37 is rapidly bactericidal against *B. subtilis* and *S. aureus*, yet despite this killing activity, in both species recovery of the culture occurs soon after treatment (Fig. 3.14b & 4.7d). This rapid recovery indicates not all cells are being killed by LL-37, meaning the surviving cells can grow and recover the culture. It is unclear whether the *B. subtilis* cells that grow in the presence of LL-37 have specific characteristics to enable their survival or if instead their survival is purely a stochastic matter of insufficient LL-37 binding, combined with association of LL-37 with dead cells. For example, LL-37 was found to preferentially bind septating *E. coli* cells, however this preference did not exist against *B. subtilis* (Sochacki *et al.*, 2011; Barns & Weisshaar, 2013). Establishing whether surviving cells are distinct from those that die would provide an important insight into the mechanism of action of LL-37, as if characteristics exist to confer protection these could be targeted to enhance LL-37 activity. Conversely if LL-37 killing is purely stochastic, this simply suggests higher concentrations of LL-37 should be effective, as then more cells would be bound by the peptide.

There are multiple factors that may impact the potency of LL-37 to kill *B. subtilis*, including the possibility of rapidly emerging genetic mutations that confer resistance. A range of bacterial species produce extracellular proteases that are active against LL-37, these degrade the peptide to prevent its antibacterial activity (Schmidtchen *et al.*, 2002; Sieprawska-Lupa *et al.*, 2004). Another potential survival mechanism could involve endospores. To survive adverse conditions *B. subtilis* can divide asymmetrically to give endospores, these have a multi-layered proteinaceous coat that enables their survival under stressful conditions. Spores can then germinate and return to vegetative growth once conditions improve (McKenney *et al.*, 2013). It may be that spores present within the culture are able to survive LL-37 and then resume vegetative growth once all the LL-37 has bound the growing cells. These potential strategies for *B. subtilis* to evade or degrade LL-37 were the initial focus of this chapter. A further focus pertained to *B. subtilis* cells treated with low concentrations of LL-37, these cells are depolarised but not permeabilised by the AMP (Fig. 4.3). A major question emerging from this observation is whether these depolarised cells can recover, and if so, whether these transiently depolarised cells are responsible for growth recovery of the culture.

In the previous chapter heterogeneous populations of cells treated with LL-37 were observed, with polarised, depolarised, and permeabilised cells being present (Fig. 4.3). Heterogeneous populations when treated with LL-37 have previously been reported in *E. coli*, with two sub-populations observed upon treatment with LL-37: a non-growing population that absorbs LL-37 and a growing population that survives due to sequestration of LL-37 by the non-growing cells (Snoussi *et al.*, 2018). This was soon followed up by the observation that the non-growing *E. coli* cells that absorb LL-37 continue to absorb LL-37 when dead, further protecting the growing cells of the culture – in this research they hypothesised that negatively charged DNA was responsible for LL-37 sequestration by dead cells (Wu & Tan, 2019). Research is required to find if these observations of LL-37 sequestration by dead cells in *E. coli* also hold true in the Gram-positive model organism *B. subtilis*.

In this chapter I first investigated whether the rapid recovery of *B. subtilis* cultures from LL-37 treatment was due to evasion or degradation of LL-37, focussing on genetic mutations, extracellular protease activity and spore formation. I also looked into whether the cells that survive LL-37 were in any way distinct from their dead sister cells or if their survival was instead due to stochastic lack of LL-37 binding. Finally, I aimed to expand on existing research to establish – whether *B. subtilis* treated with LL-37 also led to growing and non-growing subpopulations; if *B. subtilis* dead cell debris sequesters LL-37; and, if so, what component of dead cell debris was responsible for this sequestration activity.

5.2 Results

5.2.1 Rapid recovery from LL-37 is not due to mutation, adaptation, spores or extracellular proteases

I first wanted to establish whether *B. subtilis* was able to recover so rapidly from LL-37-induced lysis due to specific properties of the culture. The most obvious option would be the rapid emergence of genetic mutations that confer resistance to LL-37. To test whether genetic mutations had occurred, I treated a *B. subtilis* wild-type culture with LL-37 and allowed the culture to recover and grow to stationary phase. The recovered culture was then plated and grown to single colonies, 10 of these single colonies were then grown in liquid culture, and again treated with LL-37 (Fig. 5.1a). This experiment tests for genetic adaptation, as genetic mutations would be

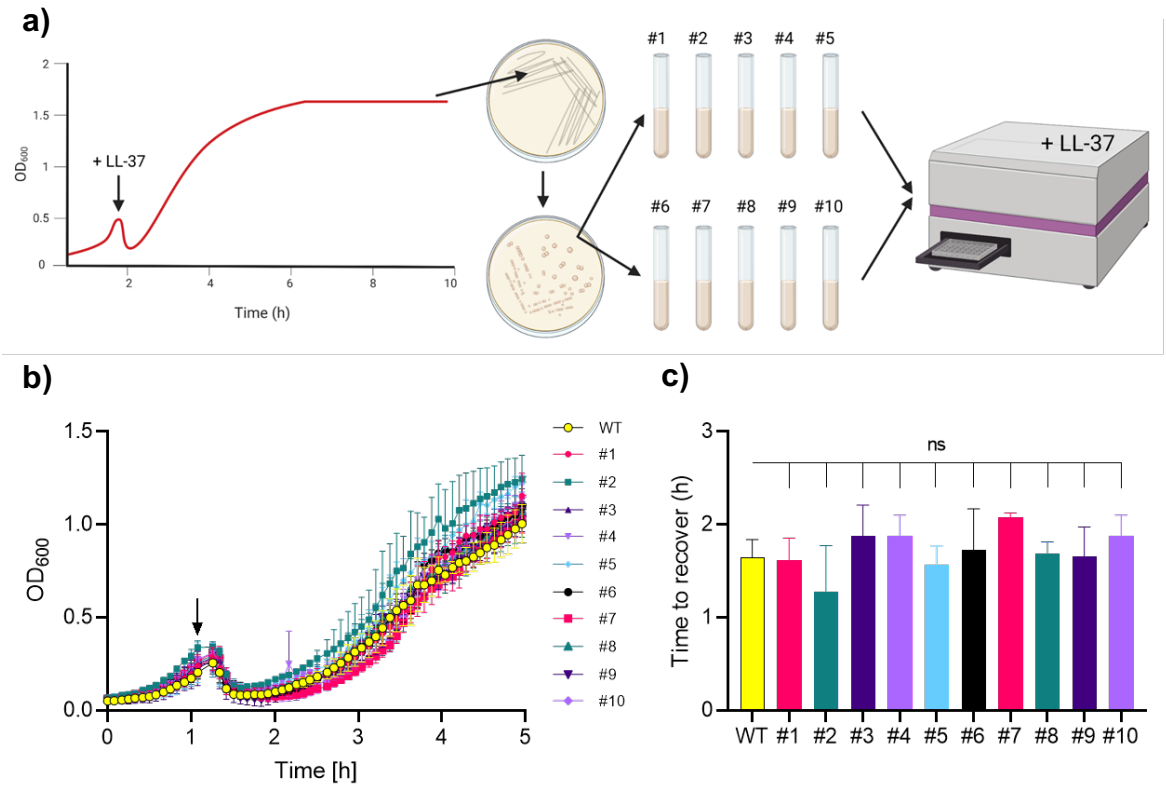

Figure 5.1. Rapid recovery from LL-37 is not due to genetic mutation. **a**) Generation of potential LL-37 suppressor mutant workflow – a culture recovered from LL-37 treatment was plated to single colonies, 10 of these were grown in liquid culture and again treated with LL-37 to assess their susceptibility. **b**) Growth/lysis of *B. subtilis* wild-type (WT) and cultures treated and recovered from LL-37 (#1-10) upon the addition of 20 μg mL^{-1} LL-37 (indicated by arrow). **c**) Analysis of the time taken for each strain treated with 20 μg mL^{-1} LL-37 to recover to the initial optical density at which LL-37 was added; analysed by unpaired ordinary ANOVA with Dunnet's multiple comparisons test comparing to wild-type, p value is not significant (ns). Data represented as mean±SD (n=3).

maintained through plating and growth and, if present, would immediately confer resistance to the cultures. The assay showed all 10 single colony-derived cultures to have the same susceptibility as wild-type LL-37-naïve *B. subtilis*, as all experienced the same rapid lysis and recovery dynamics, as indicated by a reduction followed by an increase in OD_{600} (Fig. 5.1b). When the times to recover of the 10 single colony-derived cultures were compared to that of wild-type, no culture recovered significantly faster than wild-type (Fig. 5.1c). This demonstrates cells that recover from LL-37 are not able to do so due to genetic mutations conferring resistance against the peptide.

I next tested whether *B. subtilis* was degrading LL-37 by extracellular protease activity, thereby inactivating its bactericidal activity and so enabling some cells in the culture to grow, as has previously been seen in other bacterial species (Schmidtchen *et al.*, 2002;

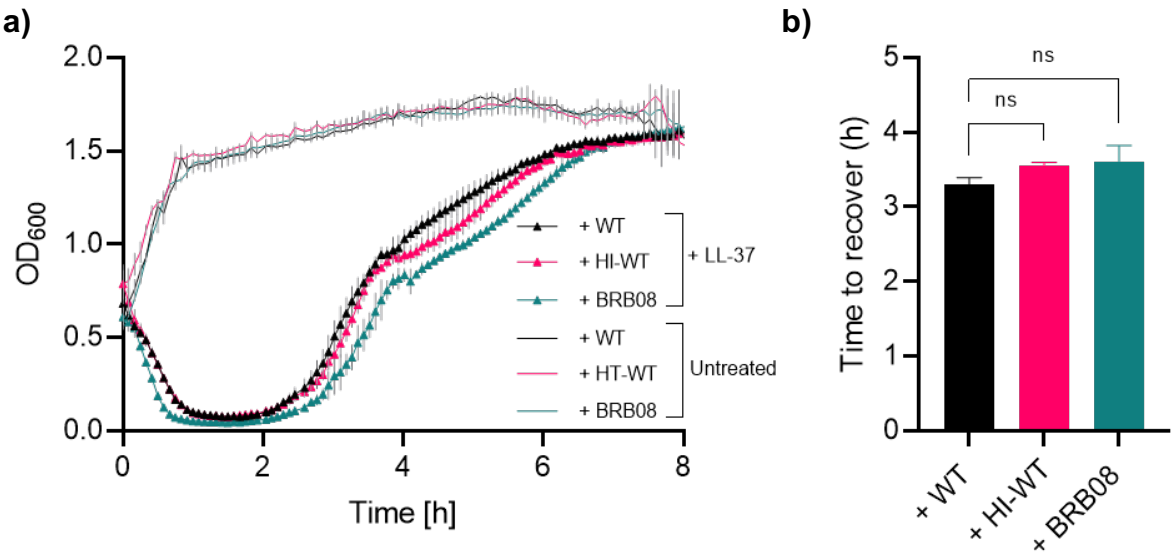

Figure 5.2. Extracellular protease activity does not impact *B. subtilis* recovery from LL-37. a) Growth/lysis of *B. subtilis* wild-type (WT) grown in supernatants untreated or pre-incubated for 1 hour with 20 µg mL^{-1} LL-37, supernatants were WT, heat-inactivated (HI)-WT and BRB08. **b**) Analysis of the time taken for each condition with 20 µg mL^{-1} LL-37 to recover to the initial optical density at which LL-37 was added; analysed by unpaired ordinary ANOVA with Dunnet's multiple comparisons test comparing to wild-type, p value is not significant (ns). Data represented as mean±SD (n=3).

Sieprawska-Lupa *et al.*, 2004). To do this, I used the BRB08 extracellular protease deficient strain constructed by Pohl *et al.* (2013). LL-37 was incubated in the supernatant of wild-type, heat-inactivated (HI) wild-type and BRB08 supernatants before being used to treat wild-type *B. subtilis*. The wild-type supernatant would contain extracellular proteases, whereas these should be inactivated or not present in the HI and BRB08 supernatants, respectively. Thus, if the extracellular proteases of *B. subtilis* were active against LL-37, the LL-37 incubated with wild-type supernatant would be less active, as it had been degraded, than that incubated with HI and BRB08 supernatants. This assay showed LL-37 in wild-type supernatant to be no less potent than HI or BRB08 supernatants, as all 3 cultures suffered the same degree of lysis and recovery (Fig. 5.2a). Analysis of the time taken for each culture to recover showed HI and BRB08 supernatants to be equal to that of wild-type supernatant, with no significant differences between the wild-type and protease-lacking cultures (Fig. 5.2b). Therefore, protease activity can also be ruled out as a means by which *B. subtilis* could recover its culture growth so rapidly after LL-37 treatment.

The next potential strategy I investigated that *B. subtilis* could employ to enable rapid recovery from LL-37 was the presence of spores in the culture. As these could resist LL-37 activity and then resume vegetative growth to recover the culture. To assess the role of spores in LL-37 susceptibility and recovery, I used a Δ*spoIIE* deletion mutant. SpoIIE is essential for the localisation of the division septum between the mother cell and spore, meaning in its absence the asymmetric division required for spore formation cannot occur and so a Δ*spoIIE* culture does not contain any spores (Feucht *et al.*, 1996). When treated with LL-37, this mutant exhibited the same lysis and recovery dynamics as wild-type at high concentrations of LL-37 (10 & 20 µg mL^{-1}) and at the lowest concentration of LL-37 no discernible difference in growth to untreated occurred in either the wild-type or Δ*spoIIE* strains (Fig. 5.3a&b). Furthermore, comparison of the time to recover of each strain from 20 µg mL^{-1} showed both strains to be very similarly affected by LL-37, with no significant difference between their recoveries (Fig. 5.3c). Altogether, these experiments demonstrated that the rapid ability of *B. subtilis* to

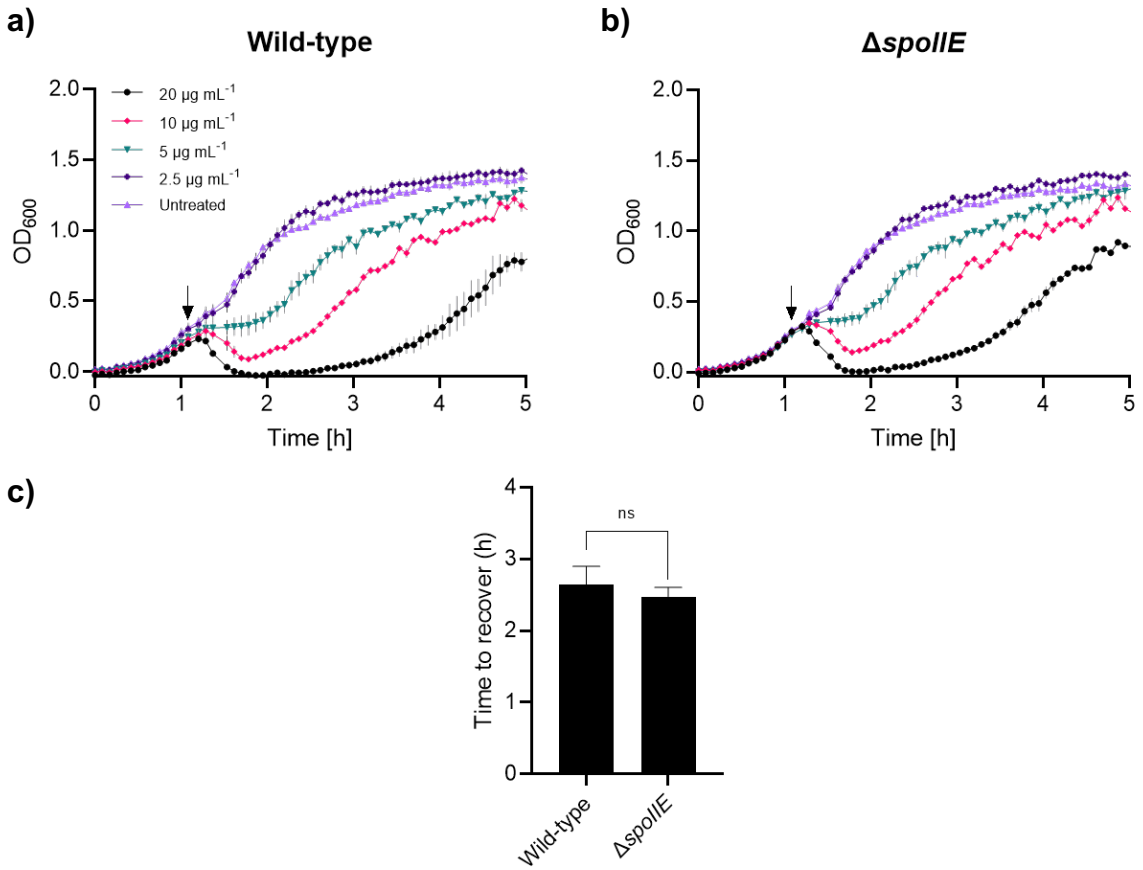

Figure 5.3. *B. subtilis* spores do not impact the lysis and recovery dynamics of LL-37 treatment. Growth/lysis of (**a**) wild-type and (**b**) Δ*spoIIE B. subtilis* upon the addition of LL-37 (indicated by arrow). **c**) Analysis of the time taken for each strain treated with 20 µg mL^{-1} LL-37 to recover to the initial optical density at which LL-37 was added; analysed by unpaired two-tailed t-test, p value is not significant (ns). Data represented as mean±SD (n=3).

recover from LL-37-induced lysis is not due to the selection of resistance, protease-mediated degradation of LL-37 or the presence and resumption of vegetative growth by spores.

5.2.2 Cells that survive LL-37 treatment are still susceptible to LL-37

As the rapid recovery of *B. subtilis* from LL-37 was not due to specific qualities of the culture previously tested (Fig. 5.1-3), I decided to conduct an experiment that would test the susceptibility of recovering cells. In this assay, I treated cells with 20 μg mL^{-1} LL-37, waited 15 minutes and then again treated cells with 20 μg mL^{-1} LL-37. Alongside, I treated cells with 40 μg mL^{-1} LL-37 as a comparison for the total dose that these doubly treated cells would receive. If these twice-treated cells were in anyway less susceptible to LL-37 that would suggest a subpopulation of more resilient cells exists in *B. subtilis* cultures. If they were still susceptible to LL-37 it instead would suggest that these cells stochastically survived the initial LL-37 and have no discernible characteristics from their dead sister cells, as sufficient LL-37 will have been added to bind and kill these cells as well. Fifteen minutes was used as this is sufficient time for the rapid permeabilising and bactericidal activity of LL-37 to take place (Fig. 4.3). This assay revealed that *B. subtilis* treated with 40 μg mL^{-1} LL-37 suffers rapid lysis like cultures treated with 20 μg mL^{-1}, however they take longer to recover, with OD_{600} remaining low for another hour after 20 μg mL^{-1} treated cells have resumed growth (Fig. 5.4a). The culture treated with 20 μg mL^{-1} and 20 μg mL^{-1} 15 minutes later had an OD_{600} profile almost identical to that of the culture treated with 40 μg mL^{-1} LL-37, with both lysing to the same extent and starting to recover growth at the same time ~4 hours into the assay (Fig. 5.4a). When the time to recover of the LL-37 treated cultures were compared, the 20 μg mL^{-1} treated culture took ~2 hours, whereas both the 40 and double 20 μg mL^{-1} treated cultures took to ~3 hours to recover; with both 20 + 20 and the 40 μg mL^{-1} cultures being significantly different from the 20 μg mL^{-1} recovery time, but not significantly different from each other (Fig. 5.4b). Thus, this indicates that the surviving proportion of cells in cultures that recover growth following LL-37 treatment are not resistant to LL-37, and instead are stochastically not bound by sufficient LL-37 – something that can be overcome by increasing the concentration of LL-37.

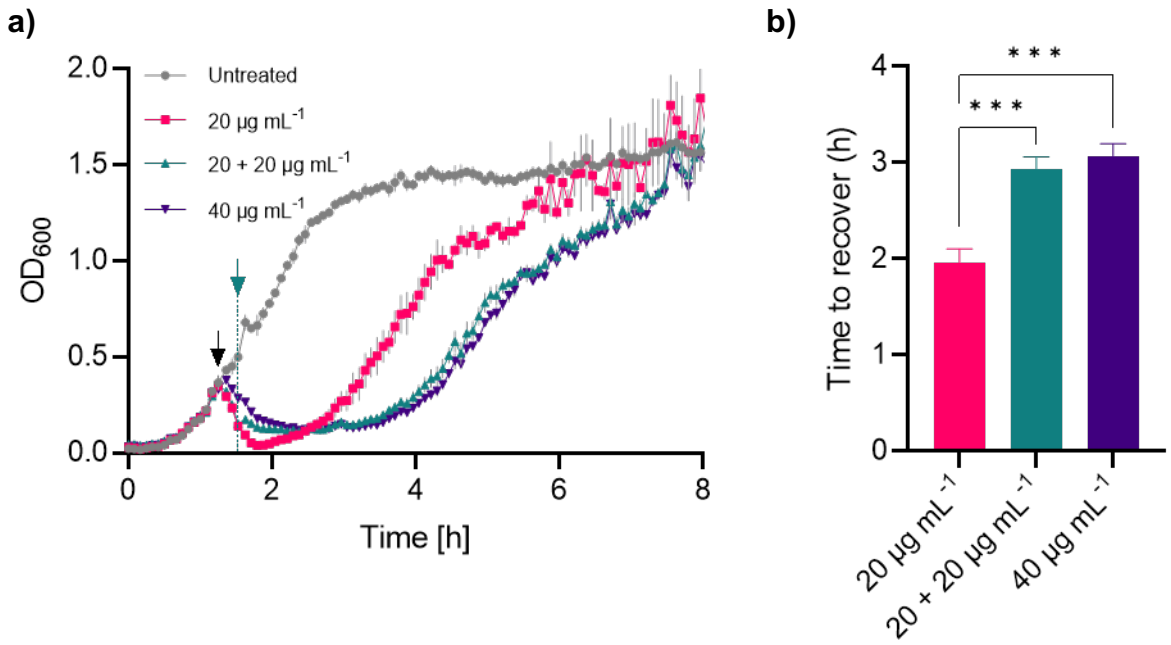

Figure 5.4. *B. subtilis* cells that survive LL-37 are initially still susceptible to subsequent treatment. a) Growth/lysis of wild-type *B. subtilis* upon the addition of 20 and 40 µg mL^{-1} LL-37 (indicated by black arrow), the 20 + 20 culture was subsequently treated with LL-37 again after 15 minutes (green arrow). **b**) Analysis of the time taken for each culture treated with LL-37 to recover to the initial optical density at which LL-37 was added; analysed by unpaired ordinary ANOVA with Tukey's multiple comparisons test to compare between all conditions, *** represents $p > 0.001$. Data represented as mean±SD (n=3).

5.2.3 B. subtilis cells that recover the culture from LL-37 treatment are neither depolarised or permeabilised

I next wanted to directly visualise cells that survive LL-37 treatment, to see if these cells were in any way impacted by the LL-37 present. To do this I used time-lapse microscopy of wild-type *B. subtilis* with the permeability dye SYTOX Green. In this assay (which stains and follows growing cells, as opposed to taking samples from a culture at time points and staining them for immediate imaging) I could not use the membrane polarisation dye $DiSC_3(5)$ as it is growth-inhibitory against *B. subtilis* (te Winkel *et al.*, 2016). This microscopy revealed that the vast majority of cells in a culture treated with 20 µg mL^{-1} LL-37 were rapidly permeabilised, with high SYTOX Green fluorescence after 5 minutes of incubation with the peptide (Fig. 5.5). Within the field of view, only one cell was not permeabilised, indicated by its lack of SYTOX Green fluorescence; it was only this non-permeabilised cell that was able to grow throughout the time-lapse, whereas the other cells all became phase light within 30 minutes, indicating they had subsequently lysed (Fig. 5.5). The non-permeabilised cell remained

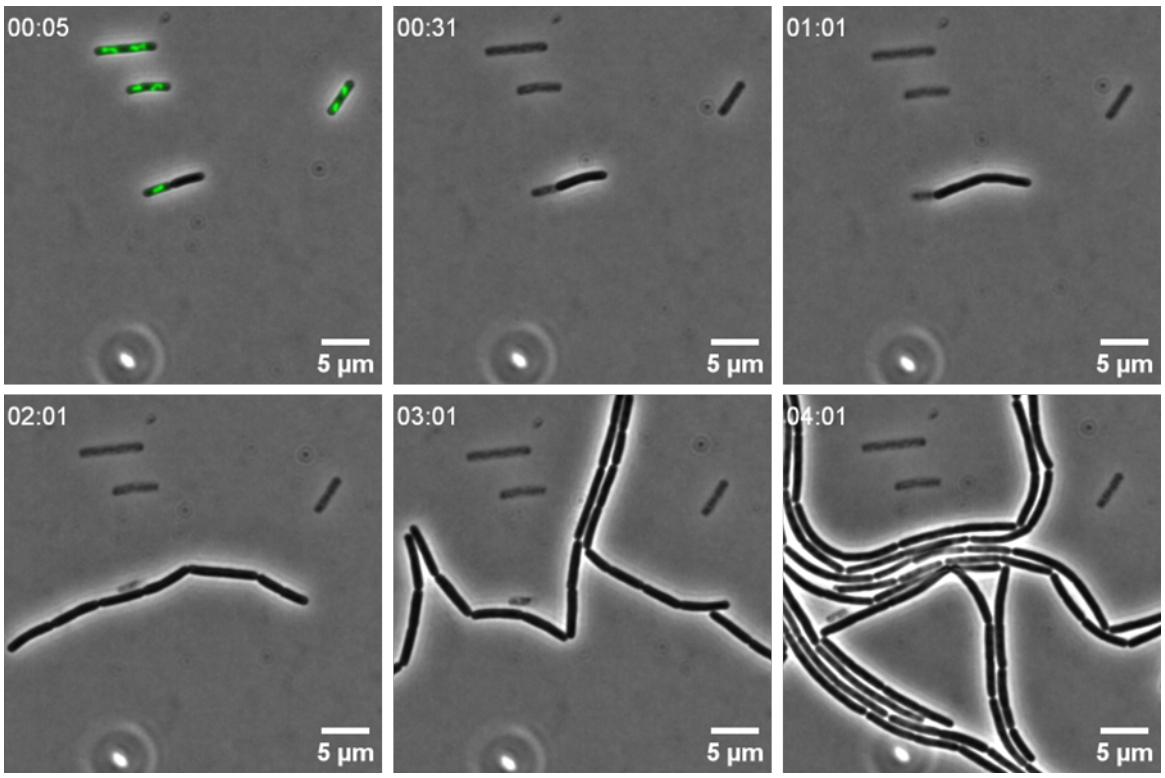

Figure 5.5. *B. subtilis* cells that survive LL-37 treatment are not permeabilised. Time-lapse fluorescent microscopy of wild-type *B. subtilis* treated with 20 µg mL^{-1} LL-37, images are a merge of phase contrast (grey) and SYTOX Green (green, 200 nM); scale bar is 5 µm.

phase dark and cell growth had occurred within 30 minutes, as the cell was elongated; by 1 hour the cell had divided into 2 cells with the division septa of the next cell division event becoming clear, by 4 hours the daughter cells of the sole non-permeabilised cell numbered far more than the number of cells at the initial time point – showing how very few surviving cells can recover an entire culture within a short time window (Fig. 5.5). Altogether, this time-lapse microscopy showed the cells that survive LL-37 treatment are not permeabilised by LL-37. However, this approach did not inform about the membrane polarisation of cells that recover cultures from LL-37 treatment.

To investigate whether the surviving cells were initially polarised or depolarised and so recovering membrane polarisation in the presence of LL-37 was my next focus. To achieve this, different fluorescent dyes had to be used to indicate membrane polarisation and permeabilisation, due to the growth inhibitory effects of $DiSC_3(5)$ in *B. subtilis*. Instead, $DiBAC_4(3)$ and propidium iodide were used as membrane polarisation and permeabilisation indicators, respectively. In contrast to the cationic membrane polarisation indicator $DiSC_3(5)$, $DiBAC_4(3)$ is anionic, meaning it is excluded from polarised cells and can only enter and stain depolarised cells (Bräuner *et al.*, 1984).

$DiBAC_4(3)$ has similar excitation and emission wavelengths to SYTOX Green, meaning they cannot be used together, so instead of SYTOX Green propidium iodide was used. Propidium iodide functions like SYTOX Green, it is excluded from non-permeabilised cells and fluoresces upon entry of permeabilised cells as it binds DNA (Stiefel *et al.*, 2015). For this experiment I used a lower concentration of LL-37, as previous experiments have proven cells that survive LL-37 result from a stochastic lack of LL-37 binding, this means lower concentrations of LL-37 should give a higher proportion of surviving and so recovering cells. Time-lapse microscopy with $DiBAC_4(3)$ and propidium iodide in wild-type *B. subtilis* treated with 5 μg mL^{-1} LL-37 revealed that the cells that grow in the presence of LL-37, in addition to not being permeabilised, as seen in Fig. 5.5, are also not depolarised – as indicated by a lack of $DiBAC_4(3)$ fluorescence in these phase dark cells (Fig. 5.6). In contrast, the permeabilised cells (propidium iodide positive) were also depolarised ($DiBAC_4(3)$ positive) at just 5 minutes of treatment, these cells went on to turn phase light, indicating subsequent lysis (Fig. 5.5a). To assess whether the surviving cells were transiently growth limited by the LL-37 present, I conducted an untreated time-lapse alongside, to enable comparison of growth. In both conditions, single cells were seen at 5 minutes, these had divided to two cells by 30 minutes, these were elongated at 1 hour and by 2 hours four cells could be delineated from each initial single cell population (Fig. 5.6). These similar growth and division rates between treated and untreated cultures indicate that *B. subtilis* cells that survive LL-37 treatment do not experience even a transient growth inhibition.

The above results clarified many features of the cells that survive LL-37 treatment and so recover growth of the culture, including that these cells are neither depolarised or permeabilised. However, these results did not clarify what happens to the small subpopulation of cells that are depolarised but not permeabilised when treated with low concentrations of LL-37, as seen in Fig. 4.3; thus, it remained unclear whether cells that were depolarised but not permeabilised could recover from this depolarisation. I searched through all fields of view of $DiBAC_4(3)$ and propidium iodide time-lapses to find cells that were depolarised but not permeabilised. Only one occurrence of a depolarised only cell was found. Within this field of view, three cell types were present: permeabilised and depolarised; depolarised only; polarised and non-permeabilised. Cells 1, 2 and 3 are examples of polarised and non-permeabilised cells, these cells grew and divided over time; cell 4 was depolarised only, as indicated by its blue $DiBAC_4(3)$ fluorescence (Fig. 5.7). The remaining cells were all depolarised and

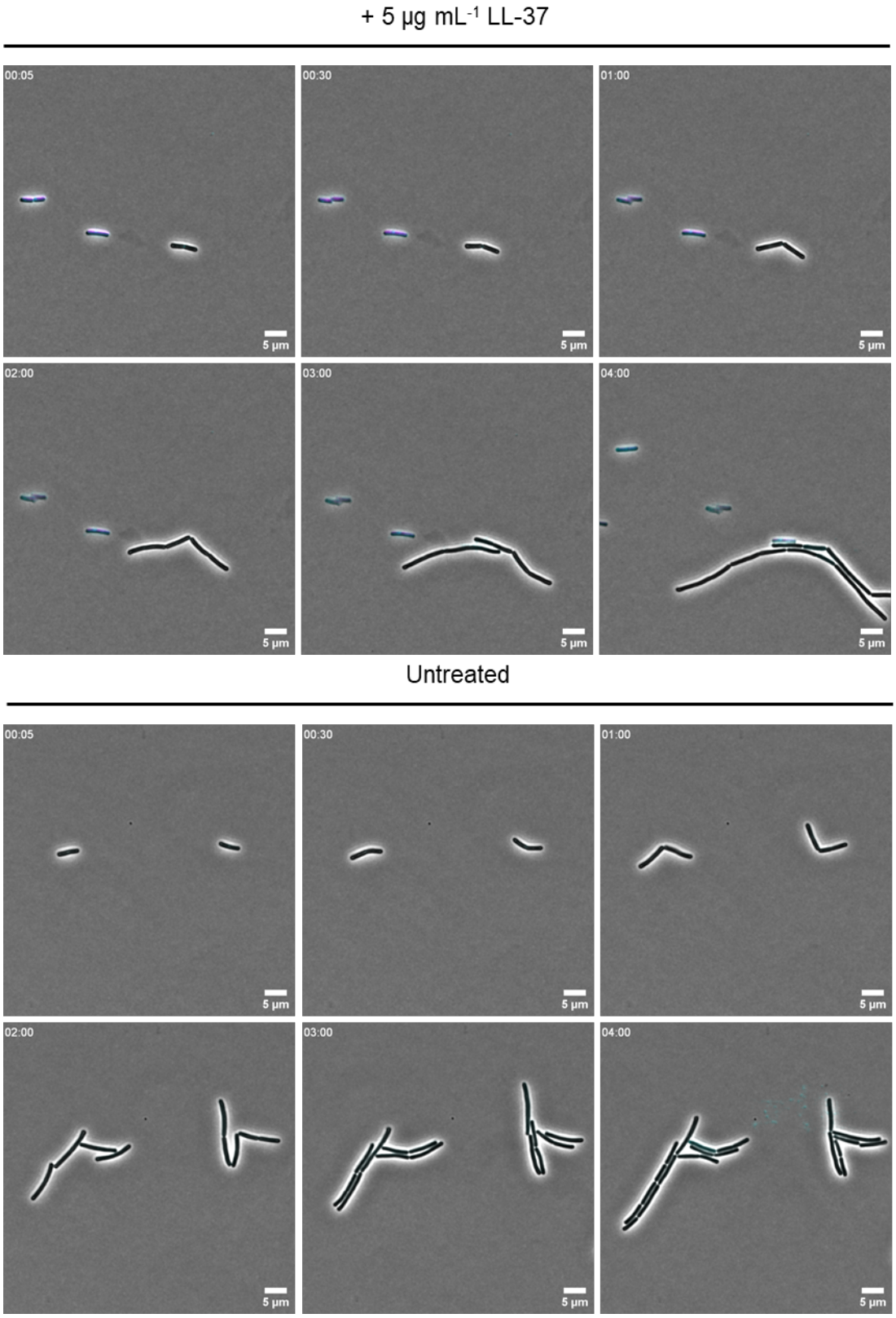

Figure 5.6. *B. subtilis* cells that survive LL-37 treatment are not permeabilised or depolarised. Time-lapse fluorescent microscopy of wild-type *B. subtilis* treated with 5 µg mL^{-1} LL-37 or untreated, images are a merge of phase contrast (grey), $DiBAC_4(3)$ (blue, 2.5 µM) and propidium iodide (pink, 10 µM); scale bar is 5 µm.

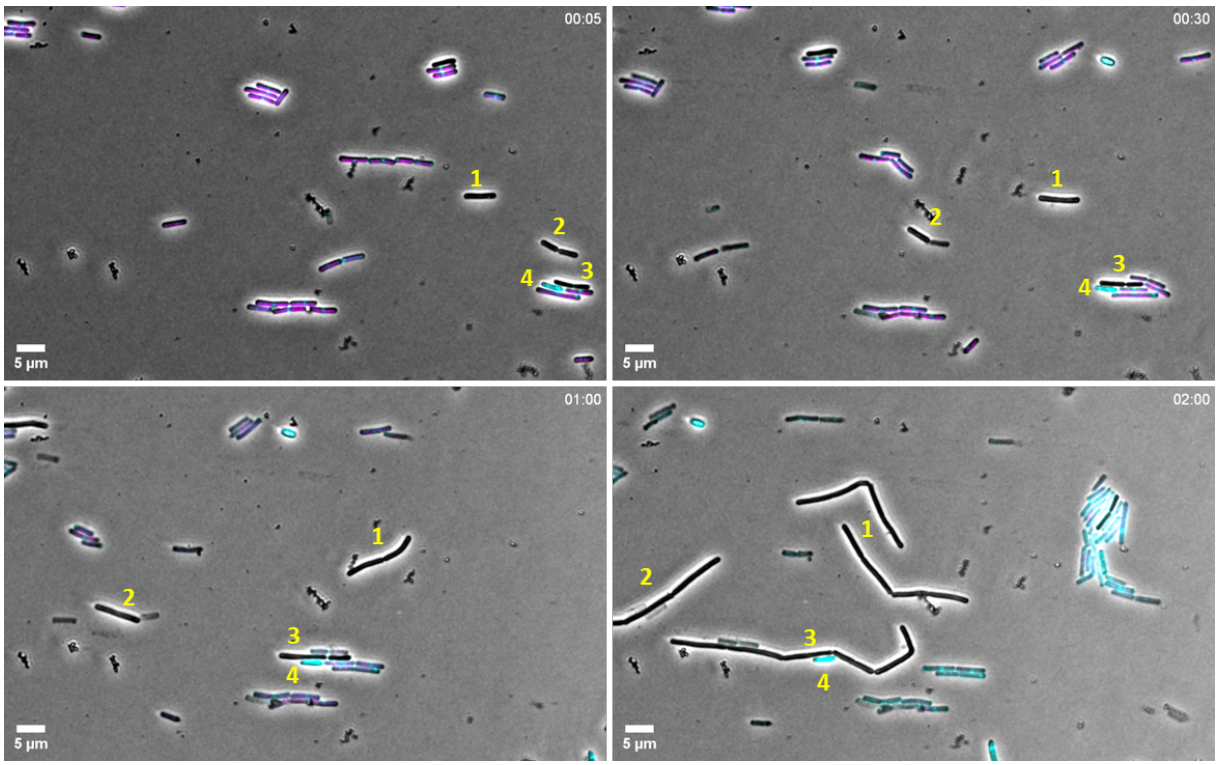

Figure 5.7. *B. subtilis* cells that are depolarised by LL-37 cannot recover. Time-lapse fluorescent microscopy of wild-type *B. subtilis* treated with 5 µg mL^{-1} LL-37, images are a merge of phase contrast (grey), DiBAC$_4$(3) (blue, 2.5 µM) and propidium iodide (pink, 10 µM); drift caused cells to move across the field of view, so numbers are used to identify the same cell at each time point; scale bar is 5 µm.

permeabilised at 5 minutes and went on to turn phase light and lyse by 1 hour. With this lysis the cell contents were released, meaning these dead cells became less fluorescent over time. Whereas the depolarised only cell, cell 4, retained its DiBAC$_4$(3) fluorescence throughout the 2 hour period, indicating this cell did not lyse. The different experimental conditions used in time-course and time-lapse microscopy mean comparisons cannot be made between 'the same' treatments, for example in Fig. 4.3 a significant number of cells treated with 5 µg mL^{-1} LL-37 are depolarised only, whereas in a time-lapse setting the vast majority of cells treated with 5 µg mL^{-1} LL-37 are both depolarised and permeabilised (Fig. 5.6&7). This microscopy suggests that *B. subtilis* is not able to recover from LL-37 induced depolarisation, and that LL-37 induced depolarisation is not sufficient to trigger autolysis. However, as only one depolarised but not permeabilised cell has been observed across the microscopy I have conducted this result is not conclusive, as further observations are required to support this.

5.2.4 S. aureus can recover from LL-37-induced depolarisation

Having found that *B. subtilis* cells that grow in the presence of LL-37 are neither depolarised or permeabilised, I wanted to see if this was also the case in the

pathogenic Gram-positive species *S. aureus*. I first conducted $DiSC_3(5)$ and SYTOX Green time-course microscopy in ΔL-PG *S. aureus* treated with 25 μg mL^{-1} LL-37. As controls for depolarisation and permeabilisation, respectively, gramicidin ABC and nisin were used – nisin is not normally effective in *S. aureus*, but as the strain used here was deficient for lysyl-phosphatidyl glycerol (L-PG) it was susceptible (Peschel *et al.*, 2001). The coccoid shape of *S. aureus* is visible in this microscopy, untreated cells were phase dark, strongly $DiSC_3(5)$ stained indicating they were polarised, and lacked SYTOX Green staining, meaning they were not permeabilised (Fig. 5.8). Incubation with nisin caused *S. aureus* to become 'phase bright' as the interior of the cells became light without the cell membrane being overtly compromised, the cells were also SYTOX Green positive, indicating permeabilisation, and were depolarised as no $DiSC_3(5)$ staining occurred. This 'phase bright' phenomenon shows that the optical properties of the cells have changed and 'phase bright' is distinct from phase light, lysed cells. 'Phase bright' *S. aureus* cells have previously been observed with other antimicrobial agents but to the best of my knowledge the mechanism behind it has not yet been characterised. With gramicidin ABC, *S. aureus* was depolarised without being permeabilised, seen in the lack of both $DiSC_3(5)$ and SYTOX Green staining (Fig. 5.8). Within 10 minutes of incubation with LL-37, *S. aureus* was depolarised, permeabilised and 'phase bright', this state continued in the majority of cells imaged across the 120 minute time-course. However, by 120 minutes a single cell was observed that was not permeabilised, as it lacked SYTOX Green fluorescence, but the cell was still depolarised, as it also lacked $DiSC_3(5)$ fluorescence (Fig. 5.8). This microscopy indicates that like *B. subtilis, S. aureus* is also rapidly permeabilised by LL-37 and supports previous observations that *S. aureus* is not liable to lyse when treated with LL-37 (Fig. 3.14), as no lysed (phase light) cells were visible at any time point. Instead 'phase bright' cells were seen – these coincided with SYTOX Green positive cells, indicating *S. aureus* cells are 'phase bright' when permeabilised (Fig. 5.8). The existence of a depolarised but not permeabilised cell in this microscopy shows LL-37 also likely results in 3 cell subpopulations in *S. aureus*: polarised, depolarised, and depolarised and permeabilised – leading to questions regarding whether LL-37-induced depolarisation in *S. aureus* is also unrecoverable like it seems to be in *B. subtilis*.

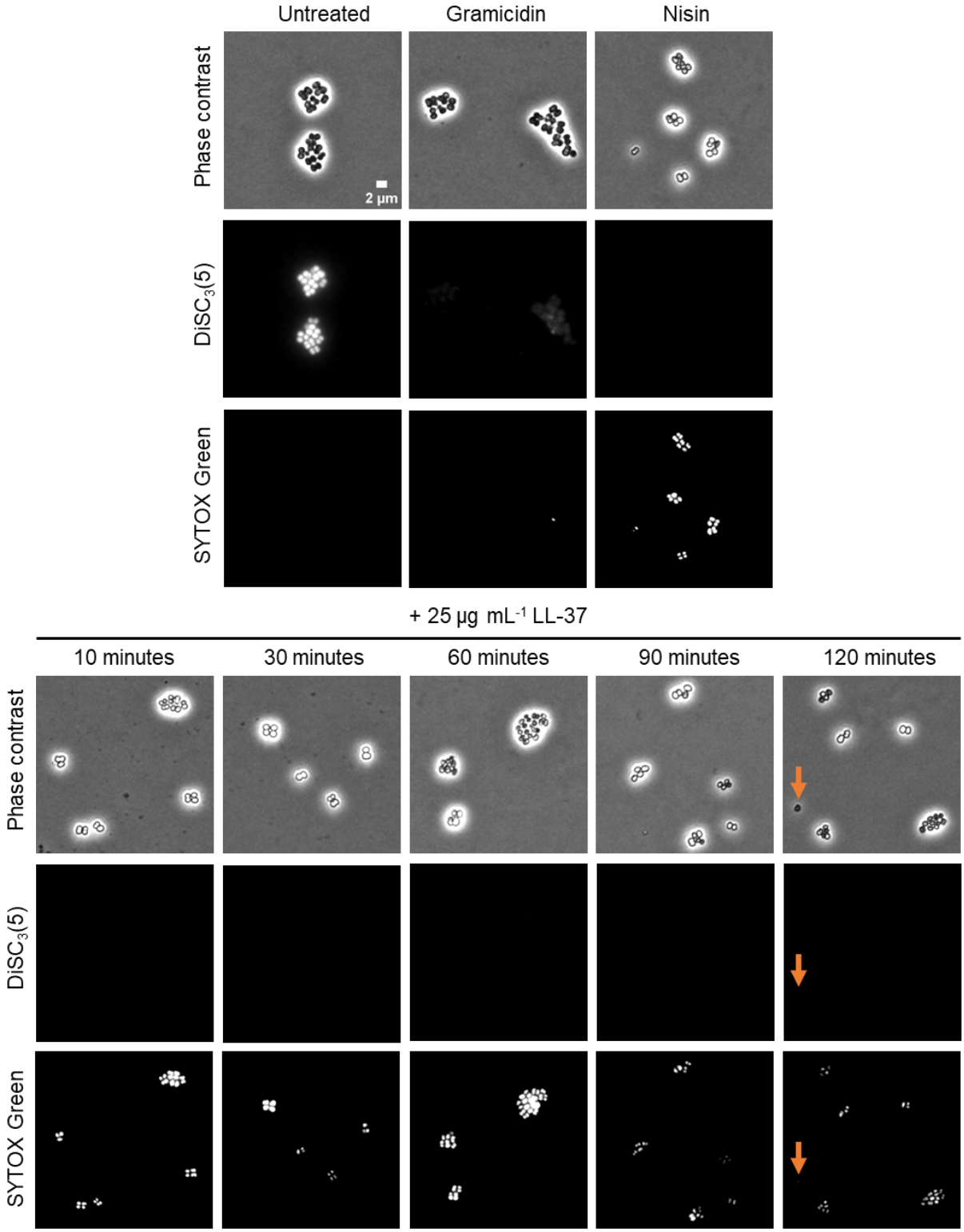

Figure 5.8. LL-37 induces rapid permeabilisation and depolarisation of *S. aureus*. Time-course fluorescent microscopy images of ΔL-PG *S. aureus* with $DiSC_3(5)$ (2 µM) and SYTOX Green (200 nM) fluorescence untreated, with nisin (5 µM) and gramicidin ABC (5 µM) after 5 minutes treatment, and of cells treated with 25 µg mL^{-1} LL-37 over time; orange arrow indicates depolarised but not permeabilised cell treated with LL-37; scale bar is 2 µm.

I next followed LL-37 treatment of *S. aureus* in a time-lapse format, for this $DiSC_3(5)$ and SYTOX Green could be used as $DiSC_3(5)$ is not growth inhibitory in *S. aureus* (Laborda Anadón, 2022). This showed the majority of *S. aureus* cells to be permeabilised and depolarised, seen in SYTOX Green fluorescence and lack of $DiSC_3(5)$ fluorescence, respectively, after just 5 minutes incubation with LL-37, reaffirming the rapid permeabilising activity of LL-37 against *S. aureus* (Fig. 5.9). Some cells within the bottom right cluster were polarised at 5 minutes, shown by their $DiSC_3(5)$ fluorescence, and these cells went on to divide, with more cells present in this cluster by 2 hours. Additionally, two cells in the top left cluster were initially depolarised but not permeabilised, indicated by their lack of both $DiSC_3(5)$ and SYTOX Green fluorescence; by 1 hour these two cells regained polarisation and by 3 hours had resumed growth. By 4 hours three actively dividing clusters existed from the original cells in the field of view, with both the initially polarised and initially depolarised cells contributing to culture growth (Fig. 5.9). To establish whether *S. aureus* that grows after LL-37 treatment experiences a growth lag, I conducted an untreated time-lapse alongside. The untreated *S. aureus* cell clusters took ~2 hours for the first instance of cell division to occur, this was also the case for the lower right LL-37 treated cluster that remained polarised throughout. However, the cells that were initially depolarised but then recovered polarisation took until 3 hours to divide, meaning the transient depolarisation of these cells caused a growth delay (Fig. 5.9). Overall, this microscopy indicates that *S. aureus* is able to recover from LL-37 treatment from two sub-populations within cultures: cells that have not been bound by LL-37 meaning they are polarised, and depolarised cells that can recover membrane polarisation and resume growth after a delay, in contrast cells that have been permeabilised by LL-37 cannot recover.

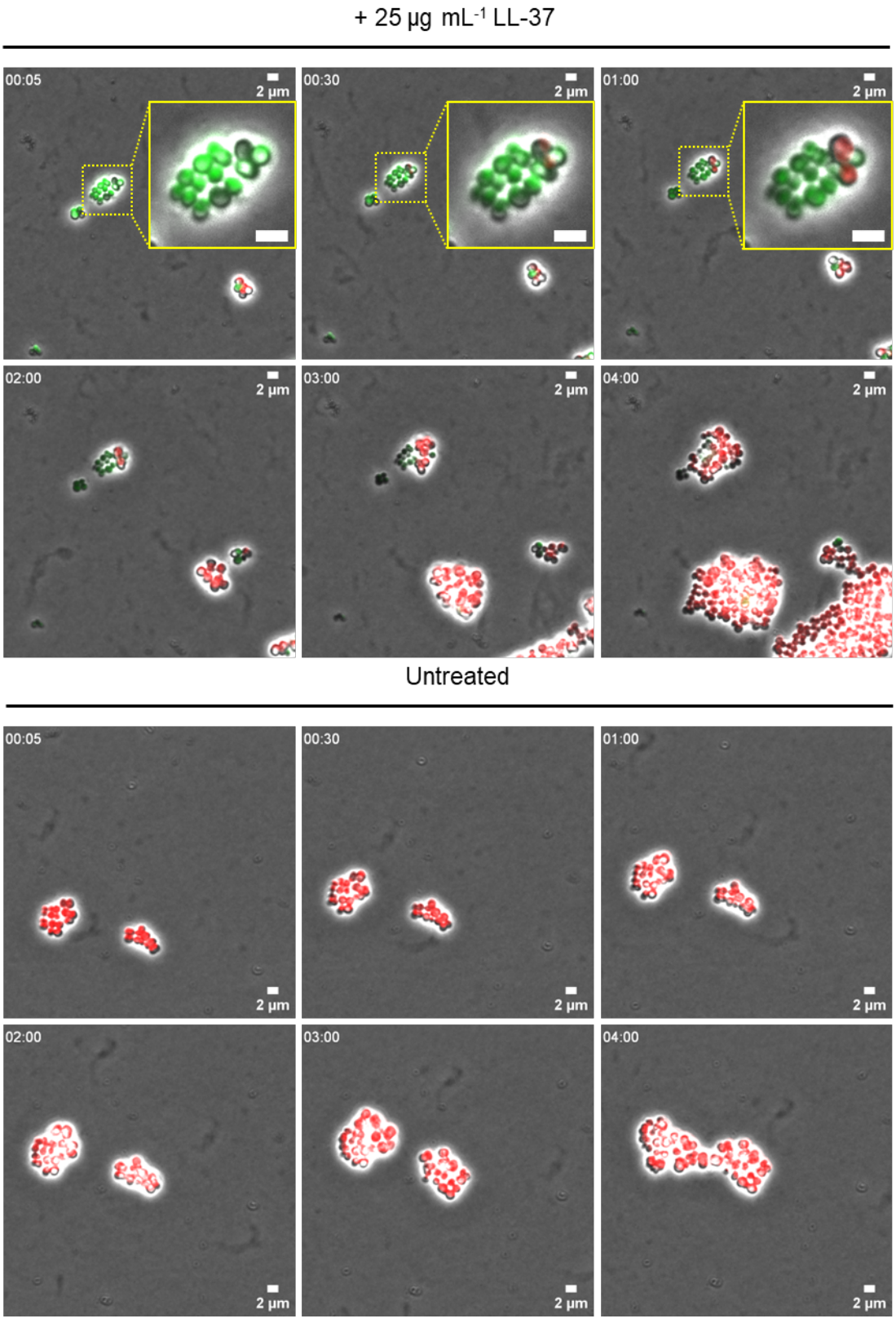

Figure 5.9. *S. aureus* can recover from LL-37-induced depolarisation. Time-lapse fluorescent microscopy of ΔL-PG *S. aureus* treated with 25 µg mL^{-1} LL-37 and untreated, images are a merge of phase contrast (grey), $DiSC_3(5)$ (red, 2 µM) and SYTOX Green (green, 200 nM); yellow boxes zoom on region containing depolarised but not permeabilised cells that recover; scale bar in all images is 2 µm.

5.2.5 *Cultures are protected from subsequent LL-37 exposure by dead cell debris*

I next wanted to examine how the susceptibility of *B. subtilis* cultures that have regrown following LL-37 treatment is impacted by their previous exposure to LL-37. I have already established that these cells are not genetically resistant to LL-37 (Fig. 5.1), and subsequently saw that this is due to the *B. subtilis* cells that recover from LL-37 being unaffected by the AMP (Fig. 5.6). Instead of giving a second dose immediately after the first, as I did in Fig. 5.4, I wanted to assess the susceptibility of cultures once they had regrown to the initial OD_{600} at which LL-37 was added. I treated wild-type *B. subtilis* with 20 µg mL^{-1} LL-37 and waited until the culture had recovered OD_{600} to ~ 0.3 before then giving a second 20 µg mL^{-1} dose. The culture lysed upon addition of the first dose of LL-37, seen in the reduction in OD_{600}, before recovering growth after ~2 hours; however, upon addition of the second dose of LL-37, no change in OD_{600} occurred relative to the singly treated culture, with the culture continuing to grow at the same rate as the culture that did not receive a second dose of LL-37 (Fig. 5.10). Overall, this shows cultures that have received LL-37, whilst initially still susceptible to LL-37 (Fig. 5.4), are no longer susceptible to LL-37 once they have resumed growing (Fig. 5.10).

Next, I wanted to investigate how recovered cultures were able to survive subsequent exposure to LL-37. As, whilst previous experiments suggested cells that recover from LL-37 are not affected by the treatment, it is still possible that these cells may have induced stress responses that would enable better survival of subsequent LL-37

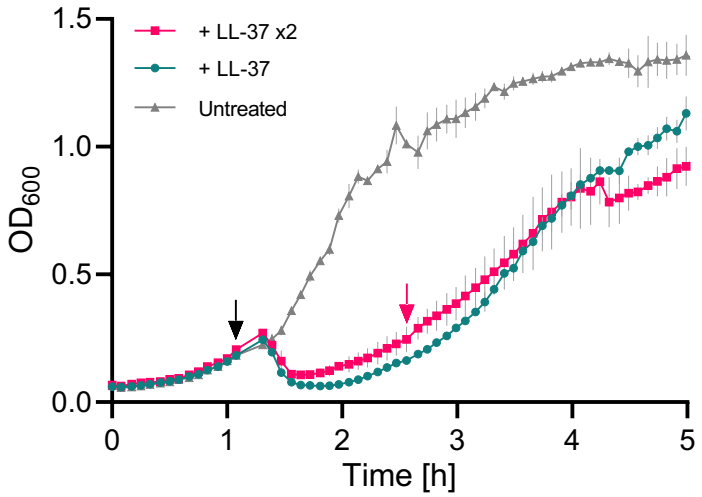

Figure 5.10. *B. subtilis* cultures are not susceptible to LL-37 once regrown. Growth/lysis of wild-type *B. subtilis* upon the addition of 20 µg mL^{-1} LL-37 (indicated by black arrow), the LL-37 x2 culture was subsequently treated with LL-37 again once the culture had regrown to the initial OD_{600} at which LL-37 was added (pink arrow). Data represented as mean±SD (n=3).

treatment. I first looked for previous observations of this subsequent exposure survival phenomenon. Wu and Tan (2019) previously found that *E. coli* is able to survive LL-37 exposure through the presence of dead cell debris within the culture sequestering the AMP; therefore, I looked to see if this was also the case in *B. subtilis*. Wild-type *B. subtilis* lysate was generated by the sonication of a stationary phase culture, this was then diluted in LB to mimic the equivalent debris of an OD_{600} 0.3 culture. Wild-type *B. subtilis* was grown in this cell lysate-enriched-LB and in normal LB for comparison, once cultures had grown to OD_{600} 0.3 LL-37 was added. The presence of cell lysate did not impact the growth of untreated cultures, as + lysate and untreated grew similarly. The presence of cell lysate in a culture treated with LL-37 prevented LL-37-induced lysis, and instead this culture continued to grow in the presence of LL-37 (Fig. 5.11a), supporting the hypothesis that cell debris protects *B. subtilis* from LL-37. I looked to see if this "dead cell binding" of LL-37 could be seen in action, by imaging *B. subtilis* over time that had been treated with fluorescently labelled LL-37. LL-37 was highly bound to cells within 10 minutes and exhibited the diffuse throughout cell binding I observed previously in Fig. 4.4&5 (Fig. 5.11b). Of note, at 30 and 60 minutes phase light cells were seen (Fig. 11b); these lysed cells, which were obviously non-viable, were still highly bound by LL-37, visually confirming the binding of LL-37 to dead cells.

To verify that it was the presence of cell debris in recovered cultures that protected them from subsequent exposure to LL-37, I decided to conduct the double dose assay of Fig. 5.10 but with a wash before the second dose of LL-37. A wash step should remove the cell debris from the culture and if the debris is responsible for protection, should re-sensitise the culture to LL-37. In this assay, I compared the growth of these conditions to naïve cells which had not been previously exposed to LL-37. The culture that had been washed lysed when the second dose of LL-37 was added, seen in its reduction in OD_{600} from ~0.25 to ~0.15, whereas the culture that was not washed had only a minimal effect from a second dose of LL-37 and had resumed growth within 30 minutes. The lysis of the washed culture was similar to that of naïve cells, with both taking ~2 hours to recover to the initial OD_{600} at which LL-37 was added (Fig. 5.12). The renewed susceptibility that washing a culture caused supports the previous finding that cell debris confers protection against LL-37 in *B. subtilis*, as the wash removes this debris. This also indicates that cells that survive LL-37 are not adapted to grow in

its presence, which is consistent with a lack of growth effect on cells that grow in the presence of LL-37.

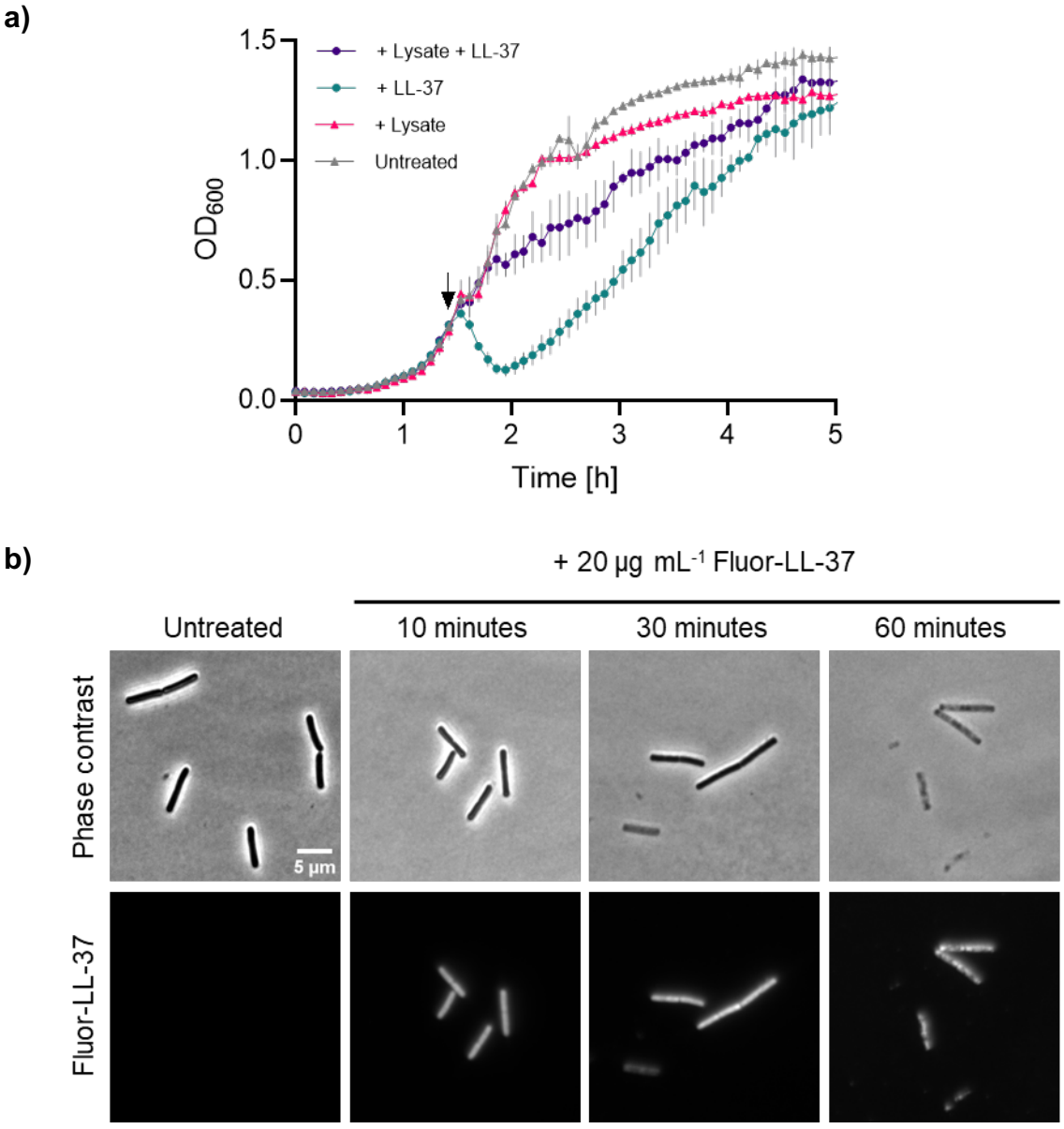

Figure 5.11. Cell debris protects *B. subtilis* from LL-37-induced lysis. **a**) Growth/lysis of wild-type *B. subtilis* grown with and without wild-type *B. subtilis* cell lysate upon the addition of 20 µg mL^{-1} LL-37 (indicated by arrow); cell lysate was generated by the sonication of a stationary phase culture, this was then diluted in LB to mimic the cell debris of an OD_{600} 0.3 culture. Data represented as mean±SD (n=3). **b**) Time-course fluorescent microscopy images of wild-type *B. subtilis* untreated and of cells treated with 20 µg mL^{-1} 5-Fam-LC-LL-37 (Fluor-LL-37); scale bar is 5 µm.

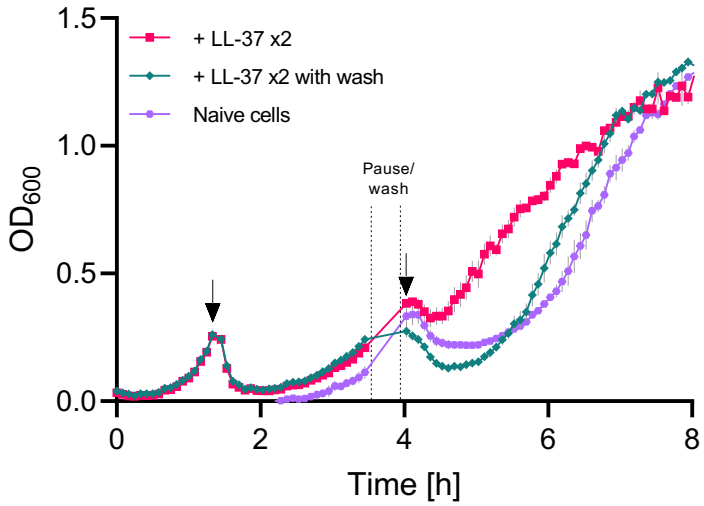

Figure 5.12. Washing away cell debris restores *B. subtilis* susceptibility to LL-37. Growth/lysis of wild-type *B. subtilis* upon the addition of 20 µg mL^{-1} LL-37 (indicated by first arrow), once the cultures had regrown to the initial OD_{600} at which LL-37 was added the 'LL-37 x2 culture with wash' culture was removed from the plate reader, centrifuged and resuspended in fresh LB twice before being returned to the plate reader, both the LL-37 x2 cultures were then treated with LL-37 again (second arrow). Data represented as mean±SD (n=3).

5.2.6 Membrane debris is responsible for the LL-37-sequestering activity of dead cell debris

The protective effect of dead cell debris against LL-37 is shared between *E. coli* and *B. subtilis*. Wu and Tan (2019) hypothesised that this protective effect was due to the release of anionic DNA from dead cells binding and sequestering LL-37, preventing it from interacting with live cells in the culture. However, as I had already observed that LL-37 does not exhibit a preference for DNA-containing regions of *B. subtilis* cells (Fig. 4.5) this did not seem likely to be the case. To identify what component of dead cell debris was sequestering LL-37, I separated cell lysate into an insoluble fraction, a cytoplasmic fraction and a membrane fraction through sonication and ultracentrifugation. Additionally, I used lysate from wild-type and L-form cells, which lack a cell wall, to definitively distinguish between protection by the cell wall and membrane components (Kawai *et al.*, 2014). Addition of the insoluble fraction, which is composed of large cell components such as the cell wall and ribosomes, and of the cytoplasmic fraction, which contains DNA, did not confer protection against LL-37, as cells still lysed in their presence (Fig. 5.13a). Whereas the addition of the membrane fraction from both wild-type and L-form cells protected the cells from lysis, and instead they were able to continue growing similar to an untreated culture (Fig. 5.13a). I looked

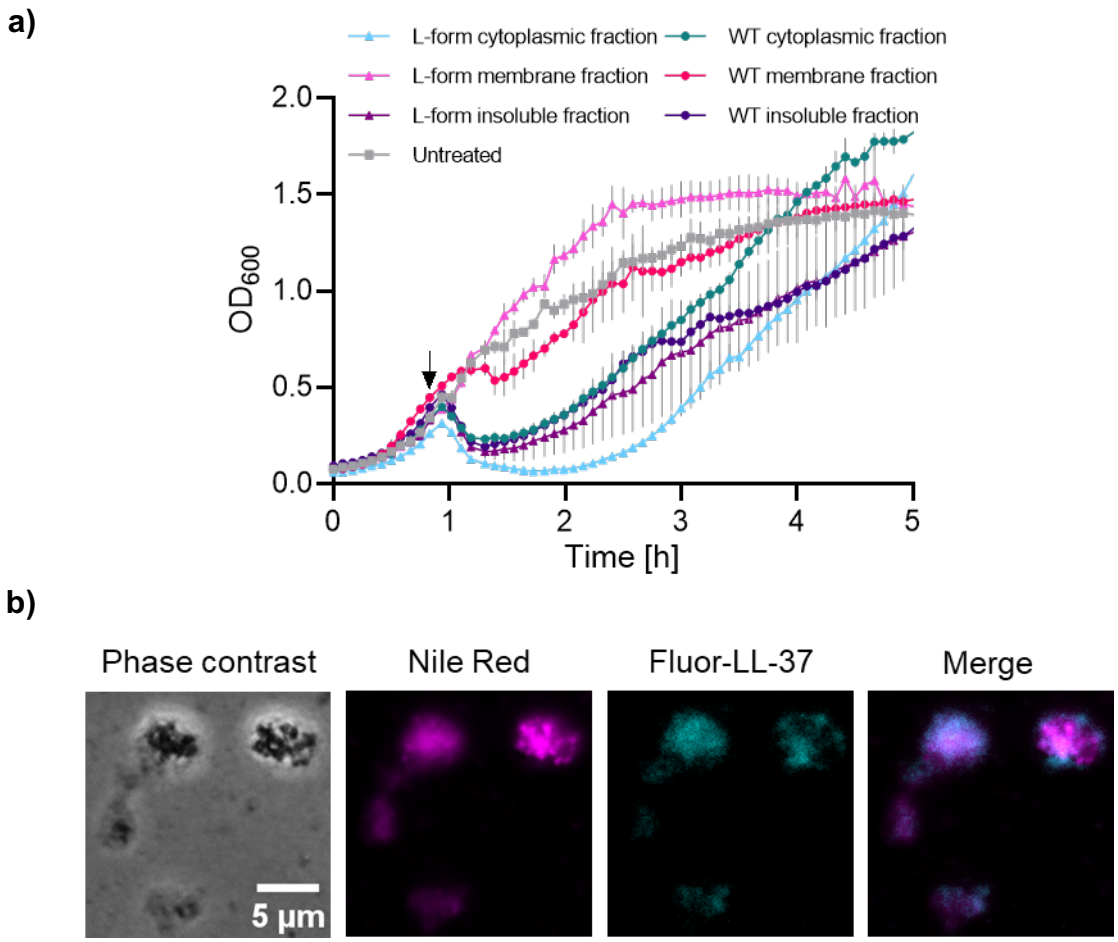

Figure 5.13. Membrane debris protects *B. subtilis* from LL-37. a) Growth/lysis of wild-type (WT) *B. subtilis* grown with the cytoplasmic fraction, membrane fraction and insoluble fraction of WT or L-form *B. subtilis*, upon the addition of 20 µg mL^{-1} LL-37 (indicated by arrow). Insoluble fraction obtained from centrifugation pellet of sonicated culture, the supernatant was ultra-centrifugated and the pellet formed the membrane fraction, and the supernatant gave the cytoplasmic fraction; the fractions were diluted to give debris akin to that of an OD_{600} 0.3 culture. Data represented as mean±SD (n=3). **b**) Fluorescent microscopy images of L-form membrane fraction with Nile Red (50 µg mL^{-1}) and 5-Fam-LC-LL-37 (Fluor-LL-37; 20 µg mL^{-1}), scale bar is 5 µm.

to visualise the sequestering activity of the membrane fraction by conducting fluorescence microscopy of the L-form membrane fraction, as this was the most protective, with Nile Red, a membrane stain, and fluorescently-labelled LL-37 (Greenspan *et al.*, 1985). This confirmed the debris present in the fraction to be membrane, as it was highly bound by Nile Red, and the fluorescently-labelled LL-37 colocalised to these regions, proving the LL-37-binding activity of cell membrane debris (Fig. 5.13b). Hence, the presence of membrane debris within a culture protects cells from LL-37, as the debris appears to adsorb the LL-37, preventing its interaction with live cells in the culture.

Having established that the membrane component of dead cell debris is responsible for sequestering LL-37 from live cells in recovered cultures, I wanted to examine how teichoic acids and their modification could impact this sequestration activity. I previously observed that teichoic acids and their D-alanylation protect *B. subtilis* from LL-37, as when these are deficient *B. subtilis* is significantly more sensitive to LL-37 (Fig. 3.3&4). Thus, I decided the test the protective effect of cell lysate from WTA, LTA and D-alanylation deficient *B. subtilis*, in comparison to lysate from wild-type. Addition of these lysates had no effect on the normal growth of *B. subtilis*, as all conditions had very similar growth curves (Fig. 5.14a). When LL-37 was added wild-type lysate protected the culture from the dramatic lysis experienced by the lysate free culture, instead only a small decrease in OD_{600} occurred before the wild-type lysate culture resumed growing again (Fig. 5.14b). The protection conferred by the ΔWTA lysate was almost identical to that of wild-type lysate, with their growth/lysis profiles being very similar. Whereas the culture with ΔLTA lysate lysed more, yet its reduction in OD_{600} was not as rapid or prolonged as the culture without lysate. Finally, the addition of Δ*dltA* lysate was extremely protective, as this culture experienced no reduction in OD_{600} and instead continued to grow immediately after the addition of LL-37 (Fig. 5.14b). Comparison of culture recovery time showed that whilst the addition ΔWTA lysate did not significantly differ from wild-type lysate, the lack of LTAs in the ΔLTA lysate resulted in a significantly longer time to recover (Fig. 5.14c). The addition of the Δ*dltA* was so strikingly protective that the culture continued to grow without delay. Altogether, this assay showed that LTA is a component of dead cell debris that is involved in LL-37 sequestration, as lysate is less protective in its absence, this however is not also the case for WTA, as lysate lacking WTA was as protective as wild-type lysate. The striking protection conferred by Δ*dltA* lysate confirms that the normal presence of D-alanylation suppresses LL-37 interaction with teichoic acids.

5.3 Discussion

Unpicking how some bacterial cells are able to survive and grow when treated with antimicrobials is key to enhancing strategies against antibiotic tolerance and resistance. To establish whether *B. subtilis* employs any strategies to evade the bactericidal activity of LL-37, I looked into the roles of genetic mutations, extracellular proteases and the presence of spores in cultures in surviving LL-37 treatment. In *S. aureus* resistance to LL-37 has been characterised to be mediated through an increase in cellular net charge and proteolytic degradation (Peschel *et al.*, 2001; Sieprawska-

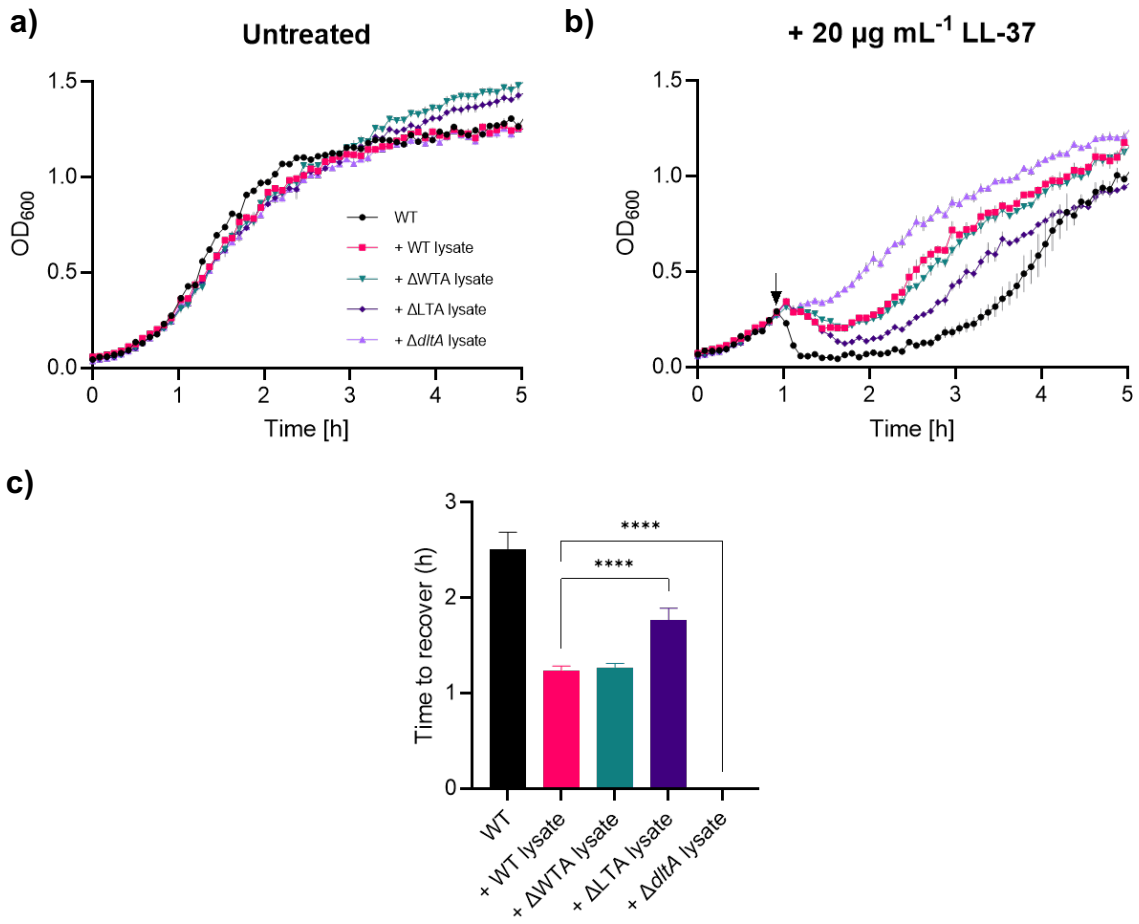

Figure 5.14. Teichoic acids contribute to the sequestering activity of dead cell debris. Growth/lysis of wild-type (WT) *B. subtilis* (**a**) untreated and (**b**) upon the addition of 20 µg mL^{-1} LL-37 (indicated by arrow), cultures were grown with and without cell lysate from WT, wall teichoic acid deficient (ΔWTA), lipoteichoic acid deficient (ΔLTA) and D-alanylation deficient (Δ*dltA*) *B. subtilis*; cell lysates were generated by the sonication of stationary phase cultures, these were diluted in LB to mimic the cell debris of an OD_{600} 0.3 culture. **c**) Analysis of the time taken for each culture treated with LL-37 to recover to the initial optical density at which LL-37 was added; analysed by unpaired ordinary ANOVA with Dunnet's multiple comparisons test comparing to + WT lysate (excludes WT), **** represents p > 0.0001. Data represented as mean±SD (n=3).

Lupa *et al.*, 2004). Peschel *et al*. (2001) were the first to describe MprF, the protein responsible for adding an L-lysine residue to PG to confer a positive charge to the membrane phospholipid. However, I have already shown that this resistance mechanism, whilst conserved, is not effective in *B. subtilis*; as a strain lacking L-PG was as susceptible as wild-type to LL-37, whereas D-alanylation was protective in *B. subtilis* (Fig. 3.12b & 3.4). In addition, I analysed the possibility of any genetic resistance mechanism that may be selected for when *B. subtilis* is treated with LL-37, following the workflow described in Fig. 5.1a. This failed to identify any isolates that

were more resistant to LL-37 than wild-type, indicating that genetic resistance is not responsible for the proportion of cells that survive during LL-37 treatment. I next analysed the role of proteolytic degradation of LL-37, as this has already been characterised in other Gram-positive species, such as *S. aureus* and *B. anthracis* (Sieprawska-Lupa *et al.*, 2004; Thwaite *et al.*, 2006). I looked to see if the extracellular proteases of *B. subtilis* could protect a growing culture from LL-37, but there was no difference in the lytic activity of LL-37 incubated in protease-containing and lacking supernatants (Fig. 5.2), meaning that proteolytic degradation is also not employed by *B. subtilis* to enable survival of LL-37. A lack of protease activity against LL-37 has also been observed in *E. coli*, with no LL-37 degradation occurring when it was incubated in the supernatant of protease-producing cells (Wu & Tan, 2019). Additionally, the role of proteolytic degradation in resistance to LL-37 is questionable, due to the finding that LL-37 is resistant to proteolytic degradation when in solution and when bound to membranes (Oren *et al.*, 1999). This may mean that even if LL-37 is experimentally susceptible to proteases, this may not be the case *in vivo*. The final mechanism I explored was spore formation, a phenomenon that is limited to a subset of the Gram-positive Firmicutes phylum (Fritze, 2004). This however proved to not contribute to the survival and rapid recovery of *B. subtilis* from LL-37 treatment under these experimental conditions, as cells lacking the ability to form spores recovered as quickly as a wild-type culture (Fig. 5.3). This does not rule out that spores, if present under other conditions, could contribute to LL-37 resistance in *B. subtilis*.

Having ruled out specific potential mechanisms for survival of LL-37, I then undertook a more general approach that would instead show if the surviving sub-population of cells were somehow resistant to LL-37. By adding LL-37 to a culture, and then adding LL-37 to the culture again 15 minutes I could test whether the sub-population of cells that recover so rapidly from LL-37 treatment do so because they are in anyway distinct, or if their survival is just stochastic. As the twice treated cells lysed to the same extent as those that received an initial double dose (Fig. 5.4), this showed the recovery of cells in a *B. subtilis* culture to be likely driven by a stochastic lack of LL-37 binding rather than specific characteristics of the surviving cells. I previously showed that LL-37 exhibits cooperative binding (Fig. 4.1), together with these results this indicates that when treated with LL-37 the majority of cells are bound by sufficient LL-37 and they permeabilise and die; however, a small proportion, that diminishes as the LL-37 concentration is increased, are not bound by LL-37 and instead continue to grow and

recover the growth of the culture. A lack of specific characteristics that protect cells that recover from LL-37 was supported by the later finding that cells are susceptible to further LL-37 if they are resuspended in fresh media (Fig. 5.12), as this showed that the cells themselves are not tolerant of LL-37. Whilst these data indicate the stochastic nature of LL-37 survival, this on its own is an interesting phenomenon that warrants further investigation. RNA sequencing of recovered cultures had been considered for this project however it was not undertaken for the following reasons: i) the results from Fig. 5.4 indicated survival is stochastic, thus the likelihood of transcriptome changes seemed low; ii) to have sufficient c.f.u. for RNA sequencing the cultures had to recover to OD_{600} 0.3 which would mean several generations of bacterial division would have occurred, meaning any transient transcriptome changes would already be lost. This issue of timing could be overcome by a combination of techniques. Firstly, the cells that survived the LL-37 treatment would need to be isolated, they make up a small proportion of the culture, so to achieve a sufficient number of cells a very large culture would be required. Surviving cells could be isolated from their dead sister cells by flow cytometry fluorescence-activated cell sorting (FACS), this technique would also enable quantification of the dead and viable cells in a whole culture. FACS would require labelling of the cells dependent on their viability, using a permeability indicator such as SYTOX Green. FACS has recently been employed to sort *B. subtilis* spore-germinating populations, in this study they effectively used propidium iodide as an indicator of compromised cytoplasmic membranes (Zhang *et al.*, 2020b). I have shown that only SYTOX Green/ propidium iodide negative cells recover from LL-37 treatment, as all permeability positive cells lyse (Fig. 5.5-7). When using FACS to sort LL-37 treated cells, SYTOX Green positive cells would make up the dead proportion of the culture and SYTOX Green negative cells would contain the viable cells remaining. This may be complicated by the presence of depolarised but not permeabilised cells, as it remains unclear whether or not these cells are viable in *B. subtilis* (Fig. 5.7). Once FACS has isolated a sufficient number of surviving cells, these could then be rapidly sampled for RNA sequencing. RNA sequencing would enable characterisation of the transcriptome of LL-37 recovered cells, which when compared to that of untreated cells should indicate whether these cells are in anyway distinct and reveal any adaptations they may have.

The non-growing depolarised cell in Fig. 5.7 suggests that *B. subtilis* cells depolarised by LL-37 are not viable; however, definitive conclusions cannot be drawn from a single

observation so more research of this is required. This could be achieved by conducting $DiBAC_4(3)$ and propidium iodide time-lapses where the fields of view are chosen dependent on the presence of $DiBAC_4(3)$ only positive cells, as opposed to the random selection of fields of view I conducted. By selecting $DiBAC_4(3)$ only positive cells, a number of these cells can be followed to reveal whether any regain membrane polarisation. The lack of propidium iodide staining in the depolarised only cell across the 2 hour time-lapse suggests that LL-37-induced depolarisation is not sufficient to trigger rapid autolysis (Fig. 5.7) – again further observations are required to support this. Of note, when Barns & Weisshaar (2013) conducted real-time single cell microscopy of *B. subtilis*, they found that cells treated with low concentrations of LL-37 experienced a growth rate decrease that could be recovered if the LL-37 was washed away. These growth rate decreased cells would not have been permeabilised by LL-37, as I have shown that to be bactericidal; however, there is the possibility that this growth rate decrease could be related to depolarisation, as this is not something that Barns & Weisshaar (2013) monitored. Therefore, an important follow-up experiment would be to conduct the same real-time single cell time-lapses as Barns & Weisshaar, but to include a non-toxic membrane polarisation indicator too, such as $DiBAC_4(3)$. Additionally, the ability to restore the growth of these cells with the washing away of LL-37 indicates LL-37 had not interacted strongly with the cell envelopes. It seems that low concentrations of LL-37 cause weak interactions with cells that whilst disruptive are not bactericidal. Only higher levels of binding, caused by cooperative binding (when the threshold is passed) are sufficient to fully disrupt the cytoplasmic membrane, resulting in permeabilisation and cell death. Whilst the outcome of LL-37-induced depolarisation is unclear in *B. subtilis*, in *S. aureus* it is clear that cells initially depolarised by LL-37 can go on to recover membrane polarisation and eventually resume growth (Fig. 5.9). Overall *S. aureus* appears to be a more resilient species to LL-37 than *B. subtilis*, as wild-type *S. aureus* cannot be killed by LL-37 within the confines of our experimental set-up (Table 3.2) and whilst bactericidal concentrations induce rapid lysis in *B. subtilis*, ΔL-PG *S. aureus* cells whilst dead remain intact (Fig. 3.12). This resilience of *S. aureus* to LL-37 could be due to its co-evolution with the AMP in the human body, as *S. aureus* will have been exposed to LL-37 when infecting humans, whereas *B. subtilis*, being a soil microbe, has likely had little evolutionary exposure to LL-37. Thus, the ability of *S. aureus* to recover its membrane polarisation following LL-37 treatment should not be taken as an indication that *B. subtilis* will be able to do likewise.

The ability of cell debris to prevent the lytic activity of LL-37 (Fig. 5.11a) shows the previously observed protective capacity of *E. coli* cell debris to also hold true in *B. subtilis* (Snoussi *et al.*, 2018; Wu & Tan, 2019). In *B. subtilis* this protection is also conferred by the sequestering activity of the cell debris, as dead cells continue to bind LL-37 following their lysis (Fig. 5.11b). This means that as more LL-37 is added to a culture, it binds dead cell debris instead of the remaining live cells, conferring collective tolerance to the culture, enabling it to survive and grow. This sequestration is likely aided by the cooperative binding property of LL-37, resulting in LL-37 being preferentially recruited to dead cells already bound by LL-37 as opposed to the LL-37-free growing cells in the culture. Retention of LL-37 internalised by *E. coli* has also been observed by Snoussi *et al.* (2018), they also observed rapid cytoplasmic localisation of LL-37, as I also saw in *B. subtilis* in Fig. 4.4&5. Thus, whilst LL-37 is initially interacting with the cell membrane, and also binding membrane debris from dead cells, these observations again indicate that LL-37 is somehow also attracted to the cytoplasm by an unknown mechanism. Previous experiments in this thesis have shown LL-37 internalisation to be independent of DNA or transmembrane polarisation, ruling out a voltage driven uptake mechanism (Fig. 4.4&5); thus, identifying what LL-37 is attracted to within the cytoplasm remains an important research question.

Fractionation of dead cell debris revealed that in contrast to the DNA sequestration hypothesis of Wu & Tan (2019), membrane debris of dead cells was responsible for the sequestration of LL-37. This protection was strong, with no lysis occurring in the membrane-containing cultures, whereas lysis occurred similar to wild-type when cytoplasmic and insoluble fractions were added (Fig. 5.13a). This leads to an interesting contradiction, in that LL-37 is somehow attracted to the cytoplasm of bound cells, yet the cytoplasmic fraction confers no protection when added to growing cultures. It may be that instead if LL-37 being actively attracted to a cytoplasmic component, the interaction of many LL-37 peptides with the membrane results in its transfer to the cytoplasm, without it being actively attracted to it. As I previously saw that teichoic acids, and specifically their D-alanylation, confer protection against LL-37 (Fig. 3. 3&4), I tested the role of teichoic acids in the protection conferred by cell debris. This showed that LTAs contribute, as debris from a ΔLTA strain was less protective than wild-type, whereas ΔWTA was as protective as wild-type (Fig. 5.14), indicating WTAs do not contribute to LL-37 sequestration. Debris containing teichoic acids lacking D-alanylation was extremely protective, which shows the effectiveness of D-

alanylation in suppressing LL-37 interaction with the cytoplasmic membrane, as in the absence of D-alanylation interaction of LL-37 with cell debris must have been very high (Fig. 5.14). Therefore, decoration of teichoic acids with cationic D-alanine is important in live cells to repel LL-37, as seen in Fig. 3.4 and shown by Saar-Dover *et al.* (2012); but then detrimental when present in dead cells as it reduces the sequestration of LL-37 by dead cell debris.

The possibility of LL-37 sequestration by the pathogenic Gram-positive species *S. aureus* should be investigated. Findings within this thesis make it unclear whether sequestration could also occur in *S. aureus* as cells killed by LL-37 do not lyse (Fig. 3.14). *S. aureus* cultures take much longer to recover from LL-37 treatment than *B. subtilis*, despite being treated with a sub-MIC concentration (25 μg mL^{-1} for growth/lysis; 40 μg mL^{-1} MIC (Table 3.2)) when *B. subtilis* is treated with MIC concentration (20 μg mL^{-1} for both (Table 3.1)) and *B. subtilis* recovers within ~2 hours (Fig. 4.7d) whereas *S. aureus* takes ~5 hours to do the same (Fig. 3.14b). Sequestration of LL-37 to already dead cells likely enables the rapid recovery of *B. subtilis* cultures, as *S. aureus* cultures are not recovering so quickly this suggests this mechanism may not be occurring in this species. Additionally, microscopy showed that *S. aureus* cells killed by LL-37 are permeabilised but are not phase light rather they turn ‘phase bright’, suggesting a lack of lysis – the unknown nature of ‘phase bright’ cells means this cannot be known for certain (Fig. 5.8). Thus, whilst dead cells accrue in these cultures, they do not break apart to disperse cell debris. Yet, it is now well established that LL-37 also exhibits cooperative binding (Fig. 4.1; Turner *et al.*, 1998; Snoussi *et al.*, 2018), meaning dead, permeabilised (but not lysed cells) should still recruit more LL-37 to themselves as they already contain LL-37. To clarify this issue, firstly a double dose treatment of ΔL-PG *S. aureus* should be conducted, where a culture is treated with LL-37 and once growth resumes then treated again to see if it is tolerant of a second dose. If tolerant, a wash should be conducted between the first and second doses of the same assay, to see if tolerance is abolished when the cells are resuspended in fresh media. Once these preliminary experiments have been conducted, and dependent on their results, further specific fractionation experiments could be conducted to identify the specific component responsible for sequestration.

Overall, in this chapter I have shown that *B. subtilis* that has been exposed to LL-37 exhibits tolerance not through protease activity or spore formation, but instead through the collective tolerance mechanism of LL-37 sequestration by the membranes of dead

cells. This protection by membrane debris is contributed to by teichoic acids, but these are not wholly responsible. This research also revealed contrasting populations resulting from LL-37 treatment, with unaffected polarised cells growing to recover the culture, whilst dead cells retain and sequester more LL-37 to protect their surviving sister cells.

Chapter 6 – Concluding remarks and future directions

The research in this thesis aimed to elucidate further aspects of the mechanism of action of the human AMP LL-37, using the Gram-positive model organism *B. subtilis*. This research was divided into the 3 following foci: the impact of cell envelope composition on LL-37 susceptibility; the immediate mechanism of action of LL-37; and bacterial recovery and protection from LL-37. By collating the findings of these chapters together, a summary of the mechanism of action of LL-37 against *B. subtilis* can be described as shown in Fig. 6.1.

In chapter 3 I investigated the role of cell envelope composition in susceptibility to LL-37. This revealed that in *B. subtilis*, the common LL-37 resistance mechanism of L-PG in the cytoplasmic membrane is surprisingly not effective. In fact, no membrane headgroup was found to majorly alter susceptibility to LL-37 other than GLs to a minor degree. This impact from GLs is likely due to their role in the synthesis of LTAs, as the lack of LTAs and WTAs increased susceptibility to LL-37. Protection by teichoic acids against LL-37 is contributed to by their decoration with D-alanine. Therefore, whilst in *B. subtilis* positively charged L-PG does not protect against LL-37, the species can increase its cellular net charge via D-alanylation to repel LL-37. Having ruled out phospholipid headgroup composition in impacting LL-37 susceptibility, I then looked at the role of phospholipid fatty acid tails, via membrane fluidity. This showed no change in LL-37 susceptibility with high or low fluidity states. I then explored similar research in the Gram-positive pathogenic species *S. aureus*, which successfully uses L-PG to protect itself from LL-37. This work revealed that *S. aureus* experiences different effects following LL-37 treatment – where *B. subtilis* rapidly lyses and recovers, *S. aureus* instead suffers extended growth inhibition but not lysis, before recovering the ability to grow. Finally, I aimed to establish similar membrane fluidity tuneable strains in *S. aureus*, but this preliminary work revealed *S. aureus* to have more complex genetic requirements in the synthesis of a BCFA-precursor auxotroph strain.

These insights in the Gram-positive model organism *B. subtilis* are useful as such genetic tractability is not possible in Gram-positive pathogenic species, as these are less well characterised and genetically malleable. For example, the important protective role of LTAs in reducing susceptibility to LL-37 and sequestering the AMP in dead cell debris would not have been so easily observed in *S. aureus*, as LTAs are essential in this species (Gründling & Schneewind, 2007b). These discoveries in *B.*

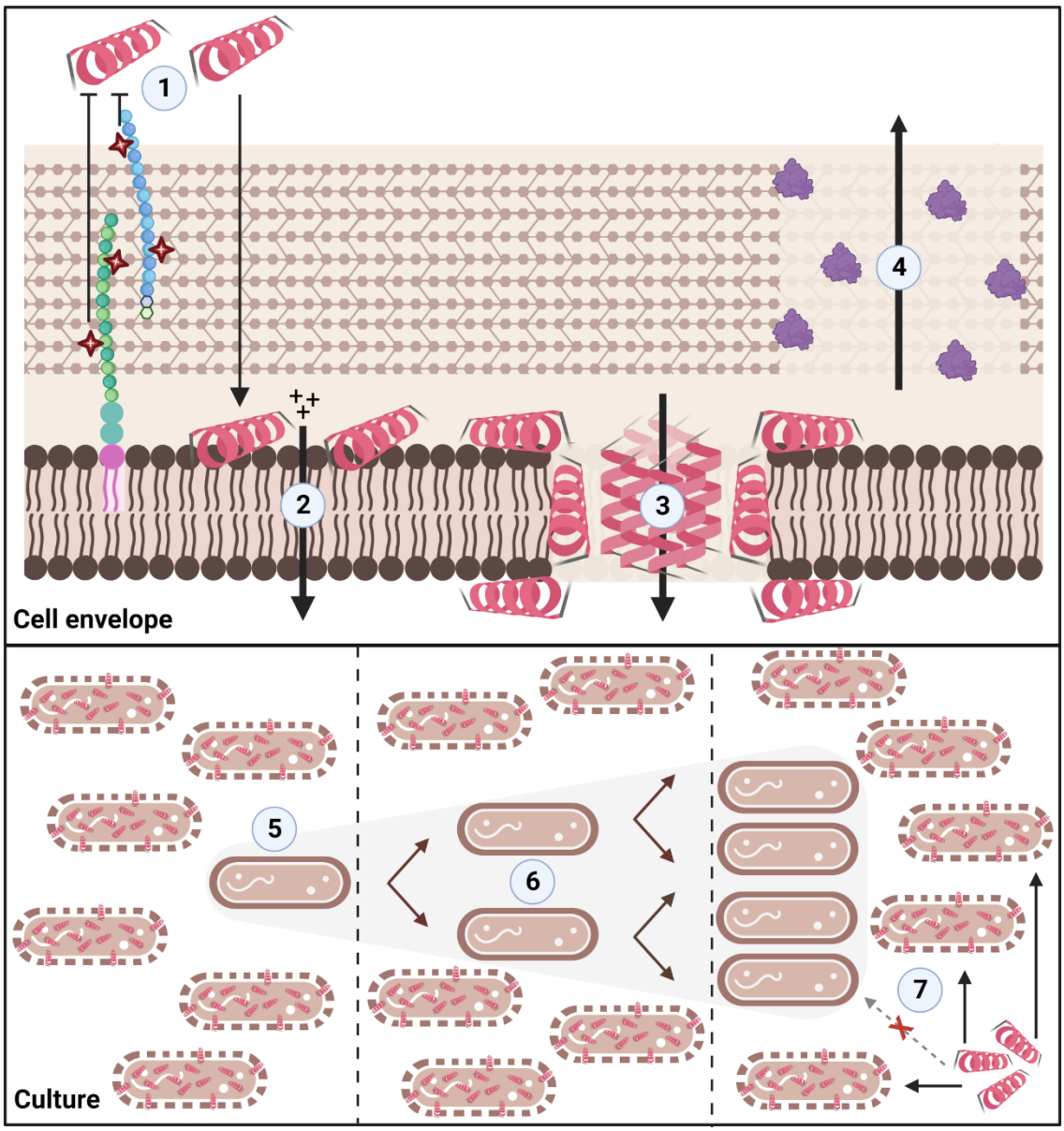

Figure 6.1. The mechanism of action of LL-37 against *B. subtilis*. **1**: LL-37 targets cell irrespective of their lipid headgroup and fatty acid composition, only teichoic acids and their modification with cationic D-alanine act to repel LL-37. **2**: LL-37 binds the cytoplasmic membrane, causing low-level disruption that can depolarise the cell. **3**: LL-37 recruits more LL-37 via cooperative binding, high binding enables permeabilisation of the cell, likely through pore formation. **4**: LL-37 triggers autolysis (by an as yet uncharacterised molecular mechanism). **5**: Lysed cells accumulate in the culture, however some cells survive due to a stochastic lack of LL-37 binding. **6**: Unbound cells are polarised and grow/divide to recover the population. **7**: The culture recovers and is protected from subsequent LL-37 exposure by membrane debris from lysed cells that sequesters LL-37.

subtilis can then be used to undertake informed experimental approaches in other pathogenic species, such as *S. aureus* and *B. anthracis*. Interestingly, whilst *B. subtilis* and *B. anthracis* belong to the same genus, published research and experiments in

this thesis have shown *B. anthracis* to be more similar to *S. aureus* in the context of LL-37 susceptibility. Both pathogenic species successfully use L-PG to repel LL-37 and both achieve proteolytic degradation of LL-37, whereas my research has shown *B. subtilis* cannot do either (Sieprawska-Lupa *et al.*, 2004; Thwaite *et al.*, 2006; Ernst *et al.*, 2009; Samant *et al.*, 2009). This indicates that in the future, whilst *B. subtilis* provides an invaluable starting tool for research into uncharacterised processes, observations in this non-pathogenic species should not be assumed to be applicable to even closely related pathogenic bacteria. Despite this, my research has highlighted the role of teichoic acids and their D-alanylation in protecting against LL-37, something that has also been seen in *S. aureus* (Saar-Dover *et al.*, 2012). Future work should focus on targeting teichoic acids, or more precisely D-alanine residues on teichoic acids, to prevent their repulsion of LL-37 away from the bacterial cell envelope. This could employ similar strategies to the MprF-targeting antibodies developed by Slavetinsky *et al*. (2022); instead, antibodies that target the membrane spanning DltBD complex, which mediates decoration of teichoic acids with D-alanine, could be developed (Debabov *et al.*, 2000; Pohl *et al.*, 2013; Reichmann *et al.*, 2013).

As a common resistance mechanism like L-PG-mediated repulsion of LL-37 is not shared between *B. subtilis* and *S. aureus*, it cannot be assumed that because membrane fluidity does not impact susceptibility to LL-37 in *B. subtilis* that this will also be the case in *S. aureus*. Therefore, development of a *S. aureus* tuneable membrane fluidity strain should be a priority in future work, as this would aid not only antimicrobial susceptibility research but also fundamental cell biology research too. Research by Singh *et al*. (2008 & 2018) has shown the synthesis of BCFAs in *S. aureus* to be more complex than *B. subtilis* (Mercier *et al.*, 2012; Gohrbandt *et al.*, 2022), as the BKD complex is not solely responsible for their synthesis. Thus, the first priority should be uncovering all BCFA synthesis mechanisms in *S. aureus*, after this a BCFA precursor auxotroph strain can be developed through the deletion of these mechanisms and growth with BCFA precursors.

In chapter 4 I investigated the specific pathway of the mechanism of action of LL-37. This showed LL-37 to exhibit cooperative binding, in which cells either have very low LL-37 binding or, once a threshold has been passed, very high LL-37 binding, as LL-37 molecules recruit more to themselves. This also revealed highly permeabilised cells to exhibit extremely high binding of LL-37, showing the sequestering activity of dead cells, described further in chapter 5, in action. Cells with low LL-37 binding were

depolarised, whereas highly bound cells were both depolarised and permeabilised by the AMP. I showed the binding and internalisation of LL-37 to be independent of transmembrane polarisation or DNA localisation and revealed that despite LL-37 being a membrane-interacting antimicrobial, it rapidly accumulates in the cytoplasm by an unknown mechanism. I then found that the rapid permeabilisation that LL-37 induces is independent of autolysis. However, autolysins are required for bacteriolysis. I was then able to identify LytD and LytE as the autolysins triggered by LL-37, with LytD having a dominant role.

A major enigma remaining from this, and other, research of LL-37 is the type of pore that LL-37 forms in the cytoplasmic membrane. The depolarising activity of low concentrations of LL-37 indicate that the AMP is able to interact with and disrupt the membrane even when only few peptides have bound, this direct interaction with the membrane is suggestive of the carpet or toroidal pore mechanisms (Jenssen *et al.*, 2006). Methods to characterise pore-forming peptides interacting with membranes are continuously being developed and improved. A recent study used fluorescently-labelled LL-37 as a means to follow LL-37 localisation in the membrane based on the amount of surface-induced fluorescence attenuation (SIFA) (Li *et al.*, 2016). This showed LL-37 to be positioned on the membrane in states conducive with toroidal pore formation; however, as other studies have indicated LL-37 to coat the membrane as in the carpet model a conclusive mechanism is still sought (Oren & Shai, 1998). The solution to this may lie in both mechanisms, as the carpet model may be followed at low concentrations, with sufficient disruption so as to depolarise cells as my research has shown; then, at high concentrations, this may shift to a toroidal pore mechanism, with the peptide coating causing the membrane to bend in and form a peptide and membrane lined pore. I am not the first the suggest this mechanism, and the research described in Chapter 4 does not argue against this hypothesis either, however much more characterisation is required to prove this model (Xhindoli *et al.*, 2013). In the SIFA study with LL-37, only a high concentration (~ 18 μg mL^{-1}) of LL-37 was used, repeating this with both high and low concentrations should be informative in this matter (Li *et al.*, 2016). These studies should also be conducted in multiple bacterial species, to allow for the differences within and between Gram-positive and Gram-negative bacteria. Against *E. coli* LL-37 exhibits septal preference and growth-phase dependent killing, phenomena that have been observed in multiple studies now (Sochacki *et al.*, 2011; Snoussi *et al.*, 2018). However, against *B. subtilis* neither of these have been

observed, both in previous publications and in the research presented in this thesis (Barns & Weisshaar, 2013). This difference in LL-37 activity suggests the potential of different mechanisms of action in different bacterial species. A priority in future LL-37 mechanism of action research should be the use of at least one Gram-positive and Gram-negative bacterial species in these studies, and before making general conclusions the relevance of these findings should then be tested in other bacterial species. It is important to include Gram-negative bacterial species as they have the additional outer membrane composed of LPS, which LL-37 has also been shown to interact with (Turner *et al.*, 1998).

This research has also revealed another important question, of what is LL-37 attracted to and interacting with in bacterial cells. Microscopy revealed a diffuse intracellular binding of LL-37, with no obvious preference for the cytoplasmic membrane. Additionally, the rapid triggering of autolysis by LL-37 could mean LL-37 is interacting directly with the cell wall machinery to activate autolysin activity. It has previously been found that teichoic acids regulate the activity of certain autolysins (Flores-Kim *et al.*, 2019; Guyet *et al.*, 2023); thus it may be that LL-37 interacting with teichoic acids disturbs the normal teichoic acid-mediated regulation of autolysins, leading to their misregulation and so autolysis. Investigating these potential additional targets of LL-37 would aid in unravelling the remaining unknown factors in the mechanism of action of LL-37. I had hypothesised that translocation of LL-37 to the cytoplasm could be driven by the transmembrane potential of a cell, as the interior of the cell is more negatively charged than the exterior and LL-37 is cationic so would likely be pushed into this negative interior, as occurs with cell-penetrating peptides (Hoffmann *et al.*, 2018). However, this was disproven by my use of CCCP to depolarise cells, as this assay showed that LL-37 still accumulates within the interior of depolarised cells. I also showed that DNA is not responsible for this intracellular localisation either. Thus, it appears LL-37 is either moved to the cytoplasm as a result of its interaction with the membrane or it is attracted to a component of the cytoplasm I have not studied, such as RNA. To decipher this, the activity of LL-37 against liposomes should be studied. Previous work has already established that LL-37 remains active against liposomes, but they did not perform experiments using fluorescently labelled LL-37 (Shahmiri *et al.*, 2016). If fluorescently labelled LL-37 is still recruited to the interior space of liposomes, which are devoid of cellular cytoplasmic contents, this would show translocation of LL-37 to the cytoplasm to be an unspecific process caused by its

interaction with the membrane. Whereas if this translocation is abolished this would instead suggest LL-37 is attracted to a specific component of the cytoplasm. To characterise whether LL-37 also exhibits any interactions with the cell wall, two approaches should be used. Firstly, the activity of LL-37 against L-forms should be tested. Secondly, its activity should be tested against cells that have already been treated with cell wall-interacting antibiotics. If these antibiotics reduce the killing activity of LL-37 this would suggest that LL-37 is also a cell wall-targeting peptide, such dual-targeting activity has previously been observed in daptomycin (Müller *et al.*, 2016; Grein *et al.*, 2020).

In chapter 5, I studied the ability of *B. subtilis* to rapidly recover from LL-37-induced lysis and protect itself against further LL-37 treatment. I showed the survival of cells within a culture to be most likely due to a stochastic lack of LL-37 binding, rather than specific characteristics of the cells or culture. These stochastically unbound cells enable rapid growth recovery as they are unaffected by the AMP and so suffer no growth inhibition. Preliminary data suggested that these *B. subtilis* cells that go on to grow in the presence of LL-37 are polarised, and that LL-37-induced depolarisation cannot be recovered from in this species, however more research is needed to support this hypothesis. Contrastingly, I showed that *S. aureus* cells could recover from LL-37-induced depolarisation to recover the culture, in addition to unbound polarised cells. I then established the tolerance of cultures to subsequent LL-37 treatment is due to the accumulation of cell debris, as this continues to bind LL-37 after death. This sequestering activity was shown to be due to the presence of membrane debris, rather than DNA as previous publications have hypothesised. I showed this protection to be due in part to the presence of lipoteichoic acids, supporting the link between teichoic acids, and their D-alanylation, and LL-37 susceptibility I presented in Chapter 3. The presence of this membrane debris means further LL-37 exposure is sequestered by dead cells, conferring collective tolerance to the growing cells in the culture.

My research has shown that *S. aureus* can recover from LL-37 induced depolarisation. This indicates that low-level exposure to LL-37 could be disadvantageous to tackling a *S. aureus* infection, as this exposure could trigger adaptations, such as increased L-PG synthesis, to make the cells more resistant to LL-37. This is of concern as these adaptations confer resistance to not only LL-37, but other commonly used antibiotics, such as daptomycin and vancomycin (Friberg *et al.*, 2020; Ledger *et al.*, 2022). These observations bring into question the efficacy of LL-37 *in vivo* as its presence may make

infecting bacterial cells harder to treat. However, this and previous work has shown the cooperative binding activity of LL-37, which implies that even at low concentrations of LL-37, some cells will be highly bound and killed by the AMP (Melo *et al.*, 2009). It may be that this is the core physiological function of LL-37, opposed to large-scale bacterial killing, as even if just a few cells are highly bound this is sufficient to trigger and modulate an immune response to the infection (Lande *et al.*, 2007; Vandamme *et al.*, 2012; Kim *et al.*, 2017; Mookherjee *et al.*, 2020). If this is the case, this process, whilst sufficient to induce an immune response, would also establish selection pressure for LL-37 resistance to evolve. Thus, to expand on the potential of LL-37-induced adaptations, RNA sequencing should be undertaken. In Chapter 5 I discussed using a combination of FACS and RNA sequencing to isolate and characterise cells that survive LL-37 treatment. This should be undertaken in *B. subtilis* to verify that survival in this species is due to a stochastic lack of LL-37 binding. Additionally, this should be performed in *S. aureus* to also test this hypothesis, but then also performed at a later stage to look at the adaptations that exposure to LL-37 triggers in this pathogenic species.

Further attention should be paid to the collective tolerance conferred by membrane debris that accumulates within cultures treated with LL-37. It should be investigated whether this mechanism is also effective in the pathogenic species *S. aureus*. The difference in lysis and recovery that *S. aureus* experiences when treated with LL-37 makes it unclear whether membrane debris will accumulate to the same degree as in *B. subtilis*. The cell debris tolerance mechanism implies that eventually cell debris will become saturated with LL-37, meaning further LL-37 would then be able to interact with live cells. This of course would lead to feedback cycles in which LL-37 kills cells, dead cells sequester further LL-37, dead cells become saturated, so LL-37 kills more cells but then the cycle repeats - it may be that these cycles exist in bacterial infections of the human body. To reduce this sequestering activity, a peptide that also binds membrane debris could be used to compete for membrane debris binding, freeing LL-37 to bind living bacterial cells. A similar approach was used by Wu & Tan (2019), in which a peptide adjuvant was used to counteract the LL-37 sequestering activity of *E. coli* cell debris. If found effective, such peptides could be used *in vivo* to enhance the activity of LL-37 and reduce the survival of cells that would otherwise go on to adapt and become less susceptible to LL-37 and other antibiotics.

In my opinion, there were three key findings in this thesis. Firstly, the complete lack of a role phospholipid head group and membrane fluidity in the susceptibility of *B. subtilis* to LL-37. This was surprising as LL-37 is well characterised to have a membrane-interacting mechanism of action. Thus, it seemed likely that phospholipid composition, with its variation in charge and structure, would impact the targeting of LL-37 and the disruption it causes, however this was shown to not be the case. This means LL-37 must have much more elasticity in its targeting than previously hypothesised. The second key finding relates to the stochasticity of LL-37 binding, as this work showed this stochasticity to be vital to the survival and recovery of bacterial cells in the presence of LL-37. These observations raise an interesting query about the potential of bacteria to develop resistance to LL-37, as this mechanism enables the survival of cells within a culture. However, as I have already discussed, it may be that LL-37 functions only to alert the immune system of an infection by killing some cells so that they release immune activating cell components. This finding does not detract from the bactericidal activity of LL-37, which can be enhanced through increased concentration and perhaps the use of synergistic compounds. The third key finding relates LTA and aspects of its activity across the three results chapters of this thesis. This research is closely related to the recently published paper of Guyet *et al.*, 2023; in this work, it was found that the production of L-PG positively influences the production of LTA in both *B. subtilis* and *S. aureus*, meaning with increased L-PG there is also increased LTA in the cell envelope. In *B.* subtilis, LTA was found to regulate the activity of LytE, thus changes in L-PG or LTA synthesis have the potential to dysregulate LytE cell wall metabolism activity and cause autolysis. In fact, it was shown that sensitivity to the lipopeptide daptomycin is increased in a strain lacking LTA compared to strains lacking D-alanine or L-PG; this means LTA protects against daptomycin by a means that is not only charge related, instead it is likely that the loss of LTA dysregulates LytE activity, making the strain more susceptible to lysis by daptomycin. These observations, made in *B. subtilis* were also found to be true in *S. aureus*, suggesting this is a common feature amongst Gram-positive bacteria. Overall, the research of Guyet *et al.* (2023) suggests that much of what has been assumed to be charge repulsion in the protection conferred by L-PG and LTA may in fact be due to the regulatory network linking these and autolysis. In chapter 3 I saw that *B. subtilis* lacking LTA was significantly more susceptible to LL-37 and this wasn't fully accounted for by D-alanylation. Thus, it seems likely that LTA has another role in protection against LL-37, which could be via regulation of LytE activity. However, the lack of increased susceptibility of L-PG lacking

cells is contrary in this regard, as L-PG production should be inherently linked to LTA production and as such the lack of increased susceptibility with the loss of L-PG is surprising. In chapter 4 I explored the role of autolysis in the mechanism of action of LL-37 and showed that whilst permeabilisation of *B. subtilis* is independent of autolysis, the subsequent bacteriolysis requires autolysin expression, specifically by LytD and LytE. Therefore, as LTA regulates LytE activity, it is likely that cells lacking LTA are more likely to undergo autolysis, as their cell wall will already be weaker due to the dysregulation of LytE – however, it should be noted that the precise mechanisms by which teichoic acids regulate autolysins are still very poorly understood. In chapter 5 I showed the protective effect conferred to cultures by the presence of LTA debris. This shows that LTA is itself protective against LL-37, in addition to its potential regulatory activity of LytE. Thus, by combining the findings of Guyet *et al*. (2023) and this thesis, the charge repulsion protection conferred by teichoic acids is reaffirmed for LL-37, but a second interesting possibility is raised, of the potential LTA-LytE regulatory system.

Overall, in this thesis I have contributed further understanding to the mechanism of action of LL-37, and these results provide useful insights and starting points for future research. Key questions surround the specific role of LL-37 *in vivo*, as whilst its antibacterial activity is evident, the relevance of this at native concentrations within the human body is questionable. However, this does not detract from antibacterial research of LL-37, as understanding its mechanism of action not only enhances our understanding of amphipathic AMPs, but also provides potential avenues for LL-37 application. For example, LL-37 derived synthetic peptides are being developed with increased potency and LL-37 is being explored as a means to clear bacterial biofilms on titanium alloy prostheses (Ridyard & Overhage, 2021; Wei *et al.*, 2021; Piller *et al.*, 2022). Additionally, LL-37 has been found to enhance the activity of a range of antibiotics in clearing biofilm infections, showing it still has relevance clinically (Wuersching *et al.*, 2021). This could mean that future healthcare strategies may involve treating infections with exogeneous LL-37 or LL-37 derivatives, an exciting potential given the current opposing rates of antibiotic resistance and development.

References

Abou Alaiwa, M.H., Reznikov, L.R., Gansemer, N.D., Sheets, K.A., Horswill, A.R., Stoltz, D.A., Zabner, J. & Welsh, M.J. (2014) pH modulates the activity and synergism of the airway surface liquid antimicrobials β-defensin-3 and LL-37. *Proceedings of the National Academy of Sciences*. 111 (52), 18703–18708.

Adams, D.W. & Errington, J. (2009) Bacterial cell division: assembly, maintenance and disassembly of the Z ring. *Nature Reviews Microbiology*. 7 (9), 642–653.

Aguilar, P.S., Cronan, J.E. & de Mendoza, D. (1998) A *Bacillus subtilis* gene induced by cold shock encodes a membrane phospholipid desaturase. *Journal of Bacteriology*. 180 (8), 2194–2200.

Alalwani, S.M., Sierigk, J., Herr, C., Pinkenburg, O., Gallo, R., Vogelmeier, C. & Bals, R. (2010) The antimicrobial peptide LL-37 modulates the inflammatory and host defense response of human neutrophils. *European Journal of Immunology*. 40 (4), 1118–1126.

Albada, H.B., Chiriac, A.-I., Wenzel, M., Penkova, M., Bandow, J.E., Sahl, H.-G. & Metzler-Nolte, N. (2012) Modulating the activity of short arginine-tryptophan containing antibacterial peptides with N-terminal metallocenoyl groups. *Beilstein Journal of Organic Chemistry*. 8 (1), 1753–1764.

Alborn, W.E., Allen, N.E. & Preston, D.A. (1991) Daptomycin disrupts membrane potential in growing *Staphylococcus aureus*. *Antimicrobial Agents and Chemotherapy*. 35 (11), 2282–2287.

Andersen, O.S. & Koeppe, R.E. (2007) Bilayer thickness and membrane protein function: an energetic perspective. *Annual Review of Biophysics and Biomolecular Structure*. 36 (1), 107–130.

Arthur, M. & Courvalin, P. (1993) Genetics and mechanisms of glycopeptide resistance in enterococci. *Antimicrobial Agents and Chemotherapy*. 37 (8), 1563–1571.

Atilano, M.L., Pereira, P.M., Yates, J., Reed, P., Veiga, H., Pinho, M.G. & Filipe, S.R. (2010) Teichoic acids are temporal and spatial regulators of peptidoglycan cross-

linking in *Staphylococcus aureus*. *Proceedings of the National Academy of Sciences of the United States of America*. 107 (44), 18991–18996.

Balhuizen, M.D., van Dijk, A., Jansen, J.W.A., van de Lest, C.H.A., Veldhuizen, E.J.A. & Haagsman, H.P. (2021) Outer membrane vesicles protect Gram-negative bacteria against host defense peptides. *mSphere*. 6 (4), e00523-21.

Balhuizen, M.D., Versluis, C.M., van Grondelle, M.O., Veldhuizen, E.J.A. & Haagsman, H.P. (2022) Modulation of outer membrane vesicle-based immune responses by cathelicidins. *Vaccine*. 40 (16), 2399–2408.

Barbe, V., Cruveiller, S., Kunst, F., Lenoble, P., Meurice, G., Sekowska, A., Vallenet, D., Wang, T., Moszer, I., Médigue, C. & Danchin, A. (2009) From a consortium sequence to a unified sequence: the *Bacillus subtilis* 168 reference genome a decade later. *Microbiology*. 155 (6), 1758–1775.

Barns, K.J. & Weisshaar, J.C. (2013) Real-time attack of LL-37 on single *Bacillus subtilis* cells. *Biochimica et Biophysica Acta (BBA) - Biomembranes*. 1828 (6), 1511–1520.

Batson, S., de Chiara, C., Majce, V., Lloyd, A.J., Gobec, S., Rea, D., Fülöp, V., Thoroughgood, C.W., Simmons, K.J., Dowson, C.G., Fishwick, C.W.G., de Carvalho, L.P.S. & Roper, D.I. (2017) Inhibition of D-Ala:D-Ala ligase through a phosphorylated form of the antibiotic D-cycloserine. *Nature Communications*. 8 (1), 1939.

Baumgart, T., Hammond, A.T., Sengupta, P., Hess, S.T., Holowka, D.A., Baird, B.A. & Webb, W.W. (2007) Large-scale fluid/fluid phase separation of proteins and lipids in giant plasma membrane vesicles. *Proceedings of the National Academy of Sciences of the United States of America*. 104 (9), 3165–3170.

Bayer, A.S., Kupferwasser, L.I., Brown, M.H., Skurray, R.A., Grkovic, S., Jones, T., Mukhopadhay, K. & Yeaman, M.R. (2006) Low-level resistance of *Staphylococcus aureus* to thrombin-induced platelet microbicidal protein 1 in vitro associated with *qacA* gene carriage is independent of multidrug efflux pump activity. *Antimicrobial Agents and Chemotherapy*. 50 (7), 2448–2454.

Beaumont, P.E., McHugh, B., Findlay, E.G., Mackellar, A., Mackenzie, K.J., Gallo, R.L., Govan, J.R.W., Simpson, A.J. & Davidson, D.J. (2014) Cathelicidin host

defence peptide augments clearance of pulmonary *Pseudomonas aeruginosa* infection by its influence on neutrophil function *in vivo*. *PLOS ONE*. 9 (6), e99029.

Beltrán-Heredia, E., Tsai, F.-C., Salinas-Almaguer, S., Cao, F.J., Bassereau, P. & Monroy, F. (2019) Membrane curvature induces cardiolipin sorting. *Communications Biology*. 2 (1), 1–7.

Benson, T.E., Filman, D.J., Walsh, C.T. & Hogle, J.M. (1995) An enzyme–substrate complex involved in bacterial cell wall biosynthesis. *Nature Structural Biology*. 2 (8), 644–653.

Beranová, J., Jemioła-Rzemińska, M., Elhottová, D., Strzałka, K. & Konopásek, I. (2008) Metabolic control of the membrane fluidity in *Bacillus subtilis* during cold adaptation. *Biochimica et Biophysica Acta (BBA) - Biomembranes*. 1778 (2), 445–453.

Bergsson, G., Reeves, E.P., McNally, P., Chotirmall, S.H., Greene, C.M., Greally, P., Murphy, P., O'Neill, S.J. & McElvaney, N.G. (2009) LL-37 complexation with glycosaminoglycans in cystic fibrosis lungs inhibits antimicrobial activity, which can be restored by hypertonic saline. *Journal of Immunology (Baltimore, Md.: 1950)*. 183 (1), 543–551.

Berkebile, A.R. & McCray, P.B. (2014) Effects of airway surface liquid pH on host defense in cystic fibrosis. *The International Journal of Biochemistry & Cell Biology*. 52, 124–129.

Berman, H.M., Westbrook, J., Feng, Z., Gilliland, G., Bhat, T.N., Weissig, H., Shindyalov, I.N. & Bourne, P.E. (2000) The Protein Data Bank. *Nucleic Acids Research*. 28 (1), 235–242.

Bhavsar, A.P., Truant, R. & Brown, E.D. (2005) The TagB protein in *Bacillus subtilis* 168 is an intracellular peripheral membrane protein that can incorporate glycerol phosphate onto a membrane-bound acceptor *in vitro*. *Journal of Biological Chemistry*. 280 (44), 36691–36700.

Bierbaum, G. & Sahl, H.-G. (1985) Induction of autolysis of staphylococci by the basic peptide antibiotics Pep 5 and nisin and their influence on the activity of autolytic enzymes. *Archives of Microbiology*. 141 (3), 249–254.

Bisicchia, P., Noone, D., Lioliou, E., Howell, A., Quigley, S., Jensen, T., Jarmer, H. & Devine, K.M. (2007) The essential YycFG two-component system controls cell wall metabolism in *Bacillus subtilis*. *Molecular Microbiology*. 65 (1), 180–200.

Biswas, S., Brunel, J.-M., Dubus, J.-C., Reynaud-Gaubert, M. & Rolain, J.-M. (2012) Colistin: an update on the antibiotic of the 21st century. *Expert Review of Anti-infective Therapy*. 10 (8), 917–934.

Bociek, K., Ferluga, S., Mardirossian, M., Benincasa, M., Tossi, A., Gennaro, R. & Scocchi, M. (2015) Lipopolysaccharide phosphorylation by the WaaY kinase affects the susceptibility of *Escherichia coli* to the human antimicrobial peptide LL-37. *The Journal of Biological Chemistry*. 290 (32), 19933–19941.

Bolger, A., Lohse, M. & Usadel, B. (2014) Trimmomatic: a flexible trimmer for Illumina Sequence Data. *Bioinformatics*. btu170.

Bouhss, A., Crouvoisier, M., Blanot, D. & Mengin-Lecreulx, D. (2004) Purification and characterization of the bacterial MraY translocase catalyzing the first membrane step of peptidoglycan biosynthesis. *Journal of Biological Chemistry*. 279 (29), 29974–29980.

Bräuner, T., Hülser, D.F. & Strasser, R.J. (1984) Comparative measurements of membrane potentials with microelectrodes and voltage-sensitive dyes. *Biochimica et Biophysica Acta (BBA) - Biomembranes*. 771 (2), 208–216.

Breijyeh, Z., Jubeh, B. & Karaman, R. (2020) Resistance of Gram-negative bacteria to current antibacterial agents and approaches to resolve it. *Molecules*. 25 (6).

Breukink, E., Wiedemann, I., Kraaij, C. van, Kuipers, O.P., Sahl, H.-G. & de Kruijff, B. (1999) Use of the cell wall precursor lipid II by a pore-forming peptide antibiotic. *Science*. 286 (5448), 2361–2364.

Brown, E.D., Vivas, E.I., Walsh, C.T. & Kolter, R. (1995) MurA (MurZ), the enzyme that catalyzes the first committed step in peptidoglycan biosynthesis, is essential in *Escherichia coli*. *Journal of Bacteriology*. 177 (14), 4194–4197.

Brown, S., Santa Maria, J.P. & Walker, S. (2013) Wall teichoic acids of Gram-positive bacteria. *Annual review of microbiology*. 67.

Büchau, A.S., Morizane, S., Trowbridge, J., Schauber, J., Kotol, P., Bui, J.D. & Gallo, R.L. (2009) The host defense peptide cathelicidin is required for NK cell-mediated suppression of tumor growth. *The Journal of Immunology*. 184 (1), 369–378.

Bucki, R., Byfield, F.J. & Janmey, P.A. (2007) Release of the antimicrobial peptide LL-37 from DNA/F-actin bundles in cystic fibrosis sputum. *The European Respiratory Journal*. 29 (4), 624–632.

Bush, K. (2012) Antimicrobial agents targeting bacterial cell walls and cell membranes. *Revue scientifique et technique (International Office of Epizootics)*. 31 (1).

Bush, K. (2016) Overcoming β-lactam resistance in Gram-negative pathogens. *Future Medicinal Chemistry*. 8 (9), 921–924.

Buttress, J.A. (2022) *Membrane-targeting antimicrobials as promising resistance-breaking antibiotic candidates*. Newcastle University.

Cáceres, N.E., Harris, N.B., Wellehan, J.F., Feng, Z., Kapur, V. & Barletta, R.G. (1997) Overexpression of the D-alanine racemase gene confers resistance to D-cycloserine in *Mycobacterium smegmatis*. *Journal of Bacteriology*. 179 (16), 5046–5055.

Carballido-López, R., Formstone, A., Li, Y., Ehrlich, S.D., Noirot, P. & Errington, J. (2006) Actin homolog MreBH governs cell morphogenesis by localization of the cell wall hydrolase LytE. *Developmental Cell*. 11 (3), 399–409.

Castuma, C.E., Crooke, E. & Kornberg, A. (1993) Fluid membranes with acidic domains activate DnaA, the initiator protein of replication in *Escherichia coli*. *Journal of Biological Chemistry*. 268 (33), 24665–24668.

Cebrián, G., Condón, S. & Mañas, P. (2016) Influence of growth and treatment temperature on *Staphylococcus aureus* resistance to pulsed electric fields: relationship with membrane fluidity. *Innovative Food Science & Emerging Technologies*. 37, 161–169.

Chantson, J.T., Vittoria Verga Falzacappa, M., Crovella, S. & Metzler-Nolte, N. (2006) Solid-phase synthesis, characterization, and antibacterial activities of metallocene–peptide bioconjugates. *ChemMedChem*. 1 (11), 1268–1274.

Chen, C.I.-U., Schaller-Bals, S., Paul, K.P., Wahn, U. & Bals, R. (2004) β-defensins and LL-37 in bronchoalveolar lavage fluid of patients with cystic fibrosis. *Journal of Cystic Fibrosis*. 3 (1), 45–50.

Chen, J.M., Uplekar, S., Gordon, S.V. & Cole, S.T. (2012) A point mutation in *cycA* partially contributes to the D-cycloserine resistance trait of *Mycobacterium bovis* BCG vaccine strains. *PLOS ONE*. 7 (8), e43467.

Choi, K.-H., Heath, R.J. & Rock, C.O. (2000) β-ketoacyl-acyl carrier protein synthase III (FabH) is a determining factor in branched-chain fatty acid biosynthesis. *Journal of Bacteriology*. 182 (2), 365–370.

Chung, M.-C., Dean, S.N. & Van Hoek, M.L. (2015) Acyl carrier protein is a bacterial cytoplasmic target of cationic antimicrobial peptide LL-37. *Biochemical Journal*. 470 (2), 243–253.

Claunch, K.M., Bush, M., Evans, C.R., Malmquist, J.A., Hale, M.C. & McGillivray, S.M. (2018) Transcriptional profiling of the *clpX* mutant in *Bacillus anthracis* reveals regulatory connection with the *lrgAB* operon. *Microbiology (Reading, England)*. 164 (4), 659–669.

Coleman, J. (1992) Characterization of the *Escherichia coli* gene for 1-acyl-*sn*-glycerol-3-phosphate acyltransferase (*plsC*). *Molecular and General Genetics MGG*. 232 (2), 295–303.

Collins, L.V., Kristian, S.A., Weidenmaier, C., Faigle, M., van Kessel, K.P.M., van Strijp, J.A.G., Götz, F., Neumeister, B. & Peschel, A. (2002) *Staphylococcus aureus* strains lacking d-alanine modifications of teichoic acids are highly susceptible to human neutrophil killing and are virulence attenuated in mice. *The Journal of Infectious Diseases*. 186 (2), 214–219.

Coster, H.G.L. & Laver, D.R. (1986) The effect of benzyl alcohol and cholesterol on the acyl chain order and alkane solubility of bimolecular phosphatidylcholine membranes. *BBA - Biomembranes*. 861 (C), 406–412.

Cullen, T.W., Giles, D.K., Wolf, L.N., Ecobichon, C., Boneca, I.G. & Trent, M.S. (2011) *Helicobacter pylori* versus the host: remodeling of the bacterial outer

membrane is required for survival in the gastric mucosa. *PLoS Pathogens*. 7 (12), e1002454.

Culp, E. & Wright, G.D. (2017) Bacterial proteases, untapped antimicrobial drug targets. *The Journal of Antibiotics*. 70 (4), 366–377.

Cybulski, L.E., Ballering, J., Moussatova, A., Inda, M.E., Vazquez, D.B., Wassenaar, T.A., de Mendoza, D., Tieleman, D.P. & Killian, J.A. (2015) Activation of the bacterial thermosensor DesK involves a serine zipper dimerization motif that is modulated by bilayer thickness. *Proceedings of the National Academy of Sciences*. 112 (20), 6353–6358.

Cybulski, L.E., Martín, M., Mansilla, M.C., Fernández, A. & de Mendoza, D. (2010) Membrane thickness cue for cold sensing in a bacterium. *Current biology: CB*. 20 (17), 1539–1544.

van Dalen, A. & de Kruijff, B. (2004) The role of lipids in membrane insertion and translocation of bacterial proteins. *Biochimica et Biophysica Acta (BBA) - Molecular Cell Research*. 1694 (1), 97–109.

Debabov, D.V., Kiriukhin, M.Y. & Neuhaus, F.C. (2000) Biosynthesis of lipoteichoic acid in *Lactobacillus rhamnosus*: role of DltD in d-alanylation. *Journal of Bacteriology*. 182 (10), 2855–2864.

D'Elia, M.A., Millar, K.E., Beveridge, T.J. & Brown, E.D. (2006a) Wall teichoic acid polymers are dispensable for cell viability in *Bacillus subtilis*. *Journal of Bacteriology*. 188 (23), 8313–8316.

D'Elia, M.A., Pereira, M.P., Chung, Y.S., Zhao, W., Chau, A., Kenney, T.J., Sulavik, M.C., Black, T.A. & Brown, E.D. (2006b) Lesions in teichoic acid biosynthesis in *Staphylococcus aureus* lead to a lethal gain of function in the otherwise dispensable pathway. *Journal of Bacteriology*. 188 (12), 4183–4189.

Deva, T., Baker, E.N., Squire, C.J. & Smith, C.A. (2006) Structure of *Escherichia coli* UDP-N-acetylmuramoyl:l-alanine ligase (MurC). *Acta Crystallographica Section D: Biological Crystallography*. 62 (12), 1466–1474.

Di Nardo, A., Vitiello, A. & Gallo, R.L. (2003) Cutting edge: mast cell antimicrobial activity is mediated by expression of cathelicidin antimicrobial peptide. *The Journal of Immunology*. 170 (5), 2274–2278.

van Dijk, A., Tersteeg-Zijderveld, M.H.G., Tjeerdsma-van Bokhoven, J.L.M., Jansman, A.J.M., Veldhuizen, E.J.A. & Haagsman, H.P. (2009) Chicken heterophils are recruited to the site of *Salmonella* infection and release antibacterial mature Cathelicidin-2 upon stimulation with LPS. *Molecular Immunology*. 46 (7), 1517–1526.

Diomande, S., NGUYEN-THE, C., Guinebretière, M.-H., Broussolle, V. & Brillard, J. (2015) Role of fatty acids in *Bacillus* environmental adaptation. *Frontiers in Microbiology*. 6.

Domínguez-Cuevas, P., Porcelli, I., Daniel, R.A. & Errington, J. (2013) Differentiated roles for MreB-actin isologues and autolytic enzymes in *Bacillus subtilis* morphogenesis. *Molecular Microbiology*. 89 (6), 1084–1098.

Domínguez-Escobar, J., Chastanet, A., Crevenna, A.H., Fromion, V., Wedlich-Söldner, R. & Carballido-López, R. (2011) Processive movement of MreB-associated cell wall biosynthetic complexes in bacteria. *Science*. 333 (6039), 225–228.

Du, L., He, Y. & Luo, Y. (2008) Crystal structure and enantiomer selection by d-alanyl carrier protein ligase DltA from *Bacillus cereus*. *Biochemistry*. 47 (44), 11473–11480.

Dürr, U.H.N., Sudheendra, U.S. & Ramamoorthy, A. (2006) LL-37, the only human member of the cathelicidin family of antimicrobial peptides. *Biochimica et Biophysica Acta (BBA) - Biomembranes*. 1758 (9), 1408–1425.

Edwards, D.H. & Errington, J. (1997) The *Bacillus subtilis* DivIVA protein targets to the division septum and controls the site specificity of cell division. *Molecular Microbiology*. 24 (5), 905–915.

Egan, A.J.F., Errington, J. & Vollmer, W. (2020) Regulation of peptidoglycan synthesis and remodelling. *Nature Reviews Microbiology*. 18 (8), 446–460.

Elborn, J.S. (2016) Cystic fibrosis. *The Lancet*. 388 (10059), 2519–2531.

Ellwood, D.C. & Tempest, D.W.Y. 1972 (1972) Influence of culture pH on the content and composition of teichoic acids in the walls of *Bacillus subtilis*. *Microbiology*. 73 (2), 395–402.

Elson, E.L., Fried, E., Dolbow, J.E. & Genin, G.M. (2010) Phase separation in biological membranes: integration of theory and experiment. *Annual Review of Biophysics*. 39 (1), 207–226.

Epand, R.M. & Epand, R.F. (2009) Domains in bacterial membranes and the action of antimicrobial agents. *Molecular BioSystems*. 5 (6), 580–587.

Epand, R.M., Walker, C., Epand, R.F. & Magarvey, N.A. (2016) Molecular mechanisms of membrane targeting antibiotics. *Biochimica et Biophysica Acta (BBA) - Biomembranes*. 1858 (5), 980–987.

Ernst, C.M. & Peschel, A. (2011) Broad-spectrum antimicrobial peptide resistance by MprF-mediated aminoacylation and flipping of phospholipids. *Molecular Microbiology*. 80 (2), 290–299.

Ernst, C.M., Staubitz, P., Mishra, N.N., Yang, S.-J., Hornig, G., Kalbacher, H., Bayer, A.S., Kraus, D. & Peschel, A. (2009) The bacterial defensin resistance protein MprF consists of separable domains for lipid lysinylation and antimicrobial peptide repulsion. *PLoS Pathogens*. 5 (11), e1000660.

Ernst, R., Ejsing, C.S. & Antonny, B. (2016) Homeoviscous adaptation and the regulation of membrane lipids. *Journal of Molecular Biology*. 428 (24, Part A), 4776–4791.

Falord, M., Mäder, U., Hiron, A., Débarbouillé, M. & Msadek, T. (2011) Investigation of the *Staphylococcus aureus* GraSR regulon reveals novel links to virulence, stress response and cell wall signal transduction pathways. *PLOS ONE*. 6 (7), e21323.

Fedtke, I., Mader, D., Kohler, T., Moll, H., Nicholson, G., Biswas, R., Henseler, K., Götz, F., Zähringer, U. & Peschel, A. (2007) A *Staphylococcus aureus ypfP* mutant with strongly reduced lipoteichoic acid (LTA) content: LTA governs bacterial surface properties and autolysin activity. *Molecular Microbiology*. 65 (4), 1078–1091.

Feucht, A., Magnin, T., Yudkin, M.D. & Errington, J. (1996) Bifunctional protein required for asymmetric cell division and cell-specific transcription in *Bacillus subtilis*. *Genes & Development*. 10 (7), 794–803.

Fischer, W., Rösel, P. & Koch, H.U. (1981) Effect of alanine ester substitution and other structural features of lipoteichoic acids on their inhibitory activity against autolysins of *Staphylococcus aureus*. *Journal of Bacteriology*. 146 (2), 467–475.

Flagg, J.L. & Wilson, T.H. (1977) A protonmotive force as the source of energy for galactoside transport in energy depleted *Escherichia coli*. *The Journal of Membrane Biology*. 31 (3), 233–255.

Flores-Kim, J., Dobihal, G.S., Fenton, A., Rudner, D.Z. & Bernhardt, T.G. (2019) A switch in surface polymer biogenesis triggers growth-phase-dependent and antibiotic-induced bacteriolysis. *eLife*. 8, e44912.

Friberg, C., Haaber, J.K., Vestergaard, M., Fait, A., Perrot, V., Levin, B.R. & Ingmer, H. (2020) Human antimicrobial peptide, LL-37, induces non-inheritable reduced susceptibility to vancomycin in *Staphylococcus aureus*. *Scientific Reports*. 10 (1), 13121.

Friedlander, G., Le Grimellec, C., Giocondi, M.-C. & Amiel, C. (1987) Benzyl alcohol increases membrane fluidity and modulates cyclic AMP synthesis in intact renal epithelial cells. *Biochimica et Biophysica Acta (BBA) - Biomembranes*. 903 (2), 341–348.

Fritze, D. (2004) Taxonomy of the genus *Bacillus* and related genera: the aerobic endospore-forming bacteria. *Phytopathology*. 94 (11), 1245–1248.

Fuchs, S., Mehlan, H., Bernhardt, J., Hennig, A., Michalik, S., Surmann, K., Pané-Farré, J., Giese, A., Weiss, S., Backert, L., Herbig, A., Nieselt, K., Hecker, M., Völker, U. & Mäder, U. (2018) *Aureo*Wiki – The repository of the *Staphylococcus aureus* research and annotation community. *International Journal of Medical Microbiology*. 308 (6), 558–568.

Gale, R.T., Li, F.K.K., Sun, T., Strynadka, N.C.J. & Brown, E.D. (2017) *B. subtilis* LytR-CpsA-Psr enzymes transfer wall teichoic acids from authentic lipid-linked

substrates to mature peptidoglycan *in vitro*. *Cell Chemical Biology*. 24 (12), 1537-1546.e4.

Ganz, T. (2004) Defensins: antimicrobial peptides of vertebrates. *Comptes Rendus Biologies*. 327 (6), 539–549.

Gautier, R., Douguet, D., Antonny, B. & Drin, G. (2008) HELIQUEST: a web server to screen sequences with specific α-helical properties. *Bioinformatics*. 24 (18), 2101–2102.

Ghoul, M., Pommepuy, M., Moillo-Batt, A. & Cormier, M. (1989) Effect of carbonyl cyanide m-chlorophenylhydrazone on *Escherichia coli* halotolerance. *Applied and Environmental Microbiology*. 55 (4), 1040–1043.

Ginsberg, C., Zhang, Y.-H., Yuan, Y. & Walker, S. (2006) *in vitro* reconstitution of two essential steps in wall teichoic acid biosynthesis. *ACS Chemical Biology*. 1 (1), 25–28.

Goffin, C. & Ghuysen, J.-M. (2002) Biochemistry and comparative genomics of SxxK superfamily acyltransferases offer a clue to the mycobacterial paradox: presence of penicillin-susceptible target proteins versus lack of efficiency of penicillin as therapeutic agent. *Microbiology and Molecular Biology Reviews*. 66 (4), 702–738.

Goffin, C. & Ghuysen, J.-M. (1998) Multimodular penicillin-binding proteins: an enigmatic family of orthologs and paralogs. *Microbiology and Molecular Biology Reviews*. 62 (4), 1079–1093.

Gohrbandt, M., Lipski, A., Grimshaw, J.W., Buttress, J.A., Baig, Z., Herkenhoff, B., Walter, S., Kurre, R., Deckers-Hebestreit, G. & Strahl, H. (2022) Low membrane fluidity triggers lipid phase separation and protein segregation in living bacteria. *The EMBO journal*. e109800.

Goldman, M.J., Anderson, G.M., Stolzenberg, E.D., Kari, U.P., Zasloff, M. & Wilson, J.M. (1997) Human β-defensin-1 is a salt-sensitive antibiotic in lung that is inactivated in cystic fibrosis. *Cell*. 88 (4), 553–560.

Goldman, R.C. & Gange, D. (2000) Inhibition of transglycosylation involved in bacterial peptidoglycan synthesis. *Current Medicinal Chemistry*. 7 (8), 801–820.

Golla, R.M., Mishra, B., Dang, X., Lakshmaiah Narayana, J., Li, A., Xu, L. & Wang, G. (2020) Resistome of *Staphylococcus aureus* in response to human cathelicidin LL-37 and its engineered antimicrobial peptides. *ACS Infectious Diseases*. 6 (7), 1866–1881.

Gooderham, W.J., Gellatly, S.L., Sanschagrin, F., McPhee, J.B., Bains, M., Cosseau, C., Levesque, R.C. & Hancock, R.E.W. (2009) The sensor kinase PhoQ mediates virulence in *Pseudomonas aeruginosa*. *Microbiology*. 155 (3), 699–711.

Gordon, E., Flouret, B., Chantalat, L., Heijenoort, J. van, Mengin-Lecreulx, D. & Dideberg, O. (2001) Crystal structure of UDP-*N*-acetylmuramoyl-l-alanyl-d-glutamate:*meso*-diaminopimelate ligase from *Escherichia Coli*. *Journal of Biological Chemistry*. 276 (14), 10999–11006.

Greenspan, P., Mayer, E.P. & Fowler, S.D. (1985) Nile red: a selective fluorescent stain for intracellular lipid droplets. *The Journal of Cell Biology*. 100 (3), 965–973.

Grein, F., Müller, A., Scherer, K.M., Liu, X., Ludwig, K.C., Klöckner, A., Strach, M., Sahl, H.-G., Kubitscheck, U. & Schneider, T. (2020) Ca 2+ -Daptomycin targets cell wall biosynthesis by forming a tripartite complex with undecaprenyl-coupled intermediates and membrane lipids. *Nature Communications*. 11 (1), 1455.

Gründling, A. & Schneewind, O. (2007a) Genes required for glycolipid synthesis and lipoteichoic acid anchoring in *Staphylococcus aureus*. *Journal of Bacteriology*. 189 (6), 2521–2530.

Gründling, A. & Schneewind, O. (2007b) Synthesis of glycerol phosphate lipoteichoic acid in *Staphylococcus aureus*. *Proceedings of the National Academy of Sciences*. 104 (20), 8478–8483.

Gudmundsson, G.H., Agerberth, B., Odeberg, J., Bergman, T., Olsson, B. & Salcedo, R. (1996) The human gene *FALL39* and processing of the cathelin precursor to the antibacterial peptide LL-37 in granulocytes. *European Journal of Biochemistry*. 238 (2), 325–332.

Guyet, A., Alofi, A. & Daniel, R.A. (2023) Insights into the roles of lipoteichoic acids and MprF in *Bacillus subtilis*. *mBio*. 14 (1), e02667-22.

Ha, S., Walker, D., Shi, Y. & Walker, S. (2000) The 1.9 Å crystal structure of *Escherichia coli* MurG, a membrane-associated glycosyltransferase involved in peptidoglycan biosynthesis. *Protein Science*. 9 (6), 1045–1052.

Haas, R., Koch, H.U. & Fischer, W. (1984) Alanyl turnover from lipoteichoic acid to teichoic acid in *Staphylococcus aureus*. *FEMS Microbiology Letters*. 21 (1), 27–31.

Hamoen, L.W. & Wenzel, M. (2017) Editorial: antimicrobial peptides - interaction with membrane lipids and proteins. *Frontiers in Cell and Developmental Biology*. 5.

van Harten, R.M., van Woudenbergh, E., van Dijk, A. & Haagsman, H.P. (2018) Cathelicidins: Immunomodulatory Antimicrobials. *Vaccines*. 6 (3), 63.

Hashimoto, M., Ooiwa, S. & Sekiguchi, J. (2012) Synthetic lethality of the *lytE cwlO* genotype in *Bacillus subtilis* is caused by lack of D,L-endopeptidase activity at the lateral cell wall. *Journal of Bacteriology*. 194 (4), 796–803.

Hasper, H.E., Kramer, N.E., Smith, J.L., Hillman, J.D., Zachariah, C., Kuipers, O.P., de Kruijff, B. & Breukink, E. (2006) An alternative bactericidal mechanism of action for lantibiotic peptides that target lipid II. *Science*. 313 (5793), 1636–1637.

He, K., Ludtke, S.J., Heller, W.T. & Huang, H.W. (1996) Mechanism of alamethicin insertion into lipid bilayers. *Biophysical Journal*. 71 (5), 2669–2679.

Heberle, F.A. & Feigenson, G.W. (2011) Phase separation in lipid membranes. *Cold Spring Harbor Perspectives in Biology*. 3 (4), a004630.

Helmann, J.D. (2016) *Bacillus subtilis* extracytoplasmic function (ECF) sigma factors and defense of the cell envelope. *Current Opinion in Microbiology*. 30, 122–132.

Hemshekhar, M., Choi, K.-Y.G. & Mookherjee, N. (2018) Host defense peptide LL-37-mediated chemoattractant properties, but not anti-inflammatory cytokine IL-1RA production, is selectively controlled by Cdc42 Rho GTPase via G protein-coupled receptors and JNK mitogen-activated protein kinase. *Frontiers in Immunology*. 9, 1871.

Henzler Wildman, K.A., Lee, D.-K. & Ramamoorthy, A. (2003) Mechanism of lipid bilayer disruption by the human antimicrobial peptide, LL-37. *Biochemistry*. 42 (21), 6545–6558.

Heydanek, M.G.Jr., Struve, W.G. & Neuhaus, F.C. (1969) Initial state in peptidoglycan synthesis. III. Kinetics and uncoupling of phospho-N-acetylmuramyl-pentapeptide translocase (uridine 5'-phosphate). *Biochemistry*. 8 (3), 1214–1221.

Hines, K.M., Alvarado, G., Chen, X., Gatto, C., Pokorny, A., Alonzo, F., Wilkinson, B.J. & Xu, L. (2020) Lipidomic and ultrastructural characterization of the cell envelope of *Staphylococcus aureus* grown in the presence of human serum. *mSphere*. 5 (3), e00339-20.

Hjort Ipsen, J., Karlström, G., Mourtisen, O.G., Wennerström, H. & Zuckermann, M.J. (1987) Phase equilibria in the phosphatidylcholine-cholesterol system. *Biochimica et Biophysica Acta (BBA) - Biomembranes*. 905 (1), 162–172.

Ho, S.W., Jung, D., Calhoun, J.R., Lear, J.D., Okon, M., Scott, W.R.P., Hancock, R.E.W. & Straus, S.K. (2008) Effect of divalent cations on the structure of the antibiotic daptomycin. *European biophysics journal: EBJ*. 37 (4), 421–433.

Hoffmann, K., Milech, N., Juraja, S.M., Cunningham, P.T., Stone, S.R., Francis, R.W., Anastasas, M., Hall, C.M., Heinrich, T., Bogdawa, H.M., Winslow, S., Scobie, M.N., Dewhurst, R.E., Florez, L., Ong, F., Kerfoot, M., Champain, D., Adams, A.M., Fletcher, S., Viola, H.M., Hool, L.C., Connor, T., Longville, B.A.C., Tan, Y.-F., Kroeger, K., Morath, V., Weiss, G.A., Skerra, A., Hopkins, R.M. & Watt, P.M. (2018) A platform for discovery of functional cell-penetrating peptides for efficient multi-cargo intracellular delivery. *Scientific Reports*. 8 (1), 12538.

Horsburgh, G.J., Atrih, A., Williamson, M.P. & Foster, S.J. (2003) LytG of *Bacillus subtilis* is a novel peptidoglycan hydrolase: the major active glucosaminidase. *Biochemistry*. 42 (2), 257–264.

Horsburgh, M.J., Aish, J.L., White, I.J., Shaw, L., Lithgow, J.K. & Foster, S.J. (2002) σB modulates virulence determinant expression and stress resistance: characterization of a functional *rsbU* strain derived from *Staphylococcus aureus* 8325-4. *Journal of Bacteriology*. 184 (19), 5457–5467.

Hosoi, S., Mochizuki, N., Hayashi, S. & Kasai, M. (1980) Control of membrane potential by external H+ concentration in *Bacillus subtilis* as determined by an ion-selective electrode. *Biochimica et Biophysica Acta (BBA) - Biomembranes*. 600 (3), 844–852.

Hu, Y., Chen, L., Ha, S., Gross, B., Falcone, B., Walker, D., Mokhtarzadeh, M. & Walker, S. (2003) Crystal structure of the MurG:UDP-GlcNAc complex reveals common structural principles of a superfamily of glycosyltransferases. *Proceedings of the National Academy of Sciences*. 100 (3), 845–849.

Huang, L.C., Petkova, T.D., Reins, R.Y., Proske, R.J. & McDermott, A.M. (2006) Multifunctional roles of human cathelicidin (LL-37) at the ocular surface. *Investigative Ophthalmology & Visual Science*. 47 (6), 2369–2380.

Humphrey, M., Abdelmesseh Nekhala, I., Scheinpflug, K., Krylova, O., Schäfer, A.-B., Buttress, J.A., Wenzel, M. & Strahl, H. (2023) Tracking Global and Local Changes in Membrane Fluidity Through Fluorescence Spectroscopy and Microscopy. In: Peter Sass (ed.). *Antibiotics: Methods and Protocols*. Methods in Molecular Biology. New York, NY, Springer US. pp. 203–229.

Ichihashi, N., Kurokawa, K., Matsuo, M., Kaito, C. & Sekimizu, K. (2003) Inhibitory effects of basic or neutral phospholipid on acidic phospholipid-mediated dissociation of adenine nucleotide bound to DnaA protein, the initiator of chromosomal DNA replication. *Journal of Biological Chemistry*. 278 (31), 28778–28786.

Inda, M.E., Oliveira, R.G., de Mendoza, D. & Cybulski, L.E. (2016) The single transmembrane segment of minimal sensor DesK senses temperature via a membrane-thickness caliper. *Journal of Bacteriology*. 198 (21), 2945–2954.

Jenssen, H., Hamill, P. & Hancock, R.E.W. (2006) Peptide Antimicrobial Agents. *Clinical Microbiology Reviews*. 19 (3), 491–511.

Jervis, A.J., Thackray, P.D., Houston, C.W., Horsburgh, M.J. & Moir, A. (2007) SigM-responsive genes of *Bacillus subtilis* and their promoters. *Journal of Bacteriology*. 189 (12), 4534–4538.

Johansson, J., Gudmundsson, G.H., Rottenberg, M.E., Berndt, K.D. & Agerberth, B. (1998) Conformation-dependent antibacterial activity of the naturally occurring human peptide LL-37. *The Journal of Biological Chemistry*. 273 (6), 3718–3724.

Jolliffe, L.K., Doyle, R.J. & Streips, U.N. (1981) The energized membrane and cellular autolysis in *Bacillus subtilis*. *Cell*. 25 (3), 753–763.

Jones, T., Yeaman, M.R., Sakoulas, G., Yang, S.-J., Proctor, R.A., Sahl, H.-G., Schrenzel, J., Xiong, Y.Q. & Bayer, A.S. (2008) Failures in clinical treatment of *Staphylococcus aureus* infection with daptomycin are associated with alterations in surface charge, membrane phospholipid asymmetry, and drug binding. *Antimicrobial Agents and Chemotherapy*. 52 (1), 269–278.

Jong, I.G. de, Beilharz, K., Kuipers, O.P. & Veening, J.-W. (2011) Live cell imaging of *Bacillus subtilis* and *Streptococcus pneumoniae* using automated time-lapse microscopy. *JoVE (Journal of Visualized Experiments)*. (53), e3145.

Joo, H.-S., Fu, C.-I. & Otto, M. (2016) Bacterial strategies of resistance to antimicrobial peptides. *Philosophical Transactions of the Royal Society B: Biological Sciences*. 371 (1695), 20150292.

Jorasch, P., Wolter, F.P., Zähringer, U. & Heinz, E. (1998) A UDP glucosyltransferase from *Bacillus subtilis* successively transfers up to four glucose residues to 1,2-diacylglycerol: expression of *ypfP* in *Escherichia coli* and structural analysis of its reaction products. *Molecular Microbiology*. 29 (2), 419–430.

Jouhet, J. (2013) Importance of the hexagonal lipid phase in biological membrane organization. *Frontiers in Plant Science*. 4.

Kahan, F.M., Kahan, J.S., Cassidy, P.J. & Kropp, H. (1974) The mechanism of action of fosfomycin (phosphonomycin). *Annals of the New York Academy of Sciences*. 235 (1), 364–386.

Kahlenberg, J.M. & Kaplan, M.J. (2013) Little peptide, big effects: the role of LL-37 in inflammation and autoimmune disease. *Journal of immunology*. 191 (10).

Kandasamy, S.K. & Larson, R.G. (2006) Effect of salt on the interactions of antimicrobial peptides with zwitterionic lipid bilayers. *Biochimica et Biophysica Acta (BBA) - Biomembranes*. 1758 (9), 1274–1284.

Kang, J., Dietz, M.J. & Li, B. (2019) Antimicrobial peptide LL-37 is bactericidal against *Staphylococcus aureus* biofilms. *PLoS ONE*. 14 (6), e0216676.

Kany, A.M., Sikandar, A., Yahiaoui, S., Haupenthal, J., Walter, I., Empting, M., Köhnke, J. & Hartmann, R.W. (2018) Tackling *Pseudomonas aeruginosa* virulence

by a hydroxamic acid-based LasB inhibitor. *ACS chemical biology*. 13 (9), 2449–2455.

Kasahara, J., Kiriyama, Y., Miyashita, M., Kondo, T., Yamada, T., Yazawa, K., Yoshikawa, R. & Yamamoto, H. (2016) Teichoic acid polymers affect expression and localization of dl-endopeptidase LytE required for lateral cell wall hydrolysis in *Bacillus subtilis*. *Journal of Bacteriology*. 198 (11), 1585–1594.

Kawai, F., Shoda, M., Harashima, R., Sadaie, Y., Hara, H. & Matsumoto, K. (2004) Cardiolipin domains in *Bacillus subtilis* Marburg membranes. *Journal of Bacteriology*. 186 (5), 1475–1483.

Kawai, Y., Mercier, R. & Errington, J. (2014) Bacterial cell morphogenesis does not require a preexisting template structure. *Current Biology*. 24 (8), 863–867.

Kepplinger, B., Morton-Laing, S., Seistrup, K.H., Marrs, E.C.L., Hopkins, A.P., Perry, J.D., Strahl, H., Hall, M.J., Errington, J. & Allenby, N.E.E. (2018) Mode of action and heterologous expression of the natural product antibiotic vancoresmycin. *ACS Chemical Biology*. 13 (1), 207–214.

Kessler, N., Schuhmann, H., Morneweg, S., Linne, U. & Marahiel, M.A. (2004) The linear pentadecapeptide gramicidin is assembled by four multimodular nonribosomal peptide synthetases that comprise 16 modules with 56 catalytic domains. *Journal of Biological Chemistry*. 279 (9), 7413–7419.

Kim, S.-H., Kim, Y.N. & Jang, Y.-S. (2017) Cutting edge: LL-37–mediated formyl peptide receptor-2 signaling in follicular dendritic cells contributes to B cell activation in Peyer's patch germinal centers. *The Journal of Immunology*. 198 (2), 629–633.

Kiriukhin, M.Y., Debabov, D.V., Shinabarger, D.L. & Neuhaus, F.C. (2001) Biosynthesis of the glycolipid anchor in lipoteichoic acid of *Staphylococcus aureus* RN4220: role of YpfP, the diglucosyldiacylglycerol synthase. *Journal of Bacteriology*. 183 (11), 3506–3514.

Kiriukhin, M.Y. & Neuhaus, F.C. (2001) d-Alanylation of lipoteichoic acid: role of the d-alanyl carrier protein in acylation. *Journal of Bacteriology*. 183 (6), 2051–2058.

Kiriyama, Y., Yazawa, K., Tanaka, T., Yoshikawa, R., Yamane, H., Hashimoto, M., Sekiguchi, J. & Yamamoto, H. (2014) Localization and expression of the *Bacillus*

subtilis DL-endopeptidase LytF are influenced by mutations in LTA synthases and glycolipid anchor synthetic enzymes. *Microbiology (Reading, England)*. 160 (Pt 12), 2639–2649.

Kitano, K. & Tomasz, A. (1979) Triggering of autolytic cell wall degradation in *Escherichia coli* by beta-lactam antibiotics. *Antimicrobial Agents and Chemotherapy*. 16 (6), 838–848.

Koch, H.U., Haas, R. & Fischer, W. (1984) The role of lipoteichoic acid biosynthesis in membrane lipid metabolism of growing *Staphylococcus aureus*. *European Journal of Biochemistry*. 138 (2), 357–363.

Konopásek, I., Strzalka, K. & Svobodová, J. (2000) Cold shock in *Bacillus subtilis*: different effects of benzyl alcohol and ethanol on the membrane organisation and cell adaptation. *Biochimica et Biophysica Acta (BBA) - Biomembranes*. 1464 (1), 18–26.

Koo, B.-M., Kritikos, G., Farelli, J.D., Todor, H., Tong, K., Kimsey, H., Wapinski, I., Galardini, M., Cabal, A., Peters, J.M., Hachmann, A.-B., Rudner, D.Z., Allen, K.N., Typas, A. & Gross, C.A. (2017) Construction and analysis of two genome-scale deletion libraries for *Bacillus subtilis*. *Cell systems*. 4 (3), 291-305.e7.

Kowalska-Krochmal, B. & Dudek-Wicher, R. (2021) The minimum inhibitory concentration of antibiotics: methods, interpretation, clinical relevance. *Pathogens*. 10 (2), 165.

Koyano, Y., Okajima, K., Mihara, M. & Yamamoto, H. (2023) Visualization of wall teichoic acid decoration in *Bacillus subtilis*. *Journal of Bacteriology*. 205 (4), e00066-23.

Kristian, S.A., Timmer, A.M., Liu, G.Y., Lauth, X., Sal-Man, N., Rosenfeld, Y., Shai, Y., Gallo, R.L. & Nizet, V. (2007) Impairment of innate immune killing mechanisms by bacteriostatic antibiotics. *The FASEB Journal*. 21 (4), 1107–1116.

Kubicek-Sutherland, J.Z., Lofton, H., Vestergaard, M., Hjort, K., Ingmer, H. & Andersson, D.I. (2017) Antimicrobial peptide exposure selects for *Staphylococcus aureus* resistance to human defence peptides. *Journal of Antimicrobial Chemotherapy*. 72 (1), 115–127.

Kuroda, A. & Sekiguchi, J. (1991) Molecular cloning and sequencing of a major *Bacillus subtilis* autolysin gene. *Journal of Bacteriology*. 173 (22), 7304–7312.

Labischinski, H., Naumann, D. & Fischer, W. (1991) Small and medium-angle X-ray analysis of bacterial lipoteichoic acid phase structure. *European Journal of Biochemistry*. 202 (3), 1269–1274.

Laborda Anadón, S. (2022) *Membrane depolarisation induced by cell wall-targeting antibiotics triggers bactericidal activity independent of cell lysis*. Newcastle University.

Lacriola, C.J., Falk, S.P. & Weisblum, B. (2013) Screen for agents that induce autolysis in *Bacillus subtilis*. *Antimicrobial Agents and Chemotherapy*. 57 (1), 229–234.

Lambert, M.P. & Neuhaus, F.C. (1972) Mechanism of d-cycloserine action: alanine racemase from *Escherichia coli* W. *Journal of Bacteriology*. 110 (3), 978–987.

Lande, R., Gregorio, J., Facchinetti, V., Chatterjee, B., Wang, Y.-H., Homey, B., Cao, W., Wang, Y.-H., Su, B., Nestle, F.O., Zal, T., Mellman, I., Schröder, J.-M., Liu, Y.-J. & Gilliet, M. (2007) Plasmacytoid dendritic cells sense self-DNA coupled with antimicrobial peptide. *Nature*. 449 (7162), 564–569.

LaRock, C.N., Döhrmann, S., Todd, J., Corriden, R., Olson, J., Johannssen, T., Lepenies, B., Gallo, R.L., Ghosh, P. & Nizet, V. (2015) Group A *Streptococcal* M1 protein sequesters cathelicidin to evade innate immune killing. *Cell host & microbe*. 18 (4), 471–477.

Larrick, J.W., Hirata, M., Balint, R.F., Lee, J., Zhong, J. & Wright, S.C. (1995) Human CAP18: a novel antimicrobial lipopolysaccharide-binding protein. *Infection and Immunity*. 63 (4), 1291–1297.

Lazarevic, V. & Karamata, D. (1995) The tagGH operon of *Bacillus subtilis* 168 encodes a two-component ABC transporter involved in the metabolism of two wall teichoic acids. *Molecular Microbiology*. 16 (2), 345–355.

Lazarevic, V., Margot, P., Soldo, B. & Karamata, D. (1992) Sequencing and analysis of the *Bacillus subtilis lytRABC* divergon: a regulatory unit encompassing the structural genes of the N-acetylmuramoyl-L-alanine amidase and its modifier. *Journal of General Microbiology*. 138 (9), 1949–1961.

Ledger, E.V.K., Mesnage, S. & Edwards, A.M. (2022) Human serum triggers antibiotic tolerance in *Staphylococcus aureus*. *Nature Communications*. 13 (1), 2041.

Lee, A.G. (2004) How lipids affect the activities of integral membrane proteins. *Biochimica et Biophysica Acta (BBA) - Biomembranes*. 1666 (1), 62–87.

Lee, C.-C., Sun, Y., Qian, S. & Huang, H.W. (2011) Transmembrane pores formed by human antimicrobial peptide LL-37. *Biophysical Journal*. 100 (7), 1688–1696.

Leeuw, E. de, Li, C., Zeng, P., Li, C., Buin, M.D., Lu, W.-Y., Breukink, E. & Lu, W. (2010) Functional interaction of human neutrophil peptide-1 with the cell wall precursor lipid II. *FEBS Letters*. 584 (8), 1543–1548.

Li, M., Cha, D.J., Lai, Y., Villaruz, A.E., Sturdevant, D.E. & Otto, M. (2007) The antimicrobial peptide-sensing system *aps* of *Staphylococcus aureus*. *Molecular Microbiology*. 66 (5), 1136–1147.

Li, Y., Qian, Z., Ma, L., Hu, S., Nong, D., Xu, C., Ye, F., Lu, Y., Wei, G. & Li, M. (2016) Single-molecule visualization of dynamic transitions of pore-forming peptides among multiple transmembrane positions. *Nature Communications*. 7 (1), 12906.

Limoli, D.H., Rockel, A.B., Host, K.M., Jha, A., Kopp, B.T., Hollis, T. & Wozniak, D.J. (2014) Cationic antimicrobial peptides promote microbial mutagenesis and pathoadaptation in chronic infections. *PLOS Pathogens*. 10 (4), e1004083.

Lin, M.-F., Tsai, P.-W., Chen, J.-Y., Lin, Y.-Y. & Lan, C.-Y. (2015) OmpA binding mediates the effect of antimicrobial peptide LL-37 on *Acinetobacter baumannii*. *PLoS ONE*. 10 (10), e0141107.

Lin, Y.-M., Wu, S.-J., Chang, T.-W., Wang, C.-F., Suen, C.-S., Hwang, M.-J., Chang, M.D.-T., Chen, Y.-T. & Liao, Y.-D. (2010) Outer membrane protein I of *Pseudomonas aeruginosa* is a target of cationic antimicrobial peptide/protein. *The Journal of Biological Chemistry*. 285 (12), 8985–8994.

Lofton, H., Pränting, M., Thulin, E. & Andersson, D.I. (2013) Mechanisms and fitness costs of resistance to antimicrobial peptides LL-37, CNY100HL and wheat germ histones. *PLoS ONE*. 8 (7), e68875.

Loll, P.J., Upton, E.C., Nahoum, V., Economou, N.J. & Cocklin, S. (2014) The high resolution structure of tyrocidine A reveals an amphipathic dimer. *Biochimica et Biophysica Acta*. 9.

Lu, Y.-J., Zhang, F., Grimes, K.D., Lee, R.E. & Rock, C.O. (2007) Topology and active site of PlsY: the bacterual acylphosphate:glycerol-3-phsophate acyltransferase. *Journal of Biological Chemistry*. 282 (15), 11339–11346.

Ludtke, S.J., He, K., Heller, W.T., Harroun, T.A., Yang, L. & Huang, H.W. (1996) Membrane pores induced by magainin. *Biochemistry*. 35 (43), 13723–13728.

Lyu, M., Ayala, J.C., Chirakos, I., Su, C.-C., Shafer, W.M. & Yu, E.W. (2022) Structural basis of peptide-based antimicrobial inhibition of a resistance-nodulation-cell division multidrug efflux pump. *Microbiology Spectrum*. 10 (5), e02990-22.

Machado, H., Weng, L.L., Dillon, N., Seif, Y., Holland, M., Pekar, J.E., Monk, J.M., Nizet, V., Palsson, B.O. & Feist, A.M. (2019) Strain-specific metabolic requirements revealed by a defined minimal medium for systems analyses of *Staphylococcus aureus*. *Applied and Environmental Microbiology*. 85 (21), e01773-19.

Macheboeuf, P., Contreras-Martel, C., Job, V., Dideberg, O. & Dessen, A. (2006) Penicillin Binding Proteins: key players in bacterial cell cycle and drug resistance processes. *FEMS Microbiology Reviews*. 30 (5), 673–691.

Maffeo, C., Yoo, J., Comer, J., Wells, D.B., Luan, B. & Aksimentiev, A. (2014) Close encounters with DNA. *Journal of physics. Condensed Matter : an Institute of Physics Journal*. 26 (41), 413101.

Majewska, M., Zamlynny, V., Pieta, I.S., Nowakowski, R. & Pieta, P. (2021) Interaction of LL-37 human cathelicidin peptide with a model microbial-like lipid membrane. *Bioelectrochemistry*. 141, 107842.

Mansilla, M.C., Cybulski, L.E., Albanesi, D. & Mendoza, D. de (2004) Control of membrane lipid fluidity by molecular thermosensors. *Journal of Bacteriology*. 186 (20), 6681–6688.

Mansilla, M.C. & de Mendoza, D. (2005) The *Bacillus subtilis* desaturase: a model to understand phospholipid modification and temperature sensing. *Archives of Microbiology*. 183 (4), 229–235.

Margot, P., Mauël, C. & Karamata, D. (1994) The gene of the N-acetylglucosaminidase, a *Bacillus subtilis* 168 cell wall hydrolase not involved in vegetative cell autolysis. *Molecular Microbiology*. 12 (4), 535–545.

Margot, P., Pagni, M. & Karamata, D. (1999) *Bacillus subtilis* 168 gene *lytF* encodes a gamma-D-glutamate-meso-diaminopimelate muropeptidase expressed by the alternative vegetative sigma factor, sigmaD. *Microbiology (Reading, England)*. 145 (Pt 1), 57–65.

Margot, P., Wahlen, M., Gholamhuseinian, A., Piggot, P. & Karamata, D. (1998) The *lytE* gene of *Bacillus subtilis* 168 encodes a cell wall hydrolase. *Journal of Bacteriology*. 180 (3), 749–752.

Márquez, L.M., Helmann, J.D., Ferrari, E., Parker, H.M., Ordal, G.W. & Chamberlin, M.J. (1990) Studies of sigma D-dependent functions in *Bacillus subtilis*. *Journal of Bacteriology*. 172 (6), 3435–3443.

Márquez-Magaña, L.M. & Chamberlin, M.J. (1994) Characterization of the *sigD* transcription unit of *Bacillus subtilis*. *Journal of Bacteriology*. 176 (8), 2427–2434.

Marr, A.G. & Ingraham, J.L. (1962) Effect of temperature on the composition of fatty acids in *Escherichia coli*. *Journal of Bacteriology*. 84 (6), 1260–1267.

Martynowycz, M.W., Rice, A., Andreev, K., Nobre, T.M., Kuzmenko, I., Wereszczynski, J. & Gidalevitz, D. (2019) *Salmonella* membrane structural remodeling increases resistance to antimicrobial peptide LL-37. *ACS infectious diseases*. 5 (7), 1214–1222.

Matsumoto, K., Okada, M., Horikoshi, Y., Matsuzaki, H., Kishi, T., Itaya, M. & Shibuya, I. (1998) Cloning, sequencing, and disruption of the *Bacillus subtilis psd* gene coding for phosphatidylserine decarboxylase. *Journal of Bacteriology*. 180 (1), 100–106.

Matsuoka, S., Hashimoto, M., Kamiya, Y., Miyazawa, T., Ishikawa, K., Hara, H. & Matsumoto, K. (2011) The *Bacillus subtilis* essential gene *dgkB* is dispensable in mutants with defective lipoteichoic acid synthesis. *Genes & Genetic Systems*. 86 (6), 365–376.

McAuliffe, O., Ross, R.P. & Hill, C. (2001) Lantibiotics: structure, biosynthesis and mode of action. *FEMS Microbiology Reviews*. 25 (3), 285–308.

McKenney, P.T., Driks, A. & Eichenberger, P. (2013) The *Bacillus subtilis* endospore: assembly and functions of the multilayered coat. *Nature Reviews Microbiology*. 11 (1), 33–44.

McQuade, R., Roxas, B., Viswanathan, V.K. & Vedantam, G. (2012) *Clostridium difficile* clinical isolates exhibit variable susceptibility and proteome alterations upon exposure to mammalian cationic antimicrobial peptides. *Anaerobe*. 18 (6), 614–620.

Melo, M.N., Ferre, R. & Castanho, M.A.R.B. (2009) Antimicrobial peptides: linking partition, activity and high membrane-bound concentrations. *Nature Reviews Microbiology*. 7 (3), 245–250.

Mercier, R., Domínguez-Cuevas, P. & Errington, J. (2012) Crucial role for membrane fluidity in proliferation of primitive cells. *Cell Reports*. 1 (5), 417–423.

Mickiewicz, K.M., Kawai, Y., Drage, L., Gomes, M.C., Davison, F., Pickard, R., Hall, J., Mostowy, S., Aldridge, P.D. & Errington, J. (2019) Possible role of L-form switching in recurrent urinary tract infection. *Nature Communications*. 10, 4379.

de Miguel Catalina, A., Forbrig, E., Kozuch, J., Nehls, C., Paulowski, L., Gutsmann, T., Hildebrandt, P. & Mroginski, M.A. (2019) The C-Terminal VPRTES tail of LL-37 influences the mode of attachment to a lipid bilayer and antimicrobial activity. *Biochemistry*. 58 (19), 2447–2462.

Mileykovskaya, E. & Dowhan, W. (2000) Visualization of phospholipid domains in *Escherichia coli* by using the cardiolipin-specific fluorescent dye 10-N-nonyl acridine orange. *Journal of Bacteriology*. 182 (4), 1172–1175.

Mishra, N.N., Yang, S.-J., Sawa, A., Rubio, A., Nast, C.C., Yeaman, M.R. & Bayer, A.S. (2009) Analysis of cell membrane characteristics of *in vitro*-selected daptomycin-resistant strains of methicillin-resistant *Staphylococcus aureus*. *Antimicrobial Agents and Chemotherapy*. 53 (6), 2312–2318.

Missiakas, D.M. & Schneewind, O. (2013) Growth and laboratory maintenance of *Staphylococcus aureus*. *Current protocols in microbiology*. CHAPTER 9, Unit-9C.1.

Monteiro, J.M., Fernandes, P.B., Vaz, F., Pereira, A.R., Tavares, A.C., Ferreira, M.T., Pereira, P.M., Veiga, H., Kuru, E., VanNieuwenhze, M.S., Brun, Y.V., Filipe, S.R. & Pinho, M.G. (2015) Cell shape dynamics during the staphylococcal cell cycle. *Nature Communications*. 6, 8055.

Mookherjee, N., Anderson, M.A., Haagsman, H.P. & Davidson, D.J. (2020) Antimicrobial host defence peptides: functions and clinical potential. *Nature Reviews Drug Discovery*. 19 (5), 311–332.

Mount, K.L.B., Townsend, C.A., Rinker, S.D., Gu, X., Fortney, K.R., Zwickl, B.W., Janowicz, D.M., Spinola, S.M., Katz, B.P. & Bauer, M.E. (2010) *Haemophilus ducreyi* SapA contributes to cathelicidin resistance and virulence in humans. *Infection and Immunity*. 78 (3), 1176–1184.

Mouritsen, O.G. & Zuckermann, M.J. (2004) What's so special about cholesterol? *Lipids*. 39 (11), 1101–1113.

Muchová, K., Wilkinson, A.J. & Barák, I. (2011) Changes of lipid domains in *Bacillus subtilis* cells with disrupted cell wall peptidoglycan. *FEMS Microbiology Letters*. 325 (1), 92–98.

Müller, A., Wenzel, M., Strahl, H., Grein, F., Saaki, T.N.V., Kohl, B., Siersma, T., Bandow, J.E., Sahl, H.-G., Schneider, T. & Hamoen, L.W. (2016) Daptomycin inhibits cell envelope synthesis by interfering with fluid membrane microdomains. *Proceedings of the National Academy of Sciences*. 113 (45), E7077–E7086.

Murakami, M., Lopez-Garcia, B., Braff, M., Dorschner, R.A. & Gallo, R.L. (2004) Postsecretory processing generates multiple cathelicidins for enhanced topical antimicrobial defense. *The Journal of Immunology*. 172 (5), 3070–3077.

Mykytczuk, N.C.S., Trevors, J.T., Leduc, L.G. & Ferroni, G.D. (2007) Fluorescence polarization in studies of bacterial cytoplasmic membrane fluidity under environmental stress. *Progress in Biophysics and Molecular Biology*. 95 (1), 60–82.

Nair, S.K. & van der Donk, W.A. (2011) Structure and mechanism of enzymes involved in biosynthesis and breakdown of the phosphonates fosfomycin, dehydrophos, and phosphinothricin. *Archives of Biochemistry and Biophysics*. 505 (1), 13–21.

Neshani, A., Zare, H., Akbari Eidgahi, M.R., Kamali Kakhki, R., Safdari, H., Khaledi, A. & Ghazvini, K. (2019) LL-37: Review of antimicrobial profile against sensitive and antibiotic-resistant human bacterial pathogens. *Gene Reports*. 17, 100519.

Neuhaus, F.C. & Baddiley, J. (2003) A continuum of anionic charge: structures and functions of D-alanyl-teichoic acids in gram-positive bacteria. *Microbiology and Molecular Biology Reviews*. 67 (4), 686–723.

Neuhaus, F.C. & Lynch, J.L. (1964) The enzymatic synthesis of D alanyl-D-alanine. III. On the inhibition of D-alanyl-D-alanine synthetase by the antibiotic D-cycloserine. *Biochemistry*. 3 (4), 471–480.

Neville, F., Cahuzac, M., Konovalov, O., Ishitsuka, Y., Lee, K.Y.C., Kuzmenko, I., Kale, G.M. & Gidalevitz, D. (2006) Lipid headgroup discrimination by antimicrobial peptide LL-37: insight into mechanism of action. *Biophysical Journal*. 90 (4), 1275–1287.

Newcastle University Image Analysis Unit (2023) *General_Fiji_Macros*. https://github.com/NCL-ImageAnalysis/General_Fiji_Macros/blob/a04f85da883a3ed4028abae2d43da74404303153/Phase_Contrast_Cell_Average_Fluorescence.py.

Nishibori, A., Kusaka, J., Hara, H., Umeda, M. & Matsumoto, K. (2005) Phosphatidylethanolamine domains and localization of phospholipid synthases in *Bacillus subtilis* membranes. *Journal of Bacteriology*. 187 (6), 2163–2174.

Noore, J., Noore, A. & Li, B. (2013) Cationic antimicrobial peptide LL-37 Is effective against both extra- and intracellular *Staphylococcus aureus*. *Antimicrobial Agents and Chemotherapy*. 57 (3), 1283–1290.

Novitsky, T.J., Chan, M., Himes, R.H. & Akagi, J.M. (1974) Effect of temperature on the growth and cell wall chemistry of a facultative thermophilic *Bacillus*. *Journal of Bacteriology*. 117 (2), 858–865.

Ohnishi, R., Ishikawa, S. & Sekiguchi, J. (1999) Peptidoglycan hydrolase LytF plays a role in cell separation with CwlF during vegetative growth of *Bacillus subtilis*. *Journal of Bacteriology*. 181 (10), 3178–3184.

Oliver, P.M., Crooks, J.A., Leidl, M., Yoon, E.J., Saghatelian, A. & Weibel, D.B. (2014) Localization of anionic phospholipids in *Escherichia coli* cells. *Journal of Bacteriology*. 196 (19), 3386–3398.

Oren, Z., Lerman, J.C., Gudmundsson, G.H., Agerberth, B. & Shai, Y. (1999) Structure and organization of the human antimicrobial peptide LL-37 in phospholipid membranes: relevance to the molecular basis for its non-cell-selective activity. *Biochemical Journal*. 341 (Pt 3), 501–513.

Oren, Z. & Shai, Y. (1998) Mode of action of linear amphipathic α-helical antimicrobial peptides. *Peptide Science*. 47 (6), 451–463.

Oshida, T., Sugai, M., Komatsuzawa, H., Hong, Y.M., Suginaka, H. & Tomasz, A. (1995) A *Staphylococcus aureus* autolysin that has an *N*-acetylmuramoyl-L-alanine amidase domain and an endo-beta-*N*-acetylglucosaminidase domain: cloning, sequence analysis, and characterization. *Proceedings of the National Academy of Sciences*. 92 (1), 285–289.

Pachón-Ibáñez, M.E., Smani, Y., Pachón, J. & Sánchez-Céspedes, J. (2017) Perspectives for clinical use of engineered human host defense antimicrobial peptides. *FEMS Microbiology Reviews*. 41 (3), 323–342.

Pag, U., Oedenkoven, M., Sass, V., Shai, Y., Shamova, O., Antcheva, N., Tossi, A. & Sahl, H.-G. (2008) Analysis of *in vitro* activities and modes of action of synthetic antimicrobial peptides derived from an α-helical 'sequence template'. *Journal of Antimicrobial Chemotherapy*. 61 (2), 341–352.

Patterson, P.H. & Lennarz, W.J. (1971) Studies on the membranes of *Bacilli*. *Journal of Biological Chemistry*. 246 (4), 1062–1072.

Pedreira, T., Elfmann, C. & Stülke, J. (2022) The current state of *Subti*Wiki, the database for the model organism *Bacillus subtilis*. *Nucleic Acids Research*. 50 (D1), D875–D882.

Pelz, A., Wieland, K.-P., Putzbach, K., Hentschel, P., Albert, K. & Götz, F. (2005) Structure and biosynthesis of staphyloxanthin from *Staphylococcus aureus*. *Journal of Biological Chemistry*. 280 (37), 32493–32498.

Percy, M.G. & Gründling, A. (2014) Lipoteichoic acid synthesis and function in Gram-positive bacteria. *Annual Review of Microbiology*. 68 (1), 81–100.

Peschel, A., Jack, R.W., Otto, M., Collins, L.V., Staubitz, P., Nicholson, G., Kalbacher, H., Nieuwenhuizen, W.F., Jung, G., Tarkowski, A., van Kessel, K.P.M. & van Strijp, J.A.G. (2001) *Staphylococcus aureus* resistance to human defensins and evasion of neutrophil killing via the novel virulence factor Mprf is based on modification of membrane lipids with L-Lysine. *Journal of Experimental Medicine*. 193 (9), 1067–1076.

Pezzulo, A.A., Tang, X.X., Hoegger, M.J., Abou Alaiwa, M.H., Ramachandran, S., Moninger, T.O., Karp, P.H., Wohlford-Lenane, C.L., Haagsman, H.P., van Eijk, M., Bánfi, B., Horswill, A.R., Stoltz, D.A., McCray, P.B., Welsh, M.J. & Zabner, J. (2012) Reduced airway surface pH impairs bacterial killing in the porcine cystic fibrosis lung. *Nature*. 487 (7405), 109–113.

Pietiäinen, M., Gardemeister, M., Mecklin, M., Leskelä, S., Sarvas, M. & Kontinen, V.P. (2005) Cationic antimicrobial peptides elicit a complex stress response in *Bacillus subtilis* that involves ECF-type sigma factors and two-component signal transduction systems. *Microbiology*. 151 (5), 1577–1592.

Piller, P., Wolinski, H., Cordfunke, R.A., Drijfhout, J.W., Keller, S., Lohner, K. & Malanovic, N. (2022) Membrane activity of LL-37 derived antimicrobial peptides against *Enterococcus hirae*: superiority of SAAP-148 over OP-145. *Biomolecules*. 12 (4), 523.

Pinho, M.G. & Errington, J. (2003) Dispersed mode of *Staphylococcus aureus* cell wall synthesis in the absence of the division machinery. *Molecular Microbiology*. 50 (3), 871–881.

Pogmore, A.-R., Seistrup, K.H. & Strahl, H. (2018) The Gram-positive model organism *Bacillus subtilis* does not form microscopically detectable cardiolipin-specific lipid domains. *Microbiology*. 164 (4), 475–482.

Pohl, S., Bhavsar, G., Hulme, J., Bloor, A.E., Misirli, G., Leckenby, M.W., Radford, D.S., Smith, W., Wipat, A., Williamson, E.D., Harwood, C.R. & Cranenburgh, R.M. (2013) Proteomic analysis of *Bacillus subtilis* strains engineered for improved production of heterologous proteins. *Proteomics*. 13 (22), 3298–3308.

Poirel, L., Jayol, A. & Nordmann, P. (2017) Polymyxins: Antibacterial Activity, Susceptibility Testing, and Resistance Mechanisms Encoded by Plasmids or Chromosomes. *Clinical Microbiology Reviews*. 30 (2), 557–596.

Porcelli, F., Verardi, R., Shi, L., Henzler-Wildman, K.A., Ramamoorthy, A. & Veglia, G. (2008) NMR structure of the cathelicidin-derived human antimicrobial peptide LL-37 in dodecylphosphocholine micelles. *Biochemistry*. 47 (20), 5565–5572.

Prenner, E.J., Lewis, R.N.A.H. & McElhaney, R.N. (1999) The interaction of the antimicrobial peptide gramicidin S with lipid bilayer model and biological membranes. *Biochimica et Biophysica Acta (BBA) - Biomembranes*. 1462 (1), 201–221.

Ratkowsky, D.A., Olley, J., McMeekin, T.A. & Ball, A. (1982) Relationship between temperature and growth rate of bacterial cultures. *Journal of Bacteriology*. 149 (1), 1–5.

Rebets, Y., Lupoli, T., Qiao, Y., Schirner, K., Villet, R., Hooper, D., Kahne, D. & Walker, S. (2014) Moenomycin resistance mutations in *Staphylococcus aureus* reduce peptidoglycan chain length and cause aberrant cell division. *ACS chemical biology*. 9 (2), 459–467.

Reichmann, N.T., Cassona, C.P. & Gründling, A. (2013) Revised mechanism of d-alanine incorporation into cell wall polymers in Gram-positive bacteria. *Microbiology*. 159 (Pt 9), 1868–1877.

Reiners, J., Lagedroste, M., Gottstein, J., Adeniyi, E.T., Kalscheuer, R., Poschmann, G., Stühler, K., Smits, S.H.J. & Schmitt, L. (2020) Insights in the antimicrobial potential of the natural nisin variant nisin H. *Frontiers in Microbiology*. 11, 573614.

Renner, L.D. & Weibel, D.B. (2011) Cardiolipin microdomains localize to negatively curved regions of *Escherichia coli membranes*. *Proceedings of the National Academy of Sciences*. 108 (15), 6264–6269.

Ridyard, K.E. & Overhage, J. (2021) The potential of human peptide LL-37 as an antimicrobial and anti-biofilm agent. *Antibiotics*. 10 (6), 650.

Rilfors, L., Lindblom, G., Wieslander, Å. & Christiansson, A. (1984) Lipid bilayer stability in biological membranes. In: Morris Kates & Lionel A. Manson (eds.). *Membrane Fluidity*. Biomembranes. Boston, MA, Springer US. pp. 205–245.

Rogers, H.J., Perkins, H.R. & Ward, J.B. (1980) Structure of peptidoglycan. In: H. J. Rogers, H. R. Perkins, & J. B. Ward (eds.). *Microbial Cell Walls and Membranes*. Dordrecht, Springer Netherlands. pp. 190–214.

Rojas, E.R., Billings, G., Odermatt, P.D., Auer, G.K., Zhu, L., Miguel, A., Chang, F., Weibel, D.B., Theriot, J.A. & Huang, K.C. (2018) The outer membrane is an essential load-bearing element in Gram-negative bacteria. *Nature*. 559 (7715), 617–621.

Roth, B.L., Poot, M., Yue, S.T. & Millard, P.J. (1997) Bacterial viability and antibiotic susceptibility testing with SYTOX green nucleic acid stain. *Applied and Environmental Microbiology*. 63 (6), 2421–2431.

Russell, N.J. (1984) Mechanisms of thermal adaptation in bacteria: blueprints for survival. *Trends in Biochemical Sciences*. 9 (3), 108–112.

Saar-Dover, R., Bitler, A., Nezer, R., Shmuel-Galia, L., Firon, A., Shimoni, E., Trieu-Cuot, P. & Shai, Y. (2012) D-Alanylation of lipoteichoic acids confers resistance to cationic peptides in Group B *Streptococcus* by increasing the cell wall density. *PLoS Pathogens*. 8 (9), e1002891.

Sabnis, A., Hagart, K.L.H., Klöckner, A., Becce, M., Evans, L.E., Furniss, R.C.D., Mavridou, D.A.I., Murphy, R., Stevens, M.M., Davies, J.C., Larrouy-Maumus, G.J., Clarke, T.B. & Edwards, A.M. (2021) Colistin kills bacteria by targeting lipopolysaccharide in the cytoplasmic membrane. *eLife*. 10, e65836.

Sáenz, J.P., Grosser, D., Bradley, A.S., Lagny, T.J., Lavrynenko, O., Broda, M. & Simons, K. (2015) Hopanoids as functional analogues of cholesterol in bacterial membranes. *Proceedings of the National Academy of Sciences*. 112 (38), 11971–11976.

Salzberg, L.I. & Helmann, J.D. (2008) Phenotypic and transcriptomic characterization of *Bacillus subtilis* mutants with grossly altered membrane composition. *Journal of Bacteriology*. 190 (23), 7797–7807.

Samant, S., Hsu, F.-F., Neyfakh, A.A. & Lee, H. (2009) The *Bacillus anthracis* protein MprF is required for synthesis of lysylphosphatidylglycerols and for resistance to cationic antimicrobial peptides. *Journal of Bacteriology*. 191 (4), 1311–1319.

Scheinpflug, K., Krylova, O., Nikolenko, H., Thurm, C. & Dathe, M. (2015) Evidence for a novel mechanism of antimicrobial action of a cyclic R-,W-rich hexapeptide. *PLOS ONE*. 10 (4), e0125056.

Scheinpflug, K., Wenzel, M., Krylova, O., Bandow, J.E., Dathe, M. & Strahl, H. (2017) Antimicrobial peptide cWFW kills by combining lipid phase separation with autolysis. *Scientific Reports*. 7 (1), 44332.

Schertzer, J.W., Bhavsar, A.P. & Brown, E.D. (2005) Two conserved histidine residues are critical to the function of the TagF-like family of enzymes. *Journal of Biological Chemistry*. 280 (44), 36683–36690.

Schertzer, J.W. & Brown, E.D. (2003) Purified, recombinant TagF protein from *Bacillus subtilis* 168 catalyzes the polymerization of glycerol phosphate onto a membrane acceptor *in vitro*. *Journal of Biological Chemistry*. 278 (20), 18002–18007.

Schindelin, J., Arganda-Carreras, I., Frise, E., Kaynig, V., Longair, M., Pietzsch, T., Preibisch, S., Rueden, C., Saalfeld, S., Schmid, B., Tinevez, J.-Y., White, D.J., Hartenstein, V., Eliceiri, K., Tomancak, P. & Cardona, A. (2012) Fiji: an open-source platform for biological-image analysis. *Nature Methods*. 9 (7), 676–682.

Schirner, K. & Errington, J. (2009) The cell wall regulator σI specifically suppresses the lethal phenotype of *mbl* mutants in *Bacillus subtilis*. *Journal of Bacteriology*. 191 (5), 1404–1413.

Schlag, M., Biswas, R., Krismer, B., Kohler, T., Zoll, S., Yu, W., Schwarz, H., Peschel, A. & Götz, F. (2010) Role of staphylococcal wall teichoic acid in targeting the major autolysin Atl. *Molecular Microbiology*. 75 (4), 864–873.

Schmid, F. (2017) Physical mechanisms of micro- and nanodomain formation in multicomponent lipid membranes. *Biochimica et Biophysica Acta (BBA) - Biomembranes*. 1859 (4), 509–528.

Schmidtchen, A., Frick, I.-M., Andersson, E., Tapper, H. & Björck, L. (2002) Proteinases of common pathogenic bacteria degrade and inactivate the antibacterial peptide LL-37. *Molecular Microbiology*. 46 (1), 157–168.

Schmitt, M., Schuler-Schmid, U. & Schmidt-Lorenz, W. (1990) Temperature limits of growth, TNase and enterotoxin production of *Staphylococcus aureus* strains isolated from foods. *International Journal of Food Microbiology*. 11 (1), 1–19.

Schujman, G.E., Paoletti, L., Grossman, A.D. & de Mendoza, D. (2003) FapR, a bacterial transcription factor involved in global regulation of membrane lipid biosynthesis. *Developmental Cell*. 4 (5), 663–672.

Scott, M.G., Davidson, D.J., Gold, M.R., Bowdish, D. & Hancock, R.E.W. (2002) The human antimicrobial peptide LL-37 is a multifunctional modulator of innate immune responses. *The Journal of Immunology*. 169 (7), 3883–3891.

Seistrup, K.H. (2018) *MreB dependent cell envelope homeostasis in* Bacillus subtilis. Newcastle University. https://theses.ncl.ac.uk/jspui/bitstream/10443/4493/1/Seistrup%20KH%202019.pdf.

Sekimizu, K. & Kornberg, A. (1988) Cardiolipin activation of DnaA protein, the initiation protein of replication in *Escherichia coli*. *Journal of Biological Chemistry*. 263 (15), 7131–7135.

Sewell, E.W. & Brown, E.D. (2014) Taking aim at wall teichoic acid synthesis: new biology and new leads for antibiotics. *The Journal of Antibiotics*. 67 (1), 43–51.

Shahmiri, M., Enciso, M., Adda, C.G., Smith, B.J., Perugini, M.A. & Mechler, A. (2016) Membrane core-specific antimicrobial action of cathelicidin LL-37 peptide switches between pore and nanofibre formation. *Scientific Reports*. 6 (1), 38184.

Sham, L.-T., Butler, E.K., Lebar, M.D., Kahne, D., Bernhardt, T.G. & Ruiz, N. (2014) MurJ is the flippase of lipid-linked precursors for peptidoglycan biogenesis. *Science (New York, N.Y.)*. 345 (6193), 220–222.

Shelton, C.L., Raffel, F.K., Beatty, W.L., Johnson, S.M. & Mason, K.M. (2011) Sap transporter mediated import and subsequent degradation of antimicrobial peptides in *Haemophilus*. *PLOS Pathogens*. 7 (11), e1002360.

Sieprawska-Lupa, M., Mydel, P., Krawczyk, K., Wójcik, K., Puklo, M., Lupa, B., Suder, P., Silberring, J., Reed, M., Pohl, J., Shafer, W., McAleese, F., Foster, T., Travis, J. & Potempa, J. (2004) Degradation of human antimicrobial peptide LL-37 by

Staphylococcus aureus-derived proteinases. *Antimicrobial Agents and Chemotherapy*. 48 (12), 4673–4679.

Silhavy, T.J., Kahne, D. & Walker, S. (2010) The bacterial cell envelope. *Cold Spring Harbor Perspectives in Biology*. 2 (5).

Simonin, J., Bille, E., Crambert, G., Noel, S., Dreano, E., Edwards, A., Hatton, A., Pranke, I., Villeret, B., Cottart, C.-H., Vrel, J.-P., Urbach, V., Baatallah, N., Hinzpeter, A., Golec, A., Touqui, L., Nassif, X., Galietta, L.J.V., Planelles, G., Sallenave, J.-M., Edelman, A. & Sermet-Gaudelus, I. (2019) Airway surface liquid acidification initiates host defense abnormalities in cystic fibrosis. *Scientific Reports*. 9 (1), 6516.

Singer, S.J. & Nicolson, G.L. (1972) The fluid mosaic model of the structure of cell membranes. *Science*. 175 (4023), 720–731.

Singh, V.K., Hattangady, D.S., Giotis, E.S., Singh, A.K., Chamberlain, N.R., Stuart, M.K. & Wilkinson, B.J. (2008) Insertional inactivation of branched-chain α-keto acid dehydrogenase in *Staphylococcus aureus* leads to decreased branched-chain membrane fatty acid content and increased susceptibility to certain stresses. *Applied and Environmental Microbiology*. 74 (19), 5882–5890.

Singh, V.K., Sirobhushanam, S., Ring, R.P., Singh, S., Gatto, C. & Wilkinson, B.J. (2018) Roles of pyruvate dehydrogenase and branched-chain α-keto acid dehydrogenase in branched-chain membrane fatty acid levels and associated functions in *Staphylococcus aureus*. *Journal of Medical Microbiology*. 67 (4), 570–578.

Slavetinsky, C.J., Hauser, J.N., Gekeler, C., Slavetinsky, J., Geyer, A., Kraus, A., Heilingbrunner, D., Wagner, S., Tesar, M., Krismer, B., Kuhn, S., Ernst, C.M. & Peschel, A. (2022) Sensitizing *Staphylococcus aureus* to antibacterial agents by decoding and blocking the lipid flippase MprF. *eLife*. 11, e66376.

Smith, T.J., Blackman, S.A. & Foster, S.J.Y. 2000 (2000) Autolysins of *Bacillus subtilis*: multiple enzymes with multiple functions. *Microbiology*. 146 (2), 249–262.

Snoussi, M., Talledo, J.P., Del Rosario, N.-A., Mohammadi, S., Ha, B.-Y., Košmrlj, A. & Taheri-Araghi, S. (2018) Heterogeneous absorption of antimicrobial peptide LL-37 in *Escherichia coli* cells enhances population survivability. *eLife*. 7, e38174.

Sochacki, K.A., Barns, K.J., Bucki, R. & Weisshaar, J.C. (2011) Real-time attack on single *Escherichia coli* cells by the human antimicrobial peptide LL-37. *Proceedings of the National Academy of Sciences*. 108 (16), E77–E81.

Sohlenkamp, C. & Geiger, O. (2016) Bacterial membrane lipids: diversity in structures and pathways. *FEMS Microbiology Reviews*. 40 (1), 133–159.

Soldo, B., Lazarevic, V. & Karamata, D. 2002 (2002) *tagO* is involved in the synthesis of all anionic cell-wall polymers in *Bacillus subtilis* 168aa. *Microbiology*. 148 (7), 2079–2087.

Sonesson, A., Przybyszewska, K., Eriksson, S., Mörgelin, M., Kjellström, S., Davies, J., Potempa, J. & Schmidtchen, A. (2017) Identification of bacterial biofilm and the *Staphylococcus aureus* derived protease, staphopain, on the skin surface of patients with atopic dermatitis. *Scientific Reports*. 7, 8689.

Sørensen, O., Arnljots, K., Cowland, J.B., Bainton, D.F. & Borregaard, N. (1997) The human antibacterial cathelicidin, hCAP-18, is synthesized in myelocytes and metamyelocytes and localized to specific granules in neutrophils. *Blood*. 90 (7), 2796–2803.

Sørensen, O.E., Follin, P., Johnsen, A.H., Calafat, J., Tjabringa, G.S., Hiemstra, P.S. & Borregaard, N. (2001) Human cathelicidin, hCAP-18, is processed to the antimicrobial peptide LL-37 by extracellular cleavage with proteinase 3. *Blood*. 97 (12), 3951–3959.

Sperotto, M.M., Ipsen, J.H. & Mouritsen, O.G. (1989) Theory of protein-induced lateral phase separation in lipid membranes. *Cell Biophysics*. 14 (1), 79–95.

Spizizen, J. (1958) Transformation of biochemically deficient strains of *Bacillus subtilis* by deoxyribonucleate. *Proceedings of the National Academy of Sciences of the United States of America*. 44 (10), 1072–1078.

Staroń, A., Finkeisen, D.E. & Mascher, T. (2011) Peptide antibiotic sensing and detoxification modules of *Bacillus subtilis*. *Antimicrobial Agents and Chemotherapy*. 55 (2), 515–525.

Staubitz, P. & Peschel, A. (2002) MprF-mediated lysinylation of phospholipids in *Bacillus subtilis* – protection against bacteriocins in terrestrial habitats? *Microbiology*. 148 (11), 3331–3332.

Stiefel, P., Schmidt-Emrich, S., Maniura-Weber, K. & Ren, Q. (2015) Critical aspects of using bacterial cell viability assays with the fluorophores SYTO9 and propidium iodide. *BMC Microbiology*. 15, 36.

Strahl, H., Bürmann, F. & Hamoen, L.W. (2014) The actin homologue MreB organizes the bacterial cell membrane. *Nature Communications*. 5 (1), 3442.

Strahl, H. & Hamoen, L.W. (2010) Membrane potential is important for bacterial cell division. *Proceedings of the National Academy of Sciences*. 107 (27), 12281–12286.

Strahl, H., Ronneau, S., González, B.S., Klutsch, D., Schaffner-Barbero, C. & Hamoen, L.W. (2015) Transmembrane protein sorting driven by membrane curvature. *Nature Communications*. 6, 8728.

Strempel, N., Neidig, A., Nusser, M., Geffers, R., Vieillard, J., Lesouhaitier, O., Brenner-Weiss, G. & Overhage, J. (2013) Human host defense peptide LL-37 stimulates virulence factor production and adaptive resistance in *Pseudomonas aeruginosa*. *PLoS ONE*. 8 (12), e82240.

Strøm, M.B., Haug, B.E., Skar, M.L., Stensen, W., Stiberg, T. & Svendsen, J.S. (2003) The pharmacophore of short cationic antibacterial peptides. *Journal of Medicinal Chemistry*. 46 (9), 1567–1570.

Thévenaz, P., Ruttimann, U.E. & Unser, M. (1998) A pyramid approach to subpixel registration based on intensity. *IEEE Transactions on Image Processing*. 7 (1), 27–41.

Thwaite, J.E., Hibbs, S., Titball, R.W. & Atkins, T.P. (2006) Proteolytic degradation of human antimicrobial peptide LL-37 by *Bacillus anthracis* may contribute to virulence. *Antimicrobial Agents and Chemotherapy*. 50 (7), 2316–2322.

Tjabringa, G.S., Ninaber, D.K., Drijfhout, J.W., Rabe, K.F. & Hiemstra, P.S. (2006) Human cathelicidin LL-37 is a chemoattractant for eosinophils and neutrophils that acts via formyl-peptide receptors. *International Archives of Allergy and Immunology*. 140 (2), 103–112.

Toon, P., Brown, P.E. & Baddiley, J. (1972) The lipid-teichoic acid complex in the cytoplasmic membrane of *Streptococcus faecalis*. *The Biochemical Journal*. 127 (2), 399–409.

Tran, T.T., Panesso, D., Mishra, N.N., Mileykovskaya, E., Guan, Z., Munita, J.M., Reyes, J., Diaz, L., Weinstock, G.M., Murray, B.E., Shamoo, Y., Dowhan, W., Bayer, A.S. & Arias, C.A. (2013) Daptomycin-resistant *Enterococcus faecalis* diverts the antibiotic molecule from the division septum and remodels cell membrane phospholipids. *mBio*. 4 (4).

Trofimenko, E., Grasso, G., Heulot, M., Chevalier, N., Deriu, M.A., Dubuis, G., Arribat, Y., Serulla, M., Michel, S., Vantomme, G., Ory, F., Dam, L.C., Puyal, J., Amati, F., Lüthi, A., Danani, A. & Widmann, C. (2021) Genetic, cellular, and structural characterization of the membrane potential-dependent cell-penetrating peptide translocation pore. *eLife*. 10, e69832.

Tsai, M., Ohniwa, R.L., Kato, Y., Takeshita, S.L., Ohta, T., Saito, S., Hayashi, H. & Morikawa, K. (2011) *Staphylococcus aureus* requires cardiolipin for survival under conditions of high salinity. *BMC Microbiology*. 11 (1), 13.

Turner, J., Cho, Y., Dinh, N.-N., Waring, A.J. & Lehrer, R.I. (1998) Activities of LL-37, a cathelin-associated antimicrobial peptide of human neutrophils. *Antimicrobial Agents and Chemotherapy*. 42 (9), 2206–2214.

Uhlmann, J., Rohde, M., Siemens, N., Kreikemeyer, B., Bergman, P., Johansson, L. & Norrby-Teglund, A. (2016) LL-37 triggers formation of *Streptococcus pyogenes* extracellular vesicle-like structures with immune stimulatory properties. *Journal of Innate Immunity*. 8 (3), 243–257.

Urashima, A., Sanou, A., Yen, H. & Tobe, T. (2017) Enterohaemorrhagic *Escherichia coli* produces outer membrane vesicles as an active defence system against antimicrobial peptide LL-37. *Cellular Microbiology*. 19 (11).

Valentine, D.L. (2007) Adaptations to energy stress dictate the ecology and evolution of the Archaea. *Nature Reviews Microbiology*. 5 (4), 316–323.

Vandamme, D., Landuyt, B., Luyten, W. & Schoofs, L. (2012) A comprehensive summary of LL-37, the factotum human cathelicidin peptide. *Cellular Immunology*. 280 (1), 22–35.

Verjans, E.-T., Zels, S., Luyten, W., Landuyt, B. & Schoofs, L. (2016) Molecular mechanisms of LL-37-induced receptor activation: An overview. *Peptides*. 85, 16–26.

Vitrac, H., Bogdanov, M. & Dowhan, W. (2013) *in vitro* reconstitution of lipid-dependent dual topology and postassembly topological switching of a membrane protein. *Proceedings of the National Academy of Sciences*. 110 (23), 9338–9343.

Volkman, B.F., Zhang, Q., Debabov, D.V., Rivera, E., Kresheck, G.C. & Neuhaus, F.C. (2001) Biosynthesis of d-alanyl-lipoteichoic acid: the tertiary structure of apo-d-alanyl carrier protein. *Biochemistry*. 40 (27), 7964–7972.

Vollmer, W., Blanot, D. & De Pedro, M.A. (2008a) Peptidoglycan structure and architecture. *FEMS Microbiology Reviews*. 32 (2), 149–167.

Vollmer, W., Joris, B., Charlier, P. & Foster, S. (2008b) Bacterial peptidoglycan (murein) hydrolases. *FEMS Microbiology Reviews*. 32 (2), 259–286.

de Vrije, T., de Swart, R.L., Dowhan, W., Tommassen, J. & de Kruijff, B. (1988) Phosphatidylglycerol is involved in protein translocation across *Escherichia coli* inner membranes. *Nature*. 334 (6178), 173–175.

Wang, G. (2015) Improved methods for classification, prediction, and design of antimicrobial peptides. In: Peng Zhou & Jian Huang (eds.). *Computational Peptidology*. Methods in Molecular Biology. New York, NY, Springer. pp. 43–66.

Wang, J.E., Jørgensen, P.F., Almlöf, M., Thiemermann, C., Foster, S.J., Aasen, A.O. & Solberg, R. (2000) Peptidoglycan and lipoteichoic acid from *Staphylococcus aureus* induce tumor necrosis factor alpha, interleukin 6 (IL-6), and IL-10 production in both T cells and monocytes in a human whole blood model. *Infection and Immunity*. 68 (7), 3965–3970.

Wecke, J., Madela, K. & Fischer, W. (1997) The absence of D-alanine from lipoteichoic acid and wall teichoic acid alters surface charge, enhances autolysis and increases susceptibility to methicillin in *Bacillus subtilis*. *Microbiology*. 143 (9), 2953–2960.

Wei, J., Cao, X., Qian, J., Liu, Z., Wang, X., Su, Q., Wang, Y., Xie, R. & Li, X. (2021) Evaluation of antimicrobial peptide LL-37 for treatment of *Staphylococcus aureus* biofilm on titanium plate. *Medicine*. 100 (44), e27426.

Weidenmaier, C., Kokai-Kun, J.F., Kristian, S.A., Chanturiya, T., Kalbacher, H., Gross, M., Nicholson, G., Neumeister, B., Mond, J.J. & Peschel, A. (2004) Role of teichoic acids in *Staphylococcus aureus* nasal colonization, a major risk factor in nosocomial infections. *Nature Medicine*. 10 (3), 243–245.

Wenzel, M., Chiriac, A.I., Otto, A., Zweytick, D., May, C., Schumacher, C., Gust, R., Albada, H.B., Penkova, M., Krämer, U., Erdmann, R., Metzler-Nolte, N., Straus, S.K., Bremer, E., Becher, D., Brötz-Oesterhelt, H., Sahl, H.-G. & Bandow, J.E. (2014) Small cationic antimicrobial peptides delocalize peripheral membrane proteins. *Proceedings of the National Academy of Sciences*. 111 (14), E1409–E1418.

Wenzel, M., Rautenbach, M., Vosloo, J.A., Siersma, T., Aisenbrey, C.H.M., Zaitseva, E., Laubscher, W.E., Rensburg, W. van, Behrends, J.C., Bechinger, B. & Hamoen, L.W. (2018) The multifaceted antibacterial mechanisms of the pioneering peptide antibiotics tyrocidine and gramicidin S. *mBio*. 9 (5).

White, S.W., Zheng, J., Zhang, Y.-M. & Rock, C.O. (2005) The structural biology of type II fatty acid biosynthesis. *Annual Review of Biochemistry*. 74 (1), 791–831.

Willecke, K. & Pardee, A.B. (1971) Fatty acid-requiring mutant of *Bacillus subtilis* defective in branched chain α-keto acid dehydrogenase. *Journal of Biological Chemistry*. 246 (17), 5264–5272.

Wilson, S., Tank, R.K.J., Hobbs, J.K., Foster, S.J. & Garner, E. (2021) An exhaustive multiple knockout approach to understanding cell wall hydrolase function in *Bacillus subtilis*. bioRxiv. 2021.02.18.431929.

te Winkel, J.D., Gray, D.A., Seistrup, K.H., Hamoen, L.W. & Strahl, H. (2016) Analysis of antimicrobial-triggered membrane depolarization using voltage sensitive dyes. *Frontiers in Cell and Developmental Biology*. 4.

Wörmann, M.E., Corrigan, R.M., Simpson, P.J., Matthews, S.J. & Gründling, A. (2011) Enzymatic activities and functional interdependencies of *Bacillus subtilis* lipoteichoic acid synthesis enzymes. *Molecular Microbiology*. 79 (3), 566–583.

Wu, F. & Tan, C. (2019) Dead bacterial absorption of antimicrobial peptides underlies collective tolerance. *Journal of The Royal Society Interface*. 16 (151), 20180701.

Wuersching, S.N., Huth, K.C., Hickel, R. & Kollmuss, M. (2021) Targeting antibiotic tolerance in anaerobic biofilms associated with oral diseases: Human antimicrobial peptides LL-37 and lactoferricin enhance the antibiotic efficacy of amoxicillin, clindamycin and metronidazole. *Anaerobe*. 71, 102439.

Xhindoli, D., Pacor, S., Guida, F., Antcheva, N. & Tossi, A. (2013) Native oligomerization determines the mode of action and biological activities of human cathelicidin LL-37. *Biochemical Journal*. 457 (2), 263–275.

Xiong, Y.Q., Mukhopadhyay, K., Yeaman, M.R., Adler-Moore, J. & Bayer, A.S. (2005) Functional interrelationships between cell membrane and cell wall in antimicrobial peptide-mediated killing of *Staphylococcus aureus*. *Antimicrobial Agents and Chemotherapy*. 49 (8), 3114–3121.

Yamaguchi, H., Furuhata, K., Fukushima, T., Yamamoto, H. & Sekiguchi, J. (2004) Characterization of a new *Bacillus subtilis* peptidoglycan hydrolase gene, *yvcE* (named *cwlO*), and the enzymatic properties of its encoded protein. *Journal of Bioscience and Bioengineering*. 98 (3), 174–181.

Yamamoto, H., Kurosawa, S. & Sekiguchi, J. (2003) Localization of the vegetative cell wall hydrolases LytC, LytE, and LytF on the *Bacillus subtilis* cell surface and stability of these enzymes to cell wall-bound or extracellular proteases. *Journal of Bacteriology*. 185 (22), 6666–6677.

Yan, Y., Munshi, S., Leiting, B., Anderson, M.S., Chrzas, J. & Chen, Z. (2000) Crystal structure of *Escherichia coli* UDPMurNAc-tripeptide d-alanyl-d-alanine-adding enzyme (MurF) at 2.3 Å resolution. *Journal of Molecular Biology*. 304 (3), 435–445.

Yang, D., Chen, Q., Schmidt, A.P., Anderson, G.M., Wang, J.M., Wooters, J., Oppenheim, J.J. & Chertov, O. (2000) LL-37, the neutrophil granule– and epithelial cell–derived cathelicidin, utilizes formyl peptide receptor–like 1 (Fprl1) as a receptor to chemoattract human peripheral blood neutrophils, monocytes, and T cells. *Journal of Experimental Medicine*. 192 (7), 1069–1074.

Yang, Y., Luo, M., Zhou, H., Li, C., Luk, A., Zhao, G., Fung, K. & Ip, M. (2019) Role of two-component system response regulator *bceR* in the antimicrobial resistance, virulence, biofilm formation, and stress response of Group B *Streptococcus*. *Frontiers in Microbiology*. 10, 10.

Yoon, Y., Lee, H., Lee, S., Kim, S. & Choi, K.-H. (2015) Membrane fluidity-related adaptive response mechanisms of foodborne bacterial pathogens under environmental stresses. *Food Research International*. 72, 25–36.

Yoshimura, M., Oshima, T. & Ogasawara, N. (2007) Involvement of the YneS/YgiH and PlsX proteins in phospholipid biosynthesis in both *Bacillus subtilis* and *Escherichia coli*. *BMC Microbiology*. 7 (1), 69.

Yuan, Y., Fuse, S., Ostash, B., Sliz, P., Kahne, D. & Walker, S. (2008) Structural analysis of the contacts anchoring moenomycin to peptidoglycan glycosyltransferases and implications for antibiotic design. *ACS Chemical Biology*. 3 (7), 429–436.

Zaritsky, A., Kihara, M. & Macnab, R.M. (1981) Measurement of membrane potential in *Bacillus subtilis*: a comparison of lipophilic cations, rubidium ion, and a cyanine dye as probes. *The Journal of Membrane Biology*. 63 (3), 215–231.

Zasloff, M. (2002) Antimicrobial peptides of multicellular organisms. *Nature*. 415 (6870), 389–395.

Zeth, K. & Sancho-Vaello, E. (2017) The human antimicrobial peptides dermcidin and LL-37 show novel distinct pathways in membrane interactions. *Frontiers in Chemistry*. 5.

Zhang, B., Liu, X., Lambert, E., Mas, G., Hiller, S., Veening, J.-W. & Perez, C. (2020a) Structure of a proton-dependent lipid transporter involved in lipoteichoic acids biosynthesis. *Nature structural & molecular biology*. 27 (6), 561–569.

Zhang, W., Yang, F.K., Han, Y., Gaikwad, R., Leonenko, Z. & Zhao, B. (2013) Surface and tribological behaviors of the bioinspired polydopamine thin films under dry and wet conditions. *Biomacromolecules*. 14 (2), 394–405.

Zhang, X., Oglęcka, K., Sandgren, S., Belting, M., Esbjörner, E.K., Nordén, B. & Gräslund, A. (2010) Dual functions of the human antimicrobial peptide LL-37—target

membrane perturbation and host cell cargo delivery. *Biochimica et Biophysica Acta (BBA) - Biomembranes*. 1798 (12), 2201–2208.

Zhang, Y., Delbrück, A.I., Off, C.L., Benke, S. & Mathys, A. (2020b) Flow cytometry combined with single cell sorting to study heterogeneous germination of *Bacillus* spores under high pressure. *Frontiers in Microbiology*. 10.

Zhang, Y.-M. & Rock, C.O. (2008) Membrane lipid homeostasis in bacteria. *Nature Reviews Microbiology*. 6 (3), 222–233.

Zhang, Z., Cherryholmes, G., Chang, F., Rose, D.M., Schraufstatter, I. & Shively, J.E. (2009) Evidence that cathelicidin peptide LL-37 may act as a functional ligand for CXCR2 on human neutrophils. *European Journal of Immunology*. 39 (11), 3181–3194.

Zielińska, A., Savietto, A., de Sousa Borges, A., Martinez, D., Berbon, M., Roelofsen, J.R., Hartman, A.M., de Boer, R., Van der Klei, I.J., Hirsch, A.K., Habenstein, B., Bramkamp, M. & Scheffers, D.-J. (2020) Flotillin-mediated membrane fluidity controls peptidoglycan synthesis and MreB movement. *eLife*. 9, e57179.

Zilberstein, D., Padan, E. & Schuldiner, S. (1980) A single locus in *Escherichia coli* governs growth in alkaline pH and on carbon sources whose transport is sodium dependent. *FEBS Letters*. 116 (2), 177–180.

Appendix

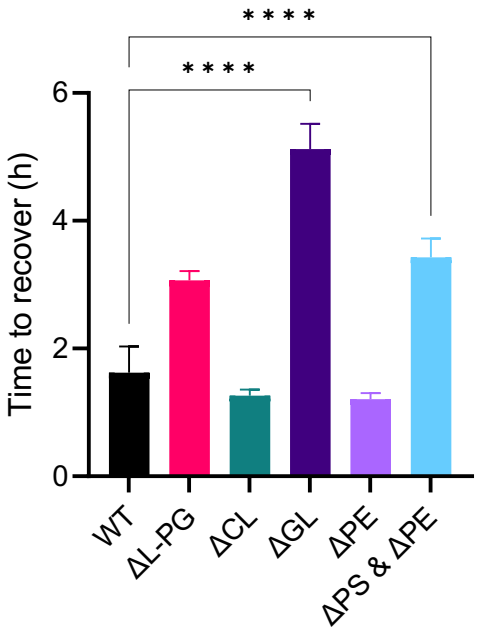

Figure A1. Second biological repeat of experiment in Figure 3.2b. Analysis of the time taken for *B. subtilis* lacking lysyl-phosphatidylglycerol (L-PG), cardiolipin (CL), glycolipids (GL), phosphatidylethanolamine (PE) or phosphatidylserine (PS) & PE to recover to the initial optical density at which 20 μg mL^{-1} LL-37 was added; analysed by unpaired ordinary ANOVA with Dunnet's multiple comparisons test comparing to wild-type (WT), **** represents $p < 0.0001$. Data represented as mean±SD (n=3).

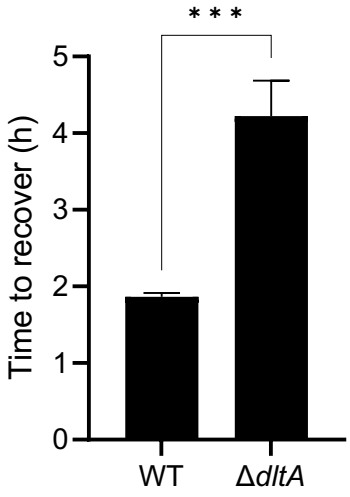

Figure A2. Second biological repeat of experiment in Figure 3.4c. Analysis of the time taken for wild-type and D-alanylation (Δ*dltA*) deficient *B. subtilis* to recover to the initial optical density at which 20 μg mL^{-1} LL-37 was added; analysed by unpaired two-tailed t-test, *** represents $p < 0.001$. Data represented as mean±SD (n=3).

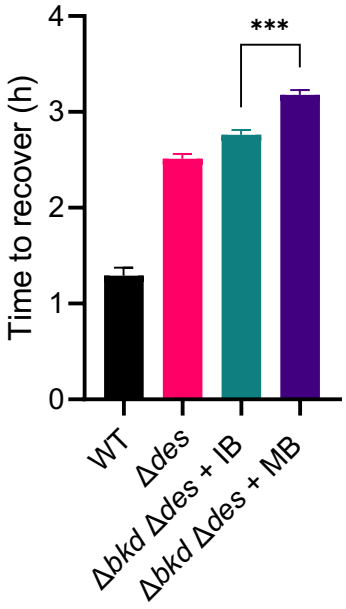

Figure A3. Second biological repeat of experiment in Figure 3.6c. Analysis of the time taken for *B. subtilis* wild-type, Δ*des* and Δ*bkd* Δ*des* with isobutyric acid (IB) or 2-methylbutyric acid (MB) to recover to the initial optical density at which 20 µg mL^{-1} LL-37 was added; Δ*bkd* Δ*des* + IB/MB analysed by unpaired two-tailed t-test, *** represents $p < 0.001$. Data represented as mean±SD (n=3).

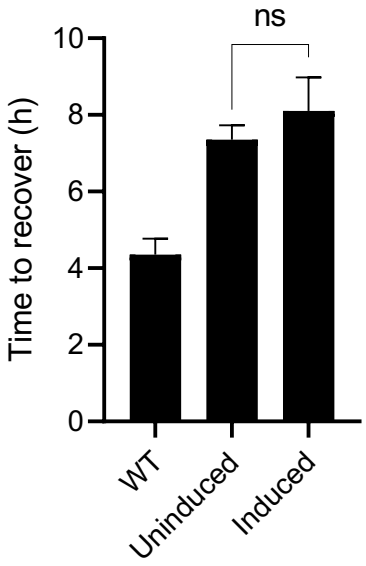

Figure A4. Second biological repeat of experiment in Figure 3.7d. Analysis of the time taken for *B. subtilis* wild-type, Δ*bkd* Δ*des* Pspac-*des* with 2-methylbutyric acid (MB) and *des* expression uninduced or induced by 1 mM IPTG to recover to the initial optical density at which 20 µg mL^{-1} LL-37 was added; Δ*bkd* Δ*des* + MB with *des* expression un/induced analysed by unpaired two-tailed t-test, p value is not significant (ns). Data represented as mean±SD (n=3).

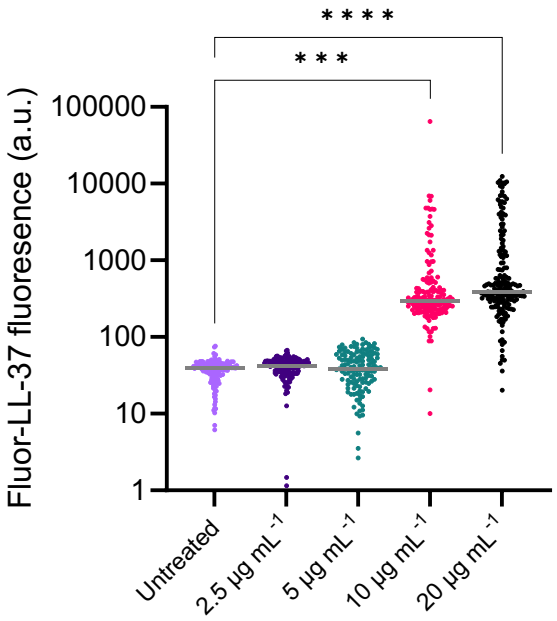

Figure A5. Second biological repeat of experiment in Figure 4.1a. Single cell fluorescent microscopy quantification of 5-Fam-LL-37 (Fluor-LL-37) binding wild-type *B. subtilis* after 5 minutes incubation; grey bar indicates median fluorescence intensity; analysed by unpaired ordinary ANOVA with Dunnet's multiple comparisons test comparing to untreated, *** represents $p < 0.0001$, **** represents $p < 0.0001$; $n \geq 139$.

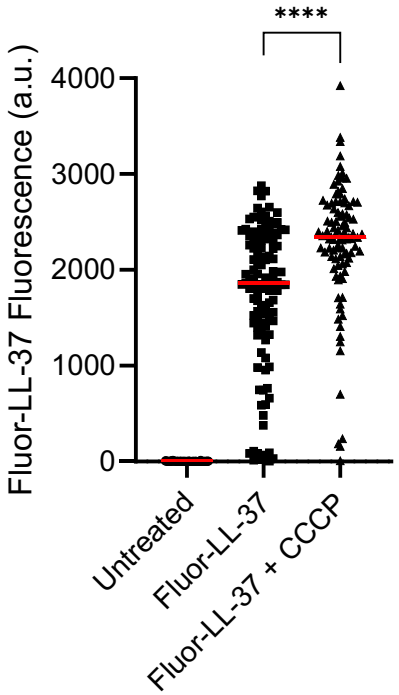

Figure A6. Second biological repeat of experiment in Figure 4.4b. Single cell quantification of wild-type *B. subtilis* treated with 5-Fam-LL-37 (Fluor-LL-37; 20 µg mL^{-1}) and CCCP (100 µM) for 5 minutes; red bar indicates median fluorescence intensity; analysed by unpaired two-tailed t-test, **** represents $p < 0.0001$; $n \geq 96$.

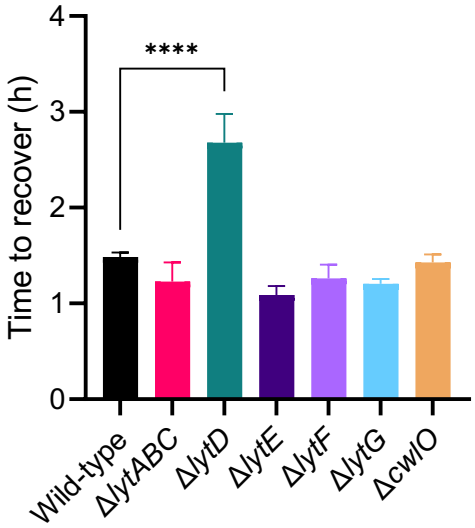

Figure A7. Second biological repeat of experiment in Figure 4.8h. Analysis of the time taken for *B. subtilis* strains: wild-type, Δ*lytABC*, Δ*lytD*, Δ*lytE*, Δ*lytF*, Δ*lytG*, Δ*cwlO* upon the addition of 20 µg mL^{-1} LL-37 to recover to the initial optical density at which LL-37 was added; analysed by unpaired ordinary ANOVA with Dunnet's multiple comparisons test comparing to wild-type, **** represents $p < 0.0001$. Data represented as mean±SD (n=3).

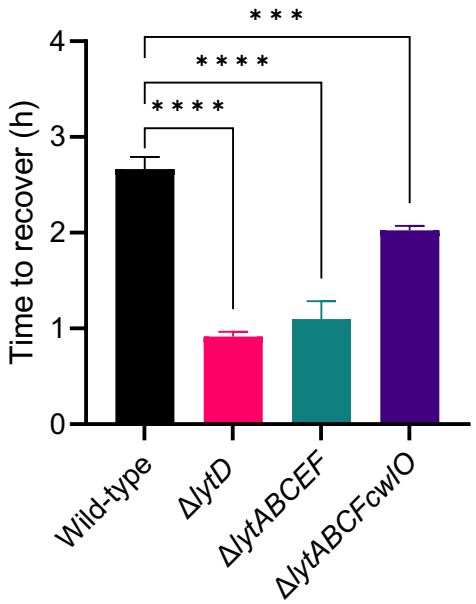

Figure A8. Second biological repeat of experiment in Figure 4.9c. Analysis of the time taken for wild-type, Δ*lytD*, Δ*lytABCEF*, Δ*lytABCFcwlO B. subtilis* strains to recover to the initial optical density at which 10 µg mL^{-1} LL-37 was added; analysed by unpaired ordinary ANOVA with Dunnet's multiple comparisons test comparing to wild-type, **** represents $p < 0.0001$. Data represented as mean±SD (n=3).

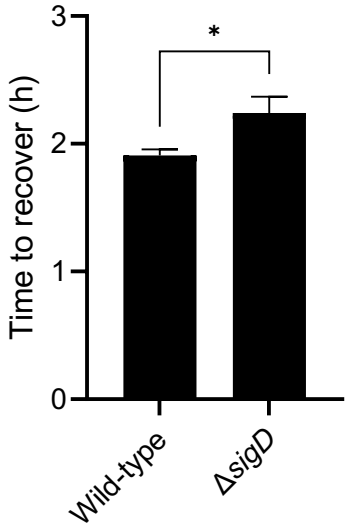

Figure A9. Second biological repeat of experiment in Figure 4.10c. Analysis of the time taken for wild-type and σ^D deficient (Δ*sigD*) *B. subtilis* treated with 20 µg mL^{-1} LL-37 to recover to the initial optical density at which LL-37 was added; analysed by unpaired two-tailed t-test, * represents $p < 0.05$. Data represented as mean±SD (n=3).

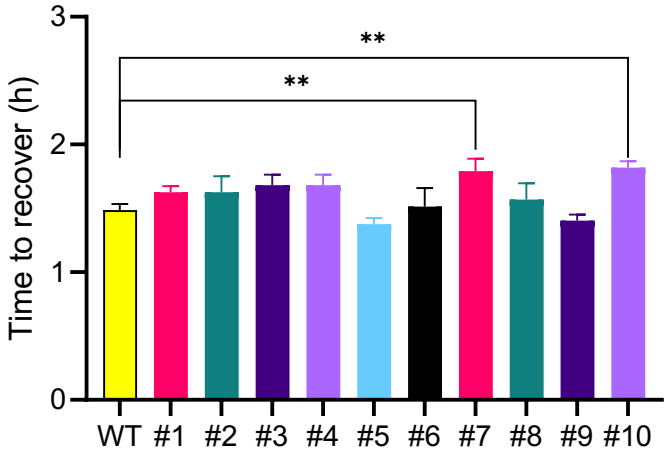

Figure A10. Second biological repeat of experiment in Figure 5.1c. Analysis of the time taken for WT and potential suppressor strains (#1-10) treated with 20 µg mL^{-1} LL-37 to recover to the initial optical density at which LL-37 was added; analysed by unpaired ordinary ANOVA with Dunnet's multiple comparisons test comparing to wild-type, ** represents $p < 0.01$. Data represented as mean±SD (n=3).

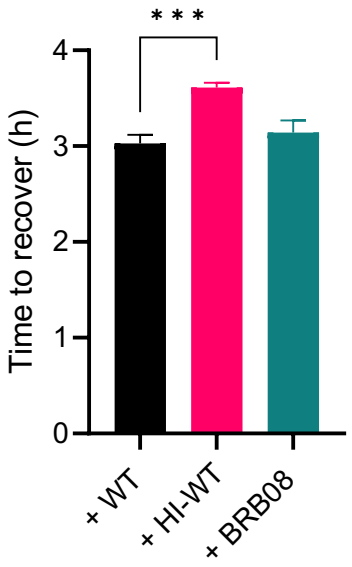

Figure A11. Second biological repeat of experiment in Figure 5.2b. Analysis of the time taken for *B. subtilis* wild-type (WT) grown in WT, heat-inactivated (HI)-WT and BRB08 supernatant treated with 20 µg mL^{-1} LL-37 to recover to the initial optical density at which LL-37 was added; analysed by unpaired ordinary ANOVA with Dunnet's multiple comparisons test comparing to wild-type, *** represents $p < 0.001$. Data represented as mean±SD (n=3).

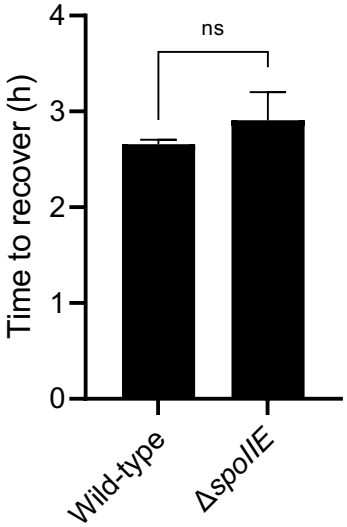

Figure A12. Second biological repeat of experiment in Figure 5.3c. Analysis of the time taken for wild-type and Δ*spoIIE B. subtilis* treated with 20 µg mL^{-1} LL-37 to recover to the initial optical density at which LL-37 was added; analysed by unpaired two-tailed t-test, p value is not significant (ns). Data represented as mean±SD (n=3).

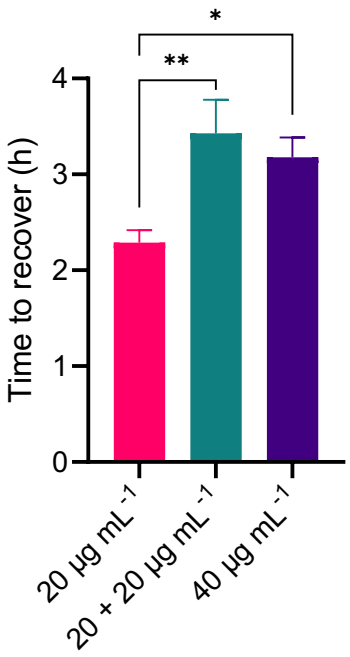

Figure A13. Second biological repeat of experiment in Figure 5.4b. Analysis of the time taken to recover to the initial optical density at which LL-37 was added for wild-type *B. subtilis* treated with 20, 20 + 20 (second dose after 15 minutes) and 40 µg mL^{-1} LL-37; analysed by unpaired ordinary ANOVA with Tukey's multiple comparisons test to compare between all conditions, * represents $p < 0.05$, ** represents $p < 0.01$. Data represented as mean±SD (n=3).

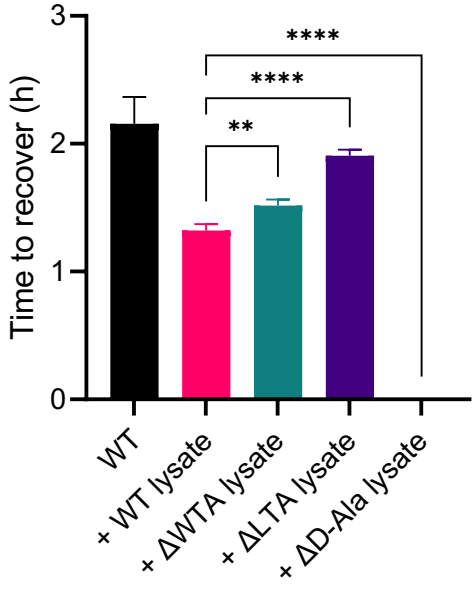

Figure A14. Second biological repeat of experiment in Figure 5.14c. Analysis of the time taken time taken to recover to the initial optical density at which LL-37 was added for wild-type *B. subtilis* grown with and without cell lysate from WT, wall teichoic acid deficient (ΔWTA), lipoteichoic acid deficient (ΔLTA) and D-alanylation deficient (Δ*dltA*) *B. subtilis* treated with 20 µg mL^{-1} LL-37; analysed by unpaired ordinary ANOVA with Dunnet's multiple comparisons test comparing to + WT lysate, **** represents $p > 0.0001$ (excludes WT). Data represented as mean±SD (n=3).